January 2004

History and Characterization of Mortars in Spanish New World Fortifications: A Case Study on El Castillo de San Cristóbal, San Juan, Puerto Rico

Jeremy C. Wells
University of Pennsylvania

Presented to the Faculties of the University of Pennsylvania in Partial Fulfillment of Requirements for the Degree of Master of Science in Historic Preservation 2004.
Advisor: Frank G. Matero

History and Characterization of Mortars in Spanish New World Fortifications: A Case Study on El Castillo de San Cristóbal, San Juan, Puerto Rico

Comments

Presented to the Faculties of the University of Pennsylvania in Partial Fulfillment of Requirements for the Degree of Master of Science in Historic Preservation 2004.
Advisor: Frank G. Matero

HISTORY AND CHARACTERIZATION OF MORTARS IN SPANISH NEW WORLD FORTIFICATIONS: A CASE STUDY ON EL CASTILLO DE SAN CRISTÓBAL, SAN JUAN, PUERTO RICO

Jeremy C. Wells

A THESIS

in

Historic Preservation

Presented to the Faculties of the University of Pennsylvania in
Partial Fulfillment of the Requirements for the Degree of

MASTER OF SCIENCE

2004

____
Advisor
Frank G. Matero
Associate Professor of Architecture

____
Reader
A. Elena Charola
Lecturer in Historic Preservation

____
Graduate Group Chair
Frank G. Matero
Associate Professor of Architecture

DEDICATION

To my wife, Jeanne, for her tireless support of my academic endeavors.

ACKNOWLEDGEMENTS

I would like to thank my advisor, Prof. Frank G. Matero, for his expertise and guidance through this rigorous, but rewarding experience; Dr. A. Elena Charola for kindly agreeing to be a reader while teaching in Spain; Mr. William Romanow at the Laboratory for the Research on the Structure of Matter for his assistance in interpreting XRD results; Ms. Beth Price at the Philadelphia Museum of Art for kindly running and interpreting FTIR and SEM/EDS tests; and Mr. Félix López, Mr. Carlos Almodovar, and the other employees at the San Juan National Historic Site for their time and generous assistance.

TABLE OF CONTENTS

LIST OF TABLES

Chapters 1-5

Appendices

LIST OF ILLUSTRATIONS

Chapters 1-5

Appendices

Structures

Maps of Sample Locations

Photographs of Sample Locations

Photomicrographs of Whole Samples

Photomicrographs of Thin Sections

CHAPTER 1: SITE SELECTION, FOCUS OF INQUIRY, AND METHODOLOGY

1.1 Introduction

Fort San Cristóbal is the largest fortification ever built by the Spanish in the New World. Its size is primarily due to its extensive outworks which extend over twenty-seven acres. If viewed as a primary document, this site has the potential to deliver a vast amount of information on Spanish building technology from the sixteenth to the nineteenth centuries. This particular investigation deals specifically with mortar formulations and use from Fort San Cristóbal. This chapter will explain the research design: why Fort San Cristóbal was selected, what questions were postulated to guide the sampling and analysis, and the overall methodology used to obtain answers to those questions.

1.2 Site selection

Fort San Cristóbal is located in the northeast corner of Old San Juan, Puerto Rico (see Appendix A). It is one of many forts on the island that were built by the Spanish from the sixteenth through nineteenth centuries as a safeguard against European predation. Fort San Cristóbal is notable for its immense size and for its historical integrity. To a large degree, it retains its late eighteenth century plan and many of its original structures are relatively intact.

Several material-based studies on mortars and surface finishes have been published on the fortifications of Old San Juan. These investigations were primarily the result of an intensive study in the mid to late 1980s of Fort San Cristóbal, El Morro (located across the city to the west), and several smaller fortifications along with the wall that surrounds much of Old San Juan.[1]

Two articles were published on the mortars from El Morro using data collected for the historic structure report.[2] These articles were important to this investigation because El Morro is structurally and materially similar to Fort San Cristóbal. No other published articles were located on the material analysis of mortars for the fortifications of Old San Juan or the Spanish Caribbean in general.

This lack of material investigations is, unfortunately, endemic to the Caribbean. While much has been published on the architectural history of this area, very little has been written on the building materials of the Caribbean and their relevance to architectural history, cultural studies, and site preservation and restoration. According to German Tellez, an expert on Caribbean fortifications, "the focus on construction issues among investigators of the Caribbean fortifications has been marginal compared to the interest on the political and military histories" (1997: 75). Moreover, Tellez hints at the potential value offered by material investigations: "the knowledge of the characteristics and performance of construction materials available and used throughout the Caribbean for military construction could decidedly impact theoretical or histographical issues" (1997: 75).

---

[1] The study in the 1980s was spearheaded by the Center for Preservation Research at Columbia University in conjunction with the North Atlantic Region of the National Park Service. The primary participants in the study included Joan Berkowitz, E. Blaine Cliver, Richard Crisson, Billy Garrett, Judy Jacob, Frank Matero, and Barbara Yocum. The fruition of the project was an historic structure report that was published in 1991 by the National Park Service and has been used extensively in the preparation of this investigation.

[2] The first article by Jacob and Cavallo was published in the *Conservation of the Iberian and Latin American Cultural Heritage* (1992). The second article by Crisson was published in the *Third International Symposium of Historic Preservation on Puerto Rico and the Caribbean* (1996).

The analysis of the mortars of Fort San Cristóbal presents a unique and rare opportunity to add to the rather limited knowledge on construction technology used in the Spanish Caribbean and to answer specific questions related to mortar formulations. Such an investigation will hopefully provide a more complete foundation for further research into this area.

1.3 Focus of inquiry

The basis of this investigation focuses on three questions related to the formulation and use of mortars in Spanish New World fortifications using Fort San Cristóbal as a case study. These questions were carefully selected in order to effectively narrow the focus of this investigation while providing a maximum amount of information. These questions are as follows:

1. Can mortar formulations be correlated with specific uses?
2. Is there a chronological pattern in mortar formulations?
3. Are there any components in the mortars that characterize regional or cultural traditions?

Questions one and two are interrelated; information obtained from mortar analysis provides answers that can be interpreted by use or time. Question three is more specific to local uses.

The information obtained from the analysis of mortars was placed into a matrix in order to fully understand the relationships between various samples. The patterns revealed by this method are interpreted in a narrative in Chapter 5.

1.4 Methodology

Once the questions were clearly framed, the chronology and layout of Fort San Cristóbal were investigated (see Chapter 2). The goal was to select a limited set of samples that would be representative of various construction periods from the seventeenth century up to the year 1900 and exhibit a wide variety of common uses. The three main categories of use were renders (e.g., stuccos), bedding mortars, and horizontal surfaces (i.e., terreplein surfaces or merlon/embrasure horizontal surfaces).

Upon researching the chronology of the site, it quickly became apparent that the Officers' Quarters, Troops Quarters, most of the North Casemates, North Bastion, Curtain, and South Bastion were heavily modified in the twentieth century. These structures would have made poor choices for sample locations because layers of change would be too difficult to interpret. Therefore, with the exception of an embrasure in the North Casemates, this project focused on the outworks of Fort San Cristóbal. Only mortar samples that appeared to date from the construction of each structure were taken in order to eliminate confusion with areas that have been modified during later periods.

Six structures were eventually selected. They are presented below along with a justification for their selection:

1. Fort of the Point. Representative of possible seventeenth-century mortars from the earliest construction period.
2. Lightning Tower on San Carlos. Documentary evidence is available to substantiate a construction date of about 1819 for this tower. Represents early- to mid-nineteenth century mortars and renders.

3. La Trinidad. Representative of the first construction period in the eighteenth century (about 1766 to 1783).
4. El Abanico. Representative of the second construction period in the eighteenth century (about 1779 to 1783).
5. St. Teresa. Representative of late nineteenth century mortars.
6. Casemate number three in the North Casemates. Most of the North Casemates were heavily modified by the U.S. Army and National Park Service in the twentieth century. Casemate number three is unique in that it exhibits what may be original renders and most certainly original bedding mortar from the first construction period in the eighteenth century.

A map of the location of the sampled structures is available (see Appendix A).

Where possible, two samples from each of the three categories (render, bedding, horizontal) were taken from each structure, for a maximum possible of six per structure. There were no horizontal mortars available from Fort of the Point and the Lightning Tower. Of these samples, fifteen were eventually chosen for analytical study. A subset of samples from the previous Columbia University study in the 1980s were used to help corroborate or refute the results of analytical tests. The Columbia University samples included the Main Ramp and South Gate as well as buildings sampled for this present investigation.

After the samples were taken, an extensive literature search was undertaken of the full spectrum of analytical techniques used in mortar analysis. A subset of possible analytical techniques was then chosen for their suitability to answer the questions posed for this inquiry (see Chapter 4).

1.5 Summary

Fort San Cristóbal was selected as a study site for its ability to provide new and hopefully useful information to supplement the paucity of available data on the materials of Caribbean fortifications. This information is intended to provide historical information as well as support future preservation and restoration efforts. Information gathered for this study was centered around three main questions relating to the chronology and use of mortars as well as unusual formulations that may be present.

Sampled structures were selected for their ability to provide a wide distribution of time periods and mortar uses. Primarily, these structures were the outworks of San Carlos, La Trinidad, El Abanico, and St. Teresa. Fifteen samples were selected for analytical study. Samples from the Columbia Study of the 1980s were used to supplement these samples.

CHAPTER 2: SITE HISTORY

2.1 Introduction

Fort San Cristóbal and El Morro are the two principal forts constructed to protect the city of San Juan. This chapter will explain the historical context and design origins of Fort San Cristóbal, followed by a technical description and chronology of buildings where samples have been taken.

2.2 Historical context

2.2.1 Design origins

The design of Fort San Cristóbal is representative of eighteenth century European fortifications. It was designed by Thomas O'Daly, an Irishman, who was influenced by the French school of fortification based on Italian Renaissance ideas. As it stands today, Fort San Cristóbal is one of the last traditional European-style fortresses and represents the culmination of centuries of slow, evolutionary change.

Until the Renaissance, the tower was the principal structure used to defend a permanent fortification. By the fifteenth century, the tall, narrow tower had evolved into a very low, broad structure in response to the development of more powerful and effective explosive weaponry. (Hughes 1991: 53). It was during this period that the design of permanent fortifications underwent substantial changes that are reflected in Fort San Cristóbal.

The basic design of Fort San Cristóbal can be traced to fifteenth-century Italy. It was there that the mobile siege gun and specialized iron shot were developed to replace early archaic weaponry. Engineers from Italy invented the *bastion*—an outward projection from the main fortification consisting of two faces and two flanks which allowed the defense of nearby walls. Its design relied on an intersection of several incident firing angles and maximized the area that could be defended from one position. Italian engineers refined fortifications into a workable defense method called the *bastion system* by designing complex outworks with very low, massive, thick walls and an overall plan that was star-shaped (Duffy 1985: 1; Hughes 1991: 68-70). This star design was no accident; according to the military historian George Rothrock, "the evolution of the complex-star shaped fortresses of the seventeenth century can be attributed almost wholly to the influence of explosives" (1966: 79). Later military engineers were to refine this system, but its essential essence remained intact.

The idea behind the bastion system was to stop an attack by creating an obstruction without providing an easily defeated target. The heart of this system is the ditch, the wall, and the *glacis* (Illustration 2.1). These elements can easily be seen at Fort San Cristóbal. The ditch helped to create a better barrier by increasing the effective height of the fortress wall. Earth left over from the excavation of the ditch was piled into a glacis on the side across from the wall. The side closest to the ditch was steeply sloped (or nearly vertical) while the other side gently sloped away from the fort. The glacis impeded artillery because a very limited firing angle was available—more often than not, artillery hit the glacis or went right over the top of the fortress. In addition, the glacis slowed the path of infantry that had to advance uphill (Rothrock 1966: 79).

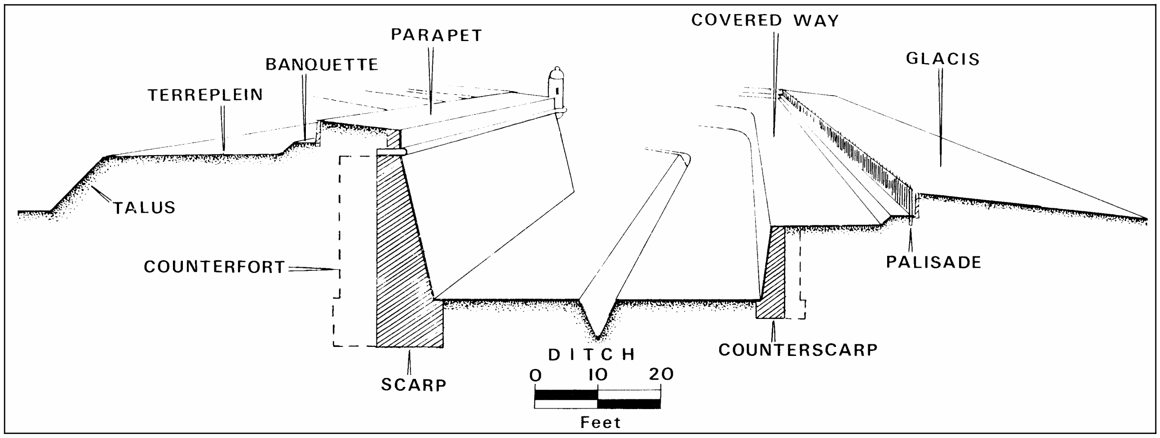

Illustration 2.1: The bastion system (Duffy 1985: 2).

Fortification design was a pan-European affair. According to *Fortification and Military Discipline*, published in 1688, the most prominent experts of fortification design in the sixteenth and seventeenth centuries were the German authors Samuel Maralois, Adam Fritach, Nicolaus Goldmann, and Matthias Dogen; English authors Richard Norwood and Jonas Moor; Italian authors Pietro Sardi and Francesco Tensini; and French authors M. de LaMont, Alain Manesson Mallet, Antoine de Ville, and Georges Fournier (Steed 1688).

The most influential military engineer that indirectly influenced the design of Fort San Cristóbal was Sébastien LePrestre de Vauban (1633-1707). Vauban worked primarily in the later half of the seventeenth century in France, but his theories and design ideas did not achieve widespread adoption until the eighteenth century. His success was legendary: over his lifetime all of the forty sieges he directed were successful; he was also directly responsible for the building of one-hundred sixty fortresses (Hughes 1991: 120).

Vauban was a prolific writer, but none of his works addressed the manner in which he built permanent fortifications—instead they exclusively addressed siegecraft. In fact, Vauban never wrote a treatise on fortification design intended for publication. In 1706 he did write a fairly definitive work addressing permanent fortifications under the name *Traité de la Défense,* but it was never meant to be published. It was, however, circulated soon after in incomplete pirated versions. (Duffy 1985: 81; introduction in Vauban 1968: ix, x). *Traité de la Défense* was eventually published in 1829, but this came too late to directly influence the design of Fort San Cristóbal.

This situation meant that in the eighteenth century Vauban's ideas on fortification design were deduced through pirated manuscripts and the interpretation of the forts he built. Many authors attempted to understand his designs through mathematical and geometric abstractions, but these attempts were only approximations (Duffy 1985: 149). Examples of this approach to Vauban's work include Abel Swall's, *The New Method of Fortification* (1691), and Abbé Du Fay's *Manière de Fortifier Selon la Methode de Monsieur de Vauban* (1692).

Vauban's brilliance was most evident in his approach to siegecraft. His fortification work was considered to be mostly derivative of his contemporaries. Vauban did introduce new ideas and variations on established design that can be seen in Fort San Cristóbal, however. Specifically, Vauban is considered to have been the first military engineer to design his fortresses to accommodate the landscape. Eschewing the classically-inspired symmetry of fort design at the time, Vauban's fortresses undulate across the landscape and appear to hug the terrain due to very low lying works (Duffy 1985: 82-84; Hughes 1991: 123).

Vauban's ideas prevailed throughout most of Western Europe for the remainder of the eighteenth century (Duffy 1985: 163). Little changed in the design of fortifications until Marc-René, Marquis de Montalembert (1714-1800) began to advance his ideas in the 1760s that fortification design should be radically changed. The French war minister attempted to keep his ideas quiet, but not for long: in 1776 Montalembert published *La Fortification Perpendicular.* In it, he argued for a huge increase in the number of guns installed in a fortress. The guns were to be placed in the casemate rather than in the open air as had been done previously. Coastal defense positions were to take form in huge lighthouse towers that could deliver a tremendous blow in firepower to the enemy. The traditional angular, star-like design of the fort was to be replaced with straight curtain walls. Montalembert also argued for an increase in the number of detached forts (Duffy 1985: 157-160).

Montalembert's ideas, however, came too late to influence the design of Fort San Cristóbal. His fortification designs eventually prevailed in the nineteenth century, especially with the Germans (Hughes 1991: 131).

2.2.2 The founding of Puerto Rico and the construction of the first fortifications

Puerto Rico was revealed to the Old World by Columbus in 1493. An attempt was made to set up a permanent habitation, but its success was marred by many mutinies. The next explorer, Juan Ponce de León, arrived in 1508 with the drive to discover wealth in the New World (Van Middeldyk 1903: 9, 17-21). In that year, he had a fortified house made of tapia constructed in Caparra. In 1937, this house was extensively excavated and its design and materials were confirmed (Hostos 1948: 13).

Ponce de León was appointed governor of the new island and put in charge of enslaving the natives to work mining for gold. The treatment of the indigenous peoples lead to insurrections that were eventually put down. A series of laws and ordinances from the King directed that the natives be treated well, converted to Christianity and given land on which to farm. Although the Friars tried admirably to prevent the extermination of the indigenous peoples, by the end of the sixteenth century, few were left (Van Middeldyk 1903: 30-57).

In the sixteenth century, Puerto Rico was not very prosperous and was subject to depredation by pirates starting with the French in the 1530s. In 1533, the first of a series of primitive fortifications were put into place in San Juan (Van Middeldyk 1903: 86, 87, 96, 109). One of these forts became what is now known as La Fortaleza, which is still standing today. By the end of the century, there were approximately three hundred houses with a total population of a thousand on the island (Hostos 1948: 30).

In the later half of the sixteenth century, the English repeatedly ambushed, tricked, and attacked various Spanish outposts. Chief among the aggressors was Sir Francis Drake who was famous in England and infamous in Spain. As early as 1540 Drake sacked San Germán on the island of Puerto Rico resulting in the city's abandonment and the end of fortification work there (Iñiguez 1942: 2-3).

In 1585 Drake decimated the Spanish outposts in Santo Domingo, Cartegena, and Saint Augustine. King Phillip II of Spain reacted by directing the creation of a grand defense plan for the Caribbean. For this task he selected Fieldmaster Juan de Tejeda and an Italian military engineer by the name of Bautista Antonelli (Manuncy and Torres-Reyes 1973: 36).

Antonelli came from a long line of civil and military engineers and was made famous by his work on many forts in the Caribbean including el Morro in Havana, San Felipe de Barajas in Cartegena de Indias, San Juan de Ulúa in Veracruz, el Morro in Puerto Rico, and Portabelo (Iñiguez 1942: 4, 5). He first arrived in the new world in 1581 to begin formulating ideas for the defense of the West Indies. He returned in 1586 with Tejeda to begin preliminary fortifications of La Habana, Portobelo, and Cartegena (Calderón Quijano 1996: 169).

From these reconnaissance missions, Antonelli developed a master plan in 1587 for shore defenses of the Caribbean. Ten locations were chosen for fortifications: San Juan (Puerto Rico); Santo Domingo (Hispaniola); Santa Marta and Cartegena (Colombia); Nombre de Dios, Portobelo, the Chagres River and Panama (the Isthmus); Havana (Cuba), and St. Augustine (Florida). The official commission for these works came from King Phillip II in 1588 (Manuncy and Torres-Reyes 1973: 36). In 1589 Antonelli and Tejeda began directing the building of fortifications in Puerto Rico (e.g., El Morro), Santo Domingo, Habana, and Veracruz (Calderón Quijano 1996: 169).

Drake attacked Puerto Rico again in 1595, but was not successful; the new fortifications did their job as intended. In 1598, however, Sir George Clifford, the third earl of Cumberland attacked and prevailed. The English fleet left several months later, severely debilitated by hunger and sickness. El Morro was rebuilt in the next years, with the newly revitalized fortifications ready in 1609 (Manuncy and Torres-Reyes 1973: 43, 49-51).

The Dutch attacked Puerto Rico in 1625 and sacked the town of San Juan. They did not stay either. The Dutch attack in particular proved how vulnerable the defenses in the Spanish West Indies were. Major work began on rebuilding and fortifying El Morro and the new fort of San Cristóbal on the landward side of San Juan was started in 1634. The work was essentially complete by 1650. The new defenses proved to be formidable enough to hold off the aspirations of English and Dutch conquest of the island for a nearly a century (Manuncy and Torres-Reyes 1973: 60-61).

2.2.3 The eighteenth century fortification campaign for Fort San Cristóbal

By the middle of the eighteenth century, the fortifications completed in the 1600s were nearly a century old and showing signs of significant decay. In addition, the Spanish king, Charles III, realized that the defenses in Caribbean had to be upgraded—especially after the English captured Havana and Manila in 1762. Charles sought out an Irishman by the name of Alexander O'Reilly to create and implement a grand vision for improved defenses on Puerto Rico. O'Reilly first arrived in Puerto Rico in 1765 and met Colonel Thomas O'Daly, a field engineer who was also an Irishman. O'Reilly and O'Daly were to create a plan for fortifications at El Morro and San Cristóbal that would take nearly twenty-five years to complete (Manuncy and Torres-Reyes 1973: 65-67).

O'Reilly, a veteran of the Spanish army, had been previously recruited in 1763 to reform the defenses in Habana and was appointed to the title of Inspector-General of Cuba. He only stayed in Puerto Rico for forty-five days, leaving the engineering and construction work up to O'Daly. As with O'Reilly, O'Daly had also enlisted in the Spanish army as a youth and rose through the ranks of the Corps of Engineers. Upon O'Reilly's arrival, O'Daly was appointed Chief of Engineers at San Juan (National Park Service 1996: 59; Calderón Quijano 1996: 234).

O'Daly made the first designs for the modernization of Fort San Cristóbal. A copy of a map dated 1678 gives an indication of what the site may have looked like before O'Daly's changes were implemented (Illustration 2.2). Construction began in 1766 with assistance from engineer Pablo Castello and architects Diego Ramos and Antonio Sein. From 1766 to 1769, work consisted of analyzing the strength and stability of the existing fortifications, modifying existing structures, adding parapets and merlons to newly constructed walls, excavating a moat, and adding underground galleries. Several earlier structures were demolished including the powder magazine. During this phase of construction, O'Daly fell ill, but continued to direct the work from his bed (Torres-Reyes 1965: 36, 38, 42-43).

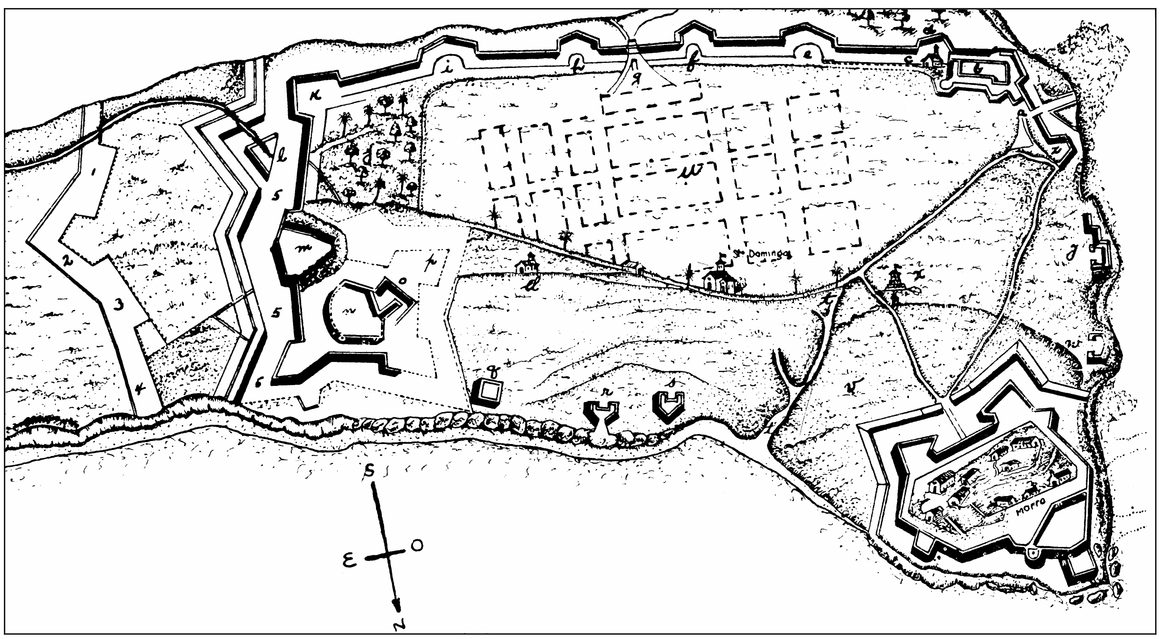

Illustration 2.2: 1678 map of San Juan (north is down). Fort San Cristóbal is on the middle left side (Hostos 1948: 498).

Work ceased briefly after an accident in January of 1769 when a wall collapsed due to a weak clay/lime mortar. Normally clay/lime mortars are acceptable as long as they are kept dry; in this instance, water was infiltrating the wall, negating any strength imparted by the mortar. This event prompted an overview of how mortars were being used and mixed in order to prevent a similar catastrophe (Manuncy and Torres-Reyes 1973: 54-57).

The second phase of construction lasted from 1769 to 1773. A copy of a site plan from 1771 gives a snapshot of the status of the works during this time (Illustration 2.3). Due to the earlier accident, much effort was spent identifying weaknesses and faults in the existing fortifications and correcting the problems. The engineer Juan Francisco Mestre headed up most of these efforts. This phase of construction created the Cavalier, the San Carlos Revelin, La Trinidad, a new redoubt constructed behind the counterscarp of the North Bastion, the curtain of the Santiago Gate (including El Príncipe), the North Bastion, the Santiago Bastion, and the main moat. Excavated material was used to build a glacis on the eastern half of the site (Torres-Reyes 1965: 61, 64-71, 73, 78).

From 1773 to 1785, the third stage of construction at Fort San Cristóbal took place. This included construction of the cisterns and Officers' Quarters. Work continued on La Trinidad, the entrance ramp, Santa Teresa, La Princesa, and El Abanico. Nine vaults were added to the North Casemates. By 1785, most construction ceased, but work continued into the 1790s on enhancing La Princesa (Manuncy and Torres-Reyes 1973: 88, 89, 92, 96, 102, 110, 113). A copy of an artist's rendering shows how Fort San Cristóbal probably looked in the nineteenth century (Illustration 2.4).

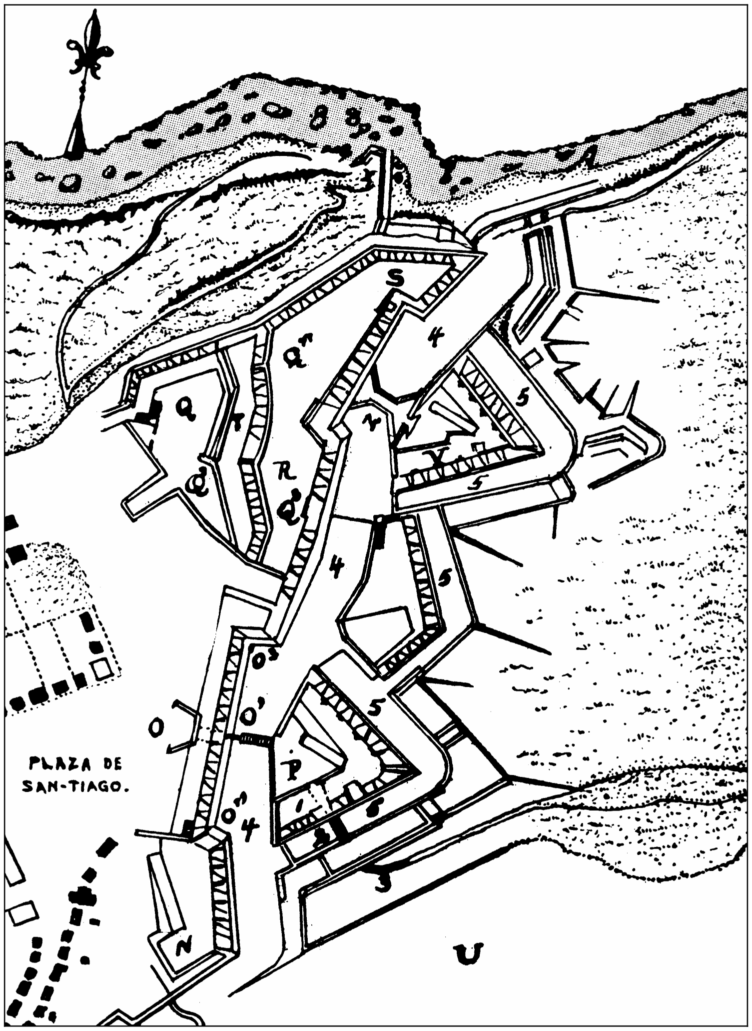

Illustration 2.3: Plan of Fort San Cristóbal in 1771 (Hostos 1948: 501).

Key:

Q & Q’: Plaza de Armas
T: Troops Quarters or Cavalier
S: North Bastion
Q”: Terreplein
R: South Bastion
4 & 5: Ditch
O: Santiago Gate (demolished)
N: Santiago Bastion (demolished)
V: San Carlos Revelin
P: Santiago Revelin (demolished)
3: Fort of the Point

(La Trinidad Counterguard is directly to the south of San Carlos)

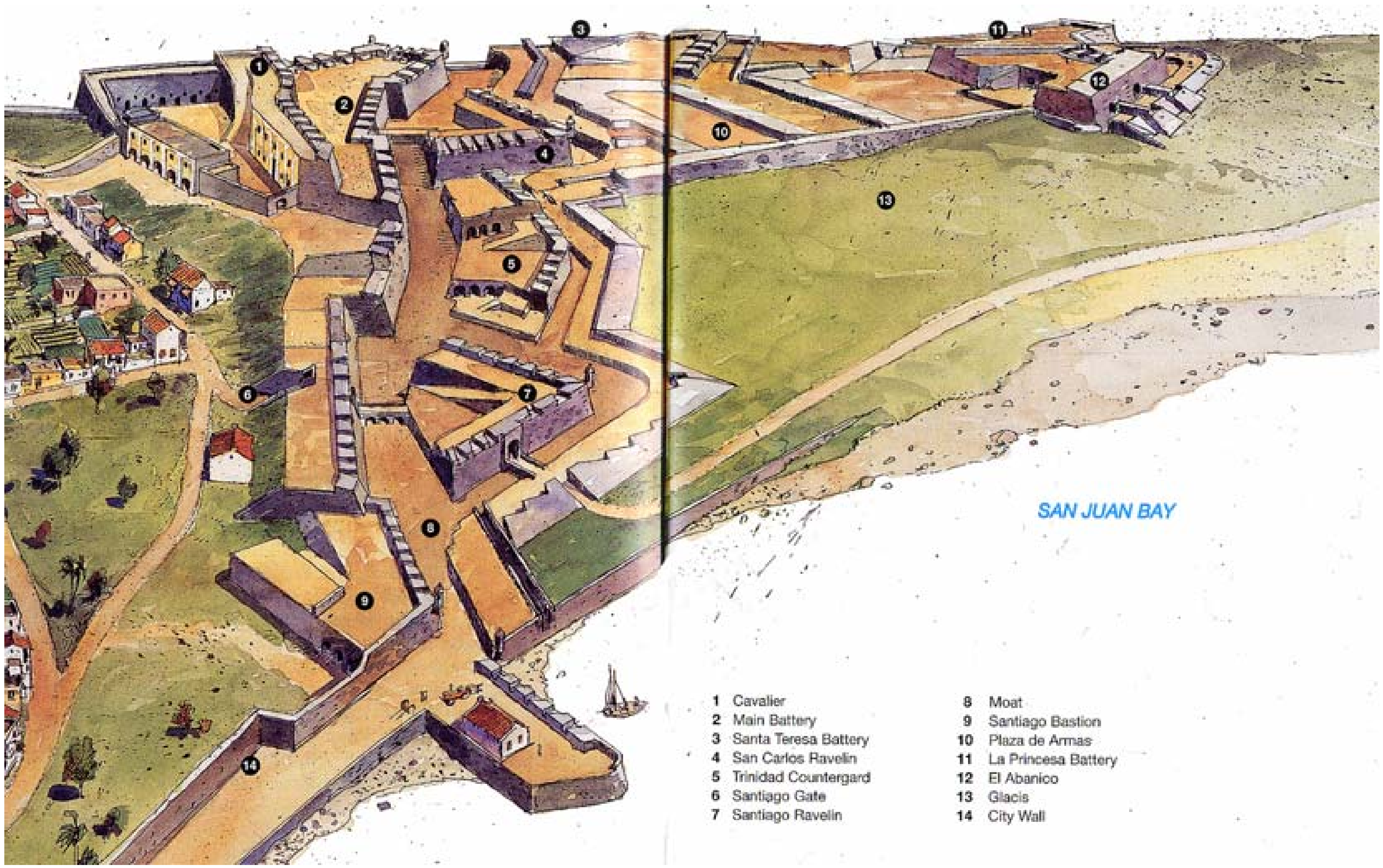

Illustration 2.4: Plan of Fort San Cristóbal in the nineteenth century. The Santiago Revelin, Santiago Bastion, and Santiago Gate have been demolished (National Park Service 1996: 63).

2.2.4 Nineteenth and twentieth centuries

After the completion of Fort San Cristóbal in the 1790s, most modifications were relatively minimal until the onset of the Spanish American War. In the early nineteenth century, the main ramp was stuccoed and one of the barrel vaults was filled with masonry, the south parapet by the South Gate was raised in order to prevent soldiers from escaping, a small guardhouse was built by the North Casemates, and a lightning tower was added to San Carlos (Berkowitz et al. 1991: 10-19, 199-203, 337-355).

In the 1890s, in preparation for the Spanish American War and to let the city of San Juan expand, many changes were made to the fortifications. Substantial portions of the fortifications in the south of the site were demolished, such as the Santiago Bastion, and the Santiago Gate. Gun emplacements were added to the North Casemates and North Bastion and a new structure replaced much of St. Teresa in the north. After the Spanish American War, the American Army occupied the site and made modifications to the North Casemates and Officers' Quarters in order to accommodate American troops (Berkowitz et al. 1991: 266-274).

From 1938 to 1940, the Army Corps of Engineers and the Works Progress Administration embarked on an extensive repair and renovation campaign. The triangular-shaped stone veneer that has been applied to embrasures of the North Bastion, Curtain, and South Bastion are from this period. Major repair work was done on the Fort of the Point to prevent the undercutting of this structure by the ocean. In 1940, the Army added a new concrete structure in the middle of the main moat, partially obscuring the lower walls of the North Bastion and La Trinidad (Berkowitz et al. 1991: 251-275).

Beginning in 1959 with an experimental restoration of El Abanico, the National Park service became intimately involved with the site. In the 1960s, the National Park Service restored much of the main fort including the North Casemates, Officers' Quarters, and Troops' Quarters. The outworks were left relatively untouched except for the upper portion of El Abanico (Berkowitz et al. 1991: 251-275).

2.3 Building description and chronology

2.3.1 Building selection

Only the chronology of those buildings or structures of Fort San Cristóbal where a mortar sample has been obtained and analyzed will be presented. Each structure heading identifies the name of the structure, its building number used for sample identification, and probable construction dates followed by modification dates. The structures are presented in order of their sample identification number. They are: the Main Entrance Ramp; South Gate; North Bastion, Curtain, and South Bastion; Fort of the Point; San Carlos; La Trinidad, including the Lightning Tower; El Abanico; and the vaulted bunker and gun emplacement from St. Teresa. A map of the locations of these structures is provided (see Appendix A).

2.3.2 Entrance ramp to main gate (ID# 01)

Built ca. 1773 to 1783; modified 1829

The entrance ramp to the main gate is located at the northwest corner of the site. The fourteen-foot wide ramp starts in a southeasterly direction and then curves through ninety degrees and heads in a northeast direction. From its beginning to the point at which it reaches the main entrance, the ramp angles upward, eventually gaining a height of twenty feet. The ramp is constructed of ashlar sandstone and hand molded brick. Two elliptical barrel vaults are located under the main section of the ramp (Berkowitz et al. 1991: 1-2).

The first evidence of the ramp in its current configuration appears in a 1783 drawing by Mestre. The ramp itself was first proposed in 1769 in a straight, rather than curved form in a slightly different location. The ramp also appeared in a 1773 plan by O'Daly with similar attributes (Berkowitz et al. 1991: 7). This information suggests a construction date between 1773 and 1783.

Many modifications to the ramp, especially in its lower section, occurred over the years. The ramp was repaired in 1829. In 1861, it appears that the ramp was first stuccoed. During this year the western most arch was filled with masonry and a window and door were added. The floor of the ramp was resurfaced in 1901. In the late 1930s, the lower curved section of the ramp was substantially altered by realignment in order to accommodate widening of the street in front of the fort. The upper section of the ramp was not altered. In 1964, the east arch of the ramp was partially infilled with masonry and a gate was added (Berkowitz et al. 1991: 10, 11, 13, 18, 19).

2.3.3 South Gate (ID# 08)

Built ca. 1773-1783; modified 1808, possibly 1849-1858, 1898, 1969-70.

The South Gate is located at the southern end of the Plaza de Armas at the end of the Troops' Quarters. It consists of two stone posts and a brick and wood lintel. The posts are of ashlar sandstone with brick spacers. Some stucco remains which appears to have originally covered the whole of the structure.

The ramp was probably constructed between 1773 and 1783 when it first appeared in Mestre's plans. From 1808-1817 the height of the southern part of the west parapet wall was increased. This change probably affected the gate, but its exact extent is not known. Sometime between 1849-1858 the gate may have been raised in height by two feet by filling in the area at its base and extending the posts. Around 1898, one side of the gate opening was filled with masonry so that a smaller door could be set within the posts. The gate was restored by the National Park Service from 1968 to 1970. Work consisted of removing the earlier masonry infill and refitting a pair of large wooden doors (Berkowitz et al. 1991: 199-203).

2.3.4 North Bastion, Curtain, and South Bastion (ID# 10)

Built 1766 to 1773; modified 1789, 1808, 1859, 1890s, 1921-22, 1938-1945, 1960s

The north bastion, curtain, and south bastion form a contiguous north south line abutting the Caballero and Troops' Quarters on the west. Historically, the north bastion was known by its Spanish name of *Baluarte del Norte* or *Baluarte Plano del Norte.* The curtain, which joins the North and South Bastions, was called *Baluarte Medio* or *La Cortina*, and the south bastion was called *Baluarte Plano* or *Baluarte Plano del Sur* (Berkowitz et al. 1991: 249). All three elements will simply be referred to collectively as the structure unless characteristics are particular to individual portions thereof.

This structure is filled with a mixture of rubble masonry and mortar and possibly earth. In Puerto Rico, this mixture was referred to as *mampostería*, a term which apparently has more general and slightly different connotations in other Spanish-speaking areas (Manuncy and Torres-Reyes 1973: 86). The walls are of ashlar stone, brick, and stucco over *mampostería*. The top of the structure has a large terreplein and a series of merlons and embrasures which were used for firing positions. The merlons are formed from rubble fill construction covered with stucco and trimmed with ashlar or brick. Banquettes near each embrasure are constructed of brick and rubble stone (Berkowitz et al. 1991: 249, 257).

An earlier version of this structure was begun as a wall in 1634. In 1749, buttresses were added as reinforcement to the wall. Before O'Daly's work commenced in 1766, work on this wall and the construction of a north bastion were frequently interrupted with structural issues. Pre-1766 masonry is visible today in the midsection of the curtain. Other than this older area, most of what is currently visible dates from O'Daly's work from 1766 to 1773. The only modification before the nineteenth century occurred in 1789. In that year possible earthquake damage necessitated repairs of the parapets of the North Bastion (Berkowitz et al. 1991: 259, 266).

The structure remained relatively intact throughout the nineteenth century. In 1808, the parapets were coated with a mortar consisting of rough aggregate (it is not known if this was the first time such an event occurred). In 1859, it is likely that the embrasures on the landward side of the structure were closed or changed, contemporaneous with changes to El Morro. During the Spanish-American War a concrete wall was built on the terreplein of the north battery and two semicircular gun emplacements were added (Berkowitz et al. 1991: 266, 269, 274).

Most changes occurred in the twentieth century. The walls of the entire structure were re-stuccoed from 1921-22. In 1938-1940, one of the largest visual changes was effected by the Army Corps of Engineers by installing a masonry veneer of polygonal slabs to the parapets. This later work exclusively used Portland cement for patching and repairs. During World War II, a watch tower of reinforced concrete was constructed on the North Bastion and the original sentry box was extensively repaired. In 1940, a large concrete structure was added in the moat and attached to the lower walls of the North and South Bastions. After the National Park Service acquired the property in 1960, extensive repairs were made to the terreplein and drainage systems of the structure. Earth that had previously been piled on top of the terreplein was removed (Berkowitz et al. 1991: 251, 270, 274-275).

2.3.5 Fort of the Point (ID# 11)

Walls built between 1635 and 1678, sentry box built between 1678 and 1765 ; modified ca. 1880-1928, 1938, 1975.

Fort of the Point or *Fuerte del Espigón* is more commonly known by the colloquial name *La Garita del Diablo* (the Garrison of the Devil) for its supposed propensity to make Spanish soldiers disappear in the night. It is the most northern and oldest of the fortifications at Fort San Cristóbal, located on the sea shore directly in front of the North Bastion. It consists of a *garita* (sentry box) and two short walls in a triangle shaped configuration. The walls are made of ashlar and stone rubble while the sentry box is a combination of these elements plus brick.

The earliest surviving records indicate that a fortification existed at the present location of the Fort of the Point as early as 1634 to 1644. The first map that shows the existing structure is from 1678. The *garita* is missing from the map and probably was constructed sometime before O'Daly's changes (Berkowitz et al. 1991: 281-284).

No changes of any major significance appeared to have occurred to the Fort of the Point for most of the nineteenth century according to available documentation. As a result, the *garita* was in serious disrepair by the 1880s. Extensive repair work was done on the *garita* between 1880 and 1928 which included a new coat of stucco. In 1938, the foundation, long eroded by the ocean, was finally repaired by the W.P.A. with concrete masonry. Portions of the *garita* were also repointed, most likely with Portland cement. While the 1938 repairs to the foundation greatly improved the structural stability of the fortification, by the 1950s, an undercut has appeared again which was repaired in 1975 (Berkowitz et al. 1991: 286-291, 294).

2.3.6 San Carlos Revelin and the Lightning Tower (ID# 13)

Revelin built ca. 1766-1770, lightning tower built ca. 1818;
modified 1897, 1938-1940, 1963.

The San Carlos Revelin is located directly to the east of the main moat between St. Teresa to the north and La Trinidad to the south. It is a triangular in shape with a salient angle of sixty-five degrees. A *garita* is located at the origin of this angle and faces more or less southeastward. San Carlos is built of coursed ashlar and rubble coated with stucco finished scored to look like ashlar. Sections of the parapets have had several coats of cement applied. The interior of the structure is earth or *mampostería* or a combination of the two. Original stucco from about 1773 is likely to still exist on the west façade of the north parapet. According to the 1991 historic structure report, original stucco was defined as that which had original faux decorative scoring marks (Berkowitz et al. 1991: 337-341).

San Carlos was constructed from 1766 to about 1770 (343-348). In 1818, plans were drawn up for the masonry lightning tower that was constructed on the edge of the south terreplein facing the South Bastion (Illustration 2.5). Three embrasures on the north parapet were filled in during 1897 with rubble and concrete. Gun emplacements were added to the south parapet and a revetment to strengthen the wall were added in the same year (Berkowitz et al. 1991: 337, 340-341, 352, 355).

The W.P.A. made extensive repairs to San Carlos from 1938 to 1940. Earth that had been piled on top of the merlons was removed and the merlons were repaired. A stone veneer was probably added during this time. The *garita* was replaced c. 1939-1940. The addition of the concrete bunker in the moat between the North and South Bastions and San Carlos in 1940 covered much of the lower section of the west side of San Carlos and obliterated original access stairs. In 1963, the walls of the structure were repaired with cement patches by the Army Corps. of Engineers (Berkowitz et al. 1991: 355-357, 358).

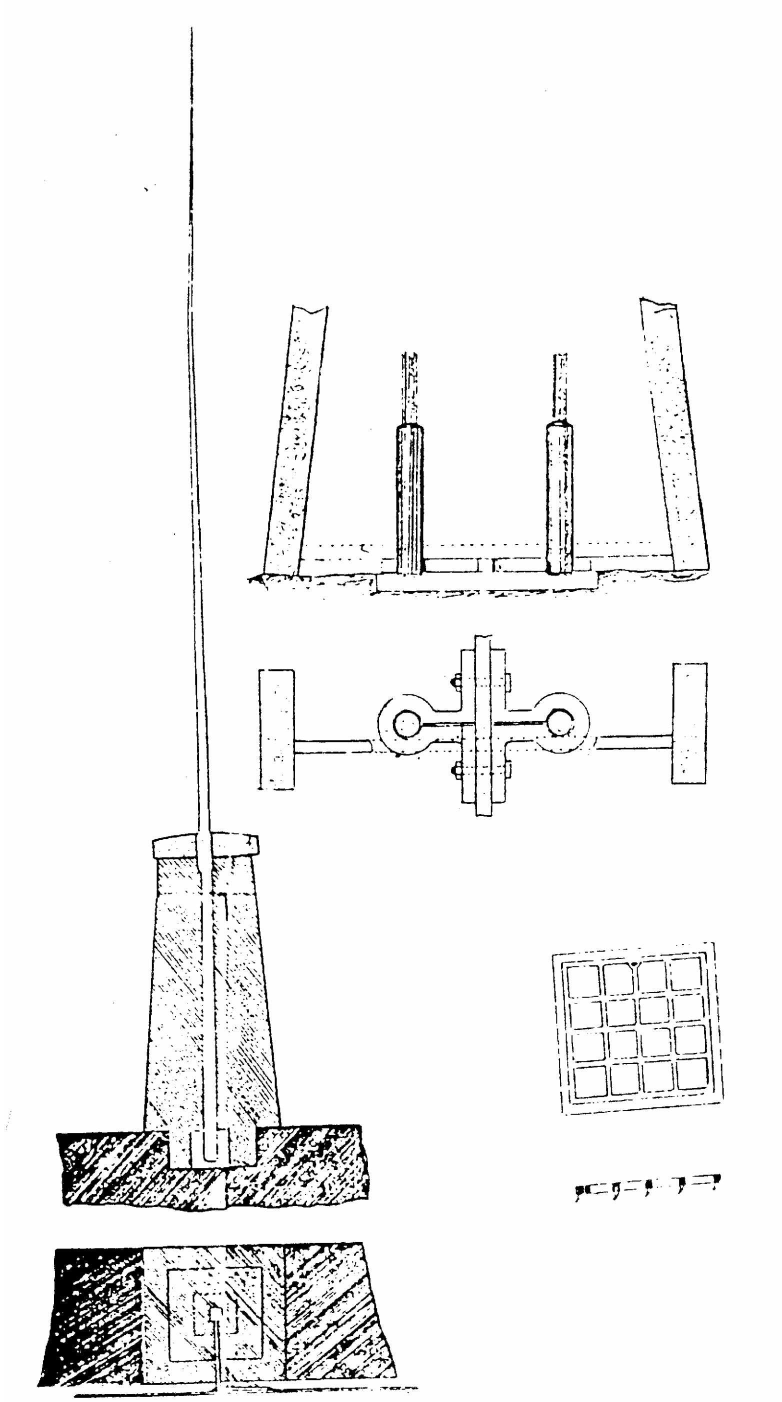

Illustration 2.5: Detail of 1818 drawings of the lightning tower and rod installed on San Carlos (Berkowitz et al. 1991: 353).

2.3.7 La Trinidad (ID# 14)

Built ca. 1766-1783 (most work before 1774);

modified ca. 1792-1861 (one event), 1892,1960s.

La Trinidad counterguard is located directly to the south of San Carlos on the east side across the main moat from the South Bastion. It was constructed in four levels to accommodate the terrain and is irregular in plan. Four embrasures facing east and a terreplein define the top level. The third level is comprised primarily of a sod terreplein with two embrasures facing east. The second level has a paved terreplein with three embrasures facing southeast. Remnants of the base level consist of a partial esplanade and banquette. A large amount of what may be original stucco remains at the northeast corner and the parapet walls and embrasure sides. Two stucco campaigns are evident: one that used raised joints and another one that used scored and penciled joints to create faux ashlar (Berkowitz et al. 1991: 362-368).

As with the other fortifications, La Trinidad is constructed of a combination of coursed ashlar, brick, and *mampostería* covered in stucco. The interior is likely to be a combination of earth and *mampostería.*

Construction of La Trinidad occurred between 1766 and 1783. The majority of the work appears to have occurred before 1774, however. A fourth embrasure on the top level was added between 1792 and 1861. In 1892, work to demolish the Santiago Revelin appeared to have partially damaged La Trinidad and primarily affected the lower levels. In the 1960s, soil and vegetation that covered the structure were removed and damaged sections of La Trinidad were repaired (Berkowitz et al. 1991: 371, 372, 374).

2.3.8 El Abanico (ID# 16)

Built 1779-1783; modified ca. 1792-1861 (one event), 1892,1960s.

El Abanico ("the fan"), is an outwork located on the far east of the site south of La Princesa. It is an equilateral triangle in overall plan with one point facing directly east. It is surrounded by a moat and access is via a bridge from the west. The northeast and southeast facing walls form a parapet and terreplein. The terreplein of the fortification is accessed by one of two ramps found in a middle indent in the west side of the structure. El Abanico is made of coursed ashlar, brick, and *mampostería* covered with stucco.

El Abanico was constructed between 1779 and 1783. Originally made of earth and fagot (bundles of sticks), the construction material was eventually changed to masonry. Although it was reported that graffiti with the date of 1783 was found on the fort in 1959, it has not been located since. According to the historic structure report of 1991, the entire fort was stuccoed between 1824 and 1832, making the 1783 date dubious. This would also mean that the graffiti of a sailing ship located on the north wall of the terreplein wall probably dates to the period between 1824 and 1832 (Berkowitz et al. 1991: 434, 427).

In 1896, changes to El Abanico occurred contemporaneously with work on La Princesa. Specifically, part of the scarp and counterscarp walls of the El Abanico were converted into a cistern. The work involved the application of hydraulic cements. In 1901-02, the U.S. Army made small changes to the access path for the fort. In 1938 to 1940, repairs to El Abanico were made consisting of the repair of firing steps, replacing brick trim, and resurfacing steps and platforms on the terreplein. The surface of the terreplein was also paved to prevent water leakage into underground rooms and tunnels (Berkowitz et al. 1991: 437, 439).

In 1959, the National Park Service embarked on campaign to test various restoration methodologies on the fort. Vegetation was removed from around the fort to expose masonry. The stucco and structural cracks were then repaired. Red colored mortar was used around the embrasure openings and walls were painted red and buff. It appears that this work was confined to the upper level of the fort, in areas where samples were not taken. In 1982, the drainage system was excavated (Berkowitz et al. 1991: 440, 441).

2.3.9 Vaulted bunker and gun emplacement from St. Teresa (ID# 20)

Built 1897; no major modifications.

The St. Teresa Battery is located directly to the east of the North Bastion and northeast from San Carlos. It is on the north edge of the glacis. St. Teresa has existed in various forms since the eighteenth century; this review, however, will only focus on the vaulted bunker and gun emplacement that were built in 1897.

Compared with the other works of St. Teresa, the connected vaulted bunker and rifle mount are located nearest to the ocean. The vaulted bunker is a short and small structure with an arched roof and a single doorway. The date of “1897,” molded from mortar, is above the door. A circular gun emplacement built at the same time of the bunker is located about ten feet to the east. The vaulted bunker is most likely constructed of concrete coated with stucco, but the gun emplacement appears to have used rubble stone construction similar to that used in order parts of the fort; the same beige-colored mortar is used for bedding material. Stucco has been applied on the surface.

The historic structure report from 1991 indicates that the work for the vaulted bunker and gun emplacement began in 1897 and used concrete for its construction. Few, if any, changes appear to have occurred to these two structures from their construction to the present time (Berkowitz et al. 1991: 327-330).

2.3.10 Casemate number three of the North Casemates (ID# 21)

Area of sample location built ca. 1774 to 1785;

modified 1830, many changes from 1898 to 1975.

The North Casemates consist of a one room deep, one to two-storey high structure located directly to the north of the Plaza de Armas. Its north side faces the ocean. A one-storey loggia fronts the plaza side of the casemates. Each casemate has been assigned a number by the National Park service starting at the far west side (casemate one) and proceeding to the far east side (casemate eleven). The casemates consist of large vaulted rooms with window embrasures facing north. The entire structure is load bearing masonry. The casemates were also the original location for the kitchen (casemate two) and latrines (casemate one). Only the chronology that affects the embrasure of casement number three, the area from which the sample was taken, will be discussed.

Work on the North Casemates began with the construction of the powder magazines (casemates ten and eleven) from 1768 to 1771. Construction of casemates one to nine occurred between 1774 and 1785. Although their initial use was possibly for cannon positions, casemates three to nine were used to house soldiers beginning in the earlier part of the nineteenth century (Berkowitz et al. 1991: 25, 30, 49).

In 1830, the interior and exterior of the casemates were replastered and possibly whitewashed. Sometime around 1868, the interior of casemate three was bisected by an east-west partition. Between 1898 and 1960 when the U.S. Army was administering the fort, casemates three through nine were restored to their original pass-through configuration without doors. By 1901, casemate three had been turned into a dining room. The interior and exterior of the casemates were whitewashed and woodwork was painted in 1900. Cement floors were also poured over the original lime mortar floors during this time. The terreplein over casemates three and four was repaired in 1908. In 1935, casemates three through five were changed back into troop quarters (Berkowitz et al. 1991: 42, 44, 51, 53, 55, 56).

A 1940 plan showed a mortar bathtub for the first time in the north window embrasure of casemate three (the general area from which samples for this structure was taken). The historic structure report from 1991 theorizes that this bathtub was added between 1935 and 1940 (Berkowitz et al. 1991: 58). Extant evidence, however, seems to point to a construction sometime in the middle to late eighteenth century when casemate three was used for troops' quarters. The technology used to make the bathtub would have been archaic in the late 1930s. The bathtub is coated with a brick dust mortar and has no metal fittings, nor any sign that there were ever any metal fittings. In addition, the area underneath a small opening inside the bathtub exhibits signs of significant loss coincident with flowing water used to fill the tub. It is highly unlikely that this much mortar loss (especially from a hydraulic mortar) would have occurred with less than five years of use.

After the National Park Service took over the operations of Fort San Cristóbal in 1960, casemate three was turned into a "museum laboratory". In 1975, the interior of the casemates were all painted white. A partition wall was built in casemate three sometime after 1961 (Berkowitz et al. 1991: 61).

2.4 Summary

The design of Fort San Cristóbal has very close ties with Europe and especially France. Its design is derivative of Vauban's work who in turn based his designs on earlier Italian Renaissance precedents. The fort is representative of the last gasp of traditional fortification design before the radical ideas of Montalembert were adopted in the nineteenth century.

Most of the fortifications at Fort San Cristóbal were built before the nineteenth century. In particular, there were two phases of construction: the main fort which was essentially complete by 1773, and the outworks which were mostly completed by 1783. The information presented on the chronology of the buildings from which samples were taken help to provide important context to the later interpretation of these samples.

CHAPTER 3: SPANISH MORTAR TECHNOLOGY

3.1 Introduction

Few, if any, of the military fortification treatises up to the nineteenth century make specific mention of the use and technology of mortars. Many architectural treatises that address mortar technology were available to the military engineers and masons in the Spanish New World (Alba 1995: 6). These architectural treatises provide valuable clues to the use of mortars and their technology that are absent from works on military fortification.

The most important Spanish edition treatises that are represented in trade invoices, wills, and New World library inventories of the sixteenth, seventeenth, and eighteenth centuries include *Los Diez Libros de Arquitectura* (The Ten Books of Architecture) by Alberti, *Diez Libros de Arquitectura* (The Ten Books of Architecture) by Vitruvius, *Arquitectura* by San Nicolas, and *De Arquitectura Anno* by Palladio (Alba 1995: 6). Although there were many more architectural treatises available during this time, such as those by Serlio and Diego, the aforementioned works are the most important because they specifically address mortar technology.

Two architectural treatises written in the New World are also important to this inquiry. They are the anonymous work titled *Arquitectura Mechanica Conforme la Practica de esta Cuidad de México* (Architectural Practice in Mexico City) published between 1783 and 1810 and *Arte de Albanileria* (The Art of Masonry and Plaster Work) by Villanueva published in 1827. There are a few other treatises written in the New

World, but as with the European treatises, they do not specifically address mortar technology.

It must be remembered that until well into the twentieth century, the techniques and traditions of the trades were orally passed from master to apprentice. Many of these people were illiterate. Therefore, any treatises on the preparation and formulations of mortar were likely to have been reflections on current practice rather than highly influential in their own right. The paucity of treatises on the subjects of mortar use and formulation before the nineteenth century—especially in the Spanish New World—makes it difficult to ascribe with certainty on current practices of the day.

This condition does not, however, negate the value of the treatises. They still offer highly valuable insight into the world of the past and are the only record of tradition and craft that has long since left the cultural memory of the current trades.

This literature review will begin by covering the major European architectural treatises through the Renaissance. An overview of their continued influence into the eighteenth century will then be presented followed by treatises written in the New World. Finally, all of the information will be synthesized into a hypothetical whole in order to understand what the mason in the Spanish New World would have known.

3.2 General European Renaissance foundations

3.2.1 Vitruvius

The earliest known treatise that describes mortar formulations and use is the *Ten Books on Architecture* by Marcus Vitruvius. The exact date of its writing is not known for certain, although it is generally assumed to have occurred between 31 BC – 14 AD during the reign of the Roman emperor Augustus (Albert Howard in preface to Vitruvius 1960: iv). The work of Vitruvius was nearly forgotten after the fall of the Roman Empire. It was first published in Rome in 1485 with many subsequent reprints and translations (Meeks 1949: 55).

Vitruvius recommends that sand used for aggregate be clean; the sand, thrown upon a white sheet, should not leave a mark. Sharp pit sand should be used for all construction except for renders. Vitruvius notes that pit sand dries quickly—a trait no doubt useful in the interior of walls. River sand should be used instead of pit sand in order to prevent excessive cracking from premature drying. Sea sand is not recommended at all because of its tendency to effloresce (Vitruvius 1960: 44, 45). It is likely that less cracking was evident from renders prepared from the generally well-graded, rounded and spherical river sand which required less water in its preparation as well. Issues with efflorescence were in no doubt due to sea salts.

Vitruvius was careful in describing the preparation and slaking of lime. The limestone selected for calcining was to be very white in color. The best lime, slaked for a long period of time and free of "crude bits," was reserved for stucco work. To test the lime for its readiness, a hoe was inserted into the slaked lime; if, when withdrawn, the hoe had lime adhered to it, the lime was ready to use. Straight lime and sand mortar was recommended for the bedding and render mortar of most walls. (Vitruvius 1960: 45, 51, 204, 205).

Pounded brick and tile were also mentioned for use in place of, or in addition to sand. These materials were recommended for use in mortars that would be exposed to damp locations, such as foundations or baths. In these cases, brick or tile was to be used in place of sand (Vitruvius 1960: 159, 203, 208). It can be assumed that the brick and tile provided a component of hydraulicity to the mortar. Vitruvius notes that when brick was added to a lime/sand mortar mix it would “make your mortar of a better composition to use” (Vitruvius 1960: 45). Vitruvius also wrote about the properties of a special kind of tufa found at Mt. Vesuvius. The addition of this pozzolana would enable mortars to set under water (Vitruvius 1960: 47).

In general, lime to aggregate ratios were in the range of one to three or two to five. Vitruvius advised that the mortar should be thoroughly mixed before use; an example is given whereby a gang of men vigorously work the mixture with wooden beetles (a heavy mallet with a large wooden head). Mixtures of one part of lime to three parts of broken stone and one part of lime to three parts pounded tile were used in creating a tiled floor; the mixture is also varied in the proportions of two to five. For stucco, three coats of mortar are recommended followed by a topping of marble dust—gypsum was not advised. Lastly, Vitruvius mentioned a kind of lime concrete made of gravel, lime, and ashes for use in leveling a floor (Vitruvius 1960: 202, 203, 206, 208, 210).

3.2.2 Leon Battista Alberti

Leon Battista Alberti (1404-1472) wrote the architectural treatise *De re Aedificatoria* out of an inspiration to clarify the earlier work of Vitruvius. Alberti completed his Latin manuscript in 1452, but it wasn’t published until 1485 in Florence. A 1512 edition was published in France followed by an Italian translation in 1546 and a

Spanish translation in 1582. An English translation was published in 1726 (Publisher's note in Alberti 1986).

As expected, Alberti's work is derivative of Vitruvius. The three types of sand, pit, river, and sea sand, were mentioned with the recommendation that pit sand was generally superior. The best sand was sharp and angular while white colored sand was to be avoided. According to Alberti and following Vitruvius, pit sand was more prone to cracking and should therefore only be used in non-render applications. For a render, river sand gave better results. Alberti wrote that in some places where lime was not available, clays were used as mortar. He made no specific mention of the use of clays in extending lime mortars, however (Alberti 1986: 37, 38).

Only limestone that lost at least one-third of its weight upon calcining was to be used. Colored limestone—especially that which was earthy—was to be avoided; white limestone gave the best results. This recommendation is supported by the fact that whiter limestone has a higher calcium carbonate content and therefore makes a better mortar. Alberti wrote that limestone should be taken from a moist quarry rather than a dry one, but in some cases limestone rocks taken from a river would be quite acceptable. In both cases, little in the way of an explanation of the recommendation is offered. Alternately, lime calcined from seashells, as was done in Vannes, France, also produced good results. Lime was to be slaked for a very long period of time—the more time the better (Alberti refers to the process as "fermentation"). One example was given of a five-hundred year old slaked lime that gave quite good results when used for construction (Alberti 1986: 35, 36).

Only lime that came from the kiln in whole lumps instead of broken pieces was to be slaked. When slaked, good lime produced "a strong thick smoke high into the air." Alberti suggested that lime which produces a weak binder should be mixed with less sand; conversely a strong binder required a greater amount of sand. For wall construction a ratio of one part lime to two parts sand was suggested, but the ratios that Vitruvius selected of one part lime to three parts pit sand and one part lime to two parts of river sand were also acceptable. In the situation where the mortar was to be more liquid in consistency, Alberti described the use of a sieve to remove larger aggregates. The addition of gravel and broken fragments of stone produced a stiffer mortar (Alberti 1986: 45).

Alberti also addresses gypsum which he refers to as plaster of Paris. He indicates that it sets much quicker than lime, but it is a poor choice in any place exposed to cold weather or moisture (Alberti 1986: 36, 54). Alberti also noted that the addition of powdered brick or tile to a mortar "will be much more tenacious" (Alberti 1986: 45). Later in the treatise Alberti specifically says that brick or tile added to a mortar "will be the less injured by the wet"—a reference to the reactive silicates present in an hydraulic mortar (Alberti 1986: 54).

Alberti made specific recommendations regarding the stiffness of mortar and its compatibility with various masonry materials. For example, he wrote that stone "agrees not ill with river-sand," but it "delights in pit-sand." Small stones were to be cemented in place with a thick, lean mortar while most other stone agreed more favorably with a "fat" mix. Very large stones were to be laid with a "very soft fluid mortar, so that it rather seems design'd to lubricate and make the bed they are laid upon slippery…[so that] they may be easy to move with the hand." Alberti wrote that a mortar of this consistency would give a desirable, pillow-like cushioning to the stones. When work was to be halted, the top of wall was covered with straw so that "the wind and sun may not exhaust the strength of the cement and make it rather useless." Alberti stressed that the newly laid masonry should be well watered. When the work was resumed, clean water was poured over the work to thoroughly soak the masonry (Alberti 1986: 52, 53).

There are several places where Alberti makes reference to "slime" to bind building stone which is probably referring to clay. He describes how a building can be built of stone or brick cemented with this slime which should then be "cloathed with a crust of mortar [i.e., lime based] outside and plaster of Paris on the inside." (53, 54).

Alberti is unique in his specific recommendations for building a battlement wall for use in fortifications. While he makes little mention of mortar formulas in this application, he does describe in great detail how the wall is to be built with a rubble stone interior cemented with lime mortar or filled with rammed earth and straw. Alberti mentions that soft stone, such as pumice, is well suited for the interior voids within such walls if the exterior is faced in harder stone (Alberti 1986: 73, 74).

3.2.3 Andrea Palladio

In 1570, Palladio published his *Four Books of Architecture* in Venice, Italy. Arguably one of the most influential architects of all time, Palladio is known more for introducing the world to a revival of Roman classicism than for his instructions on building technology. His work, however, does contain specific references to the preparation and use of mortars that are relevant to this general inquiry. Editions of *Four*

Books of Architecture were republished in 1625 in Spain, in 1682 in Amsterdam, and in London in 1736. *Four Books of Architecture* was translated into English in 1738 (Meeks 1949: 57).

From Vitruvius, Palladio knew about general recommendations regarding pit, river, and sea sand, and like Vitruvius, recommends pit sand over the other two except for use in renders. Palladio does, however, add new information regarding sands. Curiously, all white pit sand was considered less desirable and in regards to sea sand, the best was black in color and shiny like glass (Palladio 1965: 3, 4). This recommendation is indicative of aggregates that are low in quartz and from today's perspective would not usually be desirable.

The best river sand was to be found in rapid streams and under water falls because the action of the water removed the fines and dirt. Sands with large grains, nearest to the shore, were considered to be best. Palladio knew that pit sand was typically well graded, and for that reason recommended it, but like Vitruvius noted that it was prone to cracking when used in anything other than walls and vaults. For renders, river sand was considered superior. In all cases weathered sand was to be avoided (Palladio 1965: 4).

Palladio recommended that lime should be quarried from the hills, but in some cases limestone pebbles taken from rivers was quite acceptable for the best neat work. White limestone was considered to be a better choice than brown varieties. A rule of thumb for selecting a limestone high in carbonates was also offered: when calcined, the limestone must loose one-third of its weight. Once the sand has been added to a mortar, it was to be mixed quite well in order to create the most durable and strong mortar. Two ratios for mixing were offered: one part lime to three parts of pit sand or one part lime to two parts of river or sea sand (Palladio 1965: 4).

Of note is a reference Palladio made to a kind of natural cement that was available from hills of Padua "that makes an excellent lime for such buildings as are most exposed by the weather, or stand under water, because it immediately sets, grows hard, and is very lasting." Mortars made with lime calcined from this limestone were to be mixed briefly and used right away because of their quick setting time (Palladio 1965: 4).

3.2.4 Philibert Delorme

Philibert Delorme (1514-70) was a well known and highly influential French architect. His treatise, *Le Premier Tome de l'Architecture* is best known as the most thorough French architectural treatise from the Renaissance. Unfortunately, this work is still only available in French, but it is possible to understand the majority of its content via the analysis of contemporary authors. While most influential in its design aspirations, from a material standpoint, Delorme's treatise offers little additional information that has not been covered by his contemporaries (Mitchell 1994: 20-29).

3.2.5 Sebastiano Serlio

Sebastiano Serlio (1475-1554) was a practicing architect from Bolgna, Italy. He created a large body of work in several installments over his lifetime that were published as seven books under the titles *Tutte l'Opere d'Architettura et Prospetiva* and *Regole Generali di Architettura* from 1542 to 1619. Sebastiano's treatise is unique because it speaks directly to the architect as an audience rather than a noble patron as Alberti's work had done. It was also written in Italian rather than Latin and was practical in nature (introduction in Serlio 1996: i, xvii, xviii, xix). Overall, this work, while exceptional for its time, reads like an architectural pattern book with emphasis totally given to issues of visual aesthetics and geometry. Unfortunately, Serlio did not address building materials in much technical detail, including mortars.

3.3 Renaissance treatises from the Spanish speaking world

3.3.1 Diego de Sagredo

Diego de Sagredo's work is the earliest known architectural treatise that was written in Spanish by a Spaniard. It was first published in Toledo in 1526, then in Paris in 1539, Lisbon in 1541 and 1542, and Toledo again in 1549 and 1564. It gave detailed instructions for creating formal places using classical Roman design principles espoused by Vitruvius (introduction in Sagredo 1986: 7, 8, 9, 50, 142-147). This work primarily reflects design issues by dealing with proportion, symmetry, and the human form adapted to architectural design. Unfortunately, it makes no reference to mortar use or technology.

3.3.2 Lorenzo de San Nicolas

Arte y Uso de Arquitectura (Art and Use of Architecture) by Lorenzo de San Nicolas was published in 1633, 1665, and 1667. It primary value comes from its description of *enjarre* (stucco) techniques which were practiced by the Spanish in the sixteenth century (Alba 1995: 10).

San Nicolas recommended pit or river sand for use in *enjarres*. For river sand a ratio of one part lime to two parts of sand was advised; for pit sand a ratio of two parts of lime to three parts of sand was mixed in a two part process. A white, porous limestone was recommended for calcining. San Nicolas also described the use of a gypsum binder prepared from material that was dark, a "mirror" type, or white. *Enjarre* could be prepared as pure lime, pure gypsum, or mixture of the two (Alba 1995: 10, 11).

If the *enjarre* was applied to an earthen or brick wall, the wall surface was first punctured to increase the available surface area. A limewash-like mix of diluted *enjarre* was applied to the wall upon which the *enjarre* was troweled. In this particular instance, lime *enfoscado* (the first coat of stucco) served as the base coat over which a gypsum *enjarre* was spread. In total, three layers of *enjarre* were recommended with the *revoque* (top stucco layer) being the thinnest. The final surface finish was smoothed by rubbing with a river stone before the *enjarre* dried. A final coat of thin *revoque* without aggregate was recommended for the smoothest, finest finish (Alba 1995: 11, 12).

3.3.3 Other works

Alba describes several additional Spanish treatises in her thesis on architectural surface finishes in the Caribbean. They are *De Varia Comensuracion para la Escultura y la Arquitectura* (Of the Commensurate Variations for Sculpture and Architecture) by Juan de Arfe y Villafane published in 1585, *Teoria y Practica de la Fortificacion* (Theory and Practice of Fortification) by Cristobal de Rojas published in 1598, and *Regla de las Cinco Ordenes de Arquitectura* (The Five Rules of Order of Architecture) by Giacomo Vignola first published in Spanish in 1593 (Alba 1995: 4). Unfortunately, these treatises were not accessible for research for this project. It is not known if they contain specific descriptions of mortar use and technology.

3.4 Eighteenth and early nineteenth centuries

3.4.1 Reprints of earlier works

Many of the earlier major European architectural treatises such as those by Alberti, Delorme, Palladio, Serlio, and Vitruvius were reprinted and made widely available in the eighteenth century. Treatises from the Spanish-speaking world by Arfe y Villafane, San Nicolas, and Vignola were also reprinted. There does not appear to have been any new treatises of a large magnitude that were in use by the Spanish in this period, however. Of important note is a book on Roman mortar technology, *Disertacion sobre las Argamasas que Gastaban los Romanos* (Dissertation on Roman Mortars) by Lloriot, that was published in 1776 (Alba 1995: 5). Unfortunately, copies of this work are only available in archives located in Spain which were not accessible for this inquiry.

3.4.2 Transition from the theoretical to the practical

Until the nineteenth century, most works dealt with architecture from a theoretical rather than practical perspective. After this point, many practical “how to” books appeared (Alba 1995: 5). These books would not necessarily be reflective of mortar technology used in the construction of Fort San Cristóbal, but are reflective of methods that may have been used in subsequent modifications to the fort in the nineteenth century.

Examples of these kinds of publications include *Manual de Construcciones* (Manual of Masonry Construction) by Pedro Celestino Espinosa published in 1859, *Manual del Abanil-yesero* (Mason’s and Plasterer’s Manual) edited by Ignacio Boux and published in 1840, *Tesoro de Albanileria* (Masonry Treasure) by Pascual Perier y

Gallegos published in 1853, and *Arte de Albanileria* (The Art of Masonry and Plaster Work) by Villanueva published in 1827 (Alba 1995: 5).

3.4.3 Spanish New World treatises

Very few architectural treatises were written in the Spanish New World before the nineteenth century. The oldest by Andrés de San Miguel, a practicing architect in New Spain during the seventeenth century, is a treatise on his work. Unfortunately, there is no reference to mortar technology or use in it. Of the remaining treatises, two are important for their reference to mortars. They are the anonymous work *Arquitectura Mechanica Conforme la Practica de esta Cuidad de México* (Architectural Practice in Mexico City) published sometime between 1783 and 1810 and *Arte de Albanileria* (Art of Masonry and Plaster Work) by Juan de Villaneuva, published in 1827.

Arquitectura Mechanica Conforme la Practica de esta Cuidad de México recommends the sand used for mortar be clean. This requirement is met by checking to see if the sand makes a white cloth dirty and that the sand leaves no clay dust when rubbed between the fingers—a practice first mentioned by Vitruvius. The best lime was that which originated from San Marcos, a settlement to the southeast of Mexico City, because it made a large amount of noise when slaked. *Tezontale* was a unique mortar only used in the Mexico City area for leveling grades that was made from the volcanic rock *tezontle* (*Architectural practice in Mexico City* 1987: 21, 22). It is possible that this volcanic rock was pozzolanic in nature.

Several different mortar formulations were presented. *La real* (royal grade) was prepared in the ratio of one part lime to one part sand. *Mescla segunda* (second quality) consisted of one part lime to one part sand that had been sieved. *Mescla terciada* (third mix), used only for foundations, was prepared by mixing three parts of lime to three parts of sand to twelve parts of clayey earth. In order to prepare mortar for plaster, one part lime to one part of sand was mixed together and then sieved (*Architectural practice in Mexico City* 1987: 23). This treatise is the only one covered thus far that specifically indicates the Spanish were adding clayey soil to foundation mortar mixes—an important consideration when approaching the fortifications in Puerto Rico.

Arte de Albanileria by Villanueva explains how to select materials, prepare mortar mixes, apply pastes, and select proper tools. Much length is spent on the preparation and application of stuccos. It was recommended that the limestone from which the lime was slaked be white in color and all sand be relatively fine and clean. Mortar mixes in ratios of one part binder to two parts aggregate and one part binder to three parts aggregate were recommended for lime, lime and gypsum, and gypsum mortars. One part of binder to one part of aggregate was recommended for the final surface coat. A special type of pure gypsum mortar without any aggregate was also described (Alba 1995: 14-16).

Stucco was prepared from relatively freshly slaked lime. The calcined lime was not slaked by immersion in water; rather, it was sprayed with water until the lime softened and then the mass was pulverized. After preparation, the lime pile was left in the open until a crust developed on the surface. This crust apparently was protective as such piles of lime were left outside for very long periods of time. When work commenced, the crust was broken and water was added to the mixture of quicklime and slaked lime inside the pile. Water was added until the paste has a greasy consistency (Alba 1995: 15). This slaking method probably had important implications in areas where water was scarce—as in many areas the Spanish settled including Puerto Rico.

The stucco was applied in several layers to a wall. The final coat typically had a fine aggregate and was polished with the surface of a special mushroom-shaped trowel called a *fratas* (Alba 1995: 15).

3.5 Contemporary sources

Alba indicates that the original method the Spanish used for slaking lime was the *apagado* method where quicklime was fully immersed in water—in essence the common pit slaking that has been practiced for thousands of years. In the late eighteenth to early nineteenth century, the Spanish switched to the *azogado* or aspersion method where quicklime was sprayed with water until the lime softens and turns into a powder (Alba 1995: 30). This is the method described by Villanueva. Alba also reports that traditional architecture of the Antilles and Central America used aggregates composed of brick fragments, fibrous matter, ashes, lumps of old mortar, fragments of coral, and calcareous sand (Alba 1995: 32).

The use of clay/lime mortars is described in many sources with reference to the Spanish New World. In Cuba, there was a tradition of building with soils rich in calcium carbonate. Mortars were prepared directly from the soils which, over time, hardened through the migration and carbonation of soluble calcium bicarbonate (Casal 1990: 20). According to Albert Manuncy, the Spanish were known to mix clay with lime, sand, and gravel to create *tapia* walls—especially in the Caribbean (1952: 32). Manuncy also indicates that in areas where either fuel or lime was scarce, mortars were prepared with lime, sand, and clayey soils with straw sometimes added for additional strength (1983: 60).

In building of the hornwork at El Morro, Puerto Rico, workmen “laid a footing five or six inches thick—a ‘floor’ of sandstone spalls and clay soil, mixed with lime for adhesion” (Manuncy and Torres-Reyes 1973: 40). A section of a wall at Fort San Cristóbal, Puerto Rico that collapsed during work in 1769 was officially blamed in part on a weak mortar mixture of lime and clay. At the same fort construction documents specified that the outer portion of the fortifications were protected with a coating of clay and lime from excessive weathering (Torres-Reyes 1965: 59, 109). Previous analyses of masonry mortars from El Morro in Puerto Rico found clay in some of the mortars. The supposition was that clay was added because of the high cost involved in preparing lime. By adding clay, the lime could be extended (Jacob and Cavallo 1992: 74; Crisson 1996: 89).

A few sources specifically mention the use of brick dust in mortars for use on terreplein surfaces and cisterns. At Fort San Cristóbal, terrepleins were covered with mortar mixed with crushed brick (Torres-Reyes 1965: 110). In 1804, repairs to the terreplein of the Castillo de San Marcos in St. Augustine, Florida used a mixture of lime, sand, and powdered brick (Arana 1988: 141). According to the historic structure report published in 1991 on the fortifications in San Juan, Puerto Rico, the vault of the cistern at Fort San Cristóbal was plastered with brick-dust stucco (Berkowitz et al. 1991: 123).

There are a few references to organic additives for mortars. When the cisterns were constructed in Fort San Cristóbal, a water repellant coating of bitumen as added to the mortar (Torres-Reyes 1965: 90). In 1770, the British Surveyor General, William

Gerard de Brahm visited the Castillo de San Marcos in St. Augustine, Florida and wrote about the use of linseed oil in a floor:

> I advise to burn Shells into Lime and to mix it with twice the quantity of unburnt pounded Shells; these Materials together to be made up into a mortar, soon petrifying…. After the ground Floor of the House is well rammed with heavy Pestles; the above Mortar is to be laid on four or six inches thick, and beat by three or more Persons with light Pestles all over, gently and quickly until nothing of the Mortar will stick to the Pestles, then a brush of lint-seed-Oil [linseed oil] must be given all over and continue beating until the oil disappears. This brushing with Oil and beating is to be repeated until the Floor is hard, smooth and shiny; such a Floor will prove near equal to Marble, cold, easy to be cleaned with a Wet Mop, and aired to keep out Jiggers, beside all manner of Bugs and Vermin (qtd. in Manuncy 1952: 33).

Many of the fortifications in Puerto Rico are covered in stucco colored with an orange-yellow finish. Over the years, authors have speculated on what this coloring might be, but the most convincing is from an article by Jonsson and Cliver. They advance the theory that the coloring was due to the application of iron vitriol (iron sulfate, $FeSO_4$). When applied with a brush, iron vitriol is green but soon reacts with the calcium carbonate present in the stucco to form gypsum and iron oxide. The iron oxide provides the orange-yellow color. Jonsson and Cliver applied solutions of iron vitriol to test panels and produced results nearly identical to what is seen on the Puerto Rican fortifications today (Jonsson and Cliver 2003: 31-36).

3.6 Synthesis of primary and secondary sources

There is a great deal of agreement in mortar use and technology in the Renaissance treatises that were available to the Spanish builders in the New World. Table 3.1 summarizes this information. From the information collected, it is possible to synthesize a hypothetical description of mortar technology in use in the seventeenth and

Table 3.1: Summary of mortar technology

	Primary sources						Secondary sources							
	Alberti	*Arquitectura Mechanica*	Palladio	San Nicolas	Villaneuva	Vitruvius	Alba	Arana	Berkowitz	Casal	Crisson	Jacob & Cavallo	Manuncy	Torres-Reyes
Aggregate should be clean	■	■	■		■	■								
Dark colored aggregate is better (avoid white)	■		■											
River sand for renders, pit sand for all other uses	■		■			■								
No clear preference for pit or river sand				■										
Pit sand should be sharp	■					■								
Sea sand is last choice, but should be washed	■		■			■								
Brick as aggregate						■	■							
Choose whitest limestone for calcining	■		■	■	■	■								
Best limestone looses at least 1/3 its weight	■		■											
Best quicklime when slaked makes lots of noise/steam	■	■												
Remove non-burned bits from calcined lime	■					■								
Slake for long period of time	■					■								
Slake using Spanish aspersion method					■		■							
1:3 mix for pit sand mortars, 1:2 mix for river sand mortars	■		■		■	■								
Other aggregate to binder ratios				■	■	■								
Sieving	■	■												
Gypsum binders	■			■	■									
Natural cement			■											
Pozzolana		?				■								
Brick dust as hydraulic additive	■					■	■	■	■					■
Clays added to mortar	■	■					■			■	■	■	■	■
Organic additives (bitumen or linseed oil)													■	■

eighteenth centuries during the construction of Fort San Cristóbal. This synthesis is an ideal representation of the treatises and modern sources presented and would not be reflective of actual real world conditions that would have required many compromises. It is, however, a good place to begin when trying to understand the Spanish New World mason of the seventeenth and eighteenth centuries.

A mason working on Fort San Cristóbal would have been inclined to use pit sand for all uses other than renders. River sand would have been sought out for renders. Sand that was darker in color would have been preferred over light colored sand, and white pit sand would not have been used at all. All sands were checked for cleanliness by throwing them upon a white sheet and rubbing between the fingers to check for clay. Where needed, the sands were sieved. Limestone selected for calcining would have been as white as possible and preferentially quarried. Where limestone was unavailable, sea shells and coral would have been calcined. Only lime-bearing materials that lost at least one third of their weight upon calcining were selected.

Until the later part of the eighteenth century (and perhaps even later), quicklime was totally immersed for pit slaking. Around the turn of the nineteenth century, this method was changed to slaking by spraying the lime with water until a crust formed. A heap of lime was thus treated and kept indefinitely. When the lime was to be used for construction, the crust was broken and water was added until a greasy consistency was obtained.

When preparing mortars for all uses other than renders, a mixture of one part lime to three parts of sharp pit sand was used. Mortar used as bedding for large stones was quite fluid in consistency. For renders, a mixture was prepared of one part lime to two parts of river sand. Render surfaces were built up in layers with the surface finish consisting of a one to one ratio of lime to aggregate or possibly a pure lime or pure gypsum skim coat. The surface may have been colored with the application of limewashes or iron vitriol.

In situations where lime was scarce and expensive, clay/lime bedding mortars were created in the ratio of one part lime, three parts sand, and twelve parts of clayey earth. Mortars prepared for use on terreplein surfaces or cisterns were mixed with brick dust to give them hydraulic properties and better durability.

3.7 Interpretation of authors' recommendations

Most of the recommendations for mortar formulations from antiquity to the nineteenth century hold up to modern scrutiny. In the past, the process of creating a reliable mortar was primarily based on empirical knowledge: formulations that worked well were repeated and those that failed were not remade. Over time, a compendium of information on reliable mortar mixtures was created and recorded in print and in the memory of masons that was passed from generation to generation.

Clean, white, aggregates with a high quartz content are necessary to create a mortar that performs well, the aggregate being hard and chemically inert. The selection of an aggregate with a high fines content would interfere with the contact of the building lime paste with the aggregate. A sand that has a high fines content or a darker color is indicative of an undesirable level of certain mineral species such as shales or organic contaminants (English Heritage 2000: 4, 5, 8). The American Society for Testing and Materials recommends that no more than five percent of an aggregate mix should consist of fines or a mixture of sits and clays (ASTM 1999). Based on this information, the authors of the architectural treatises were correct in recommending clean sand, but Alberti's and Palladio's recommendation for darker-colored sands does not stand up to modern scrutiny.

River sands tend to be more sharp and angular than sea sands. Non-angular sands are often referred to as "soft" sands. In modern practice, sharp sands are usually recommended for all work. Sharp sands give rise to a mortar that is stronger in compressive strength than soft sands. Soft sands are sometimes recommended today for plaster work because their spherical shape reduces friction in the plastic state and helps the mortar to have a better consistency for application (English Heritage 2000: 7; Weaver and Matero 1997: 135). The authors of the architectural treatises overwhelmingly recommended sharp sand for foundations—an excellent place to put this mortar formulation which is more resistant to compressive stress due to granular interlocking. These authors also recommended soft sands for renders undoubtedly for the same reasons they are sometimes recommended today.

The range of binder to aggregate ratios mentioned by the authors' (approximately 1:1 to 1:3) are still used to this day for various repair and restoration mortars. This range of ratios was also used in a variety of other historical contexts since the time of Vitruvius (Weaver and Matero 1997: 135).

Alberti, Palladio, and Vitruvius all knew that salt was an extremely deleterious material to have in mortars. Salts in porous building materials will cause early failure through the repeated cycling of salt crystallization and dissolution (Charola 2000). Sea sand normally contains some degree of salts such as sodium chloride, but these salts can be washed away with water—a solution that these authors specifically stated.

The authors' recommendation for obtaining as white a limestone as possible for calcining is undoubtedly related to the content of clay in limestone. The higher the level of pure calcium carbonate in limestone, the whiter the resulting stone will be. Limestone with a high clay content would have produced a weak binding material due to the resulting low quicklime content. It is also possible that hydraulic components were produced upon calcining, creating a mortar with characteristics that were not traditionally desirable—such as too fast a set. Note that Palladio specifically mentioned the use of clayey limestone to produce a natural cement, but he did not recommend it for general use (Palladio 1965: 4).

Lastly, the addition of pozzolanic additives such as brick powder to mortars is a well known practice today. The addition of these compounds creates a weakly hydraulic mortar that is more durable than a pure lime mortar and can set under water. Ample analytical evidence exists today to support their appropriate use in repair and restoration mortars (Teutonico et al. 1994).

3.8 Conclusion

Up until the eighteenth century, mortar technology was still quite indebted to the Romans. The work of Vitruvius was echoed and improved upon slightly by later Renaissance authors such as Alberti, Palladio, and San Nicolas. Spanish masons working in the New World would have been likely to practice techniques presented in these works. Certainly, the later works of Villanueva and the anonymous treatise on the architectural practice in Mexico City reinforce the idea that masons were practicing techniques present in these works.

Through the analysis of these treatises, it is possible to create a synthesis of recommendations that a hypothetical Spanish New World mason would have been inclined to practice. This analysis gives a starting point in order to understand the knowledge base employed by such a mason. It does not, however, necessarily represent practical adaptations that would have been made. The recommendations made by the authors of the architectural treatises stand up—for the most part—to modern scrutiny.

CHAPTER 4: CRITICAL REVIEW OF ANALYTICAL TECHNIQUES

4.1 Introduction

The analysis and characterization of building materials—including mortars—can be broadly grouped into four categories: wet chemical analysis, spectroscopic analysis (including optical microscopy), thermal analysis, and analysis by an electron beam. Wet chemical analyses represent techniques that use water or water/acid as a solute in order to put various compounds into solution in order to engender chemical reactions. Spectroscopy uses the electromagnetic spectrum to characterize materials. While nearly the entire spectrum can be used, certain portions of it are much more valuable and useful. In particular, the wavelengths that represent X-rays, the visible spectrum, and the infrared are most important. Thermal analysis applies heat to a sample and then records various changes that occur over time as a result of this net input of energy. The scanning electron microscope (SEM) is the most common technique that uses electron beams to visually characterize the micro-features of a sample.

Not all of these methods are required to fully characterize a sample. The purpose of this critical review is to elucidate the best techniques necessary in order to answer the questions originally posited for this case study. Specifically, the selected techniques need to provide compositional information on the mortar formulations at Fort San Cristóbal that can be correlated with use and function, technological change over time, and provenance. With these prerequisites in mind, a specific set of analytical techniques will be selected and defended.

4.2 Analytical techniques

4.2.1 Analysis by wet chemical methods

One of the most common methods of analyzing mortar involves the use of hydrochloric acid to digest the matrix of a mortar and free silica-based aggregates. Jedrzejewska (1960) published one of the first articles describing the use of gravimetric acid digestion in the analysis of older mortars. Carbon dioxide liberated by the acid was analyzed for total calcium carbonate content of the mortar and the remainder, which was assumed to be aggregate, was gravimetrically analyzed and the particles visually described. Fines were assumed to be complex silicates. This method, while simple, can lead to errors especially if the aggregates are carbonate-based. Gas volumetry is mentioned in a couple of other more recent papers (Middendorf et al. 2000; Callebaut, Viaene et al. 2000).

Hydrochloric acid digestion dissolves some silicates, such as calcium silicate hydrate, that are associated with hydraulic components in mortars. These compounds are collectively known as soluble silicates. If a binder consists of significant amounts of soluble silicates, a measure of the carbon dioxide liberated will result in an inaccurate understanding of the binder. Additional analytical techniques are needed to quantify the soluble silicates and will be described in further detail below (Bläuer Böhm 2000: 106).

Most of the time, hydrochloric acid digestion is described as a precursor to other analytical techniques, such as XRD, AAS, or AES rather than to simply measure carbonate content and visually characterize the aggregate (Callebaut, Viaene et al. 2000; Middendorf et al. 2000; Charola et al. 1986; Van Balen et al. 2000; Berlucchi and Corradini 1995). In many cases, all that is needed is a gross characterization of the mortar rather than qualitative or quantitative instrumental analysis. Characterization in this sense means to free the aggregate from the binder through acid digestion so that the resulting sands can be visually typed and matched (Phillips 1994: 54). Thin sections, however, are mentioned in the surveyed literature more often as a method of visually characterizing aggregates than is hydrochloric acid digestion.

Several wet chemical tests are mentioned that are notable for their minimal corroboration in other published literature. In their article, Callebaut, Viane et al. (2000) cite the titration of a water and sucrose solution into a mortar sample in order to determine free $Ca(OH)_2$ content. In a flow chart, Middendorf et al. (2000) describe a process for identifying soluble silica in the binder of a mortar. The sample is dissolved with hydrochloric acid and the residue is dried and then boiled in a sodium carbonate solution. No further details are offered.

Charola (2001) in a comparison of European analytical techniques also describes boiling the residue from acid dissolution in sodium carbonate as part of the process in determining soluble silicates. The process is rather more complex than that supplied by Middendorf et al. After boiling the sample in sodium carbonate, it is heated to 1000ºC, dissolved in HCl, dried at 120ºC, then dissolved again in HCl, and heated to 1000ºC. After treatment with hydrogen fluoride (HF), the sample is again heated to 1000ºC. This information is described in a flow chart without a narrative, making it somewhat difficult to understand the complete process.

In an article by Goins (2001), a rather intriguing method for the "rapid qualitative estimate of hydraulic strength" of mortars is presented. Essentially, the mortar sample is dissolved in HCl and the resulting filtrate is left to stand. According to Goins, the degree of hydraulicity is directly related to the stiffness of the resulting gel. Strongly hydraulic mortars will form stiff gels in a day, while moderately weak hydraulic mortars will form a loose gel. A weakly hydraulic mortar will form a very loose gel with globules.

Lastly, mortars can be tested for salts by grinding a mortar sample and placing it in a container of deionized water. The solution is then filtered and the filtrate is tested for salt ions. Bläuer Böhm (1996) describes, in great detail, the process of preparing a mortar sample, extracting the salts, and then analyzing the filtrate. Although salt ions can be detected with simple test strips, Bläuer Böhm decided to use more precise methods such as filter and flame phototometry, AAS, and ion chromatography for accurate detection and quantification.

4.2.2 Optical microscopy / petrography

Optical microscopy uses the visible portion of the electromagnetic spectrum to characterize materials. Its main use has traditionally been in the identification of mineral phases in rocks for which the name *petrography* has been applied. A microscope consisting of a light source, stage, objective, and eye piece magnifies the sample from a typical range of forty- to one-thousand times larger than normal. Magnification greater than a few thousand times is not feasible with an optical microscope as the resolution of the instrument is limited by the wavelength of light. Greater magnification with the requisite resolution requires the use of a scanning electron microscope (SEM).

Mortar samples in a variety of physical forms can be examined with optical microscopy. A stereo microscope with a relatively low magnification (10x to 70x total magnification) is used to view whole samples of approximately five cubic centimeters or smaller. Cross sections which expose the stratigraphy of the sample for observation under reflected light are created by embedding a small piece of mortar in a mounting medium from which one- to two-millimeter wafers are removed with a micro-saw. Much thinner sections for viewing in transmitted light can be made by embedding a sample in an epoxy resin on a glass slide and grinding it down to 30μm in thickness (Reedy 1994, 115). Lastly, a dispersion of small particles from a sample can be made with a glass slide, cover slip, and mounting medium.

Samples are illuminated by reflected light and transmitted light. Opaque samples are usually illuminated with reflected light while transparent samples can be illuminated with transmitted or reflected light. Transmitted light microscopy is commonly used with particle dispersions and thin sections. Both illumination techniques can be used to characterize a sample, but transmitted light allows a more complete examination of the microstructure and various phases that are present in the sample. Using a polarizing microscope with transmitted plane polarized light it is possible to identify sample opacity and transparency, color, pleochroism, refractive index, relief, morphology, and cleavage. With crossed polars, additional characteristics such as isotropism versus anisotropism, birefringence, extinction angle, zoning, twinning, undulous extinction, and polarization colors can be determined (Reedy 1994, 116).

Optical microscopy or petrography is often recommended as a critical and primary component in the analysis of mortars. Its use is primarily to characterize the aggregate constituent of a mortar, but it is also possible to characterize the binder (Goren and Goldberg 1991; Berlucchi and Corradini 1995; Klemm and Klemm 1990; Callebaut, Viaene et al. 2000; Barnett 1991; Reedy 1994; Anderson et al. 2000). ASTM currently does not have an official testing procedure for older or historic mortars, but a recent ASTM publication recommended petrographic analysis before other analytical techniques in order to characterize the aggregates in mortars by mineral components, shape, distribution, and grading (Doebley and Spitzer 1996, 290).

Petrography offers one of the few methods of determining relatively accurate aggregate to binder ratios. While it is possible to roughly calculate this information from a gravimetric analysis after hydrochloric acid digestion, it is prone to substantial error. Since the aggregate to binder ratio is a volumetric measurement, the most accurate analytical methods will allow for calculations based on area, such as petrography. Berlucchi and Corradini (1995) noted that area calculations based on petrographic analysis of mortars tend to result in an underestimated amount of aggregates. This problem is due to the inability of this type of analysis to discern particle sizes less than 50µm to 60µm. Their solution was to supplement petrographic information with a weight to volume calculation of carbonates in the sample derived from a calcimeter. This later method tended to overestimate the aggregate content, however. A value between that derived from petrographic analysis and the calcimeter was determined to be the most accurate (Berlucchi and Corradini 1995, 8). If the aggregate is calcareous, however, any information obtained from a calcimeter will not be valid and petrographic analysis alone will have to suffice.

Porosity can also be determined by petrographic methods from area calculations. Quantitative microscopy can be used to measure the volume fraction of a constituent through the use of areal and lineal analysis and point counting. Grain size and grain surface area can also be calculated using an ASTM chart and a series of mathematical equations to determine grains per unit area, and the mean linear intercept (Callebaut, Elsen et al. 2000, 88-93; Haynes 1984).

As mentioned earlier, petrography can be used to determine the phases present in the binder. A petrographical analysis of the mortars used in the Saint Michael's Church in Leuven, Belgium was used to determine the various constituents of the binder including hydraulic phases which tend to be present in the form of "reaction rims" around particulates (Callebaut, Elsen et al. 2000, 115). Barnett (1991) argues that optical methods offer a more cost effective and faster method for determining the presence of gypsum than SEM/EDS or XRD methods. Klemm (1990) also used optical methods to determine gypsum content of mortars. Petrography can be quite effective in determining the difference between burnt and unburnt lime and identifying bioclasts and clay and organic inclusions in mortars (Goren and Goldberg 1991). Thin sections of mortars can be stained with Alizarin Red S in dilute hydrochloric acid in order to identify calcite which will stain red. Dolomite and other minerals will not stain (Reedy 1994, 120). Staining with Alizarin Red S can be particularly effective in determining if aggregates are siliceous or calcareous in composition.

4.2.3 X-ray Diffraction (XRD)

X-ray diffraction (XRD) is an important instrumental analytical technique that can identify a wide variety of crystalline compounds. Crystalline compounds will refract light in unique patterns when exposed to an X-ray beam whose angle of incidence changes over time. According to Bragg's law, when atoms are arranged in regular, repeating patterns, such as a crystalline solid, an X-ray beam will be diffracted strongly in only a few directions (Warren 1969, 15-19). An analogy can be drawn with visible light and a cut-glass crystal. When rotated, the glass reflects incident light strongly at certain angles.

Various crystalline solids will diffract X-rays in a unique, but predictable manner. Each crystalline plane diffracts the X-ray at a certain angle. A graph can be generated that indicates both the plane of diffraction and its intensity. This unique fingerprint can be compared to XRD fingerprints from other known samples in order to come up with a match (Warren 1969, 55).

XRD only works well with samples containing crystalline phases. Amorphous phases (such as obsidian) will not exhibit strong planes of diffraction. XRD works by determining the compounds in a sample through their crystalline structure. Generally speaking, XRD cannot generate useful data on amorphous substances (Warren 1969, 116-149). The more pure a sample is, the easier it is to match fingerprints. Particularly complex mixtures of crystalline solids will produce complex graphs that are difficult to interpret. In addition, many crystalline solids have quite similar fingerprints. Further qualitative analysis by other methods is usually required to determine the composition of a sample.

XRD is arguably the most important instrumental analytical technique that can be used for determining mortar composition, particularly through characterization of the binder. A large proportion of published articles on mortar analysis mention XRD in order to determine various mineral phases present. Anderson indicates that "X-ray diffraction patterns permit the identification of the main crystalline phases in…mortars" (2000, 39). According to Martinet and Quenee, XRD is "very useful for the determination of the mineralogic nature of the binder…and for the detection of the crystallized alteration products” (2000, 83). Charola et al. provides a good example of the kind of results possible with XRD. An analysis of the mortars from the Church of Saints Hermes et Alexandre in Verviers, Belgium determined that they primarily contained alpha quartz and calcite with smaller amounts of muscovite, chlorite, feldspar, and wollastonite (1986, 30, 31).

XRD has a long history of use in determining various phases in mortars. In 1982, Lewin used XRD to determine the carbonation of newly prepared lime mortars that had cured for several months. The results indicated that only calcite remained with no detectible quantities of portlandite (calcium hydroxide). The same article indicated that a six-percent addition of Portland cement to a lime mortar was not evident in the XRD fingerprint (Lewin 1982, 123). The article did not specify if the percentage was in reference to weight or volume.

4.2.4 Scanning Electron Microscopy (SEM) and Energy Dispersive Spectrometer (EDS)

Scanning electron microscopy (SEM) and energy dispersive spectrometry (EDS) are frequently mentioned in the literature. SEM creates photomicrographs of very high magnification with good resolution. EDS is an optional process that is associated with SEM that allows for the pinpoint elemental analysis of a sample.

The SEM aims a very fine beam of electrons, generated by a high voltage filament (of a similar type used to produce X-rays), at the surface of a sample. The beam is scanned across the sample in a series of parallel lines. When the beam of electrons hits the sample, they are either reflected or absorbed and then re-emitted at a lower intensity. The characteristics of the emitted or reflected beam varies substantially depending on the topography of the sample. The emitted electron beam is collected and then sent to a monitor screen or digitized and sent to a computer. The variation in the intensity of the collected electron beam exactly corresponds to the topography of the sample (Lawes 1987, 1-11).

SEM instruments are very useful because of their ability to obtain a magnification level of up to 500,000 times (depending on model) which resolves extremely small features in the tens of angstroms or less. Optical instruments can only obtain a resolution of 0.2 microns or 200 nanometers. Beyond this limit, the wavelength of light is too large to resolve the features of a sample.

SEM instruments can also perform an elemental analysis of a sample. When the electron beam hits the sample, X-rays are generated. In an Energy Dispersive Spectrometer (EDS), the wavelength and amplitude of the emitted X-rays can be used to generate a visual spectrum of peaks and valleys. Each element will emit a characteristic wavelength and energy level. This spectrum is used to create a precise qualitative and, if calibrated, quantitative breakdown of the elements contained in the sample (Lawes 1987, 54-87). EDS is also referred to by its basic characteristic of X-ray Fluorescence (XRF) or by the pseudonym, Energy Dispersive X-Ray Fluorescence Spectrometry (EDX).

SEM is primarily used to resolve morphology and topographical features of a sample. It is not capable of conveying the color of samples (i.e., in the visible spectrum) and produces a gray-scale output. Samples must be conductive enough to transmit the electron beam. Friable samples are often problematic and will not work well. The more solid a sample is, the better the results will be (Lawes 1987, 31-53).

EDS, as a byproduct of the SEM process, is an excellent way to determine what elements are in a sample. Generally, the measurement is qualitative, not quantitative, but it can give ratios of various elements present in the sample in order to determine exact quantities (Callebaut, Viaene et al. 2000, 119). Chemical compounds can not be analyzed using this method. EDS is best used with other analyses in order to determine the complete chemical makeup of a sample.

SEM can be used to further characterize phases in a sample and is particularly useful in identifying carbonates and hydrated compounds. EDS can be used in very specific areas of a sample while an SEM image is being displayed. Thus, it is possible to get an elemental analysis, in real time, of particular features in a sample (Martinet and Quenee 2000, 83). SEM is very useful in determining the presence of C-S-H (calcium silicate hydrates) or hydraulic components in a mortar. In an SEM micrograph C-S-H is clearly evident as a spider-like network of crystals (Martinet and Quenee 2000, 85, 86; Lewin 1982, 123; Charola et al. 1986, 31; Callebaut, Viaene et al. 2000, 119, 120).

4.2.5 Thermal Analysis

Thermal gravimetric analysis (TGA) is an analytical method whereby a sample is slowly heated while its weight is recorded. A known, constant rate of heat rise is programmed and a thermocouple, which consists of a bimetallic wire probe, generates an electrical current which is recorded as a temperature. The weight of the sample is also recorded at a regular basis. This data can be used to generate a graph of time/temperature versus weight. The derivative of the graphed data, which is known as derivative thermogravimetry (DTG), can be used to amplify and isolate the results of TGA for interpretation (Smykatz-Kloss 1974, 1-2, 23).

Many compounds undergo chemical changes with temperature. For instance, calcium oxalate monohydrate, which is used to calibrate TA instruments, first changes to calcium oxalate (with liberated water) at a fairly low temperature. Under further heating, the calcium oxalate changes to calcium carbonate (with liberated carbon monoxide). Finally, at a high temperature, calcium carbonate changes to calcium oxide (with liberated carbon dioxide). At each temperature point where a chemical change occurs, the weight of the sample decreases. The temperature at which the change occurs is a constant. Thus, it becomes possible to identify compounds from a sample from weight changes that occur at specific temperatures. Note that not all changes result in a weight loss. Many metals, for instance, would undergo a weight increase as the metal oxidizes (Smykatz-Kloss 1974, 21, 22, 24).

Differential thermal analysis (DTA) detects exo- or endothermic reactions that take place with heating. Phase changes, as when water changes from a solid to a liquid, require a net input of heat. This heat absorption can be detected by placing a reference thermocouple near, but not in, the sample. The reference thermocouple records the ambient temperature in the heating chamber while another thermo-couple registers the temperature in the sample. The difference in the temperature between the sample and reference indicates either an endothermic reaction, as with melting water, or an exothermic reaction that produced more heat than is being input into the chamber (Smykatz-Kloss 1974, 2-7).

Thermal analysis will only work on samples that undergo chemical or phase changes upon heating. Highly thermally stable compounds or some elemental substances are not good candidates for thermal analysis because the changes they undergo upon heating are not detectable. For instance, hydrated compounds and carbonates would be good candidates for thermal analysis as they will undergo weight changes upon heating. Silica would be a poor compound to perform DTG analysis upon, but may be a good candidate for DTA analysis as quartz compounds undergo a phase change from alpha-quartz to beta-quartz upon heating.

According to Ellis, DTA is "particularly good at distinguishing between calcium compounds" and can be used to determine if there are C-S-H (calcium silicate hydrates), sulphates, or complex hydrates in a mortar sample (2000, 133, 134). Specifically, Ellis used DTA along with DSC to determine the hydrate structure of Portland cements, free hydrated lime, the extent of conversion in high alumina cement, and the degree of pozzolanic activity of mortars. Adams and Kneller (1988) used DTA in order to determine the degree of carbonation of lime mortars from Gothic cathedrals of France. Berlucchi and Corradini (1995) used TGA on sixteen different samples of mortars from Campania, Italy in conjunction with other analytical techniques in order to reconstruct historic bedding mortars. Martinet (2000) used TGA in order to determine the water content of hydrates and the quantitative carbonate content of mortars.

Combined with other analytical techniques, such as optical microscopy and XRD, thermal analysis can help confirm mineral phases in the binder of a mortar and give exact, quantitative results.

4.2.6 Infrared (FTIR)

Through interference spectroscopy, infrared light can be used to characterize samples. The most common applied method is Fourier Transform Infrared (FTIR) spectroscopy which uses transmitted infrared light to characterize phases within a mortar sample. Depending on the chemical compounds, or groups of atoms present in a sample, some infrared radiation is absorbed while some is reflected. The FTIR instrument records the changes in the absorption and reflectance of infrared radiation and creates an absorption or transmittance spectrum. Typically the spectra covered ranges from 4000 to 500 wavenumbers (cm^{-1}), which is the reciprocal of the wavelength (Russell 1981, 133, 134).

Each chemical compound generates a unique spectral fingerprint which is generated from the various groups of atoms present in the sample. For instance, methyl (CH_3) groups, organic acids (CO-OH), and carbonates (CO_3), all generate unique variations in the spectral output generated by the FTIR instrument. Typically each group of atoms will generate various wavenumbers, intensities, and shapes. This unique fingerprint can be read and interpreted to deduce the chemical components present in the sample (Johnston 1991, 38).

According to the published literature, FTIR spectroscopy is best used to identify organic phases and clays in a mortar sample. It is a qualitative analysis which is able to identify compounds in a sample, but not the amount. It cannot indicate the elemental composition of the analyzed sample.

Some compounds and mixtures of compounds are better suited to FTIR analysis than others. For instance, various waxes tend to have nearly identical spectral fingerprints and proteins can be vary hard to differentiate using FTIR. On the other hand, synthetic resins (such as acrylics, polyesters, etc.) and corrosion products can be accurately deduced from spectral fingerprints. In general, many organic and inorganic compounds can be identified with FTIR analysis. Organic examples include carbohydrates, colorants, natural resins (can be hard to differentiate), oils and fats, proteins (another difficult case), synthetic resins, and waxes. Inorganic examples include corrosion products, minerals, pigments, fillers, stone, glass, and ceramics. Some oxide and sulfide identification will depend on the abilities of the FTIR detector (Erhardt et al. 1988, 68-70, 72, 80).

FTIR is also better suited to fairly pure samples. The more complex the mixture of compounds, the more difficult it becomes to identify the compounds. In particularly complex mixtures, pre-processing the sample to isolate components (for instance by using solvents) can help the identification process (Erhardt et al. 1988, 82).

The use of FTIR analysis to characterize mortar samples is not common judging by the sparseness of published literature on the subject. Charola et al. (1986) used FTIR as a subsidiary instrumental method in order to correlate results from XRD, SEM, and EDS techniques. Middendorf et al. (2000) mentions FTIR in a very detailed chart of analytical techniques for mortars published in *International RILEM Workshop on Historic Mortars*, but no details are given. The analysis of clays with FTIR is well known (Russell 1981).

Price et al. (1996) describe how FTIR can replace XRD in the identification of many mineral components in works in art. Stated advantages included faster analysis time, the ability to identify very small quantities of common minerals such as calcite, quartz, and kaolin. It is also possible to identify minerals with the same chemical composition, but different crystalline structures such as calcite, vaterite, and aragonite. According to this paper, the major disadvantage to FTIR is the lack of commercial mineral libraries. The Philadelphia Museum of Art is currently creating a larger database of FTIR fingerprints in conjunction with other museum laboratories and conservation professionals through the Infrared and Raman Users Group (IRUG).

The use of FTIR on mortar samples is apparently problematic due to their overwhelmingly high carbonate content. According to Hansen, the "CO peak swamps [the] spectra" (2001, 9). This note is a warning but does not negate the use of FTIR in the identification of organic constituents of mortars.

4.2.7 Emissive and Absorptive Atomic Spectroscopy (AES/AAS)

Atomic Emission Spectroscopy (AES), also known as Flame Emission Spectroscopy, is primarily used to quantify the amount of sodium, potassium, or calcium cations in a sample, but in the literature is also used to identify silicon (Callebaut, Elsen et al. 2000; Callebaut, Viaene et al. 2000). A solution containing the sample is introduced into a low-temperature flame as an aerosol upon which the salt particles evaporate and disassociate into atoms, are excited and emit a certain wavelength of light. The procedure can be calibrated in order to quantify the percentage distribution of cations in the sample (Reynolds and Aldous 1970, 1-5).

Atomic Absorption Spectroscopy (AAS) was introduced in the 1950s as a way to improve on the accuracy of AES and increase the number of detectable metals. AES is prone to spectral interference—especially with calcium and magnesium—and cannot precisely detect elements with resonance lines of less than 2700 Angstroms, such as arsenic, bismuth, cadmium, mercury, lead, and zinc. AAS functions in a fashion similar to AES, but introduces a light source and photomultiplier in order to analyze the wavelength of light that is absorbed in a flame rather than emitted (Reynolds and Aldous 1970, 1-5, 190, 191).

AES is primarily mentioned in the literature as a way to quantify the amount of SiO_2 (silica) in a sample as a prelude to determine the hydraulicity index of a mortar while AAS is used to determine the percentage of other cations such as Ca, Mg, Na, and K in a sample. It is not clear why AES is chosen for the quantification of silicon as AAS can apparently produce the same results (Reynolds and Aldous 1970, 90-93).

Callebaut, Elsen et al. (2000) indicate that a measure of soluble SiO_2 is related to the hydraulicity of mortar. In order to determine the soluble SiO_2 content, they digested the sample with a 10% hydrochloric acid solution and the remainder, which is assumed to be mostly silica, is analyzed with AES (126). Callebaut, Viane et al. (2000) also mention the use of AES for determining the hydraulicity index as well as AAS to indicate the percentage of Ca, Mg, Na, and K in a mortar sample.

Charola et al. (1986) used AAS in order to determine the percentage of aluminum and iron in mortar samples. This approach is corroborated in a flow chart by Middendorf et al. (2000) that mentions the use of AAS in order to determine the percentage of Ca, Mg, Fe, and Al in mortar sample.

4.3 Methodology used for selection of analytical techniques

The selection of each analytical technique was determined by how well it answered the questions originally posited for this case study. To recap, these questions are as follows:

1. Can mortar formulations be correlated with specific uses?
2. Is there a chronological pattern in mortar formulations?
3. Are there any components in the mortars that characterize regional or cultural traditions?

A great deal of precision was not necessary in order to answer these questions. Rather, techniques which address the overall characterization of the mortars are required.

A summary of the mortar analysis literature search for analytical techniques is presented at the end of this section. Table 4.1 presents a matrix of authors and the analytical techniques that were described. Table 4.2 is a matrix of analytical technique versus potential information that can be obtained. Table 4.3 presents a theoretical flowchart of potential analytical techniques that can be applied to mortar analysis. The authors most frequently mentioned that the determination of aggregate to binder ratio, aggregate constituents, and binder constituents were of primary consideration. Other characteristics that were mentioned included the determination of material provenance, additives (primarily organic, but also includes non-organics such as brick dust), hydraulicity index, salts, and porosity.

Presented here, briefly, is an outline of all described techniques used to characterize the overall composition of the mortar, and to quantify the phases:

1. Thin section (polished)

   Determination of micromorphology, apparent porosity, aggregate to binder ratio, and mineralogical phases (particularly gypsum, and the presence of carbonate-based aggregate).

2. Wet chemical analysis

   Gravimetric analysis by acid dissolution, salt content (presence of ions), "rapid test" for hydraulicity.

3. XRD/SEM/EDS

   Determination of mineralogical phases, hydraulic and non-hydraulic phases, and the microstructure of mortar.

4. Thermogravimetric analysis (TA/DTG/DTA)

   Identification of mineral components (primarily gypsum, calcium carbonate, calcium silicate hydrates, complex hydrates) and quantification of phases.

5. Atomic spectroscopy (AAS and AES)

   Determination of the exact percentage of mortar components (%CaO, %MgO, %Al_2O_3, %Fe_2O_3, % soluble SiO_2) and determination of hydraulicity index and the cementation index.

6. FTIR and fluorescence microscopy

   Primarily used for the identification of organic compounds, but can be used in place of XRD for some analyses.

Clearly, there are more techniques than are necessary in answering the posited questions. Many techniques also complement and overlap each other.

Five criteria were selected in order to determine the analytical techniques used in analyzing mortars from Fort San Cristóbal. They are as follows:

1. Ability of technique to answer posited question(s)
2. Easy availability of the technique within the research time frame allocated
3. Comprehensive nature of the technique
4. Support for technique in the literature
5. Ability of the technique to provide qualitative rather than quantitative information

In light of the criteria above, optical microscopy, XRD, SEM/EDS, FTIR, and wet chemical tests were chosen. Optical microscopy and XRD are able to provide most of the information required. SEM/EDS was selected in order to confirm findings and provide supplemental information on micromorphological characteristics. FTIR provides a good method to non-destructively test for the presence of organic components in renders and verify XRD data.

Thermogravimetric analysis and atomic spectroscopy were rejected because the precise quantification of phases was not a requirement of this case study. In addition, atomic spectroscopy was not easily available. Fluorescence microscopy was also rejected, primarily due to time factors and the author’s lack of experience with the technique.

Table 4.1: Analytical methods literature search matrix

Author	Optical Microscopy	XRD	TA	SEM/ EDS	Gravimetric/ Acid Digest	IR	AAS/ AES	Wet chem.
Adams (1988)		✓	✓					
Anderson (2000)	✓	✓		✓				
Barnett (1991)	✓							
Berlucchi (1995)								✓
Bläuer Böhm (1996)								✓
Callebaut (2000)	✓	✓		✓	✓		✓	
Charola (1986, 2001)	✓	✓		✓		✓	✓	
Doebley (1996)	✓	✓		✓				
Ellis (2000)			✓					
Goins (2001)	✓	✓		✓				✓
Goren (1991)	✓							
Hansen (2001)						✓		
Jedrzejewska (1960)					✓			✓
Klemm (1990)	✓	✓						
Lewin (1982)	✓	✓		✓				
Martinet (2000)	✓	✓	✓	✓	✓			✓
Middendorf (2000)	✓		✓	✓			✓	✓
Price (1996)						✓		
Reedy (1994)	✓							
Russell (1981)						✓		
Van Balen (2000)	✓	✓	✓					✓

Table 4.2: Matrix of analytical method versus information obtained

	Optical microscopy	XRD	SEM	EDS	TG	IR	AES/AAS	Wet chemical
Micromorphology	✓		✓					
Agg:bind ratio	✓							
Porosity (total)	✓							
Salt determination	✓	✓						✓
Hydraulicity index							✓ (both)	
Quantification of compounds					✓		✓	✓
Elemental analysis				✓			✓	
Crystalline or compound analyses	✓	✓	✓		✓	✓		
Organics	✓					✓		

Table 4.3: Petrographic-mineralogical analysis[1]

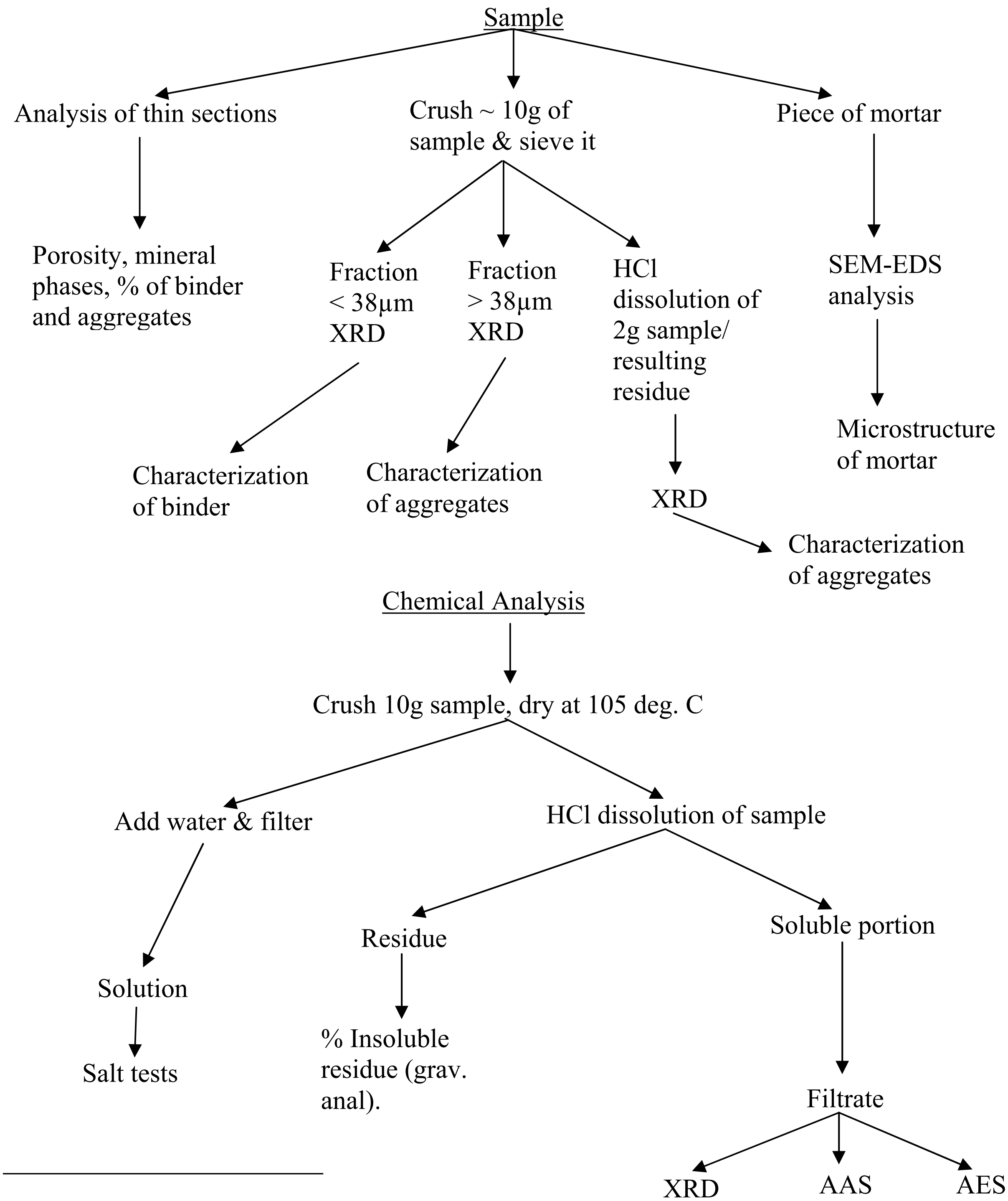

[1] Adapted from K. Callebaut et al., "Petrographical, Mineralogical and Chemical Characterization of Lime Mortars in the Saint-Michael's Church (Leuven, Belgium)," *International RILEM Workshop on Historic Mortars: Characteristics and Tests; Paisley, Scotland, 12th – 14th May 1999,* ed. P. Barton (Cachan, France: Rilem Publications, 2000), 113-123.

CHAPTER 5: RESULTS

5.1 Introduction

The previous chapters have established a referential framework that will now be used to interpret the results of the mortar analyses from Fort San Cristóbal. As previously described in Chapter 1, twenty samples from the Columbia University study in the 1980s were used to corroborate information obtained from the intensive analytical study of fifteen samples taken in October 2003. The later samples were subjected to polarized light microscopy, X-ray diffraction, infrared spectroscopy, and acid digestion followed by gravimetric analysis. The samples from the 1980s were examined under low magnification for comparison.

This chapter will begin by discussing the probable geographical sources of the materials used in Fort San Cristóbal mortars with supporting evidence from geological reports and analyses of locally available sands. The analytical results from bedding mortars, renders, and horizontal surfaces will then be presented correlated by use and time period. Finally, overall conclusions will be made and suggestions for further research offered. Raw data on the analyzed mortars is presented in appendices D through J. This information was interpreted, collated, and placed into a sample matrix in order to elucidate patterns over time and between formulations (Table 5.1).

Table 5.1: Mortar sample matrix

Sample ID	11M200	11M201	13M200	13M201	14M200	14M202	14M204	16M200	16M202	16M205	20M201	20M203	20M205	21M200	21M203
Use	white bed	render	render	white bed	render	Horiz.	beige bed	render	Horiz.	beige bed	render	Horiz.	beige bed	render	beige bed
Attributed date	1650-1700	1930s	1818	1818	1770-1820	1770s	1766-1770	1780-1820	ca. 1780	ca. 1780	1897	1897	1897	1774-1787	1774-1780
Binder to agg ratio	1:1	1:2	1:2	1:3	1:2	1:2	1:9	1:3	1:2	1:3	1:2	1:6	1:2	1:2	1:1
Porosity	13%	9%	41%	35%	<5%	29%	50%	34%	13%	10%	39%	10%	32%	34%	25%
BINDER															
Lime	X	X	X	X	X	X	X	X	X	X	X	X	X	X	X
Portland cement												X			
Clay							X						X		X
Brick dust as hydraulic additive										X					
AGGREGATE															
Grading	med	well	med	med	med	poor	med	med	med	poor	poor	well	med	med	med
Unusually large aggregate size												X			
Medium aggregate size	X	X	X	X	X	X		X	X	X	X	X	X	X	X
Unusually small aggregate size							X								X
Spherical/rounded sands	X		X	X	X	X		X			X	X		X	
Sharp sands		X					X		X	X			X		X
Beach sand w/ high bioclast content	X		X			X			X				X	X	
Beach sand w/ low bioclast content				X	X		X	X		X		X			X
No bioclasts present		X									X				
Quartz	X	X	X	X	X	X	X	X	X	X	X	X	X	X	X
Brick particles									X			X			
OTHER MINERALS															
Magnetite present	< 2%	< 2%	<2%	< 2%	< 2%	< 2%	5%	< 2%	< 2%	< 2%	5%	5%	< 2%	< 2%	< 2%
Epidote present	X	X	X	X	X	X	X	X	X				X	X	

5.2 Material sources

5.2.1 Geographic limitations

Although not readily apparent today, the Old City of San Juan is located on an island that has been recently connected to the main island of Puerto Rico. During the primary period of construction of Fort San Cristóbal in the late eighteenth century, no bridges connected the island of San Juan to the main island of Puerto Rico. Any building materials not located on the island of San Juan would have likely been brought by boat or ship from the main island of Puerto Rico. This limitation has important implications for the provenance of aggregates and lime used in the construction of Fort San Cristóbal. It is logical to conclude that the Spanish used materials immediately available near the fort for construction whenever possible. This limitation would have been especially true for heavy aggregates.

5.2.2 Sands

There are non-marine deposits of sand located in the interior of Puerto Rico, such as in the Barranquitas Triangle (Briggs and Gelabert 1962), but most of these are quite far from San Juan and would have been highly improbably sources of construction sand. The Santurce sand deposit is the closest source of non-marine sand and consists of well sorted, medium grained, white clayey quartz in a superficial deposit over much of the north coastal plain. It is over ninety-nine percent angular to subangular clear quartz without any carbonates. At its closest point, the Santurce sand deposit is located directly across the Laguna del Condado at the southeast corner of San Juan Island. In this area, however, the Santurce sands are covered by later deposits of beach sand and are not very accessible (Kaye 1959: 36).

The nearest river to San Juan Island is the Rio Piedras located approximately three miles to the south across the bay on the main island of Puerto Rico. Geological reports indicate that the lower part of this river consists mostly of floodplain alluvia, but there is no characterization or location of any specific sand deposits (Kaye 1959: plate 2). The Rio Grande de Loíza is located approximately ten miles to the east and northeast of Old San Juan. Construction sands from this river are improbable because of its distance.

A 1959 geological report indicates that all inland sands on the island of San Juan are from a recent littoral deposit (Illustration 5.1). These sands are of marine origin, cover the entirety of San Juan, and tend to be associated with older Pleistocene littoral deposits of eolianite (cemented dune sand). The littoral sands are medium to course in grain size and consist of predominantly clear quartz with smaller amounts of other minerals and calcareous fragments from marine life (Kaye 1959: 35-37, plate 2).

A sample of sand from this recent littoral deposit was obtained from a pit dug near the fort of El Morro (Table 5.2). This subspherical/subangular sand was well graded with a size range from 10µm to 500µm. It consisted of predominantly quartz with other minerals occurring at frequency of five percent. All grains were covered with a layer of beige-colored clay. Individual bioclasts were identified by chemical spot tests of the sand under low magnification with hydrochloric acid and were found to occur at a five percent frequency. Magnetite is present at a twenty-percent frequency. The magnetite appears to originate from volcanic rocks in the vicinity of San Juan that have rather high amounts of this mineral (Guillou and Glass 1957: 279).

Table 5.2: Characterization of San Juan sands

	Minerals (frequency)	Sphericity/ Roundness	Size	Grading
Pit sand from El Morro (recent littoral deposit)	Predominately quartz (>50%), magnetite (10%), bioclasts (5%), other minerals (5%), large amount of clay-like fines	Subspherical/ subangular	10µm to 500µm	Good
Beach sand near San Cristóbal	Predominately quartz (>50%), bioclasts (20%), magnetite (5%), other minerals (10%)	Subspherical/ rounded to spherical/ subrounded	Avg. 1 mm	Med to poor

The El Morro sand is relatively clean when rubbed between the fingers or dropped onto a white cloth—a small amount of beige-colored powder remains, however. The sand was subjected to acid digestion with 4M hydrochloric acid for twenty-four hours and then dried in a 60º Celsius oven for twenty-four hours. Upon gravimetric analysis it was discovered that the raw pit sand contains nearly three times as much fines as it does aggregate. Gravimetric analysis of carbonate content via acid digestion was not determined as the fines appeared to hydrate (and gain additional mass) from the application of water which was not entirely released upon heating at 60º Celsius for twenty-four hours. This reaction supports the contention that the fines may be mostly clays. The quartz grains were examined under low magnification after acid digestion and were found to be clear and free of any clay coating.

The island of San Juan is surrounded by ocean shores with an abundance of beach sand. According to a 1957 geological survey, the beach sands of this part of Puerto Rico have a large amount of calcareous material and non-metallic minerals. An analysis of sand sampled between Punta Salinas and Punta Palo Seco, an area approximately four miles to the west of San Juan, revealed a magnetite content between one and five percent by weight. Sand samples taken from the north coast of Puerto Rico near San Juan were relatively well graded with most sand grains in the range of 20µm to 125µm. A frequency analysis for mineral content of sand between Punta Salinas and Punta Palo Seco showed that diopside was present at one to five percent, epidote at fifteen to twenty-five percent, garnet at one to five percent, augite at sixty to eighty percent, and trace amounts of leucoxene (Guillou and Glass 1957: 279, 289, 290, 294).

A sample of sand taken from the beach in front of Fort San Cristóbal was analyzed for mineral content, shape and size. Under low magnification it was found to contain mostly milky to clear quartz grains. Bioclasts occur at a frequency of about twenty percent or more with various minerals present at a ten percent frequency. Magnetite is present at a low frequency of five percent. The sand grains are subspherical/rounded to spherical/subrounded and much larger than the pit sand sample from El Morro. No clay was present.

To compare, the inland pit sand taken from El Morro is sharper and better graded, has a higher magnetite content, a lower bioclast content, and contains fewer accessory minerals than the beach sand taken near El Morro. The size of the grains in the pit sand is smaller than those in the beach sand. In addition the pit sand has a very high fines content which is entirely absent from the beach sand.

With the exception of a mortar sample that represents repairs in the twentieth century, there appears to be sufficient analytical evidence to support the contention that all sands used in the construction of Fort San Cristóbal originated from local pits and beaches. This finding will be discussed in further detail later in this chapter.

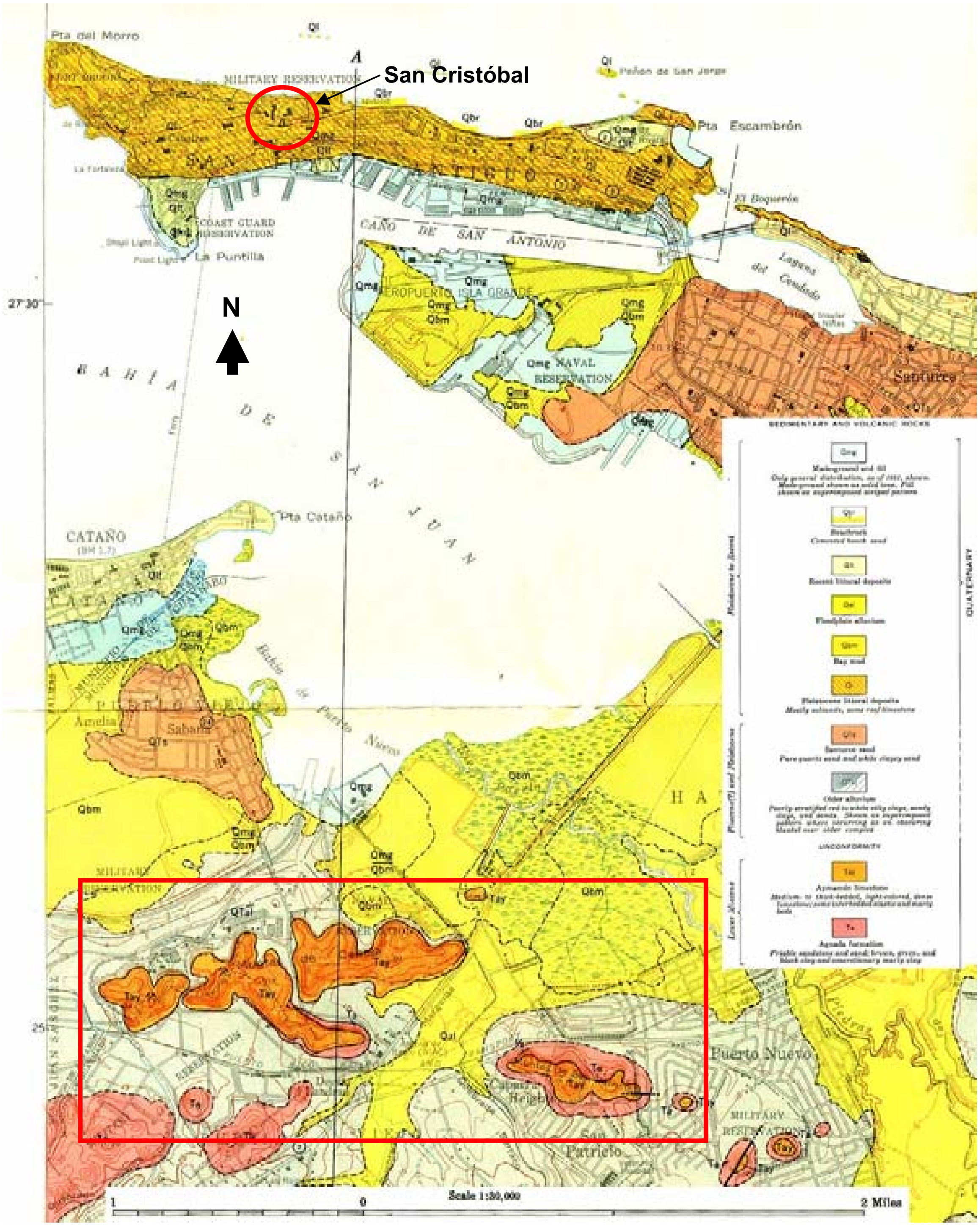

Illustration 5.1: Geological map of region around San Juan showing sands and limestone deposits. Red rectangle is the hypothesized location of the Ayamamón limestone deposits (identified as "Tay") that the Spanish used for calcining (adapted from Kaye 1959: plate 2).

5.2.3 Lime

According to the available geology reports, there are no sources of limestone present on the island of San Juan. The nearest source of limestone used for construction was probably the Ayamamón limestone deposit located four miles south near the Rio Puerto Nuevo (Illustration 5.1). The next closest source of limestone is the Trujillo Alto deposit, some ten miles to the southeast in the interior of the island. It is blue-gray in color and highly fossiliferous (Kaye 1959: 20, 21, plate 2). The composition inferred from its color makes it an unlikely source of limestone for calcining. The quality and location of the Ayamamón limestone make it the most likely candidate for use at Fort San Cristóbal. Transport by ship would have been facilitated by the close proximity of this limestone to the bay of San Juan.

The Ayamamón limestone deposit is medium- to thick-bedded and dense. It occurs in white to pinkish variations with minor amounts of marl, sand, and clay (Kaye 1959: 35, 36, plate 2). The minor clay component is an important feature of the Ayamamón limestone as many pure white mortar samples from Fort San Cristóbal appeared to have small amounts of clays. This finding will be discussed in further detail later in this chapter when the renders are analyzed.

5.3 Bedding mortars

5.3.1 General characterization

Two primary types of bedding mortars were used in the construction of Fort San Cristóbal. Bedding mortars located near the oldest and lowest portions of structures, such as foundations, tended to be beige in color[1] while bedding mortars located at higher elevations—especially on merlons and parapets—tended to be white.[2] These mortars are referred to by their color for identification purposes.

5.3.2 Clay/lime and brick powder mortars

The beige bedding mortars were divided into clay/lime mortars and brick powder mortars. The clay/lime mortars typically consisted of a homogenous dark beige binder with or without visible white lime blebs[3] while the brick powder mortar had a lighter cream colored binder without blebs and noticeable brick particles.[4] Acid digestion followed by X-ray diffraction were performed in order to confirm the presence of brick powder versus unfired clay. Sample 14M204 was chosen to represent clay/lime mortars while sample 16M205 was chosen to represent brick-powder mortars.

The samples were ground with a mortar and pestle and then subjected to acid digestion with 4M hydrochloric acid for twenty-four hours and then dried in a 60º Celsius oven for twenty-four hours. The brick powder sample (16M205) was very hard and brittle while the clay/lime sample (14M204) was quite friable. During acid digestion, the

---

[1] Beige bedding mortars: 01M016, 08M011B, 08M004, 10M027, 10M053, 14M204, 16M205, 20M205, 21M203.
[2] White bedding mortars: 01M007, 01M008, 07M003, 10M015, 13M201.
[3] Typical clay/lime bedding mortars: 01M016, 08M004, 10M053, 21M203.
[4] Brick powder mortar: 16M205.

aqueous mixture from the clay/lime sample exhibited a chocolate-brown color and soap-like bubbles. The brick powder sample colored the aqueous mixture a dark red without the bubbles found in the other sample.

X-ray diffraction was then performed on the fines from the acid-digested samples (see Appendix H). The clay/lime sample was composed of orthoclase, quartz, and kaolinite. Potassium and sodium feldspars were also present. These findings are consistent with the components of a kaolin-rich clay. The brick powder sample contained potassium feldspars, gismondine (calcium aluminum silicate hydrate), and quartz. Over thirty-five percent of the spectral energy represented a calcium aluminum silicate hydrate, a finding that could be interpreted as the hydraulic product from brick powder. Silicates that are usually found in well-fired brick, such as mullite, were not found. These compounds form as clay is heated and chemically bound water is driven off (Gurcke 1987: 28). It is likely that the firing temperature of the brick was not high enough to form detectable quantities of mullite-like compounds.

As an additional method for corroborating the analytical evidence for brick powder and unfired clays, thin sections from 14M204 and 16M205 were viewed under high magnification (400x and 1000x total). Very small brownish-red particles, less than ten microns in size were found with embedded quartz grains in sample 16M205 which would be indicative of brick. These embedded quartz grains were quite easy to see under a rotated stage with crossed polars wand the full-wave compensator (gypsum plate) inserted. Similar particles were found in 14M204, but they did not have embedded quartz grains which would be indicative of clays.

5.3.3 Aggregate and mineral composition

The beige-colored bedding mortars sampled in October 2003 were analyzed with a polarizing light microscope via thin sections (14M204, 16M205, 20M205, 21M203). All of these mortars used sharp sands. 14M204, 16M205, and 21M203 had a low bioclast content while 14M204 had the highest content of magnetite found in all of the samples that were studied for this investigation. 14M204 and 21M203 used aggregates that were smaller than the other samples. 14M204 and 16M205 had high binder to aggregate ratios. In general, the aggregates exhibited a lower than average amount non-quartz minerals.

The aggregates used in these bedding mortars most closely match pit sand that was likely excavated during the construction of Fort San Cristóbal. Based on architectural treatises examined in Chapter 3, the Spanish would have sought out sands sharper than those available on the beach for bedding mortars. Pit sand dug from the interior of the island of San Juan would have been the closest source of sharp sand. The high-clay content found in the beige bedding mortars could also be explained by the use of pit sand.

Two of the beige mortar samples (14M204 and 16M205) support the recommendations in the architectural treatises for a higher binder to aggregate ratio for bedding mortars. The other two samples (20M205, 21M203) were highly weathered and may not accurately reflect the lower binder to aggregate ratios determined from the thin section.

The white bedding mortars more closely approximated the formulation of renders which will be discussed below with the exception of 13M201 which exhibited an aggregate ratio of 1:3 instead of the expected 1:1 or 1:2.

5.3.4 Formulation changes over time

Overall, there is general consistency in the formulation of bedding mortars over time. The earliest bedding mortar, 11M200, dating from the mid to late seventeenth century and white in color, closely matches the formulation of the latest white bedding mortar, 13M201, dating from about 1818. Some differences in the beige bedding mortar are apparent over time, however.

The beige bedding mortars used for foundation work in the first phase of Fort San Cristóbal's construction in the eighteenth century (14M204 and 21M203) have significant amounts of clay—either added or naturally occurring in the sand selected for the aggregate. Sample 20M205, dating from 1897, also contains significant amounts of clay. Sample 16M205 from El Abanico is formulated with brick powder and dates to the second phase of construction in the late eighteenth century. Historical documents reviewed in Chapter 2 indicate that a wall collapsed during the first phase of construction due to the use of clay/lime mortars. Samples 14M204 and 21M203 were likely already in place by the time this wall collapsed occurred. Sample 16M205, however, clearly dates as post-wall collapse. It is possible to infer from this information that when El Abanico was constructed in the late 1780s, better mortars for foundation work were called for because of the earlier wall collapse.

The sands used in the earliest beige bedding mortars (14M204 and 21M203) dating from the first period of construction also used sands with smaller aggregate sizes than later bedding mortars. These aggregates were the smallest found in any of the samples examined.

5.4 Renders

5.4.1 General characterization

All sampled renders have white-colored binders with the exception of 13M015 which has a light beige-colored binder.[5] Of these only 03M001, 13M008, 13M200, 14M200, 16M200, and 20M201 have colored surface finishes. This surface finish is quite consistent across samples and manifests itself as a very thin transparent orange layer that does not penetrate very far into the substrate. Samples 13M008, 13M200, 14M200, and 16M200 have a very smooth polished surface.

5.4.2 Surface finish analysis

Samples 13M200, 14M200, and 16M200 were subjected to infrared-spectroscopy (FTIR) and elemental analysis (EDS) via a scanning electron microscope in order to determine the basic components of the surface finish (see appendices I and J). FTIR analysis did not reveal any organic compounds with the exception of sample 14M200 which tested positive for protein and carbohydrate. This sample, however, was also contaminated with fungal hyphae. Because 14M200 appeared identical to samples 13M200 and 16M200 as far as the surface finish is concerned, it is assumed that this test result is related to the fungal contamination.

Elemental analysis of the surface finishes on 13M200, 14M200, and 16M200 all showed a strong peak for iron. A small red particle from 14M200 was isolated from the

[5] 01M015, 03M001, 08M002, 08M006, 13P002, 13M003, 14M003, 13M008, 13P018, 13M200, 14M200, 16M200, 20M201, 21M200.

sample and tested individually. It too exhibited a strong peak for iron. The main body of the samples tested negative for iron.

From these results it can be concluded that the orange colored surface finish on mortars from Fort San Cristóbal are most likely due to iron oxides. This finding helps to support the possibility that the Spanish were applying iron vitriol to renders in order to create an orange surface (Jonsson and Cliver 2003). The application of iron vitriol (iron sulfate) to a calcium-carbonate rich surface would have produced calcium sulfate which neither XRD nor FTIR analysis revealed. It is important to note, however, that these renders have been in an exterior environment, washed by rainwater, for approximately two-hundred years. The small amounts of gypsum produced by the application of iron vitriol could have certainly been washed away leaving no detectible trace. The presence of iron oxides in the surface of the render could also be explained by the direct application of pigments to a limewash which was applied to the surface of the render.

5.4.3 Aggregate and mineral composition

All of the renders with the exception of 16M200 appeared to have been mixed in the ratio of one part binder to two parts aggregate. 16M200 was in the range of one part binder to three parts aggregate. This finding is strongly supported in the research done on contemporary architectural treatises (see Chapter 3). All of the sands were spherical and rounded. 13M200 and 21M200 had a large amount of bioclasts while 14M200 and 16M200 had a moderate amount. With the exception of 20M201 which was poorly graded, the sands had a moderate degree of grading. These results strongly point to the use of beach sand for aggregates.

FTIR results indicated that samples 13M200, 14M200, and 16M200 had some clays (see Appendix I). Illite, montmorillonite, and mixed clay fingerprints were all possibilities. These clays were present throughout the entire mortar sample and indirectly confirmed by XRD analysis which showed varying degrees of calcium aluminum silicate hydrates. Calcium aluminum silicate hydrates in these mortar samples strongly point to a limestone with some degree of clay content. When clay-bearing limestone is calcined, the clays can react with calcium creating the precursors of hydraulic compounds (Draffin 1976: 6). The FTIR results should have also indicated the presence of calcium aluminum silicate hydrates; it is uncertain why this was not the case. Further testing is recommended to confirm the presence of this compound in the samples.

5.4.4 Formulation changes over time

There is not enough documentary evidence to firmly establish the exact date of the smooth, orange surfaced renders except for 13M200 and 13M008 from the Lightning Tower on San Carlos. This structure has sufficient evidence to date these renders at about 1818. It is certainly possible that the other renders, namely 14M200 from La Trinidad and 16M200 from El Abanico, may date to a late eighteenth-century construction date. It is not possible, however, to assign a concise date to the samples from La Trinidad and El Abanico beyond a range from the 1770s to the 1820s.

All of the renders except for 20M201 and 11M201 were quite consistent and had little change that could be correlated over time. This result is not too surprising because by excluding 20M201 and 11M201, the time period analyzed is only from about 1770 to 1820.

Sample 20M201 dates to the 1897 construction of St. Teresa. Unlike all of the other renders except for 11M201, it has no bioclasts and the sand is poorly graded. In addition, it has over twice as much magnetite as the other samples. Sample 11M201 probably dates from the restoration work done in the 1930s to the Fort of the Point. Unlike the other renders, its sand is quite sharp and like 20M201 has no bioclasts. The source of sand for these two renders does not appear to be either pit sand dug near the fort, nor is it beach sand.

5.5 Horizontal surfaces

5.5.1 General characterization

The horizontal surfaces were taken from terreplein, merlon, and embrasure surfaces. Of all of the mortar samples, this category had the fewest samples primarily because some structures lacked these surfaces, such as the Fort of the Point (structure 11). There is also a wide degree of variation between samples. 14M015 and 14M202 were similar to clay/lime bedding mortars while 16M202 clearly had brick added to it. Sample 20M203 was an even gray color, quite hard and non friable, contained very large aggregates, and dates to 1897. These characteristics are strongly indicative of Portland cement, although further analytical tests would be needed for a positive confirmation.

5.5.2 Aggregate and mineral composition

Samples 14M202, 16M202, and 20M203 were analyzed using thin sections with a polarized light microscope. The sands from 14M202 and 16M202 both contained a large amount of bioclasts, but 14M202 had poorly graded spherical/rounded sand while

16M202 had sharp moderately-well graded sharp sand. Larger brick particles were clearly evident in 16M202 to the unaided eye and under low magnification, but there was no brick powder evident under high magnification. Therefore, it can be assumed that the brick particles were playing the role of a porous aggregate rather than an hydraulic component.

Sample 20M203 from St. Teresa dates to 1897 and had the most unique composition of all the samples. Its aggregate was quite large and complex consisting of quartz grains, brick, and a variety of unidentifiable mineral species. The matrix was gray in color—much like Portland cement. XRD analysis turned up a significant amount of gismondine, a calcium aluminum silicate hydrate, but other calcium aluminum silicate hydrates were also expected, but not found (see Appendix H). Based on the construction date and combined characteristics of this sample, it can be assumed that it is Portland-cement based.

5.5.3 Formulation changes over time

Because of the wide variety in formulation types for horizontal surfaces, it is not possible to clearly identify any changes over time with the exception of sample 20M203. Portland cement came into common use in the late nineteenth century in many places, and it would not be unusual to have found this binder in an 1897 sample from Puerto Rico. Thus, sample 20M203 probably represents the transition from traditional lime-based mortars into Portland-cement based ones.

5.6 Conclusions

5.6.1 Mortar formulations correlated by use

Based on the analytical evidence that has been presented, a very strong argument can be made that the formulation of mortars at Fort San Cristóbal can be associated with particular uses. With the background provided by architectural treatises in Chapter 3, it becomes clear that the Spanish were using age-proven techniques when creating mortars.

In general, the architectural treatises recommended that bedding mortars be mixed in a 1:3 (binder:aggregate) volume ratio and that the sands should be sharp. On the island of San Juan, the beach sands consist of spherical/rounded sands while pit sand dug inland tended to be more sharp. The analysis of bedding mortars strongly points to the use of pit sand in their formulation despite the readily available local beach sands. This evidence supports the contention that the Spanish were seeking out the sharpest sands on the island and using them for bedding mortars.

Most of the bedding mortars used for foundation work in the oldest structures were formulated with added clay. Quicklime is normally an expensive commodity because of the quarrying and fuel needed in its production. If the theory that the Spanish were obtaining limestone from the Ayamamón limestone deposit to the south is true, lime for calcining would have been an even more expensive commodity because of the need for transport. This environment would have encouraged the use of locally available cheap clay in extending the precious lime—especially in areas that were not supposed to be directly exposed to water, such as in foundation work. Documentary evidence (see Chapter 3) clearly shows that the Spanish were using clay/lime mortars during Fort San Cristóbal's construction. Additionally, a portion of the old Spanish-built wall near Fort

San Cristóbal collapsed in February 2004. The failure was attributed by the National Park Service to bedding mortar with added clay.

Bedding mortars that were not used lower in structures and especially those associated with merlons, embrasures, and parapets tended not to have added clay and most closely matched the formulations of renders.

Render formulation can also be correlated with use. Most of the renders analyzed exhibited a 1:1 or 1:2 binder to aggregate volume ratio which is well supported in the architectural treatises reviewed in Chapter 3. The binder is white and does not contain large amounts of clay or any brick powder. The beach sands used for renders were overwhelmingly spherical and rounded rather than sharp—characteristics that are also supported in the architectural treatises. All renders sampled that had their original smooth surface finishes had a very thin layer of orange iron oxide.

The formulation of horizontal surfaces from terrepleins, embrasures, and merlons could not be correlated with use. This finding may be in part due to a small sample size. Horizontal surfaces exhibited the widest range in formulation variations out of all of the samples that were analyzed.

5.6.2 Mortar formulations correlated by age

Mortar formulations could be correlated by age, but not in all cases. Mortars from La Teresa, built in 1897, exhibit the largest difference in formation compared to the earlier mortars. At this structure Portland cement appears and new sources of sands were used—characteristics that were found at no other sites.

The oldest mortar sampled, 11M200, is from the Fort of the Point and dates from the mid to late seventeenth century. It is a fairly pure lime mortar used in a location that later on would probably have used clay/lime mortars. In addition, it did not use sharp pit sand but instead was formulated from beach sands. Its formulation most closely matches later renders and mortars used for bedding on merlons, embrasures, and parapets.

Most foundation bedding mortars from the 1760s to the late nineteenth century were formulated with added clay. An exception is the bedding mortars sampled from El Abanico which dates from the second phase of construction in the eighteenth century. This mortar was mixed with very fine brick powder and exhibits hydraulic properties.

With the exception of renders from La Teresa, there were no obvious changes in formulation over time with renders. Mortars from horizontal surfaces were too varied in formulation to clearly establish a pattern over time.

5.6.3 Surface finishes

The analysis of surface finishes was done to determine if there were any unusual components to these renders—especially any that would have had biocidal qualities that may explain why these surfaces do not exhibit much biogrowth. Analysis of these surface finishes only found iron oxides which undoubtedly give these renders an orange color. These renders do have a rather smooth surface finish which may explain the low degree of biogrowth due to decreased surface area and porosity.

5.6.4 Questions for further research

During the process of research on this project, many questions arose that were not answered. The results determined from the analysis of mortars should be corroborated with further tests on many more mortar samples. In particular, not enough horizontal surface finishes were sampled to come to definite conclusions of formulations correlated with use and time.

Only one building, El Abanico, was found to have used brick powder in mortars. The proposed theory is that brick powder mortars are found in the foundation work in this structure as a reaction to the failure of clay/lime mortars a decade earlier. Brick powder mortars would have been water resistant, have set earlier, and been more durable. More work should be done to confirm the absence of brick-powder mortars in the first phase of For San Cristóbal's construction and to confirm their presence in the other structures not sampled from the second period of construction such as La Princesa.

Lastly, more research should be done to establish why there is a low occurrence of biogrowth on the smooth orange colored surfaces of the fort. There were no inorganic or organic additives present that could account for this characteristic. This leaves the possibility that the physical design of the surface itself may account for the low incidence of biogrowth.

APPENDIX A: STRUCTURE LOCATIONS AND PHOTOGRAPHS

All photographs by the author.

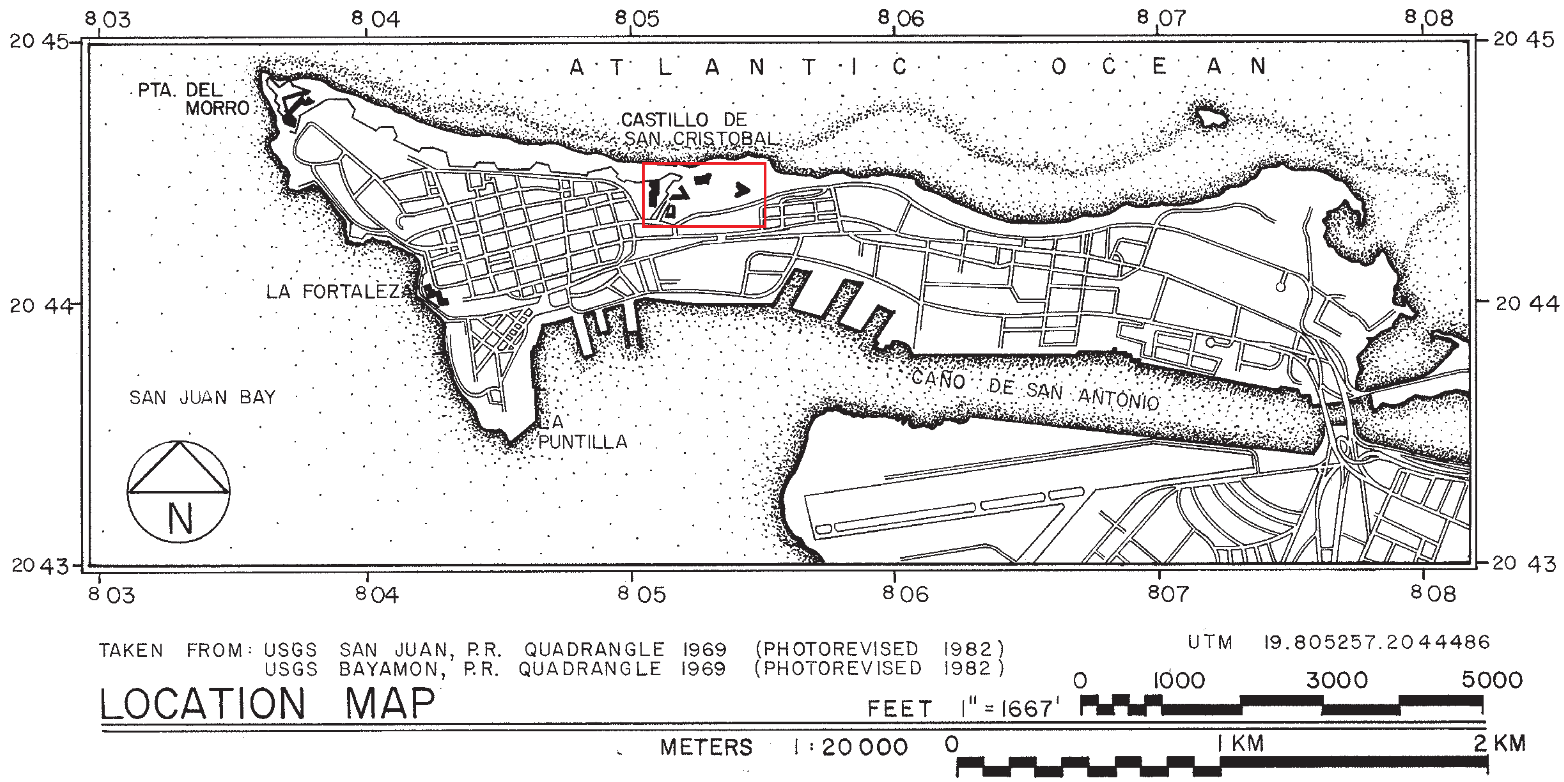

Illustration A1: Location of Fort San Cristóbal, San Juan, Puerto Rico.
Adapted from HABS survey PR-91 (call# HABS, PR,7-SAJU,53-).

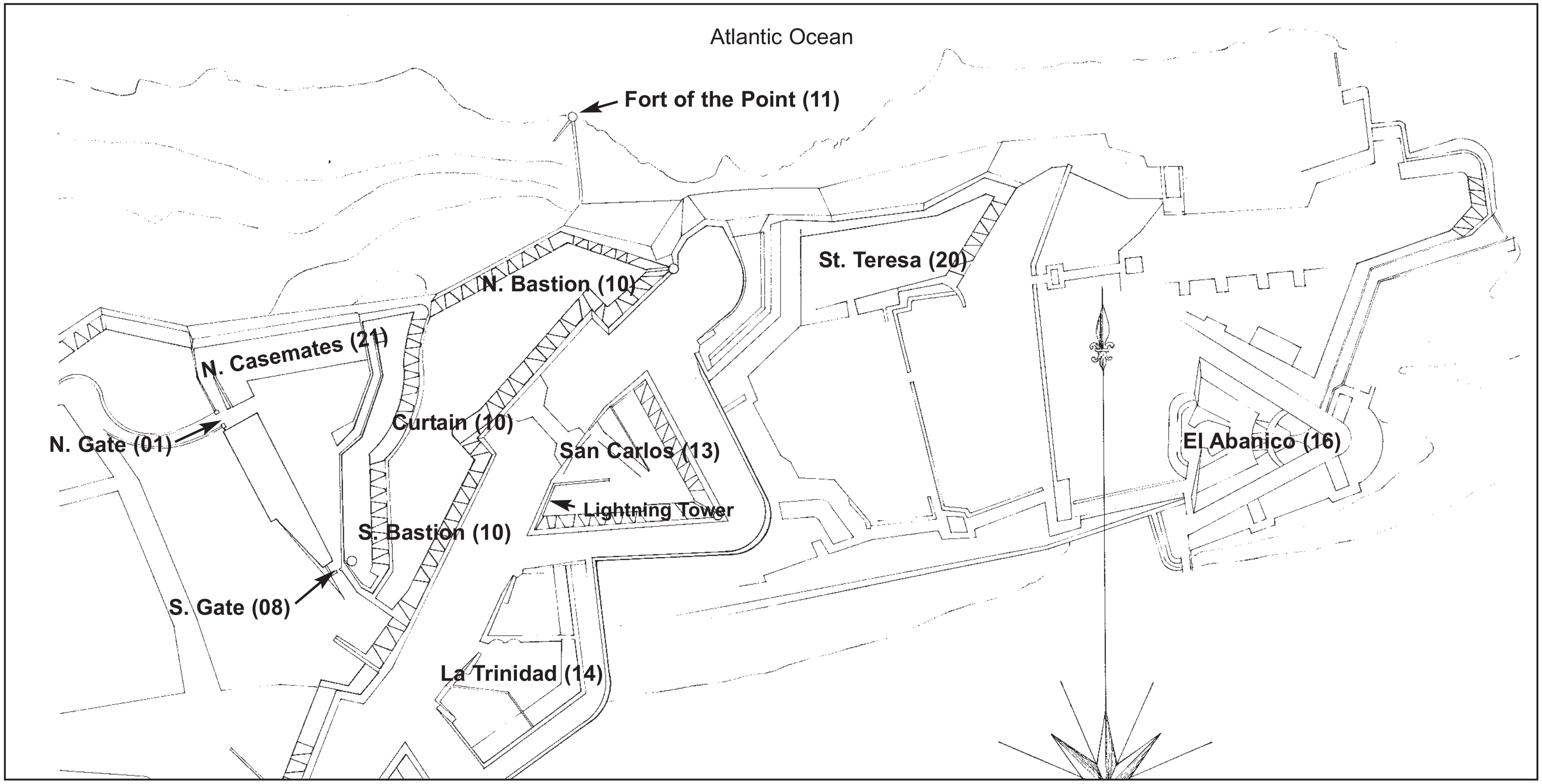

Illustration A2: Location of various structures at Fort San Cristóbal. Building IDs are in parenthesis.
Adapted from 1899 map from HABS survey HABS PR-94-C (call# HABS, PR,7-SAJU,56C-).


Illustration A3: North Gate (01), facing east.


Illustration A4: South Gate (08), facing north.

Illustration A5: Fort of the Point (11), facing east.

Illustration A6: San Carlos (13), facing northeast. Lightning Tower is circled in red.

Illustration A7: Lightning Tower located on San Carlos (13), facing west.

Illustration A8: South side of upper level of La Trinidad (14), facing northeast. San Carlos (13) is visible in the background.

Illustration A9: North side of upper level of La Trinidad (14), facing northeast.

Illustration A10: El Abanico (16), facing east. The domed structure in the background is the capitol building of Puerto Rico and is about a quarter-mile distant.

Illustration A11: St. Teresa (20), facing north.

Illustration A12: North Casemates (21), facing northwest.

APPENDIX B: MAPS OF SAMPLE LOCATIONS

Fort of the Point (11)
Plan

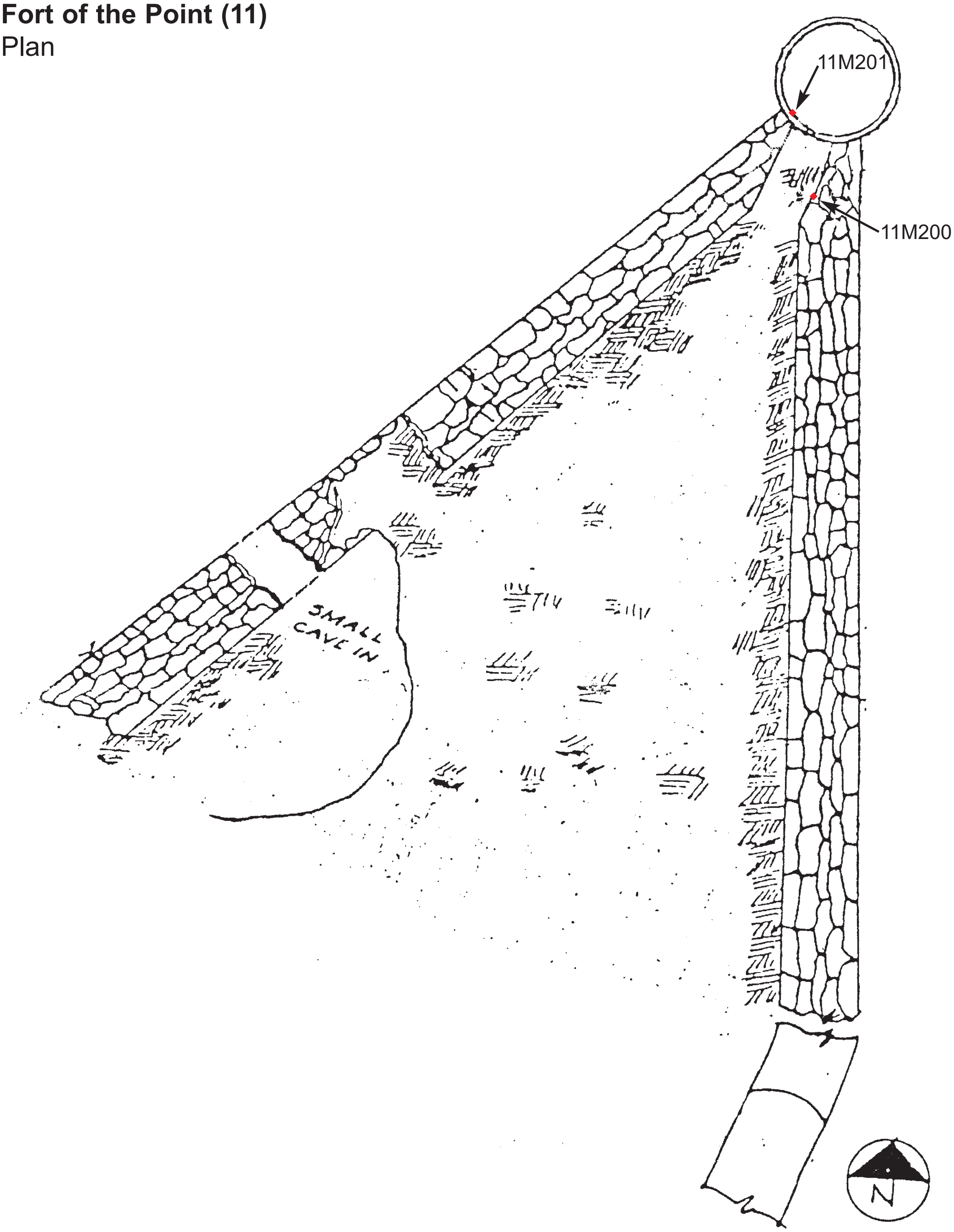

Illustration B1: Sample locations from the Fort of the Point (11).
Adapted from 1938-39 drawing by the United States Department of the Army, Engineers Office.

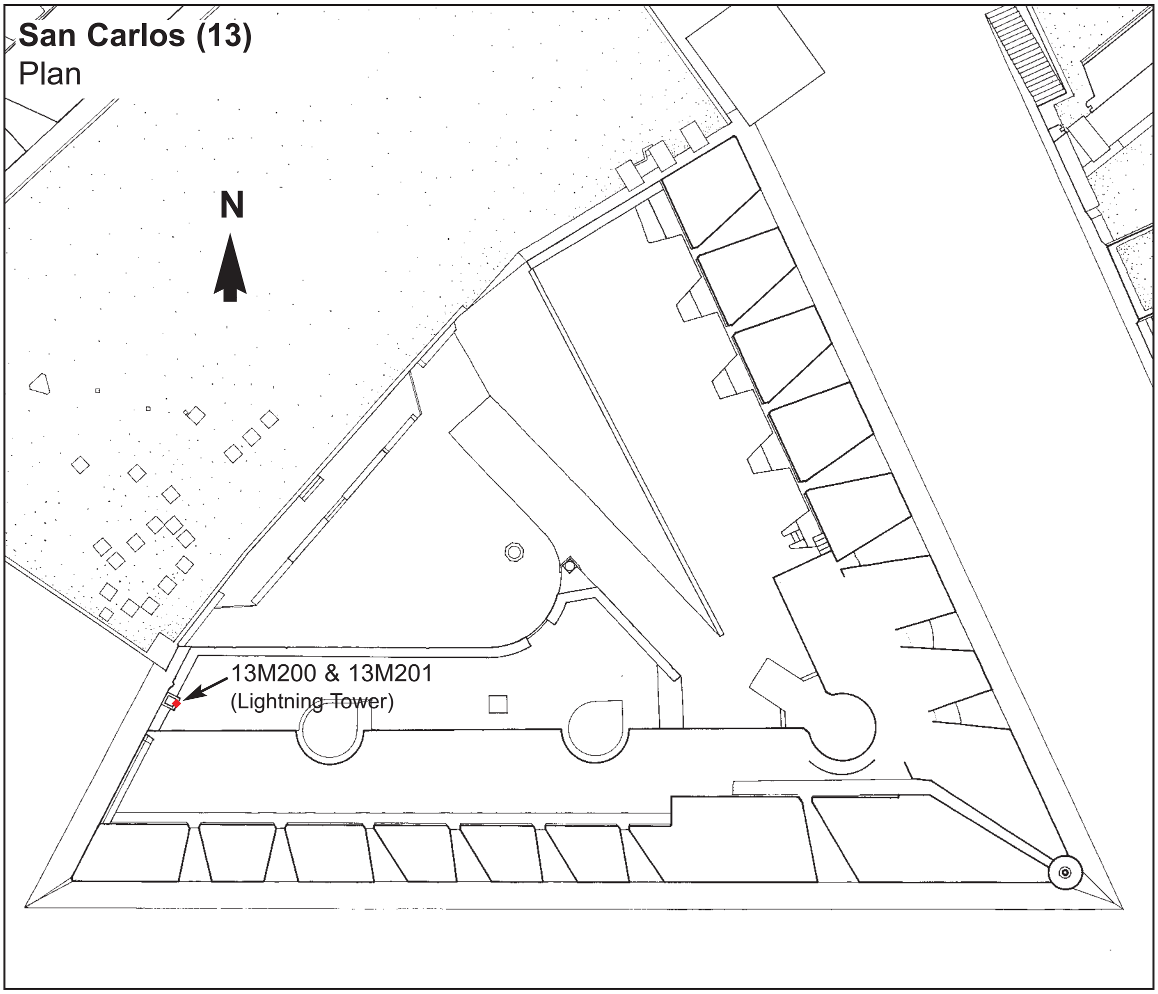

Illustration B2: Sample location from San Carlos (13).
Adapted from HABS survey HABS PR-93 (call# HABS, PR,7-SAJU,44-).

La Trinidad (14)

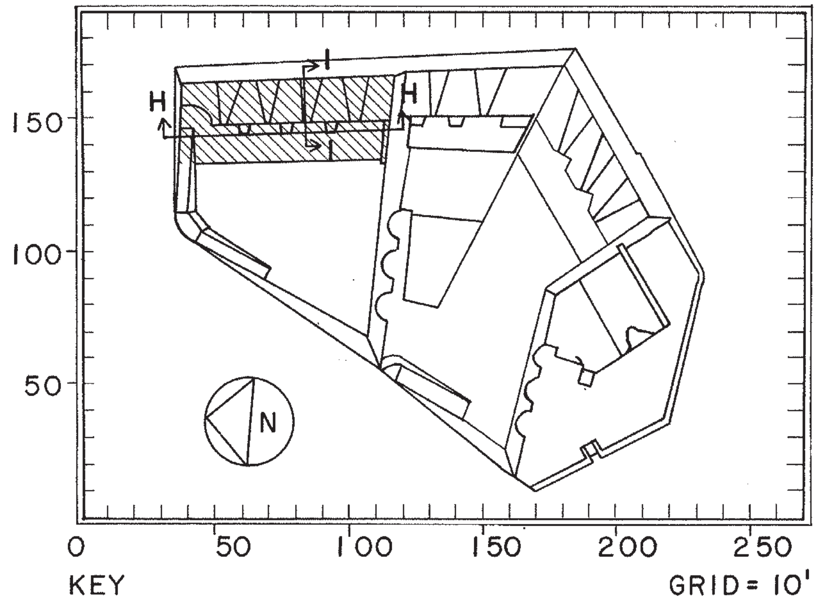

Illustration B3: Overall plan of sample location from La Trinidad (14).
Adapted from HABS survey PR-121 (call# HABS, PR,7-SAJU,59-).

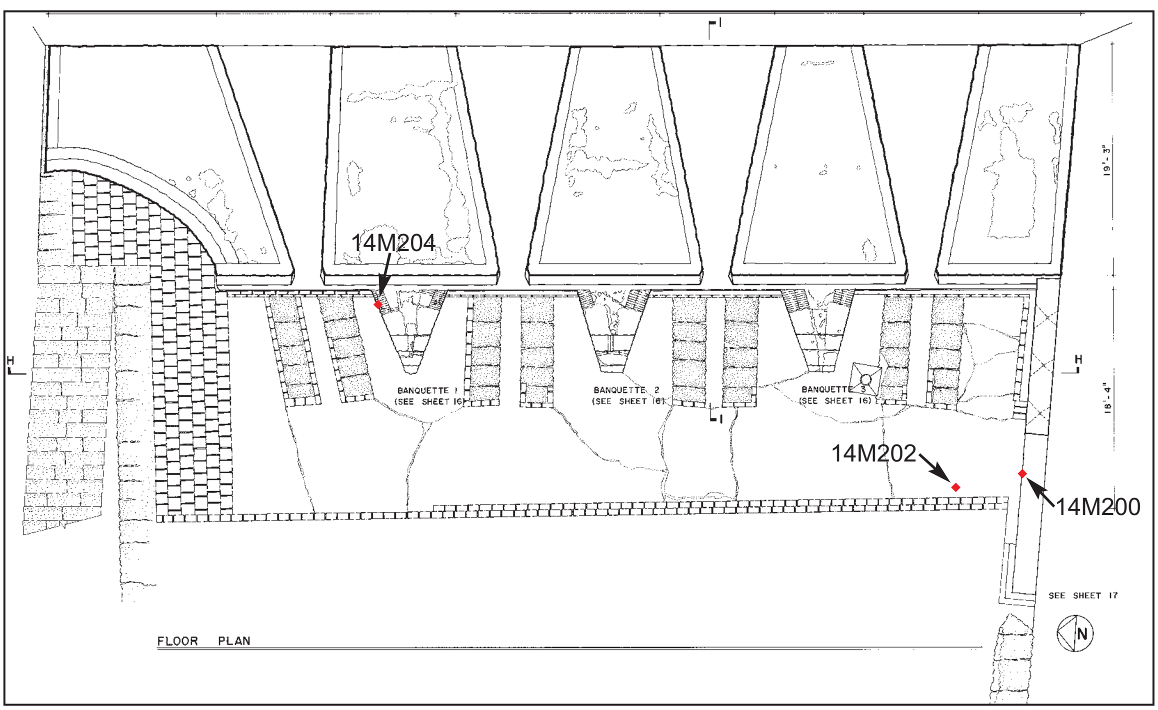

Illustration B4: Detail plan of sample location from upper level of La Trinidad (14).
Adapted from HABS survey PR-121 (call# HABS, PR,7-SAJU,59-).

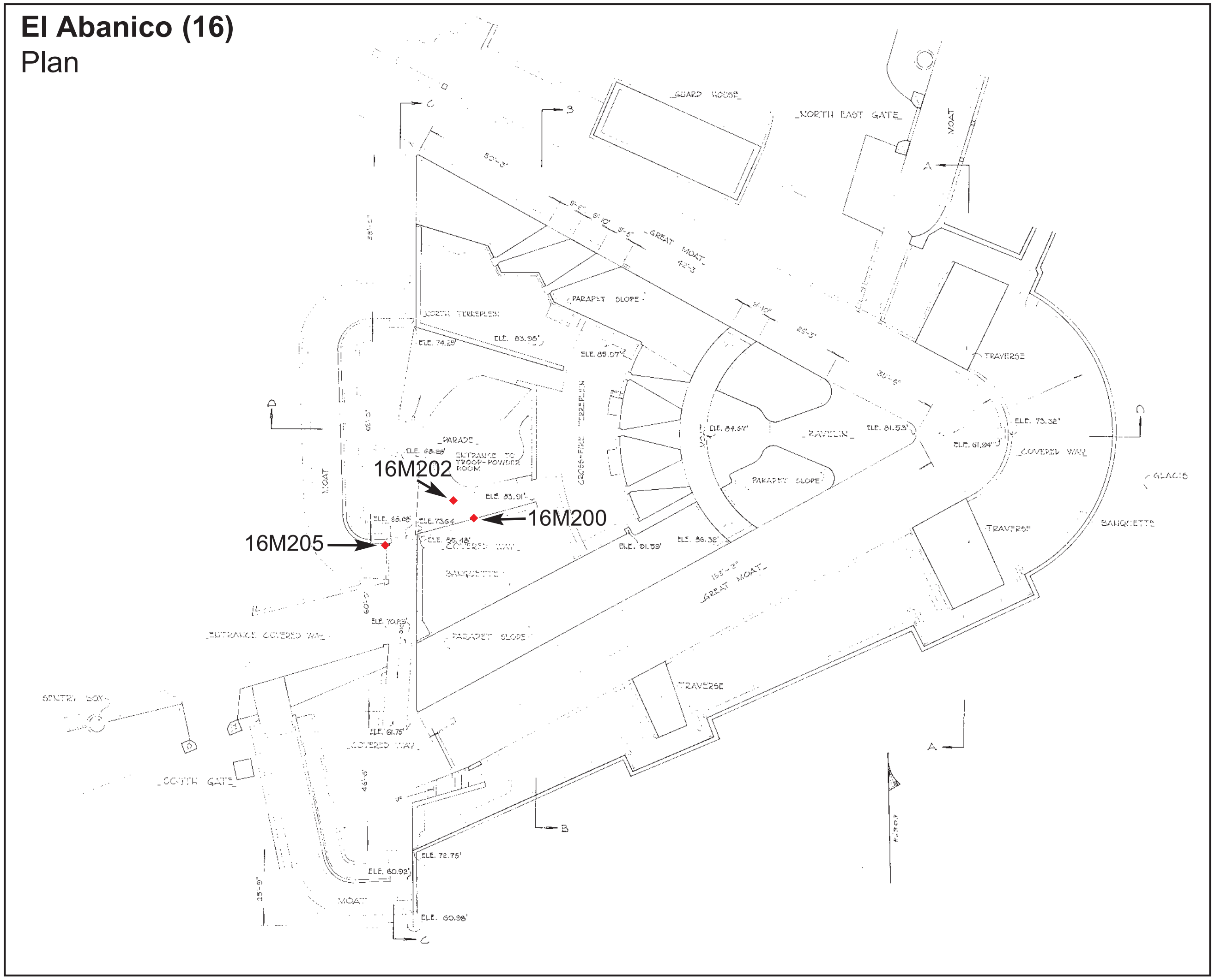

Illustration B5: Sample location from El Abanico (16).
Adapted from HABS survey HABS PR-94 (call# HABS, PR,7-SAJU,56-).

Santa Teresa (20)
Facing north

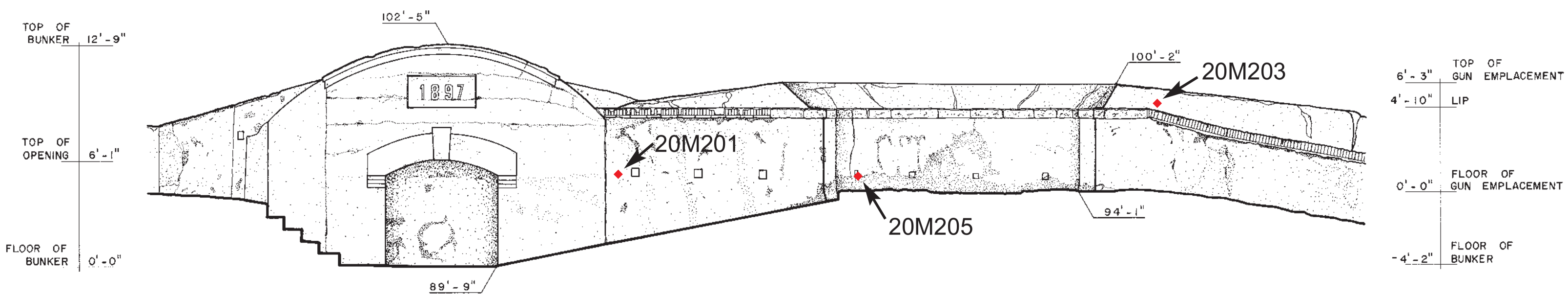

Illustration B6: Sample location from St. Teresa (20).
Adapted from HABS survey PR-91(call# HABS, PR,7-SAJU,53-).

North Casemates (21)
Plan

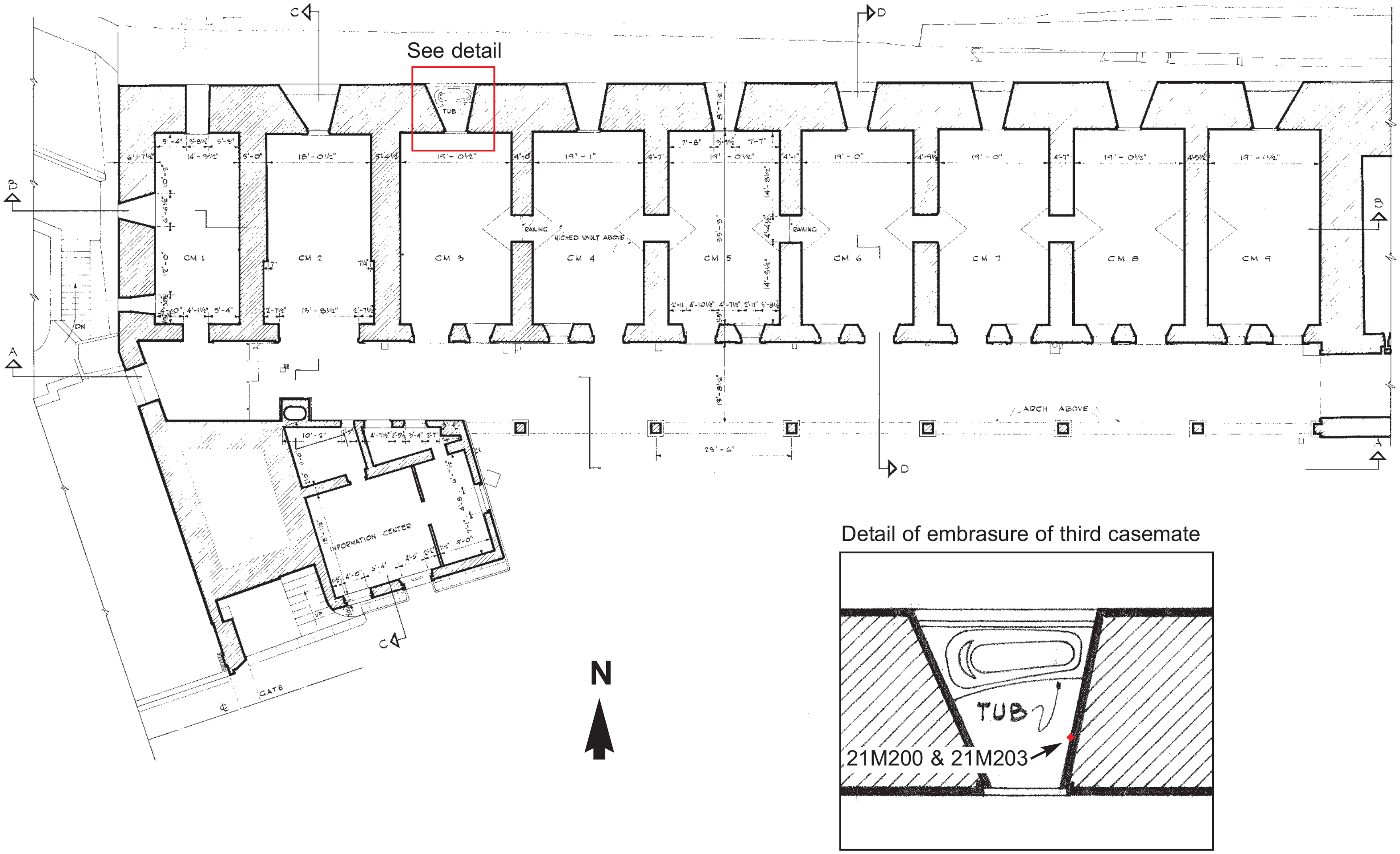

Illustration B7: Sample locations for the third casemate of the North Casemates (21).
Adapted from HABS survey PR-101 (call# HABS, PR,7-SAJU,45-).

Table B1: Location of 1980s samples

Note: These samples were taken from the mid- to late-1980s by Columbia University as part of historic structures report for Fort San Cristóbal. A mapped location for these samples was not available. Descriptions have been reproduced here, verbatim from the draft HSR.

Sample ID	**Structure**	**Location description**
01M007	North Gate	Entry gate, arch 1/ bedding mortar
01M008	North Gate	W. wall, N. of entry ramp/bedding
01M015	North Gate	Ramp, arch 2, stucco/window reveal
01M016	North Gate	Ramp, arch 2/red bedding mortar
08M002	South Gate	S. gate: concealed stucco
08M004	South Gate	S. gate: infill material
08M006	South Gate	S. gate: stucco/outer face of arch
08M011B	South Gate	S. gate: infill rubble and mortar
10M015	N. & S. Bastion	Emb. 13, N. side, bedding mortar
10M027	N. & S. Bastion	Bedding mortar/top edge embrasure
10M053	N. & S. Bastion	N. Bastion: ball pad/ br & mortar
13M003	San Carlos	Stucco on brick
13M008	San Carlos	Hard stucco from lightning tower
13M015	San Carlos	Infill from S. window / E. chamber
13P018	San Carlos	Paint/stucco from west chamber
13P022	San Carlos	Stucco from passageway to s. box
14M003	La Trinidad	W. chamber / interior stucco
14M015	La Trinidad	Ramp paving

APPENDIX C: PHOTOGRAPHS OF SAMPLE LOCATIONS


Illustration C1: Sample 11M200 (Fort of the Point).


Illustration C2: Sample 11M201 (Fort of the Point).

Illustration C3: Sample 13M200 (San Carlos).

Illustration C4: Sample 13M201 (San Carlos).

Illustration C5: Sample 14M200 (La Trinidad).

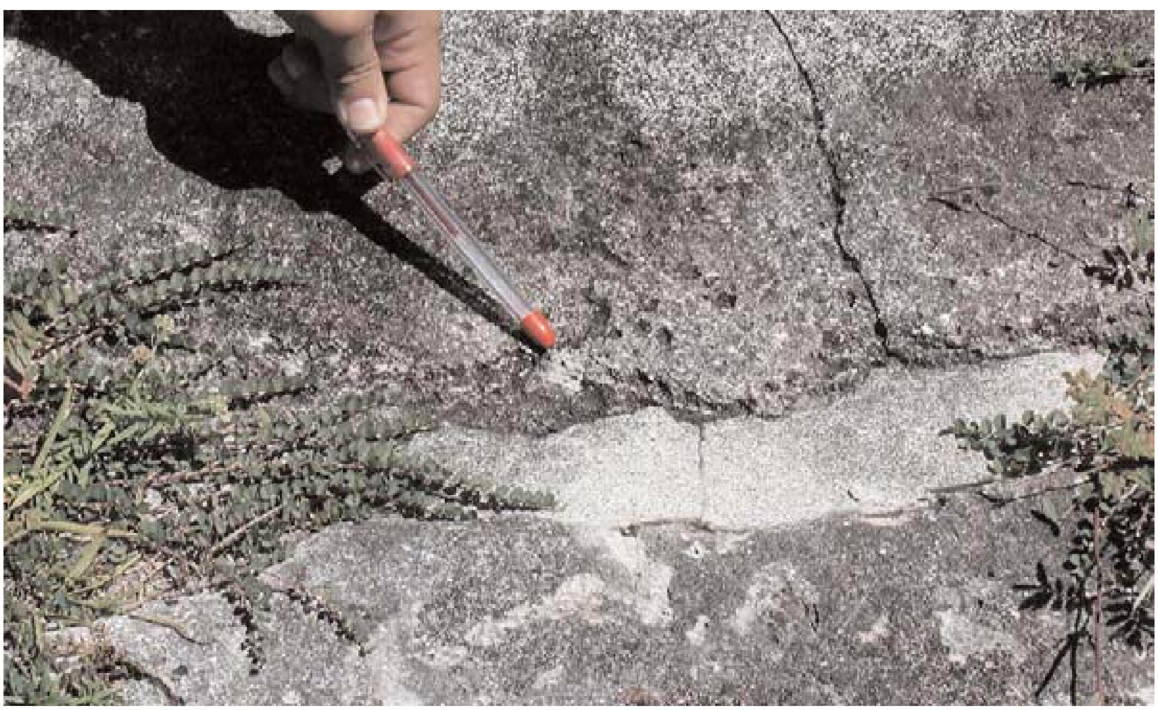

Illustration C6: Sample 14M202 (La Trinidad).

Illustration C7: Sample 14M204 (La Trinidad).

Illustration C8: Sample 16M200 (El Abanico).

Illustration C9: Sample 16M202 (El Abanico).

Illustration C10: Sample 16M205 (El Abanico).

Illustration C11: Sample 20M201 (St. Teresa).

Illustration C12: Sample 20M203 (St. Teresa).

Illustration C13: Sample 20M205 (St. Teresa).

Illustration C14: Sample 21M200 (render from St. Teresa).

Illustration C15: Sample 21M203 (bedding from the third casemate of the North Casemates).

APPENDIX D: BASIC CHARACTERIZATION OF MORTAR SAMPLES

Table D1: Basic characterization of mortar samples

Sample ID	Use	Probable Date	Color	Friability	Notes
01M007	Bedding	1783	10Y 9/1	Friable	
01M008	Bedding	1775	10Y 9/2	Not friable	
01M015	Render	1783 or earlier	Body: 10Y 9/2; surface: missing	Not friable	
01M016	Bedding	1861 or after	5YR 6/6	Friable	White blebs visible
08M002	Render	1861 or earlier	Body: 10Y 9/1; surface: 10YR 8/4	Not friable	Smooth finish
08M004	Bedding	1861 or earlier	5YR 8/4	Friable	White blebs visible
08M006	Render	1861	Body: 10Y 9/2; surface: 7.5Y 9/2 biogrowth	Not friable	
08M011B	Bedding	1861 or earlier	5YR 8/2	Friable	
10M015	Bedding	ca. 1775	10Y 9/2	Friable	
10M027	Bedding	1775	7.5YR 8/2	Not friable	
10M053	Bedding	1775-1861	5YR 6/6	Friable	White blebs visible
11M200	Bedding	Late 17th C.	10Y 9/2	Friable	Biogrowth on surface
11M201	Render	1930s	7.5Y 9/2	Not friable	Very hard repair mortar
13M003	Render	1773	Body: 10Y 9/1; surface: missing	Not friable	Bonded to brick layer beneath
13M008	Render	1818	Body: 10Y 9/2; surface: 7.5YR 7/6	Not friable	Smooth finish
13M015	Render	1775	Body: 10YR 8/2; surface: missing	Not friable	
13M200	Render	ca. 1818	Body: 10Y 9/1; surface: 7.5YR 6/6	Not friable	Smooth finish

Sample ID	Use	Probable Age	Color	Friability	Notes
13M201	Bedding	ca. 1818	10Y 9/2	Not friable	Biogrowth on surface
13P018	Render	1773	Body: 10Y 9/2; surface: missing	Friable	
13P022	Render	1861 or earlier	Body: 10Y 9/1; surface: 7.5Y 9:2 biogrowth	Not friable	
14M003	Render	1775	Body: 10Y 9/1; surface: 10Y 9/2	Friable	Layered white wash finish
14M015	Horizontal	1775	7.5YR 8/6	Not friable	Brick particles evident under low magnification
14M200	Render	1770-1820	Body: 10Y 9/1; surface: 10YR 8/3	Not friable	Smooth finish
14M202	Horizontal	1770s	7.5YR 8/6	Not friable	No brick, no blebs
14M204	Bedding	1766-1770	5YR 6/6	Not friable	Biogrowth on surface
16M200	Render	1780-1820	Body: 10Y 9/1; surface: 7.5YR 6/6	Not friable	Smooth finish
16M202	Horizontal	ca. 1780	10Y 9/2	Not friable	Large brick particles evident
16M205	Bedding	ca. 1780	5YR 7/6	Not friable	White blebs visible
20M201	Render	1897	Body: 10Y 9/1; surface: 7.5YR 6/4	Friable	Rough finish
20M203	Horizontal	1897	7.5Y 9/2	Not friable	Hard, brittle, large aggregate
20M205	Bedding	1897	7.5YR 6/6	Friable	
21M200	Render	1774-1787	Body: 10Y 9/1; surface: 10YR 8/3 (top 2mm)	Friable	
21M203	Bedding	1774-1780	5YR 7/8	Friable	White blebs visible

APPENDIX E: PHOTOMICROGRAPHS OF WHOLE SAMPLES

All photomicrographs taken under reflected light at 30X total magnification.

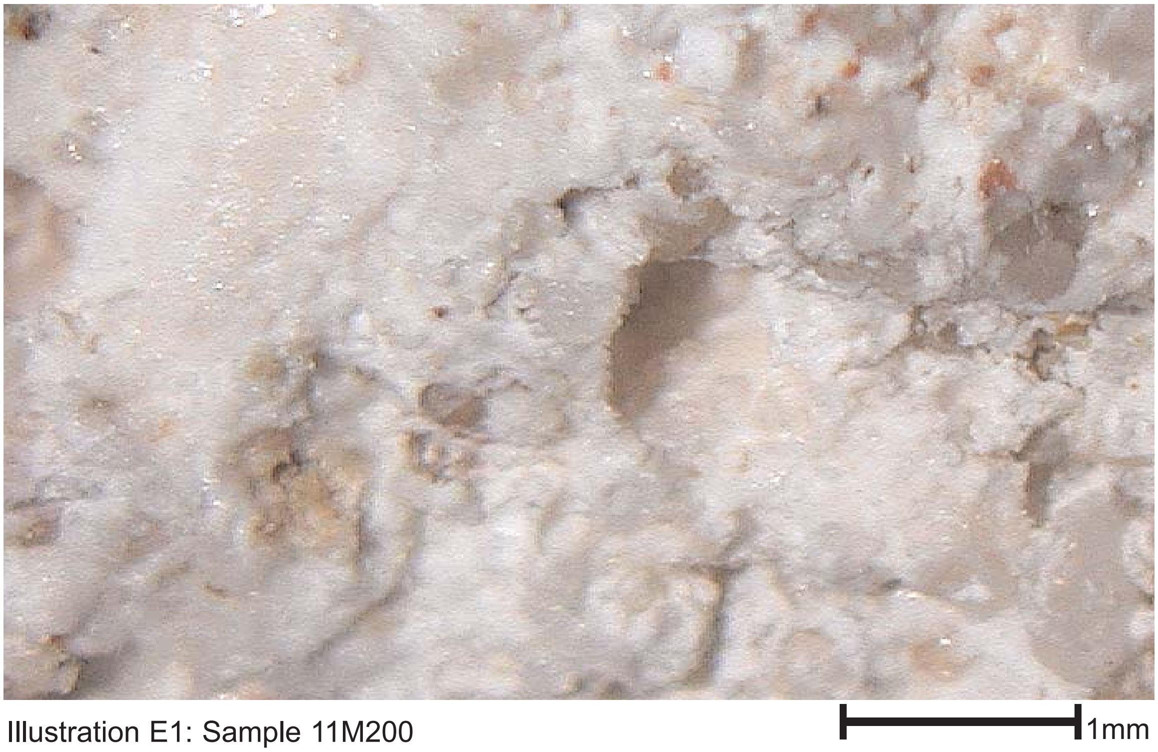

Illustration E1: Sample 11M200

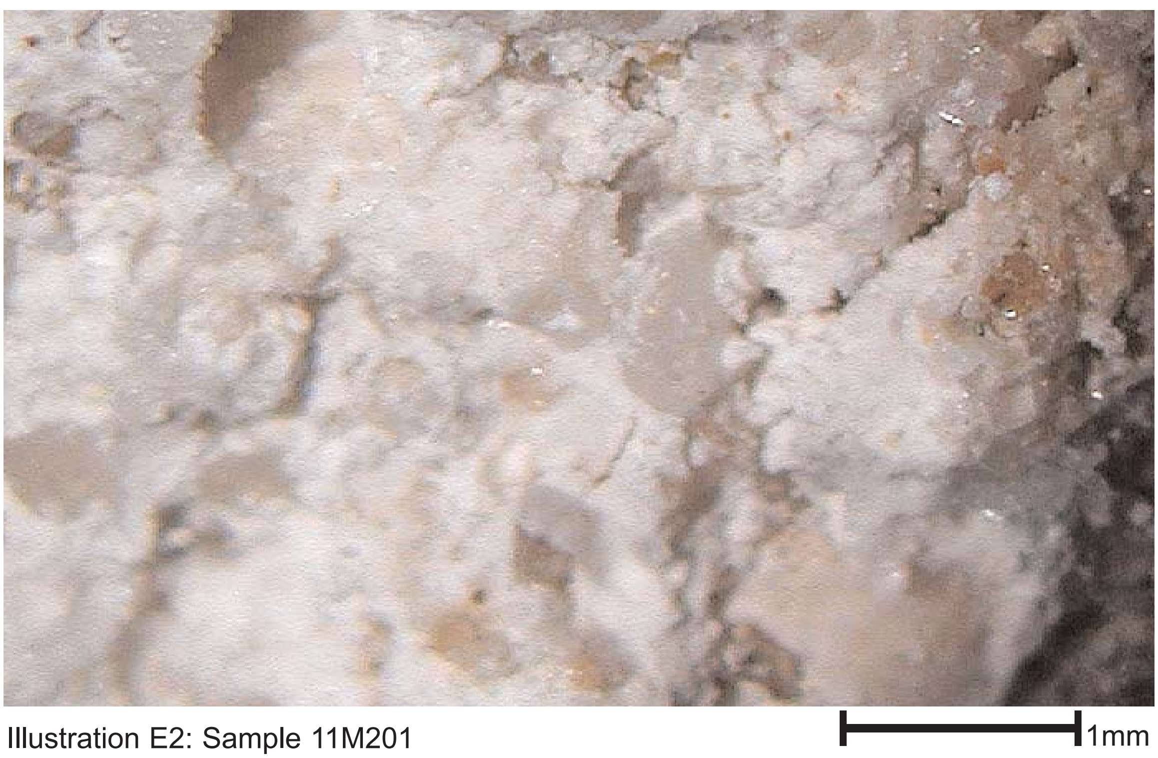

Illustration E2: Sample 11M201

Illustration E3: Sample 13M200 - body

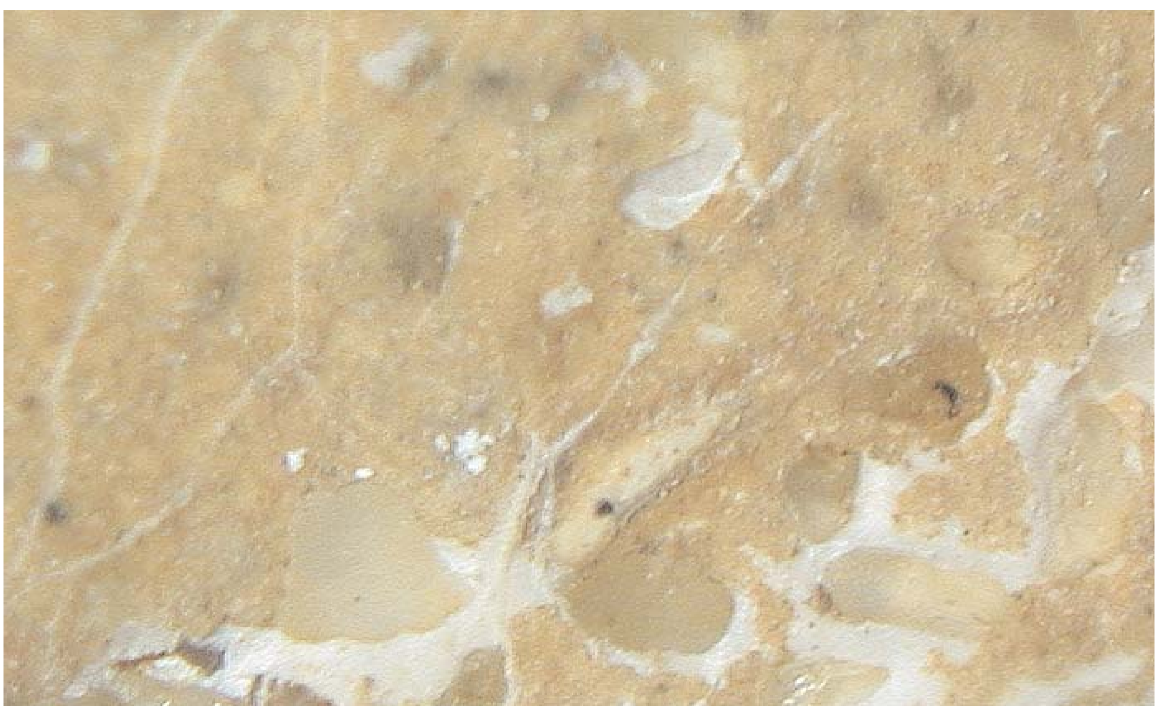

Illustration E4: Sample 13M200 - surface

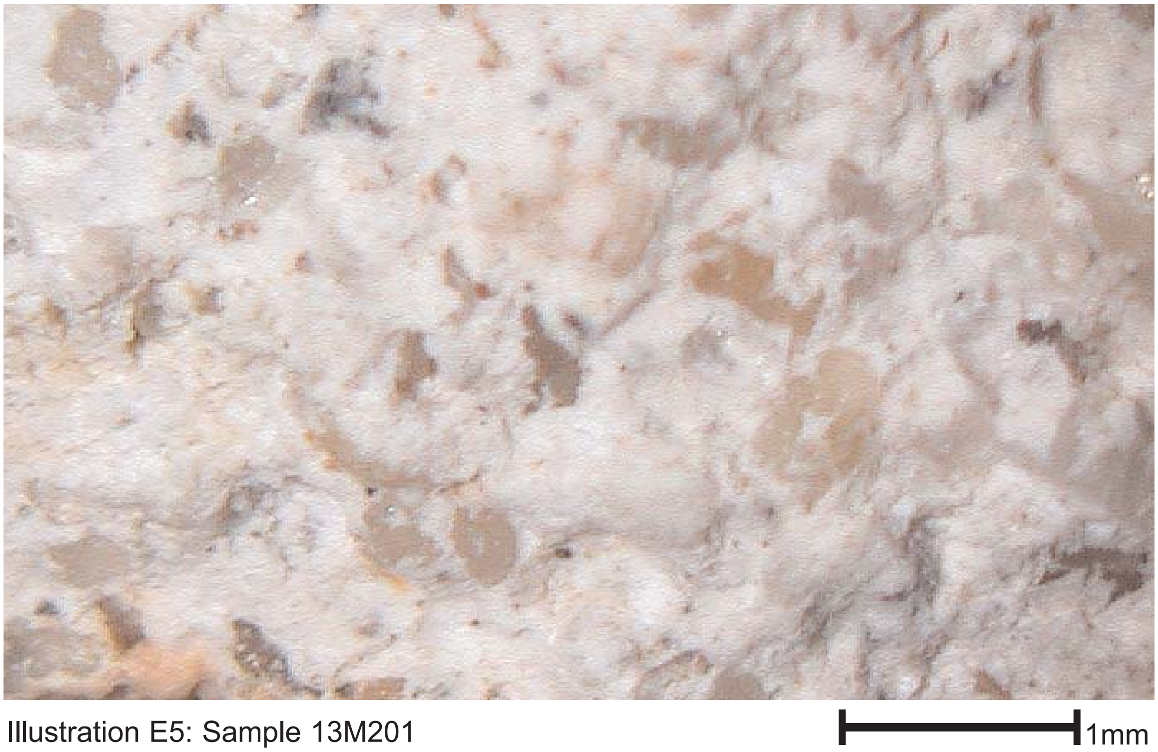

Illustration E5: Sample 13M201

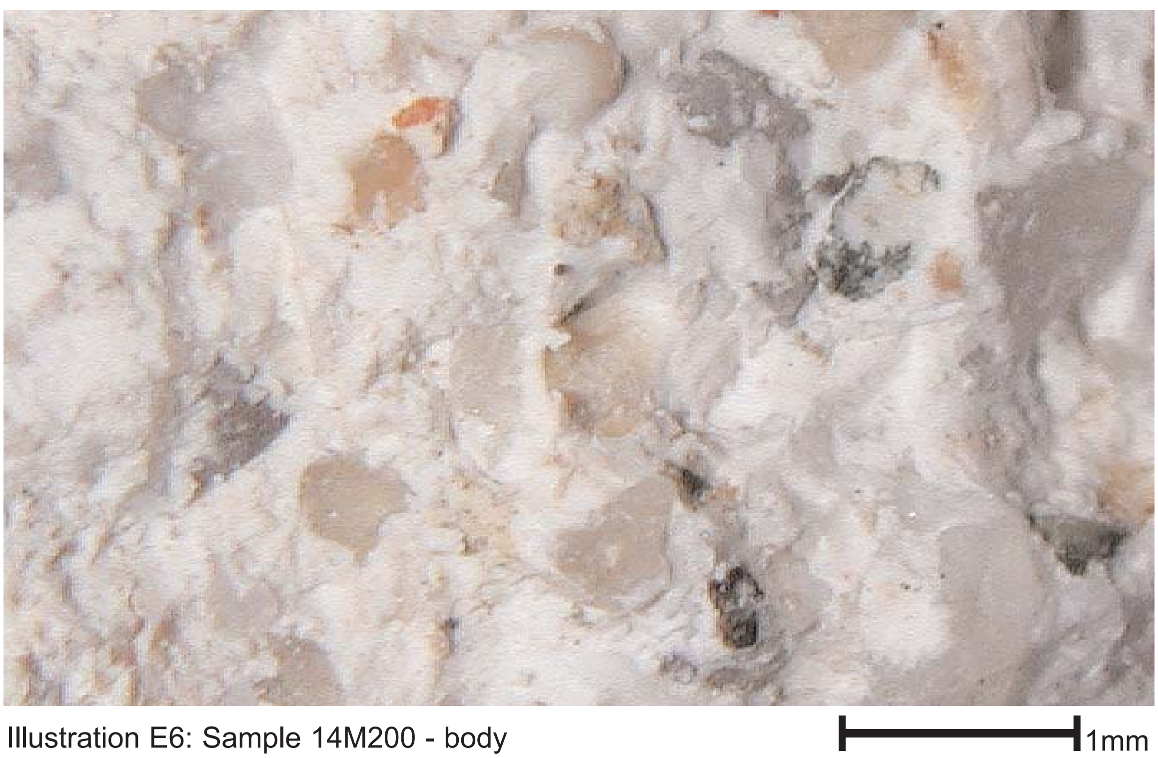

Illustration E6: Sample 14M200 - body

Illustration E7: Sample 14M200 - surface

1mm

Illustration E8: Sample 14M202

1mm

Illustration E9: Sample 14M204 1mm

Illustration E10: Sample 16M200 1mm

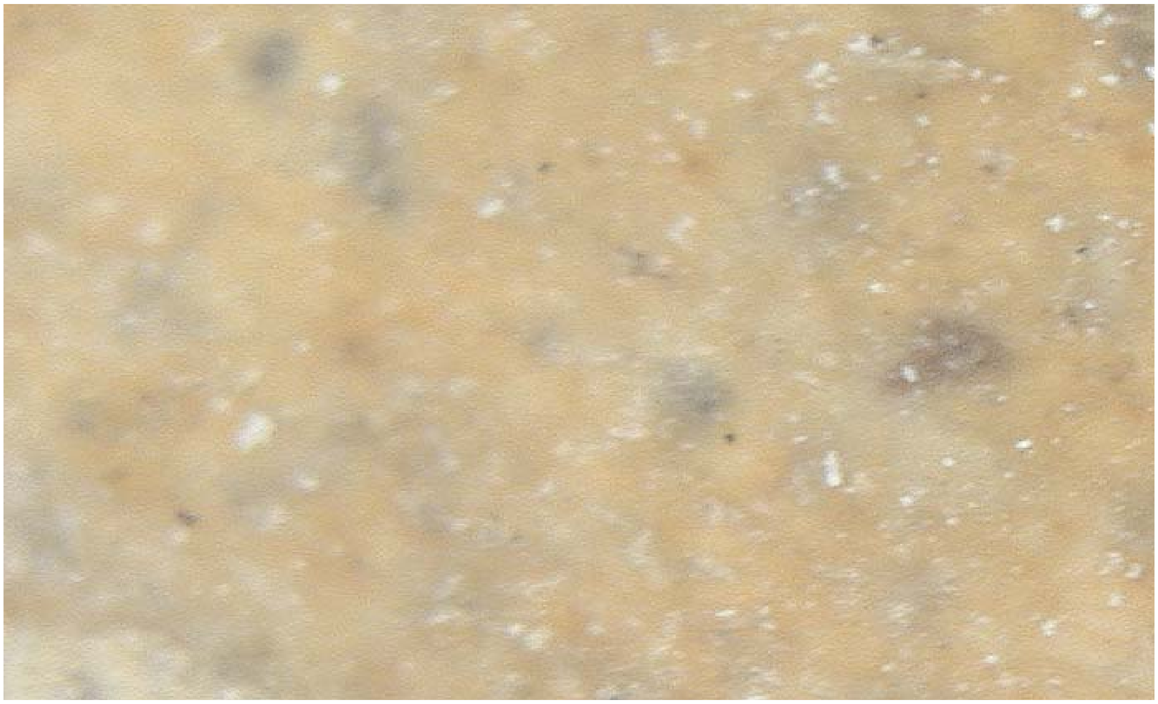

Illustration E11: Sample 16M200 - surface 1mm

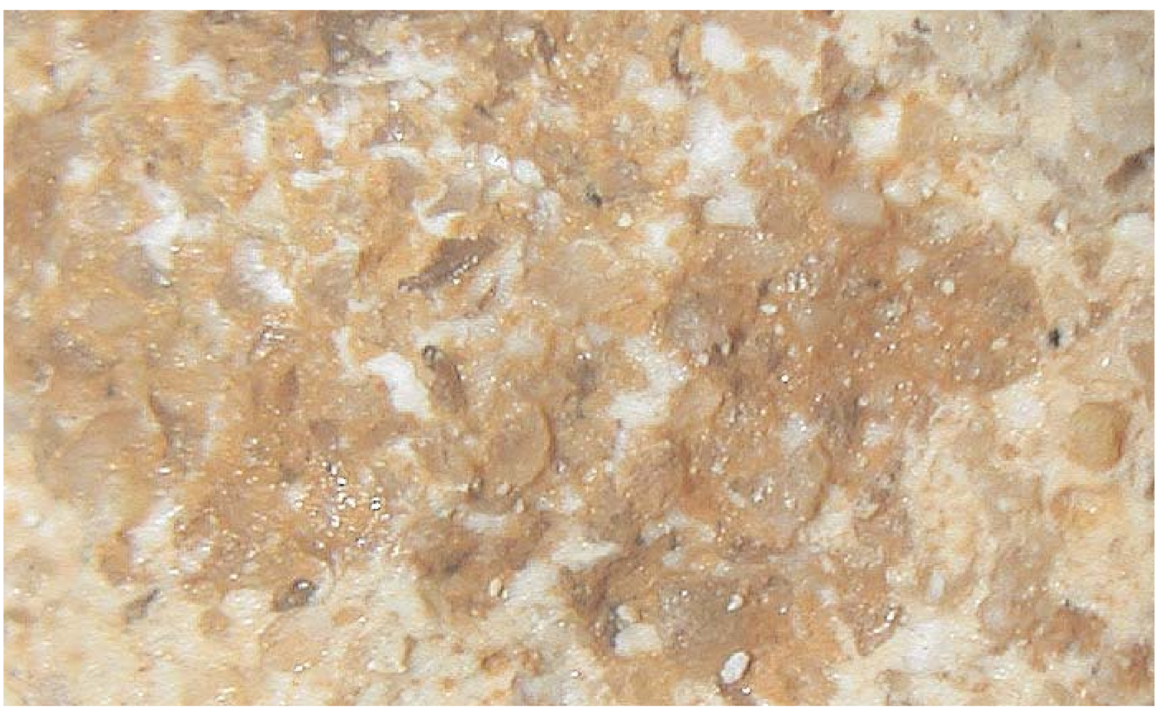

Illustration E12: Sample 16M202 1mm

Illustration E13: Sample 20M201 - body

Illustration E14: Sample 20M201 - surface

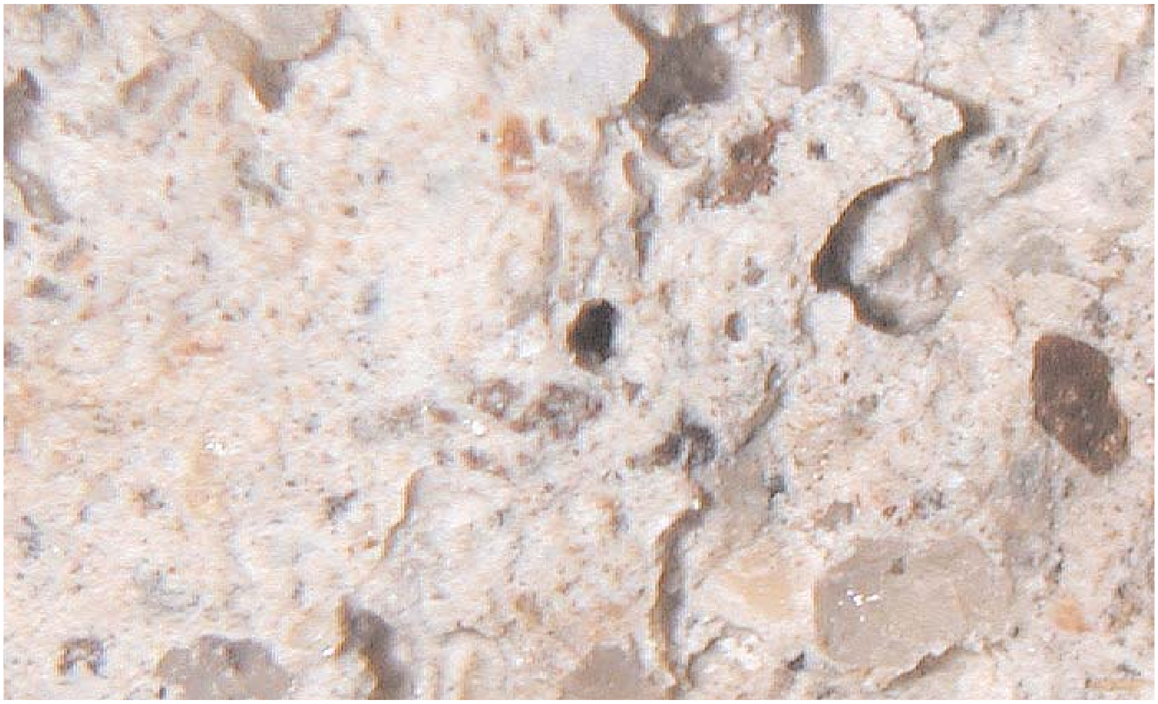

Illustration E15: Sample 20M203 1mm

Illustration E16: Sample 20M205 1mm

Illustration E17: Sample 21M200 - body

Illustration E18: Sample 21M200 - surface

Illustration E19: Sample 21M203 1mm

APPENDIX F: PHOTOMICROGRAPHS OF THIN SECTIONS

All photomicrographs taken at 100X total magnification.

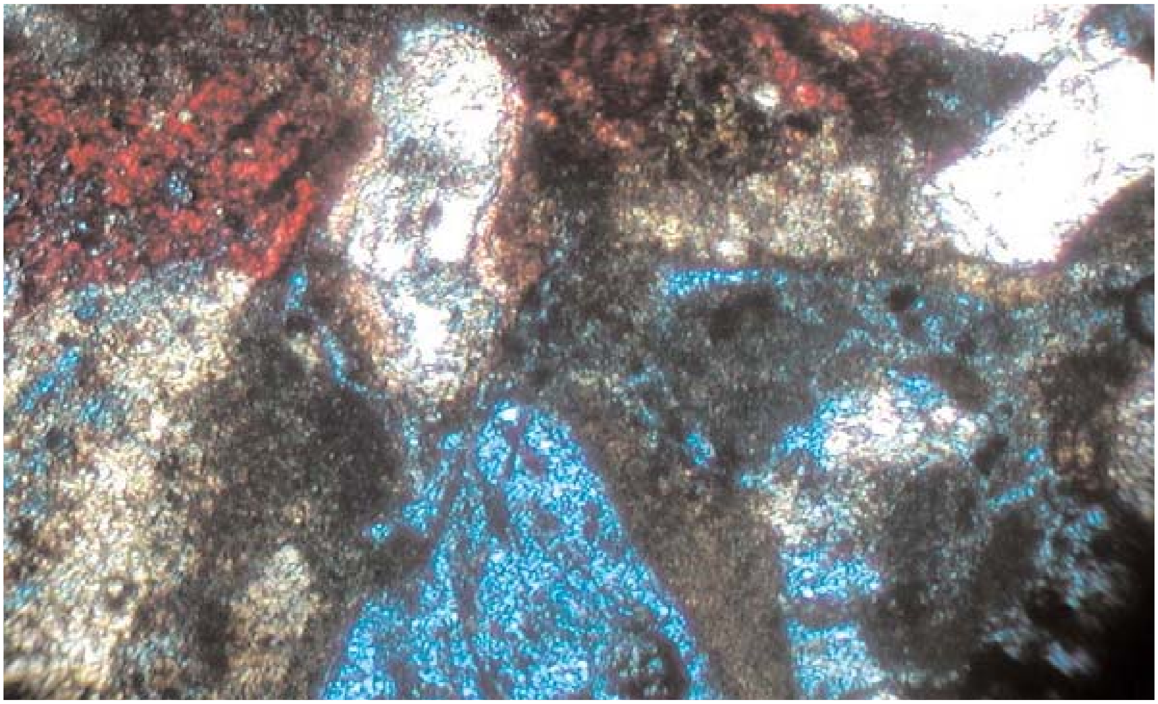

50µm

Illustration F1: Sample 11M200 in transmitted light. Red portion has been stained for calcite. Aggregate is rounded clear quartz. Binder is predominately lime which appears brown in reflected light.

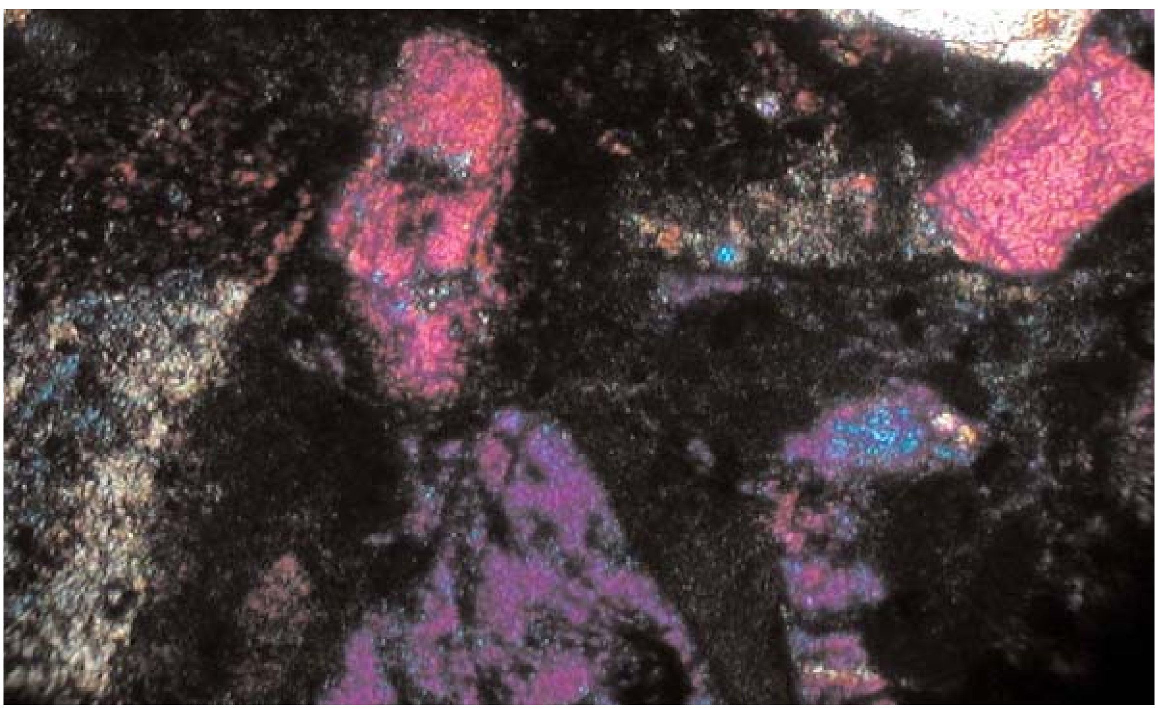

50µm

Illustration F2: Sample 11M200 in transmitted light, crossed polars and full wave compensator (gypsum plate) inserted. The quartz is pink.

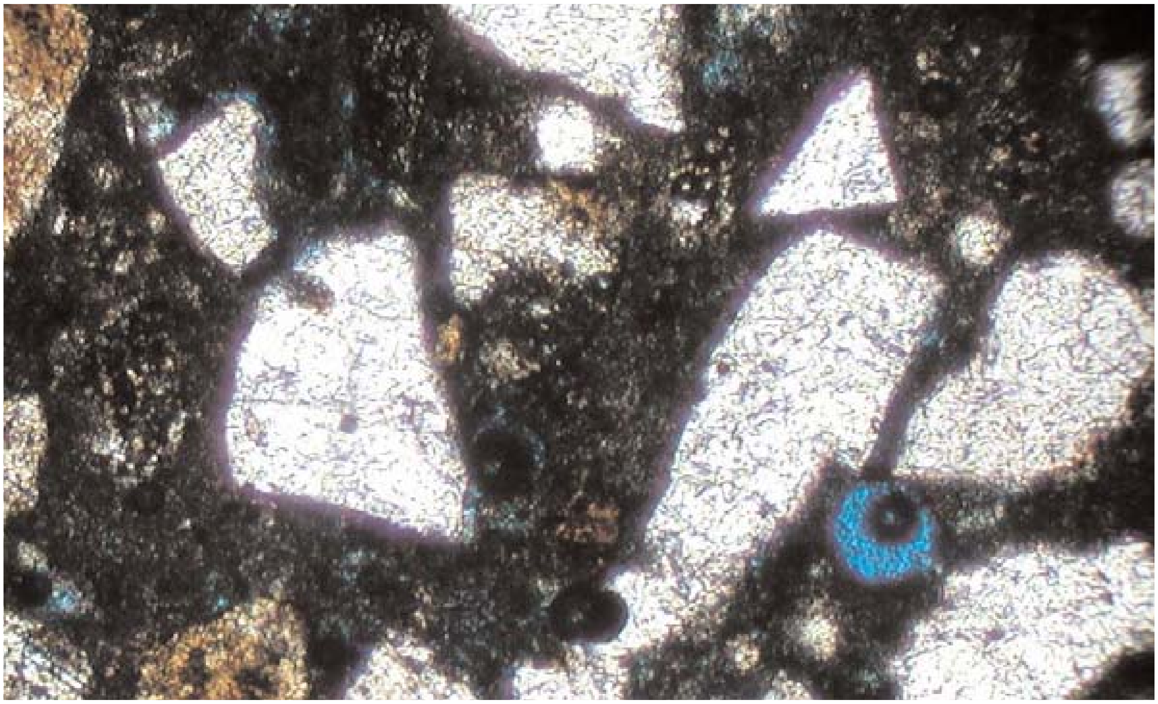

Illustration F3: Sample 11M201 in transmitted light. Note brown discoloration coating quartz aggregate caused by iron oxides. Quartz aggregate is clearly sharp. 50μm

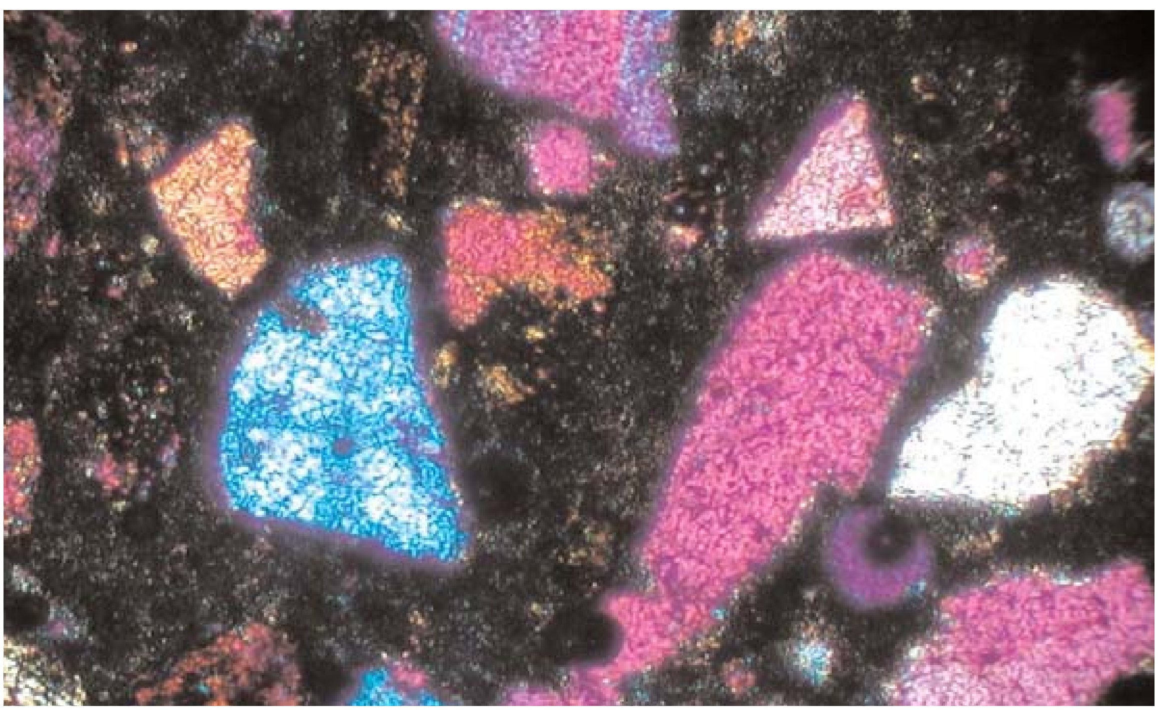

Illustration F4: Sample 11M201 in transmitted light, crossed polars and full wave compensator (gypsum plate) inserted. Quartz is pink and blue. The well-graded nature of this aggregate is clearly evident. 50μm

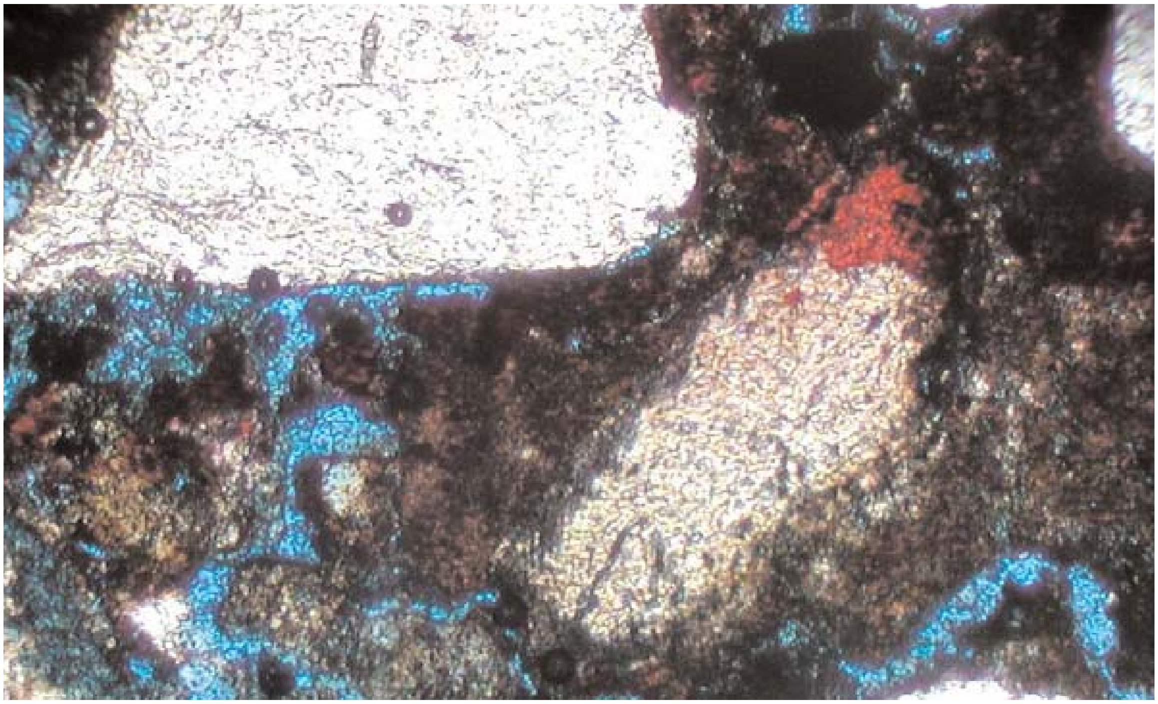

Illustration F5: Sample 13M200 in transmitted light. Red portion has been stained for calcite. Note the rounded quartz aggregate and number of pores in the lime binder.

50µm

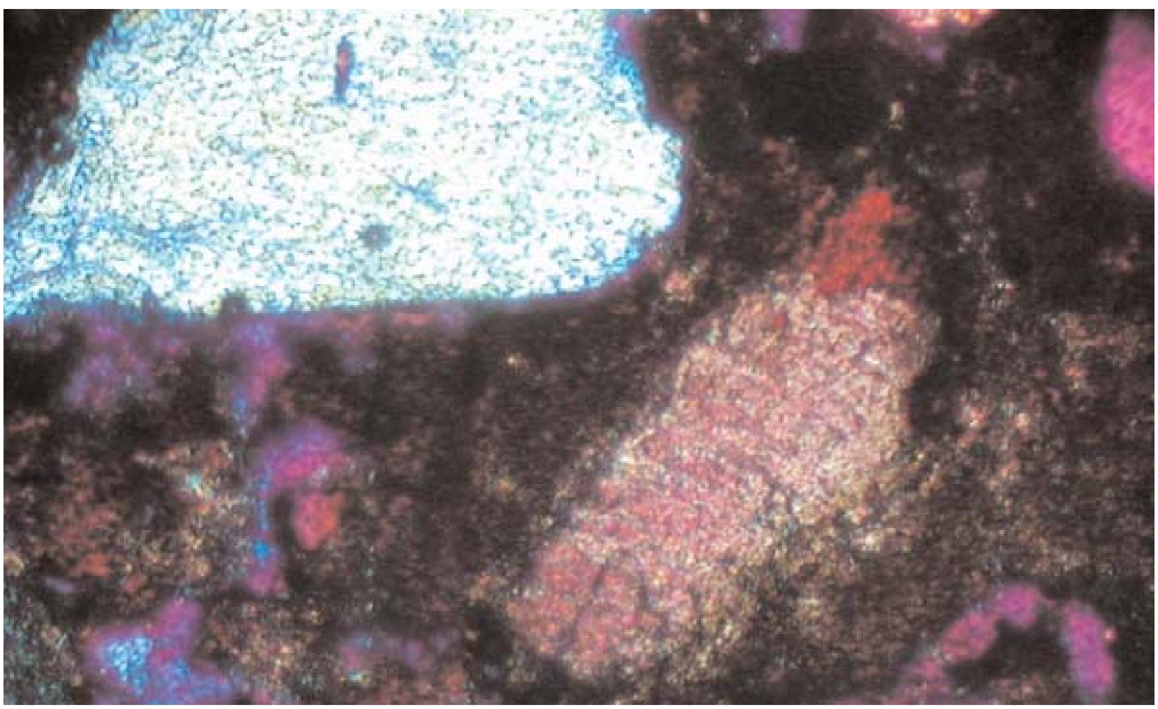

Illustration F6: Sample 13M200 in transmitted light, crossed polars and full wave compensator (gypsum plate) inserted. The grain on the lower right is a bioclast which is evident by its staining and behavior under crossed polars.

50µm

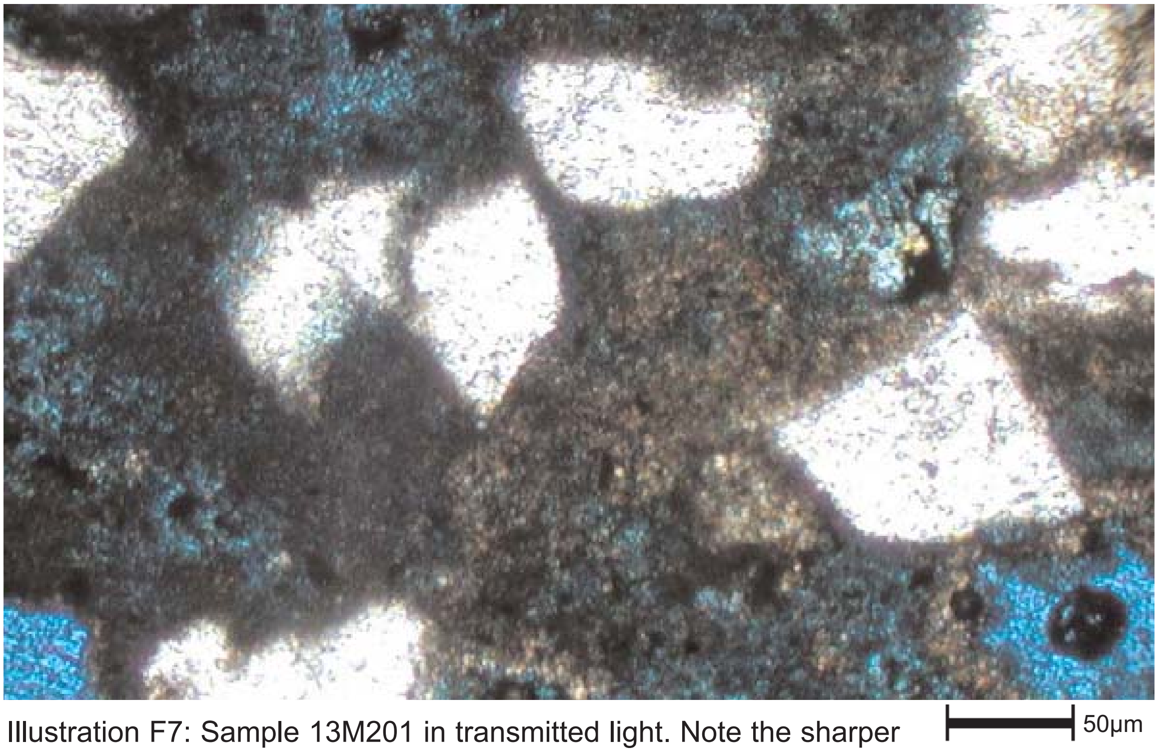

Illustration F7: Sample 13M201 in transmitted light. Note the sharper sand in this sample. This is a bedding mortar; compare with sample 13M200 which is a render.

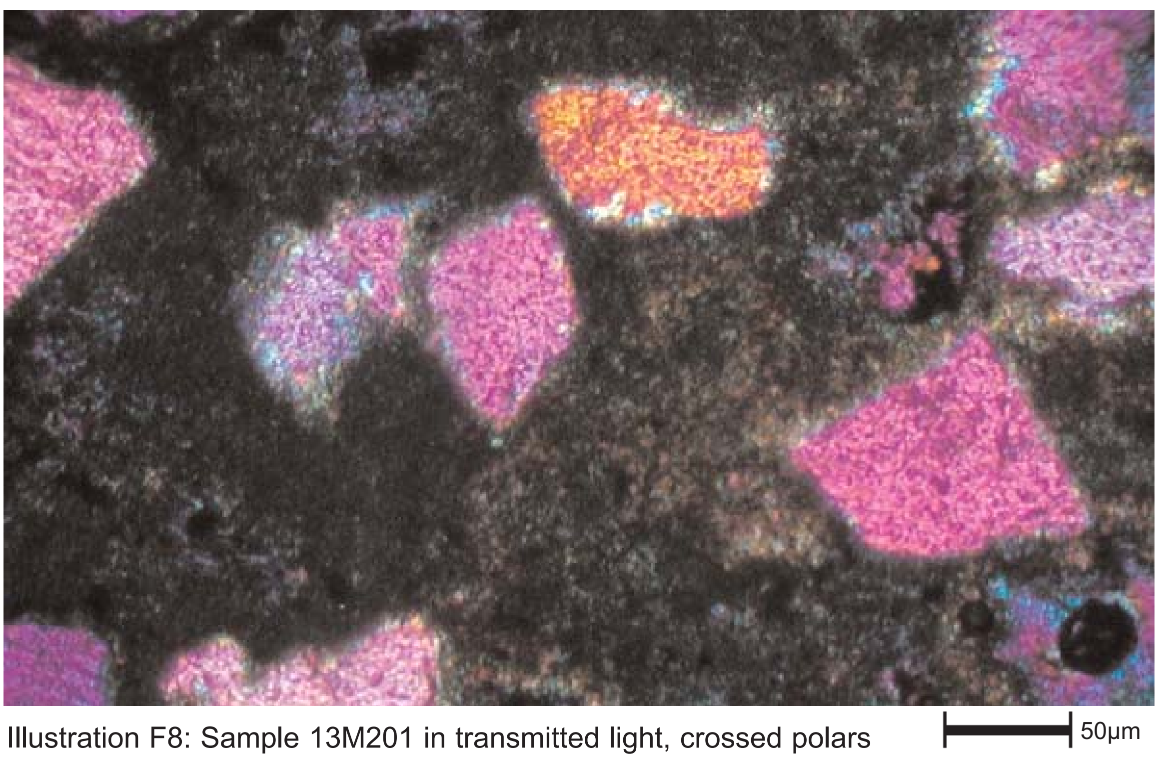

Illustration F8: Sample 13M201 in transmitted light, crossed polars and full wave compensator (gypsum plate) inserted.

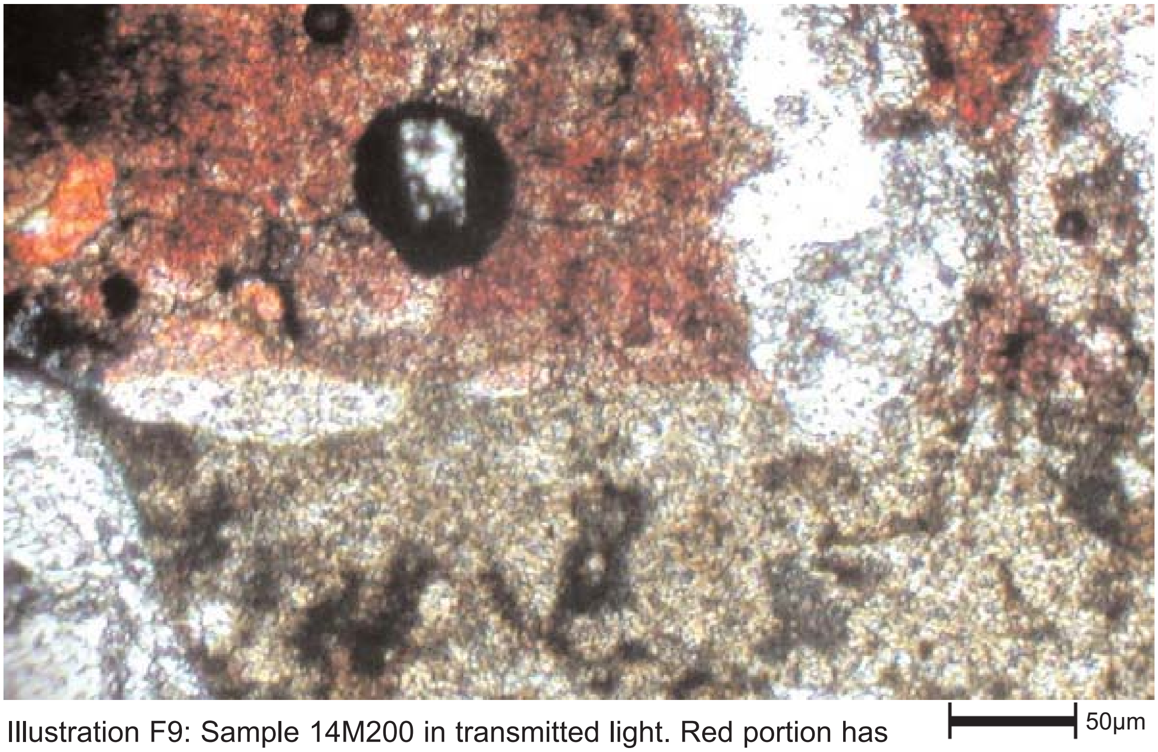

Illustration F9: Sample 14M200 in transmitted light. Red portion has been stained for calcite. The binder in this sample is notable for its low porosity.

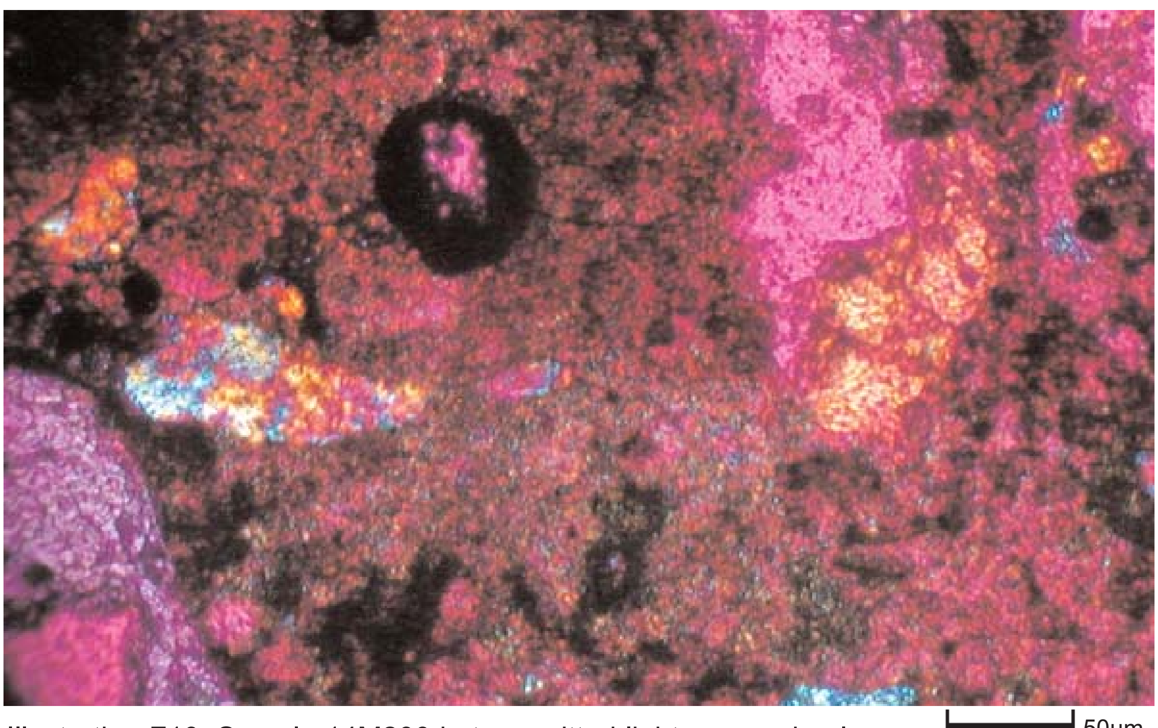

Illustration F10: Sample 14M200 in transmitted light, crossed polars and full wave compensator (gypsum plate) inserted.

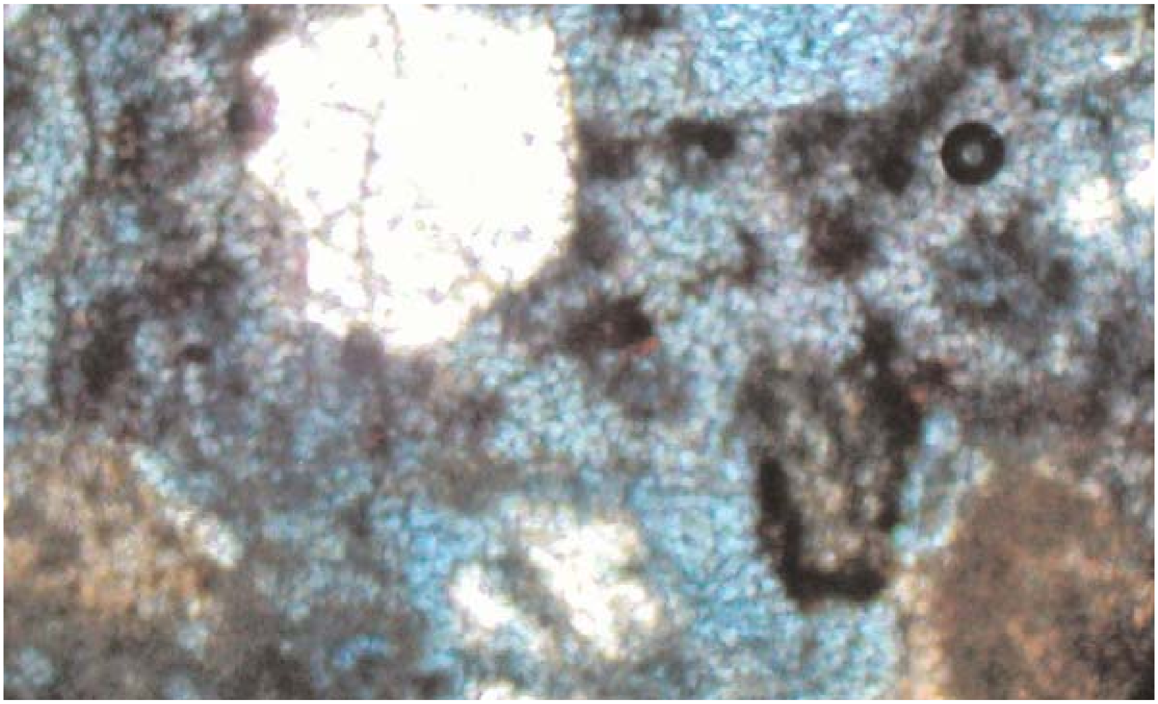

Illustration F11: Sample 14M202 in transmitted light. Red portion has been stained for calcite. This sample is quite porous.

50µm

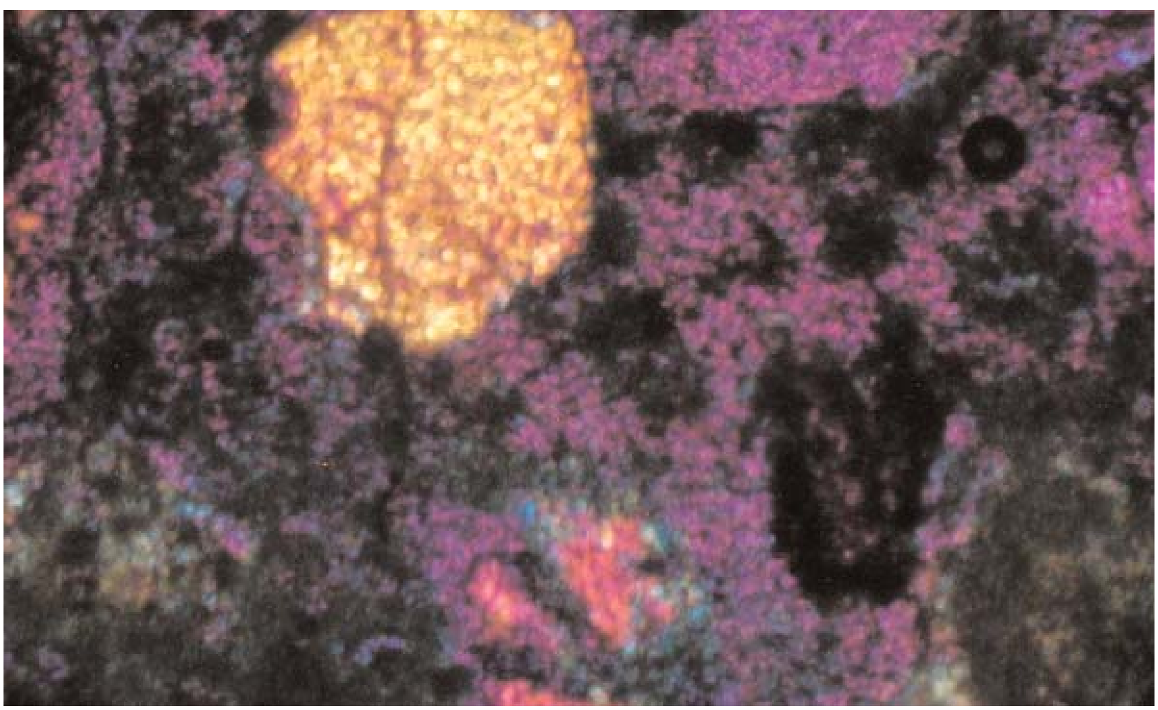

Illustration F12: Sample 14M202 in transmitted light, crossed polars and full wave compensator (gypsum plate) inserted.

50µm

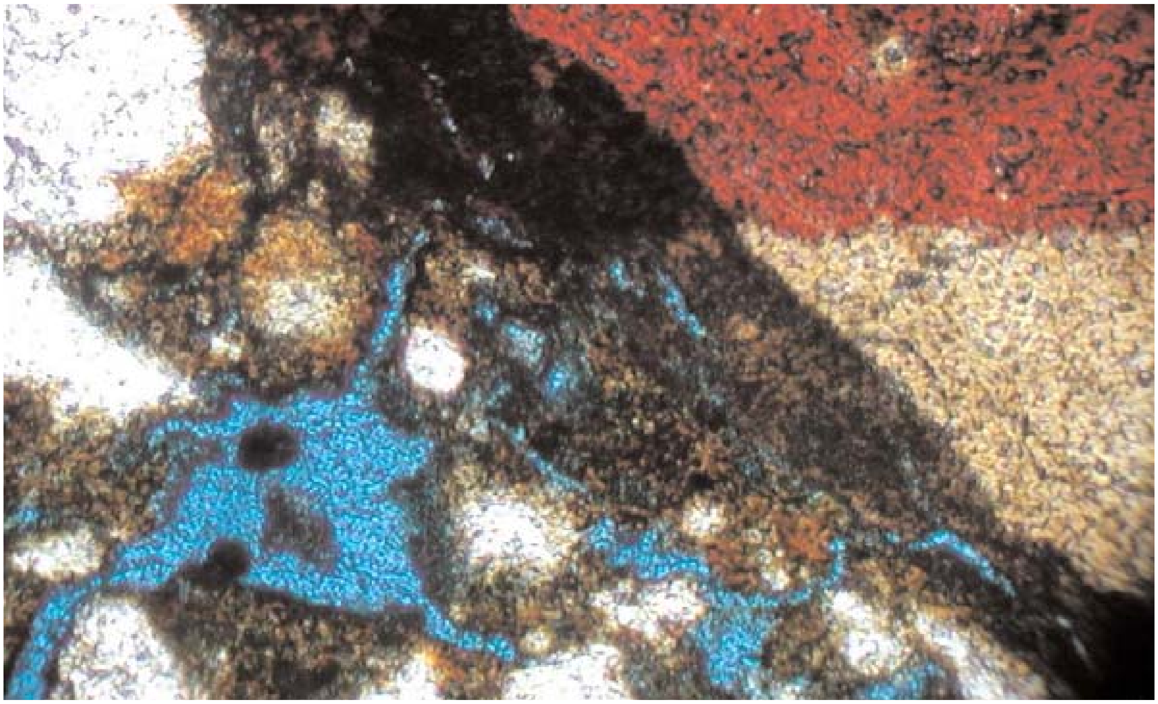

Illustration F13: Sample 14M204 in transmitted light. Red portion has been stained for calcite. This sample contains clays. Note the different color of the binder compared to the previous samples.

50µm

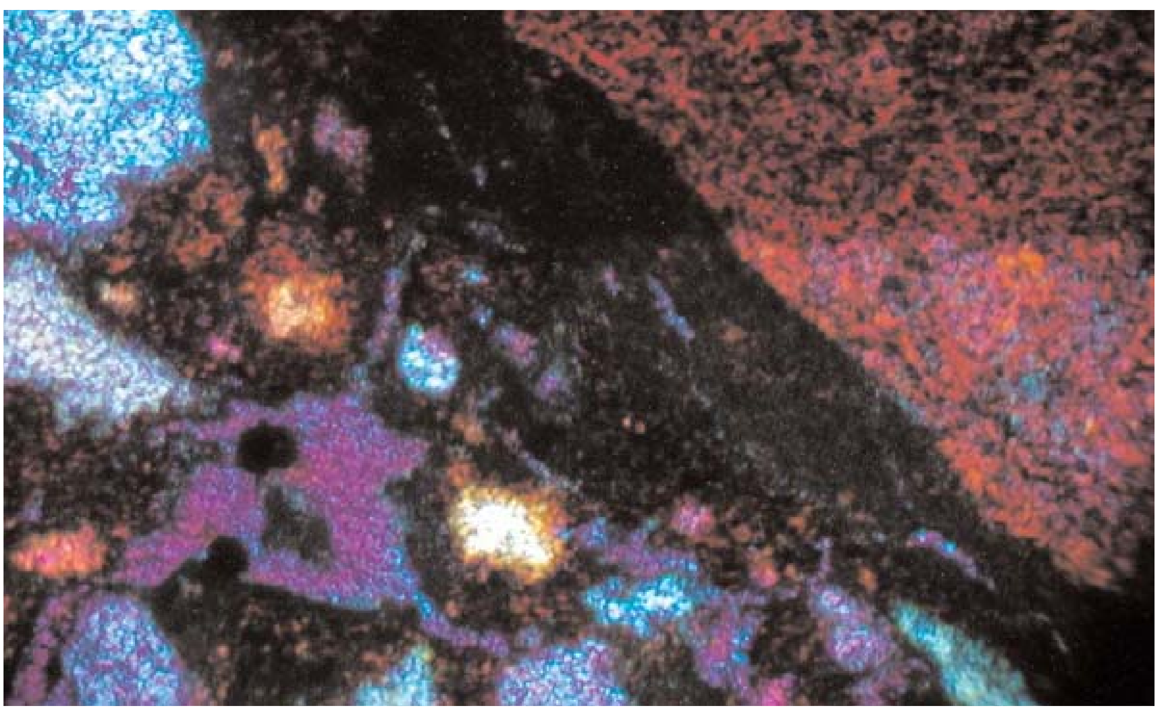

Illustration F14: Sample 14M204 in transmitted light, crossed polars and full wave compensator (gypsum plate) inserted.

50µm

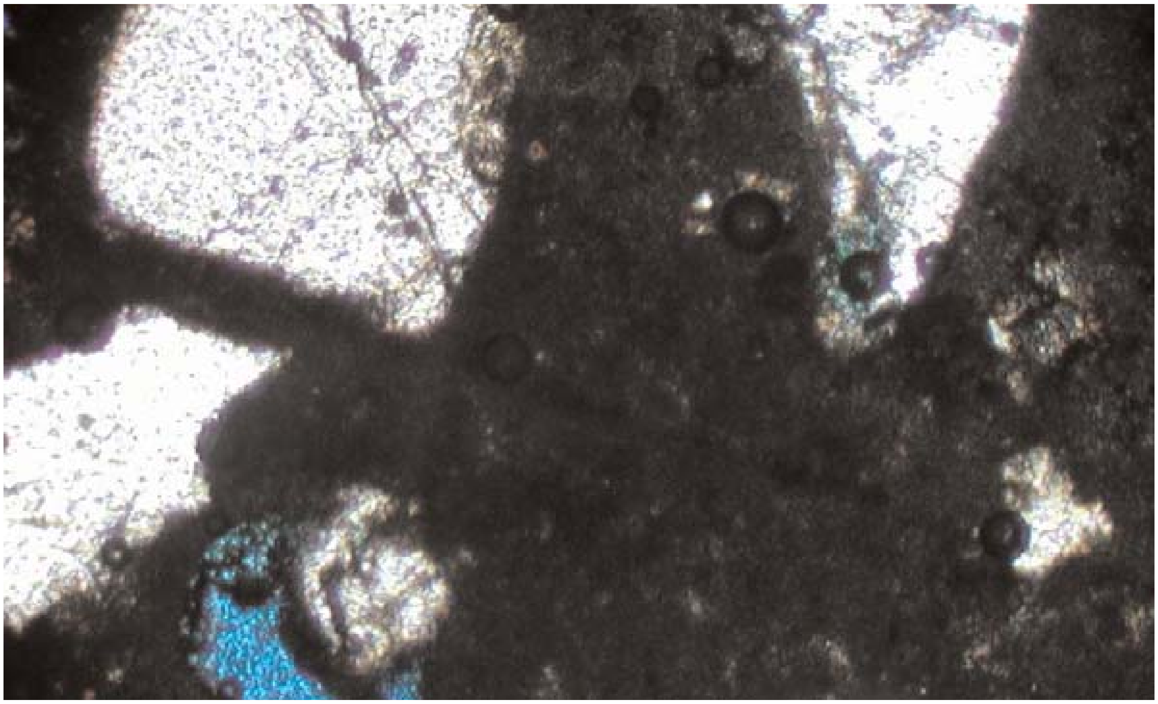

Illustration F15: Sample 16M200 in transmitted light. 50µm

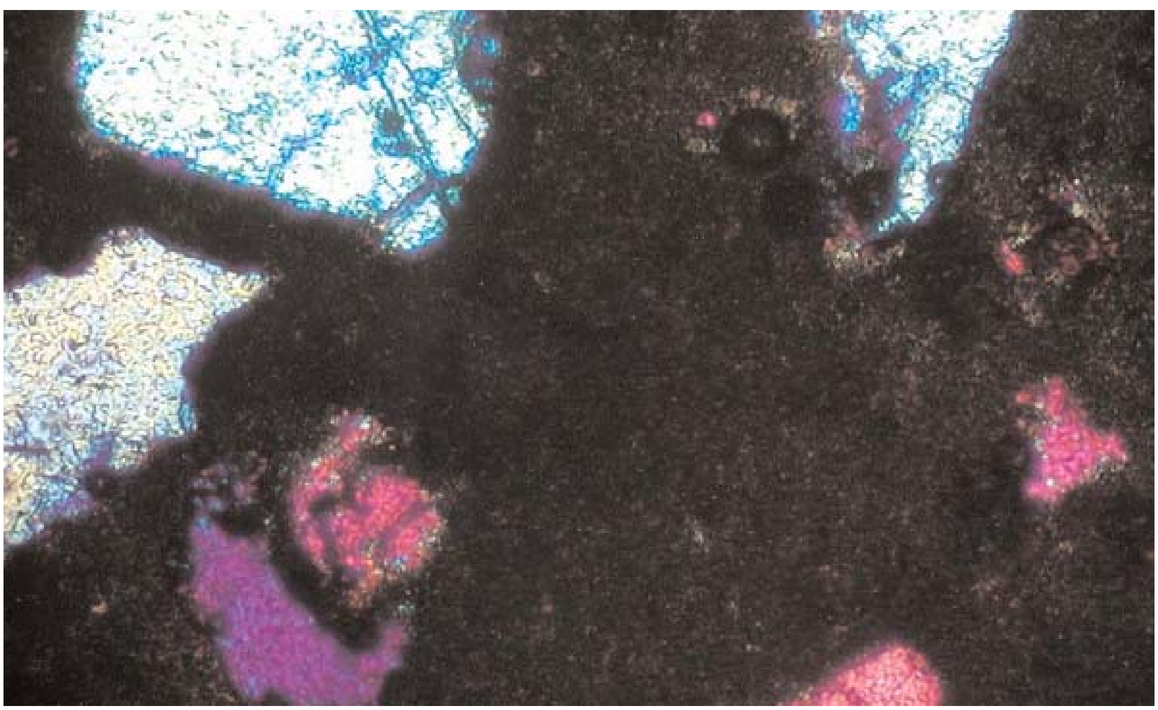

Illustration F16: Sample 16M200 in transmitted light, crossed polars and full wave compensator (gypsum plate) inserted. 50µm

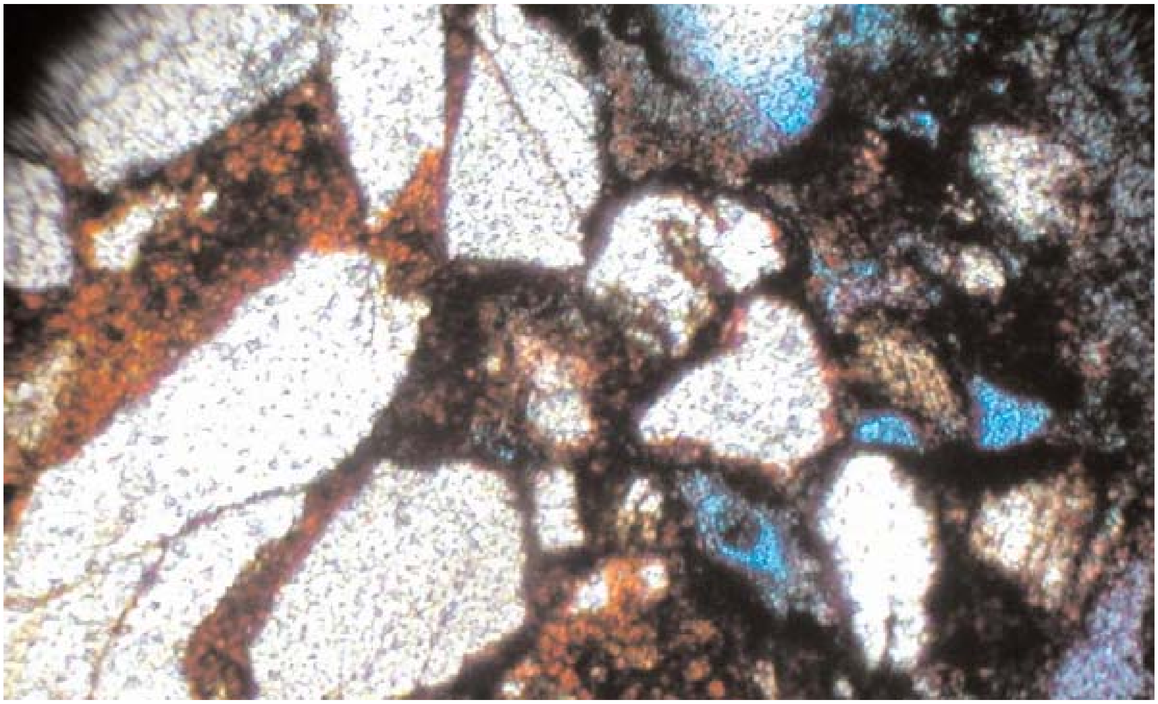

Illustration F17: Sample 16M202 in transmitted light. Red portion has been stained for calcite. The aggregate in this sample is sharper than in the previous one.

50µm

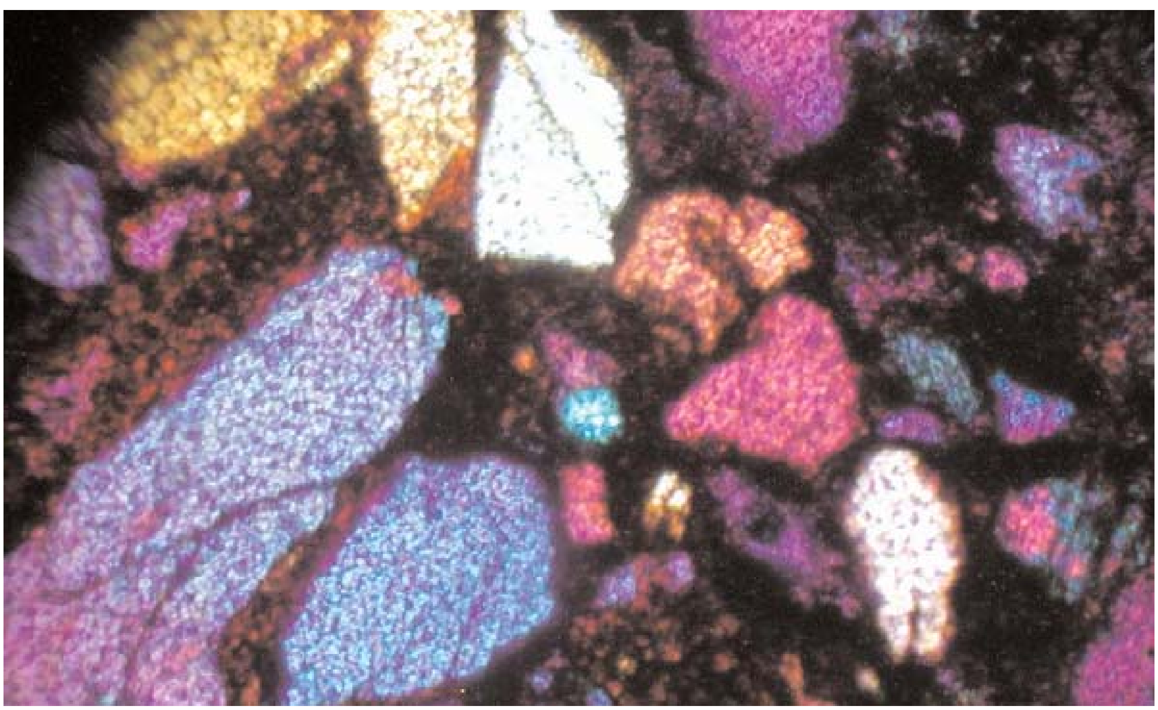

Illustration F18: Sample 16M202 in transmitted light, crossed polars and full wave compensator (gypsum plate) inserted.

50µm

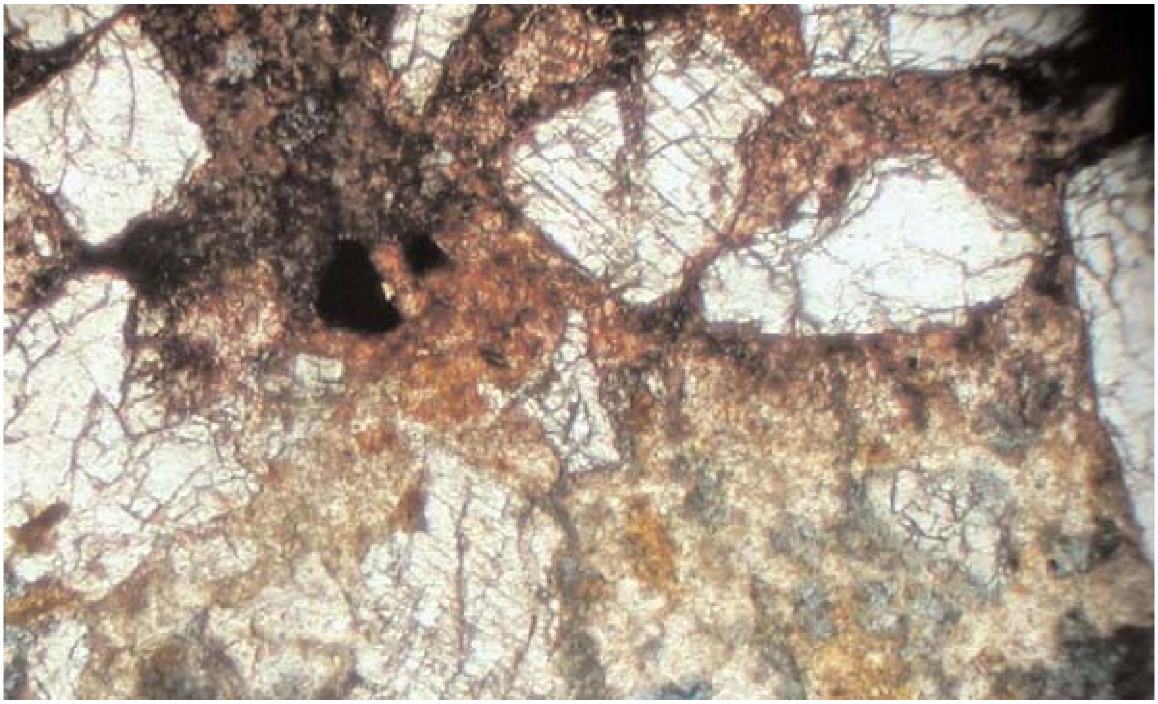

Illustration F19: Sample 16M205 in transmitted light. Red portion has been stained for calcite. This is a bedding mortar; note the sharper nature of the sand. 50µm

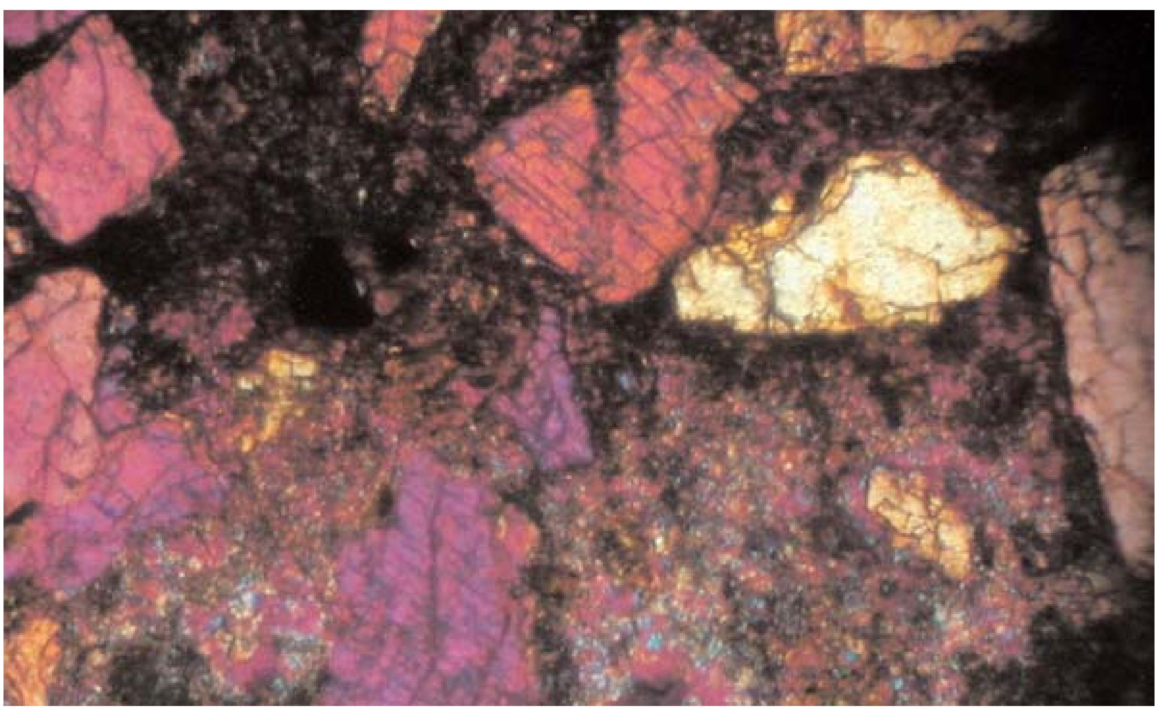

Illustration F20: Sample 16M205 in transmitted light, crossed polars and full wave compensator (gypsum plate) inserted. This sample contains brick powder which is evident from the behavior of the binder under crossed polars. 50µm

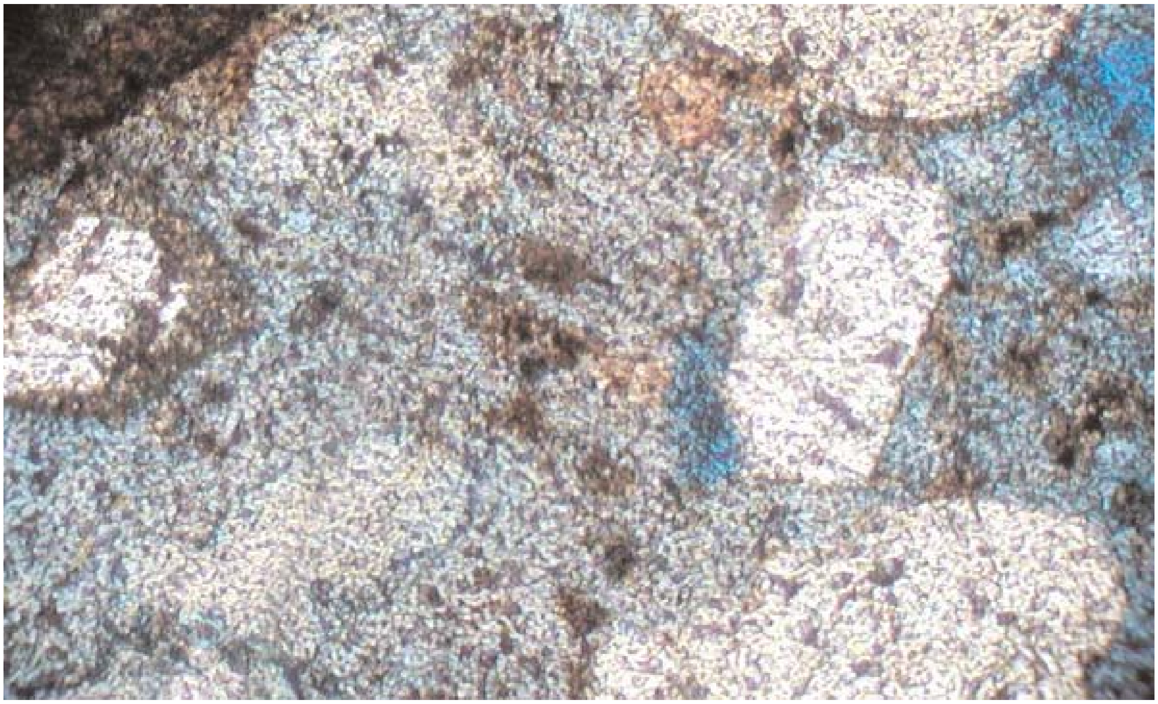

Illustration F21: Sample 20M201 in transmitted light. Note the large number of pores in the binder.

50μm

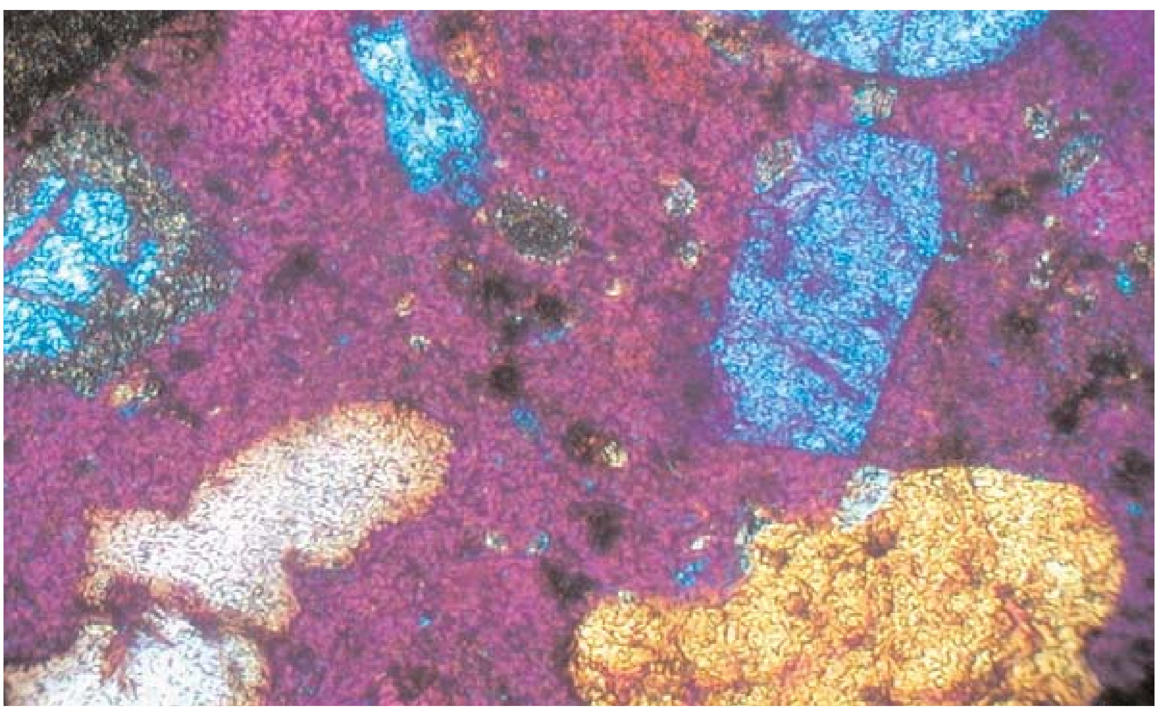

Illustration F22: Sample 20M201 in transmitted light, crossed polars and full wave compensator (gypsum plate) inserted.

50μm

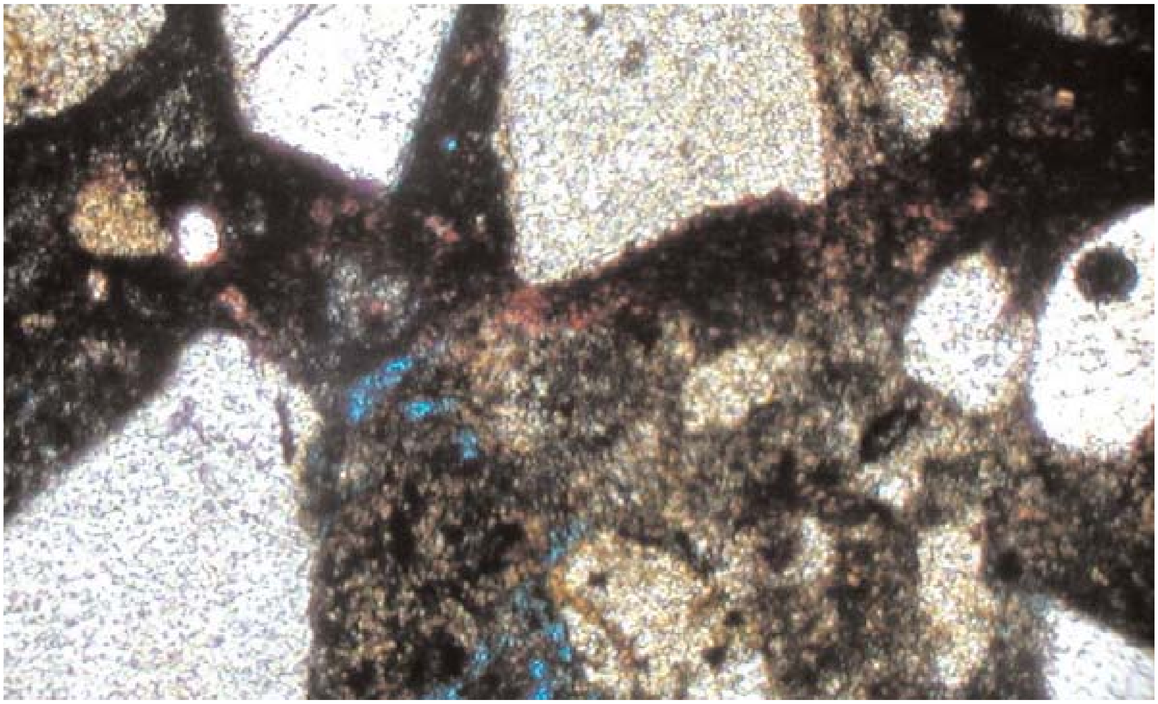

Illustration F23: Sample 20M203 in transmitted light. Red portion has been stained for calcite. Note the varied nature of the aggregate.

50µm

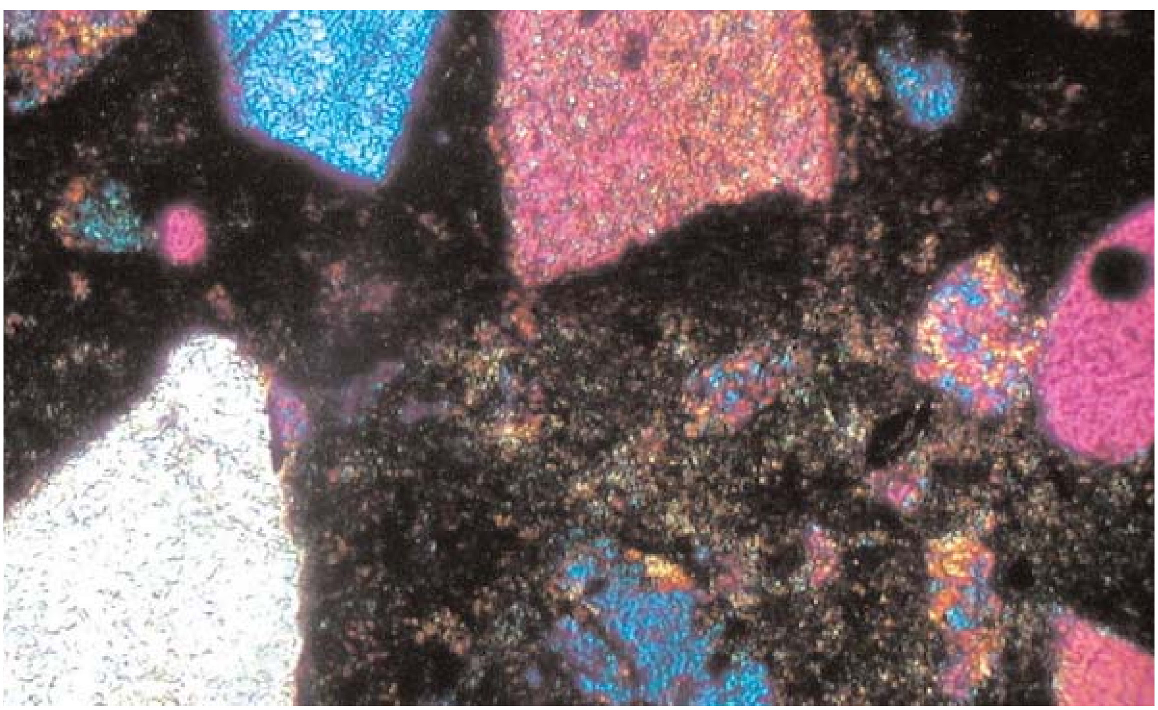

Illustration F24: Sample 20M203 in transmitted light, crossed polars and full wave compensator (gypsum plate) inserted.

50µm

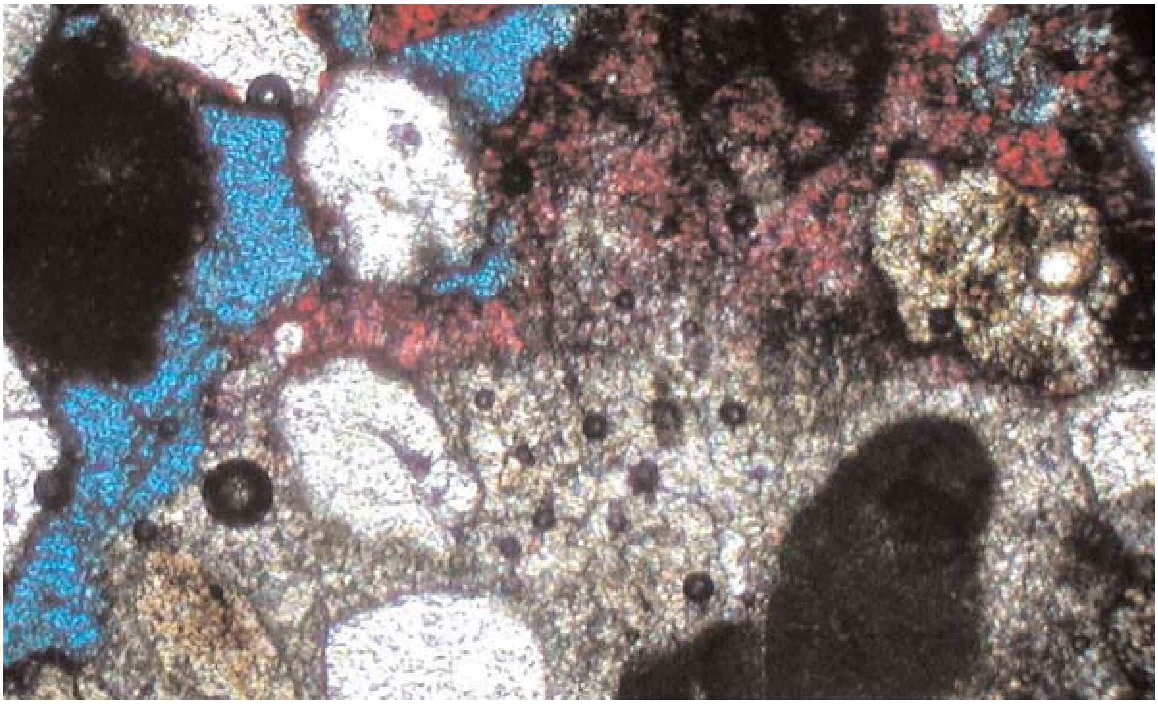

Illustration F25: Sample 20M205 in transmitted light. Red portion has been stained for calcite.

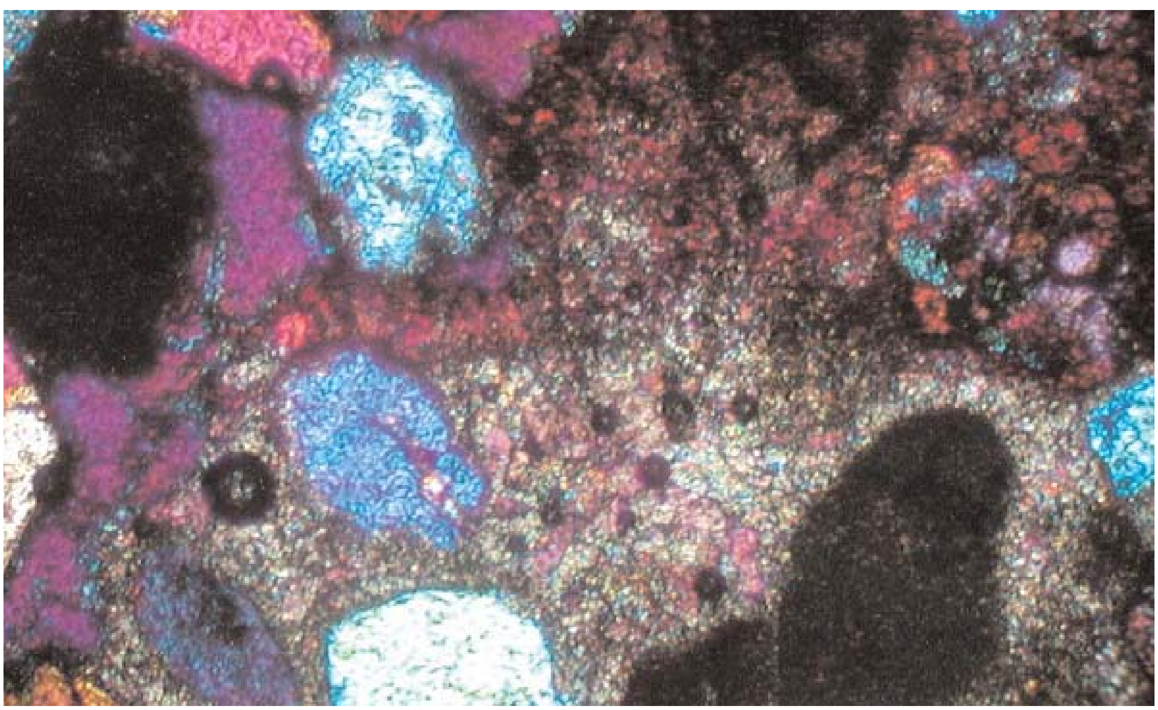

Illustration F26: Sample 20M205 in transmitted light, crossed polars and full wave compensator (gypsum plate) inserted.

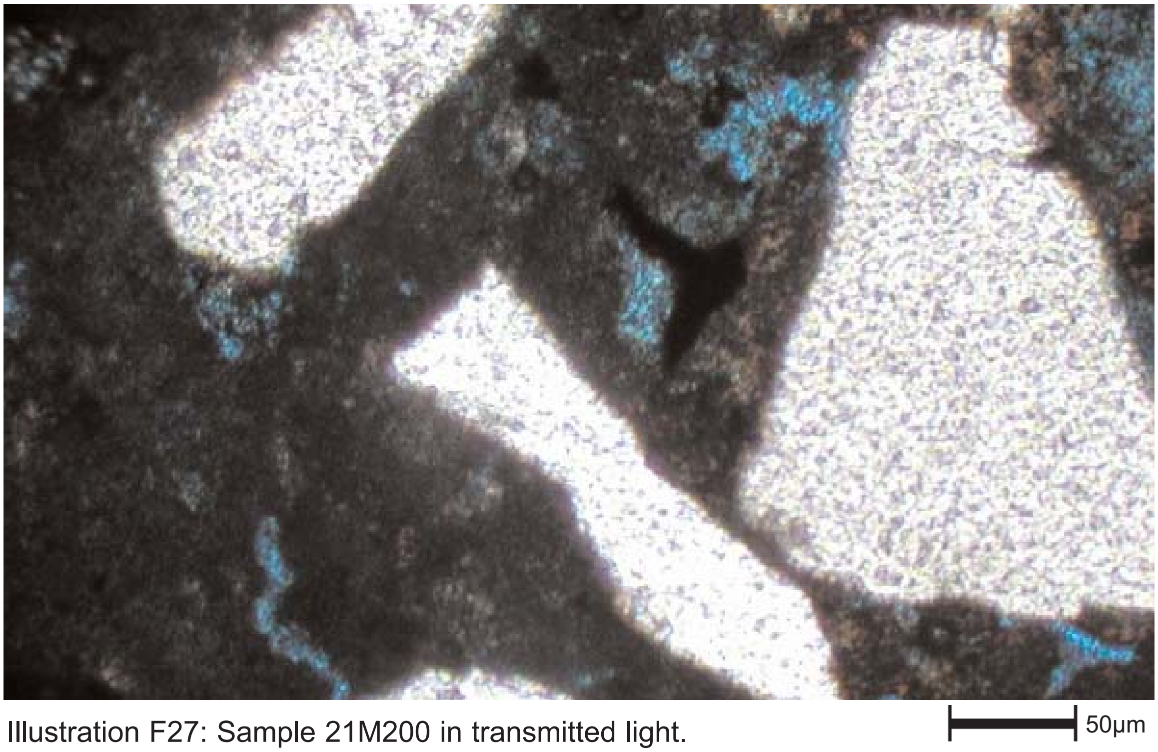

Illustration F27: Sample 21M200 in transmitted light.

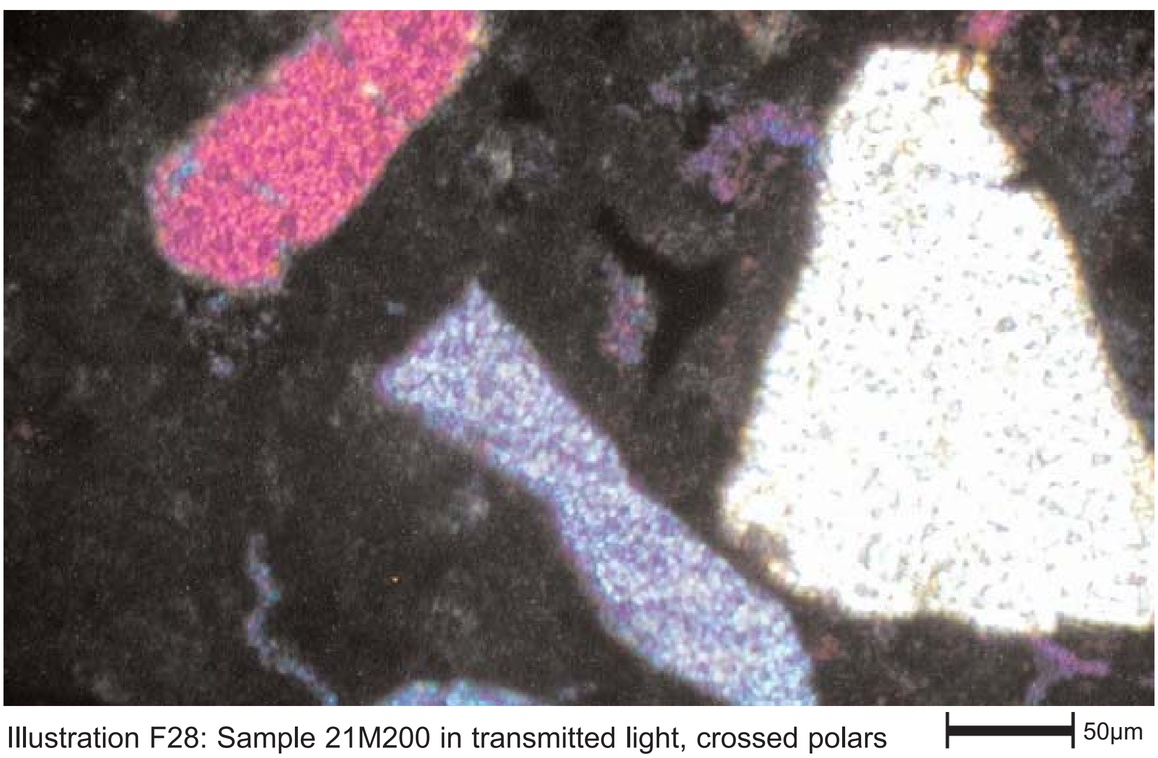

Illustration F28: Sample 21M200 in transmitted light, crossed polars and full wave compensator (gypsum plate) inserted.

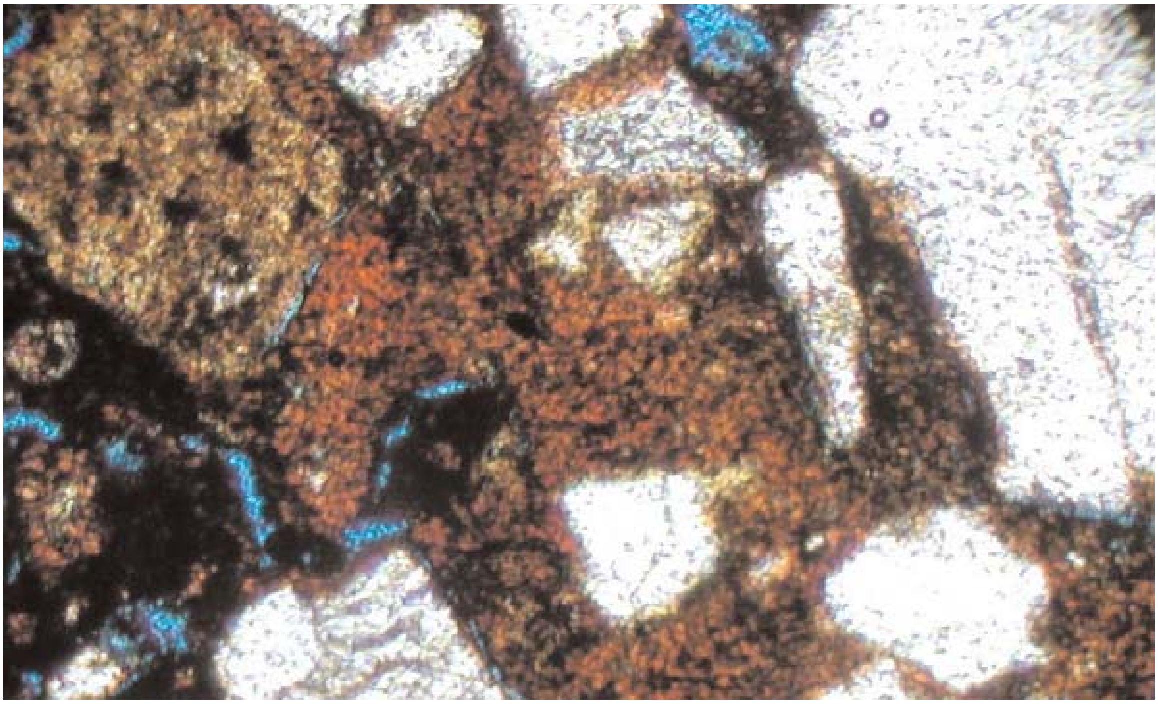

Illustration F29: Sample 21M203 in transmitted light. Red portion has been stained for calcite. This sample contains clay which is partially evident from the color of the binder.

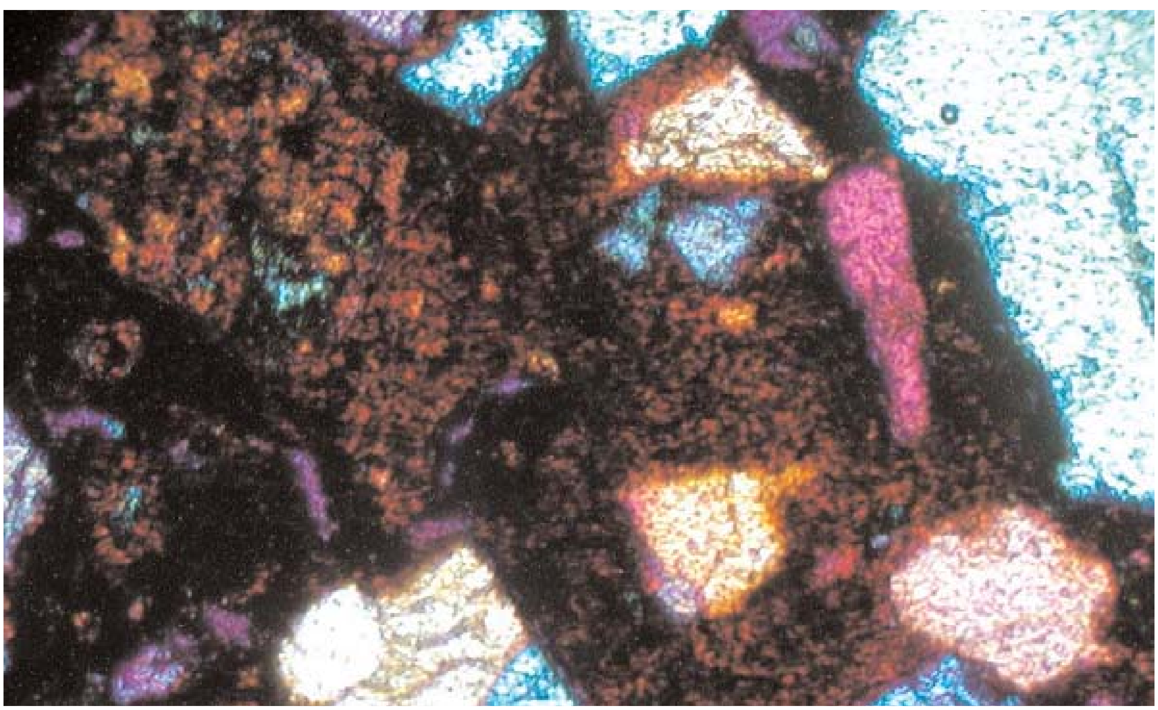

Illustration F30: Sample 21M203 in transmitted light, crossed polars and full wave compensator (gypsum plate) inserted. Compare the appearance of this binder with that of sample 16M205.

APPENDIX G: BINDER AND AGGREGATE CHARACTERIZATION

Characterization was performed using a polarizing light microscope with the methods and terminology as described in *Micromorphology of Soils* (FitzPatrick, 1984). Both reflected and transmitted light were employed; crossed polars were used for specific mineral species identification.

Aggregates are characterized by their frequency, expressed as a percentage from 0% to 50%.

Table G1: Binder characterization

Sample ID	Calcite stain	Porosity	Ratio*	Reflected light	Transmitted light	@ 1000x mag.
11M200	Nearly complete	13%	1:1	Pearly white paste with reddish tint	Dark brown-green (mottled & opaque)	Opaque white with slightly tan areas – no brick powder
11M201	Nearly complete	9%	1:2	Pearly white paste	Dark brown	Opaque white with areas of reddish particles – no brick powder
13M200	Nearly complete	41%	1:2	Quite white, pearly paste	Dark brown, fairly opaque	Very white
13M201	Complete	35%	1:3	White paste with slight red tint	Dark brown, slightly opaque	Transparent white paste
14M200	Complete	<5%	1:2	Gray-white paste	Light brown-white paste	White paste
14M202	Nearly complete	29%	1:2	Transparent white with rosy-brown tint	Mottled brown, fairly opaque	Mottled light brown with transparent white – no brick powder
14M202	Incomplete: areas of brown and green with no stain	50%	1:9	Green-brown paste, fairly opaque	Dark green-brown paste, fairly opaque	Mottled green/tan/white paste – no brick powder
16M200	No**	34%	1:3	White paste with a light red tint	Dark brown paste	Transparent white paste with a brown tint
16M202	Nearly complete	13%	1:2	Transparent white paste	Light brown to green paste (transparent)	Transparent white

Sample ID	Calcite stain	Porosity	Ratio*	Reflected light	Transmitted light	@ 1000x mag.
16M205	Irregular: tan areas incomplete	10%	1:3	Transparent white and brown paste	Green-gray and yellow brown paste	Transparent white with mottled tan and green-tan areas – brick powder is evident
20M201	Some; almost no staining of paste. Only present around quartz grains	39%	1:2	Quite transparent white paste	Light blue (resin shows through quite easily)	Very thin, pale blue—can easily see resin through paste
20M203	Incomplete stain of intercom-nected paths	10%	1:6	Transparent white	Mottled green-brown	Mottled, transparent, and dark brown areas. Brick may be present.
20M205	Nearly complete	32%	1:2	Very porous, white, transparent paste with green areas	Light brown, fairly opaque	Green-brown paste
21M200	Complete	34%	1:2	Very white, pearly paste	Dark brown, fairly opaque	Very white, thick
21M203	Stain incomplete: about ½ of paste is stained in green area, very little in brown area	25%	1:1	Yellow-brown paste and green paste	Dark reddish paste and green paste	Mottled green tint with brown and yellow-brown colors. Cracked appearance to paste.

* Binder to aggregate ratio

** The lack of a calcite stain appears to have been due to an error when the thin sections were made. XRD, FTIR, and the presence of bioclasts all point to a very high calcium carbonate content that should have stained.

Table G2: Aggregate characterization

11M200	Fort of the Point	Bedding

30% Bioclasts — Reflected: Clear centers with brownish edges

Translucent — Transmitted: Grayish brown

Size: Medium (200-2000 microns) — Refractive index: Low — Calcite stain

Prominence: Distinct — Surface: Rays from center / striated / spotted

Distribution: even — Blocky and round

Tabular Well rounded Ovoid	

20% Quartz — Reflected: gray

Translucent — Transmitted: white

Size: Medium (200-2000 microns) — Refractive index: Med

Prominence: Prominent — Surface: Fractured

Distribution: Clustered — Blocky to circular

Spherical Rounded Subspherical	Anisotropic First order white Birefringence: Low Extinction: Parallel

5% Quartz — Reflected: gray

Translucent — Transmitted: white

Size: Small (60-200 microns) — Refractive index: Med

Prominence: Prominent — Surface: Fractured

Distribution: Clustered — Blocky to circular

Spherical Well rounded	Anisotropic First order white Birefringence: Low Extinction: Parallel

Table G2: Aggregate characterization

11M201	**Fort of the Point**	**Render**

30% **Quartz** — Reflected: gray

Translucent — Transmitted: white

Size: Medium (200-2000 microns) — Refractive index: Med

Prominence: Prominent — Surface: Fractured

Distribution: Even — Blocky to circular

Subspherical	Subangular	Anisotropic	
		First order white	Birefringence: Low Extinction: Parallel

Sharp sand -- pit sand

10% **Quartz** — Reflected: gray

Translucent — Transmitted: white

Size: Small (60-200 microns) — Refractive index: Med

Prominence: Prominent — Surface: Fractured

Distribution: Even — Blocky

Ovoid	Subrounded	Anisotropic	
		First order white	Birefringence: Low Extinction: Parallel

Sharp sand -- pit sand

5% **Quartz** — Reflected: gray

Translucent — Transmitted: white

Size: Very small (2-60 microns) — Refractive index: Med

Prominence: Prominent — Surface: Fractured

Distribution: Even — Blocky to circular

Subspherical Spherical	Subrounded	Anisotropic	
		First order white	Birefringence: Low Extinction: Parallel

Smaller particles behave isotropically, but otherwise look like quartz. Orientation may be perpendicular (normal) to C-axis.

<2% Iron oxide Reflected: Saturated reddish-brown

Opaque Transmitted: Black to blackish-brown

Size: Medium (200-2000 microns) Refractive index: Med

Prominence: Prominent Surface: Embayed

Distribution: Uneven Circular to blocky

Subspherical	Rounded	Isotropic

<2% Epidote? Reflected: Slight grayish/green tint

Translucent Transmitted: Definite dark green

Size: Medium (200-2000 microns) Refractive index: Med

Prominence: Prominent Surface: Etched

Distribution: Random Rectilinear

Tabular Ovoid	Angular	Anisotropic Pleochroism: Yes - varying shades of green Particle color hides interference colors Birefringence: High Extinction: Parallel

Table G2: Aggregate characterization

13M200	Lightning Tower	Render

20% Bioclasts — Reflected: Rosy/brown

Translucent — Transmitted: Medium brown

Size: Medium (200-2000 microns) — Refractive index: Low — Calcite stain

Prominence: Distinct — Surface: Spotted

Distribution: Clustered — circular to blocky

Ovoid Subspherical Spherical — Well rounded	

20% Quartz — Reflected: gray

Translucent — Transmitted: white

Size: Medium (200-2000 microns) — Refractive index: Med

Prominence: Prominent — Surface: Fractured

Distribution: Clustered — Blocky to circular

Spherical Subspherical — Rounded	Anisotropic First order white — Birefringence: Low Extinction: Parallel

Aggregates are rather large, on the order of 1mm.

10% Quartz — Reflected: gray

Translucent — Transmitted: white

Size: Small (60-200 microns) — Refractive index: Med

Prominence: Prominent — Surface: Fractured

Distribution: Clustered — Blocky to circular

Spherical — Rounded	Anisotropic First order white — Birefringence: Low Extinction: Parallel

5% **Bioclasts** Reflected: Rosy/brown

Translucent Transmitted: Medium brown

Size: Large (2-10mm) Refractive index: Low Calcite stain

Prominence: Distinct Surface: Spotted

Distribution: Uneven Irregular

Ovoid Angular Subspherical Spherical Tabular	

Embedded quartz grains

<2% **Epidote?** Reflected: Yellow/orange

Translucent Transmitted: Similar

Size: Medium (200-2000 microns) Refractive index: Med

Prominence: Prominent Surface: Columnar

Distribution: Random Rectilinear

Tabular Angular	Anisotropic Pleochroism: Weakly - yellows to greens Particle color hides interference colors Extinction: Oblique

Table G2: Aggregate characterization

13M201	Lightning Tower	Bedding

40% Quartz Reflected: gray
Translucent Transmitted: white
Size: Medium (200-2000 microns) Refractive index: Med
Prominence: Prominent Surface: Fractured
Distribution: Even Blocky to circular

Spherical Well rounded Subspherical	Anisotropic First order white Birefringence: Low Extinction: Parallel

10% Quartz Reflected: gray
Translucent Transmitted: white
Size: Small (60-200 microns) Refractive index: Med
Prominence: Prominent Surface: Fractured
Distribution: Even Blocky

Spherical Subrounded Subspherical	Anisotropic First order white Birefringence: Low Extinction: Parallel

5% Bioclasts Reflected: Rosy/brown
Translucent Transmitted: Brown
Size: Medium (200-2000 microns) Refractive index: Low
Prominence: Distinct Surface: Rays and striations
Distribution: Uneven circular

Spherical Well rounded	

No calcite stain was evident, but these are clearly bioclasts. Assume that calcite stain was accidentally missed.

<2% Epidote? Reflected: Yellow/orange

Translucent Transmitted: Similar

Size: Medium (200-2000 microns) Refractive index: Med

Prominence: Prominent Surface: Columnar

Distribution: Random Rectilinear

Tabular	Angular	Anisotropic Pleochroism: Weakly - yellows to greens Particle color hides interference colors Extinction: Oblique

Table G2: Aggregate characterization

14M200	La Trinidad	Render

40% **Quartz** Reflected: gray

Translucent Transmitted: white

Size: Medium (200-2000 microns) Refractive index: Med

Prominence: Prominent Surface: Highly fractured

Distribution: Even Irregular to blocky

Spherical Tabular Ovoid Subspherical	Rounded	Anisotropic First order white	 Birefringence: Low Extinction: Parallel

Rather large (> 1mm) beach sand. Unusual compared to other samples.

10% **Quartz** Reflected: gray

Translucent Transmitted: white

Size: Small (60-200 microns) Refractive index: Med

Prominence: Prominent Surface: Highly fractured

Distribution: Even Irregular to blocky

Spherical Tabular Ovoid Subspherical	Rounded	Anisotropic First order white	 Birefringence: Low Extinction: Parallel

5% **Bioclasts** Reflected: Rosy/brown

Translucent Transmitted: Brown

Size: Medium (200-2000 microns) Refractive index: Low Calcite stain

Prominence: Distinct Surface: Spotted

Distribution: Clustered blocky, ovoid, spherical, irregular

Ovoid Subspherical Spherical Tabular	Well rounded	

Some bioclasts are quite large: > 2 to 3 mm and have quartz grains embedded in them

<2% Epidote? Reflected: Yellow/orange

Translucent Transmitted: Similar

Size: Medium (200-2000 microns) Refractive index: Med

Prominence: Prominent Surface: Columnar

Distribution: Random Rectilinear

Tabular Angular	Anisotropic Pleochroism: Weakly - yellows to greens Particle color hides interference colors Extinction: Oblique

Table G2: Aggregate characterization

14M202	**La Trinidad**	**Horizontal**

40% **Quartz** — Reflected: gray

Translucent — Transmitted: white

Size: Medium (200-2000 microns) — Refractive index: Med

Prominence: Prominent — Surface: Fractured

Distribution: Clustered — Blocky to circular

Subspherical	Well rounded	Anisotropic	
		First order white	Birefringence: Low Extinction: Parallel

20% **Bioclasts** — Reflected: Rosy/brown

Translucent — Transmitted: Brown

Size: Medium (200-2000 microns) — Refractive index: Low — Calcite stain

Prominence: Distinct — Surface: Spotted

Distribution: Uneven — Blocky to circular

Spherical Subspherical	Well rounded	

Similar to 14M200

5% **Quartz** — Reflected: gray

Translucent — Transmitted: white

Size: Small (60-200 microns) — Refractive index: Med

Prominence: Prominent — Surface: Fractured

Distribution: Clustered — Blocky

Subspherical	Rounded	Anisotropic	
		First order white	Birefringence: Low Extinction: Parallel

Table G2: Aggregate characterization

14M204	**La Trinidad**	**Bedding**

40% **Quartz** Reflected: gray

Translucent Transmitted: white

Size: Small (60-200 microns) Refractive index: Med

Prominence: Prominent Surface: Fractured

Distribution: Even Blocky

Subspherical Ovoid	Angular Subangular	Anisotropic First order white	 Birefringence: Low Extinction: Parallel

10% **Quartz** Reflected: gray

Translucent Transmitted: white

Size: Medium (200-2000 microns) Refractive index: Med

Prominence: Prominent Surface: Fractured

Distribution: Random Blocky to circular

Subspherical	Subrounded	Anisotropic First order white	 Birefringence: Low Extinction: Parallel

5% **Bioclasts** Reflected: Clear centers with brownish edges

Translucent Transmitted: Grayish brown

Size: Medium (200-2000 microns) Refractive index: Low Calcite stain

Prominence: Distinct Surface: Spotted

Distribution: Uneven circular to blocky

Tabular Ovoid	Well rounded Angular	

Random angular chunks of material appears to also be bioclasts.

Table G2: Aggregate characterization

16M200	El Abanico	Render

30% **Quartz** Reflected: gray
Translucent Transmitted: white
Size: Medium (200-2000 microns) Refractive index: Med
Prominence: Prominent Surface: Fractured
Distribution: Clustered Blocky to circular

Spherical Rounded	Anisotropic First order white Birefringence: Low Extinction: Parallel

10% **Quartz** Reflected: gray
Translucent Transmitted: white
Size: Small (60-200 microns) Refractive index: Med
Prominence: Prominent Surface: Fractured
Distribution: Clustered Blocky to circular

Spherical Rounded	Anisotropic First order white Birefringence: Low Extinction: Parallel

<2% **Bioclasts** Reflected: Rosy/brown
Translucent Transmitted: Brown
Size: Medium (200-2000 microns) Refractive index: Low
Prominence: Distinct Surface: Rays and striations
Distribution: Uneven circular

Spherical Well rounded	

No calcite stain was evident, but these are clearly bioclasts. Assume that calcite stain was accidentally missed.

<2% Epidote? Reflected: Slight grayish/green tint

Translucent Transmitted: Definite dark green

Size: Medium (200-2000 microns) Refractive index: Med

Prominence: Prominent Surface: Etched

Distribution: Random Rectilinear

Tabular Angular Ovoid	Anisotropic Pleochroism: Yes - varying shades of green Particle color hides interference colors Birefringence: High Extinction: Parallel

Table G2: Aggregate characterization

16M202 **El Abanico** **Horizontal**

30% **Quartz** Reflected: gray
Translucent Transmitted: white
Size: Medium (200-2000 microns) Refractive index: Med
Prominence: Prominent Surface: Fractured
Distribution: Clustered Blocky to circular

Spherical Well rounded	Anisotropic First order white Birefringence: Low Extinction: Parallel

20% **Bioclasts** Reflected: Rosy/brown
Translucent Transmitted: Brown
Size: Medium (200-2000 microns) Refractive index: Low
Prominence: Distinct Surface: Rays and striations
Distribution: Uneven circular
Calcite stain

Spherical Well rounded	

10% **Quartz** Reflected: gray
Translucent Transmitted: white
Size: Small (60-200 microns) Refractive index: Med
Prominence: Prominent Surface: Fractured
Distribution: Clustered Blocky

Subspherical Subrounded	Anisotropic First order white Birefringence: Low Extinction: Parallel

Quartz particles seem to be associated with brick particles.

10% Brick

Translucent and Opaque

Size: Small (60-200 microns)

Prominence: Distinct

Distribution: Clustered

Reflected: Dark reddish brown to red to rosy-red

Transmitted: Similar, but somewhat opaque

Refractive index: Low

Surface: Irregular

Irregular

Subspherical	Subrounded	Anisotropic Birefringence: Low

Particles are a complex mix of smaller isotropic and anisotropic particles.

<2% Epidote?

Translucent

Size: Medium (200-2000 microns)

Prominence: Prominent

Distribution: Random

Reflected: Slight grayish/green tint

Transmitted: Definite dark green

Refractive index: Med

Surface: Etched

Rectilinear

Tabular Ovoid	Angular	Anisotropic Pleochroism: Yes - varying shades of green Particle color hides interference colors Birefringence: High Extinction: Parallel

Table G2: Aggregate characterization

16M203	El Abanico	Horizontal

30% **Quartz** Reflected: gray

Translucent Transmitted: white

Size: Medium (200-2000 microns) Refractive index: Med

Prominence: Prominent Surface: Fractured

Distribution: Even Blocky to circular

Spherical Subspherical	Well rounded	Anisotropic First order white Birefringence: Low Extinction: Parallel

20% **Brick** Reflected: Dark reddish brown to red to rosy-red

Translucent and Opaque Transmitted: Similar, but somewhat opaque

Size: Medium (200-2000 microns) Refractive index: Low

Prominence: Distinct Surface: Mammilated to smooth

Distribution: Random Ovoid to circular

Spherical	Rounded	Anisotropic Birefringence: Low

Particles are a complex mix of smaller isotropic and anisotropic particles.

10% **Bioclasts** Reflected: Rosy/brown

Translucent Transmitted: Brown

Size: Medium (200-2000 microns) Refractive index: Low Calcite stain

Prominence: Distinct Surface: Spotted

Distribution: Uneven Blocky to circular

Spherical Subspherical	Well rounded	

5% **Quartz** Reflected: gray

Translucent Transmitted: white

Size: Small (60-200 microns) Refractive index: Med

Prominence: Prominent Surface: Fractured

Distribution: Clustered Blocky to circular

Spherical Well rounded Subspherical	Anisotropic First order white Birefringence: Low Extinction: Parallel

5% **Brick** Reflected: Dark reddish brown to red to rosy-red

Translucent and Opaque Transmitted: Similar, but somewhat opaque

Size: Small (60-200 microns) Refractive index: Low

Prominence: Distinct Surface: Mammilated to smooth

Distribution: Random Ovoid to circular

Spherical Rounded	Anisotropic Birefringence: Low

Particles are a complex mix of smaller isotropic and anisotropic particles.

5% **Brick** Reflected: Dark reddish brown to red to rosy-red

Translucent and Opaque Transmitted: Similar, but somewhat opaque

Size: Large (2-10mm) Refractive index: Low

Prominence: Distinct Surface: Mammilated to smooth

Distribution: Random Ovoid to circular

Ovoid Rounded	Anisotropic Birefringence: Low

Some particles are massive (>5mm)

Table G2: Aggregate characterization

16M205	**El Abanico**	**Bedding**

20% **Quartz** Reflected: gray

Translucent Transmitted: white

Size: Medium (200-2000 microns) Refractive index: Med

Prominence: Prominent Surface: Fractured

Distribution: Even Blocky

Spherical Subangular Subspherical	Anisotropic First order white Birefringence: Low Extinction: Parallel

5% **Quartz** Reflected: gray

Translucent Transmitted: white

Size: Small (60-200 microns) Refractive index: Med

Prominence: Prominent Surface: Fractured

Distribution: Even Blocky

Subspherical Subangular	Anisotropic First order white Birefringence: Low Extinction: Parallel

5% **Brick** Reflected: Dark reddish brown to red to rosy-red

Translucent and Opaque Transmitted: Similar, but somewhat opaque

Size: Small (60-200 microns) Refractive index: Low

Prominence: Distinct Surface: Mammilated to smooth

Distribution: Random Ovoid to circular

Spherical Rounded	Anisotropic Birefringence: Low

Particles are a complex mix of smaller isotropic and anisotropic particles.

2%	**Bioclasts**	Reflected: Clear centers with brownish edges	
	Translucent	Transmitted: Grayish brown	
	Size: Medium (200-2000 microns)	Refractive index: Low	Calcite stain
	Prominence: Distinct	Surface: Rays from center / striated	
	Distribution: even	circular to blocky	

Ovoid Well rounded Spherical	

Table G2: Aggregate characterization

20M201	**St. Teresa**	**Render**

40% **Quartz** Reflected: gray

Translucent Transmitted: white

Size: Medium (200-2000 microns) Refractive index: Med

Prominence: Prominent Surface: Fractured

Distribution: Even Circular to ovoid

Spherical Rounded	Anisotropic First order white Birefringence: Low Extinction: Parallel

5% **Quartz** Reflected: gray

Translucent Transmitted: white

Size: Small (60-200 microns) Refractive index: Med

Prominence: Prominent Surface: Fractured

Distribution: Even Circular to ovoid

Spherical Rounded	Anisotropic First order white Birefringence: Low Extinction: Parallel

Table G2: Aggregate characterization

20M205	St. Teresa	Bedding

40% **Quartz** Reflected: gray

Translucent Transmitted: white

Size: Small (60-200 microns) Refractive index: Med

Prominence: Prominent Surface: Fractured

Distribution: Even Blocky

Ovoid Angular Subspherical	Anisotropic First order white Birefringence: Low Extinction: Parallel

30% **Bioclasts** Reflected: Clear centers with brownish edges

Translucent Transmitted: Grayish brown

Size: Medium (200-2000 microns) Refractive index: Low

Calcite stain

Prominence: Distinct Surface: Oval with concentric rings & spotted

Distribution: Uneven circular to blocky

Spherical Well rounded Ovoid	

10% **Quartz** Reflected: gray

Translucent Transmitted: white

Size: Medium (200-2000 microns) Refractive index: Med

Prominence: Prominent Surface: Fractured

Distribution: Random Blocky to circular

Spherical Subrounded	Anisotropic First order white Birefringence: Low Extinction: Parallel

2% **Epidote?** Reflected: Slight grayish/green tint

Translucent Transmitted: Definite dark green

Size: Medium (200-2000 microns) Refractive index: Med

Prominence: Prominent Surface: Etched

Distribution: Random Rectilinear

Tabular Angular Ovoid	Anisotropic Pleochroism: Yes - varying shades of green Particle color hides interference colors Birefringence: High Extinction: Parallel

Table G2: Aggregate characterization

21M200	**N. Casemate**	**Render**

50% Bioclasts — Reflected: Clear centers with brownish edges

Translucent — Transmitted: Grayish brown

Size: Medium (200-2000 microns) — Refractive index: Low — Calcite stain

Prominence: Distinct — Surface: Rays from center / striated

Distribution: even — circular to blocky

Tabular Ovoid	Well rounded	

This is the top most 1mm layer of a interior stucco. Almost all of the aggregate in this layer is bioclasts. There are a few scattered, blocky, rounded medium size quartz grains.

20% Quartz — Reflected: gray

Translucent — Transmitted: white

Size: Medium (200-2000 microns) — Refractive index: Med

Prominence: Prominent — Surface: Fractured

Distribution: Uneven — Blocky to circular to tabular

Ovoid Subspherical	Subrounded	Anisotropic First order white — Birefringence: Low Extinction: Parallel

<2% Epidote? — Reflected: Dark greenish with black speckles

Translucent — Transmitted: Yellowish-green

Size: Medium (200-2000 microns) — Refractive index: Med

Prominence: Prominent — Surface: Etched

Distribution: Random — Rectilinear

Tabular	Angular	Anisotropic Pleochroism: Weakly - yellows to greens Particle color hides interference colors — Extinction: Oblique

Table G2: Aggregate characterization

21M201

2%	**Bioclasts**	Reflected: Clear centers with brownish edges		
	Translucent	Transmitted: Grayish brown		
	Size: Medium (200-2000 microns)	Refractive index: Low	Calcite stain	
	Prominence: Distinct	Surface: Rays from center / striated		
	Distribution: Random	circular to blocky		

Ovoid Tabular	Well rounded	

Table G2: Aggregate characterization

21M203	N. Casemate	Bedding

30% **Quartz** Reflected: gray

Translucent Transmitted: white

Size: Small (60-200 microns) Refractive index: Med

Prominence: Prominent Surface: Fractured

Distribution: Even Blocky

Tabular	Subangular	Anisotropic	
		First order white	Birefringence: Low Extinction: Parallel

Sharp sand

5% **Quartz** Reflected: gray

Translucent Transmitted: white

Size: Very small (2-60 microns) Refractive index: Med

Prominence: Prominent Surface: Fractured

Distribution: Random Blocky

Tabular	Subangular	Anisotropic	
		First order white	Birefringence: Low Extinction: Parallel

Sharp sand

5% **Quartz** Reflected: gray

Translucent Transmitted: white

Size: Medium (200-2000 microns) Refractive index: Med

Prominence: Prominent Surface: Fractured

Distribution: Even Blocky

Tabular	Subangular	Anisotropic	
		First order white	Birefringence: Low Extinction: Parallel

Sharp sand

<2% Bioclasts Reflected: Clear centers with brownish edges

Translucent Transmitted: Grayish brown

Size: Medium (200-2000 microns) Refractive index: Low Calcite stain

Prominence: Distinct Surface: Smooth with some fracturing

Distribution: Random circular to ovoid

Ovoid Well rounded	

2% Clay Reflected: Dark reddish brown to red to rosy-red

Translucent and Opaque Transmitted: Similar, but somewhat opaque

Size: Medium (200-2000 microns) Refractive index: Low

Prominence: Distinct Surface: Mammilated to smooth

Distribution: Random Ovoid to circular

Spherical Rounded	Anisotropic Birefringence: Low

Particles are a complex mix of smaller isotropic and anisotropic particles.

2% Clay Reflected: Dark reddish brown to red to rosy-red

Translucent and Opaque Transmitted: Similar, but somewhat opaque

Size: Small (60-200 microns) Refractive index: Low

Prominence: Distinct Surface: Mammilated to smooth

Distribution: Random Ovoid to circular

Spherical Rounded	Anisotropic Birefringence: Low

Particles are a complex mix of smaller isotropic and anisotropic particles.

2% **Clay** Reflected: Dark reddish brown to red to rosy-red

Translucent and Opaque Transmitted: Similar, but somewhat opaque

Size: Very small (2-60 microns) Refractive index: Low

Prominence: Distinct Surface: Mammilated to smooth

Distribution: Random Ovoid to circular

Spherical	Rounded	Anisotropic Birefringence: Low

Particles are a complex mix of smaller isotropic and anisotropic particles.

2% **Clay** Reflected: Dark reddish brown to red to rosy-red

Translucent and Opaque Transmitted: Similar, but somewhat opaque

Size: Micro (<2 microns) Refractive index: Low

Prominence: Distinct Surface: Mammilated to smooth

Distribution: Random Ovoid to circular

Spherical	Rounded	Anisotropic Birefringence: Low

Particles are a complex mix of smaller isotropic and anisotropic particles.

APPENDIX H: X-RAY DIFFRACTION RESULTS

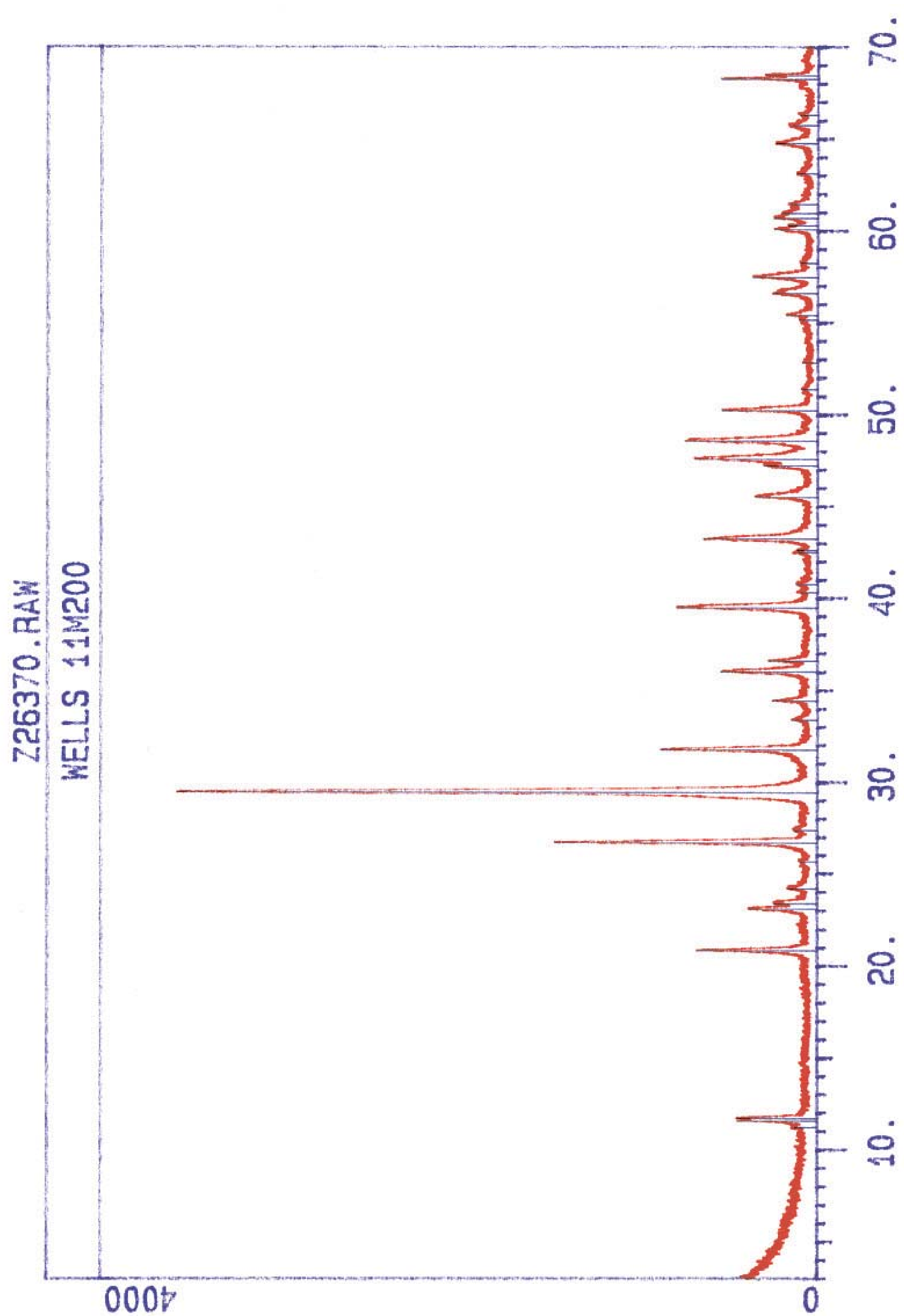
Z26370.RAW
WELLS 11M200
4000
0
10.
20.
30.
40.
50.
60.
70.

Input Pattern

WELLS 11M200
Peak search on 13-FEB-0413:59:50

d	I	d	I	d	I	d	I	d	I	d	I
7.858	3.5	3.336	41	2.2810	22	1.9093	19	1.6027	10	1.4389	6.7
7.642	12	3.253	3.7	2.2348	2.7	1.8726	21	1.5832	2.7	1.4197	4.0
7.551	13	3.029	100	2.2117	3.3	1.8152	15	1.5390	6.9	1.4091	2.9
4.253	19	2.8148	24	2.1252	3.1	1.7771	2.4	1.5340	4.7	1.3737	15
3.844	11	2.6813	4.0	2.1195	3.2	1.7320	2.4	1.5244	6.9	1.3702	8.3
3.797	6.8	2.6021	7.0	2.0909	18	1.6640	2.9	1.5185	5.6		
3.672	4.7	2.4903	15	1.9911	9.8	1.6568	5.0	1.5078	4.3		
3.466	2.7	2.4528	7.7	1.9231	8.4	1.6251	7.1	1.4721	3.3		

45 lines in pattern.

Identified Phases:

JCPDS#	SI	ML/X	At%	Identity . . .
5-0586*	284	17/1	114	*Calcium Carbonate / Calcite, syn = CaCO3
	Ierr:50,150		derr:2.0	Bground:2.4 dmax/min:29.41/1.343
46-1045*	131	10/3	87	*Silicon Oxide / Quartz, syn = SiO2
	Ierr:50,150		derr:2.0	Bground:2.4 dmax/min:29.41/1.343
5-0628*	57	4/0	24	*Sodium Chloride / Halite, syn = NaCl
	Ierr:50,150		derr:2.0	Bground:2.4 dmax/min:29.41/1.343
70-0983C	38*	6/2	14	Calcium Sulfate Hydrate / Gypsum = Ca(SO4)(H2O)2
	Ierr:50,150		derr:2.0	Bground:2.4 dmax/min:29.41/1.343
26-1286	40	4/2	9.9	Nickel Iron Carbonate Hydroxide Hydrate / Reevesite = Ni6Fe2(CO3)(OH)16.4H2O
	Ierr:50,150		derr:2.0	Bground:2.4 dmax/min:29.41/1.343
19-0696D	19	4/2	3.6	Lead Oxide = Pb2O3
	Ierr:50,150		derr:2.0	Bground:2.4 dmax/min:29.41/1.343

Summary Report (Part 1 of 2):

	Full	Resid	5-0586:114%		46-1045: 87%		5-0628: 24%		70-0983: 14%	
d	I	I	d	I	d	I	d	I	d	I
7.858	3.5	3.5								
7.642	12	None							7.6005	14
7.551	13	None								
4.253	19	None			4.2550	14			[4.2810	5.6]
3.844	11	None	3.86	14						
3.797	6.8	None							3.8003	2.1
3.672	4.7	4.7								
3.466	2.7	None								
3.336	41	None			3.3435	87				
3.253	3.7	None					3.26	3.1		
									<3.0643	11>
3.029	100	None	3.035	114						
			<2.845	3.4>					<2.8715	11>

2.8148	24	None					2.821	24		
2.6813	4.0	None							2.6855	4.7
2.6021	7.0	None							2.5953	0.4*
" "	"								2.5905	0.4*
2.4903	15	None	2.495	16					[2.4915	0.8]
2.4528	7.7	None			2.4569	7.8			[2.4520	1.0]
2.2810	22	None	2.285	21	[2.2815	6.9]			[2.2906	0.1]
2.2348	2.7	None			2.2361	3.5				
2.2117	3.3	None							2.2189	2.0
2.1252	3.1	None			2.1277	5.2				
2.1195	3.2	None								
2.0909	18	None	2.095	21					[2.0836	2.3]
1.9911	9.8	None					1.994	13		
					<1.9799	3.5>				
1.9231	8.4	None	1.927	5.7						
1.9093	19	None	1.913	19						
1.8726	21	None	1.875	19						
1.8152	15	None			1.8180	11			[1.8113	1.6]
1.7771	2.4	None							1.7764	1.3
1.7320	2.4	None								
					<1.6717	3.5>				
1.6640	2.9	None							1.6621	1.0
1.6568	5.0	None			1.6592	1.7			1.6522	0.1*
" "	"									
1.6251	7.1	None	1.626	4.6			[1.628	3.6]	[1.6230	1.1]
1.6027	10	None	1.604	9.1					[1.5996	0.1]
1.5832	2.7	None	1.587	2.3					[1.5872	0.1]
1.5390	6.9	None			1.5415	7.8				
1.5340	4.7	4.4							1.5322	0.3*
1.5244	6.9	None	1.525	5.7					[1.5229	0.1]
1.5185	5.6	None	1.518	4.6					" "	"
" "	"								[1.5194	0.1]
1.5078	4.3	None	1.510	3.4					[1.5109	0.3]
1.4721	3.3	None	1.473	2.3						
1.4389	6.7	None	1.440	5.7					[1.4394	0.4]
1.4197	4.0	None	1.422	3.4	[1.4184	0.9]			[1.4203	0.1]
1.4091	2.9	None					1.410	1.4		
					<1.3821	5.2>				
1.3737	15	9			1.3750	6.1				
1.3702	8.3	None			1.3719	4.3				

* = Obscured <..> = Missing [..] = Previously Removed

Summary Report (Part 2 of 2):

	Full	Resid	26-1286:	10%	19-0696:	4%
d	I	I	d	I	d	I
7.858	3.5	3.5				
7.642	12	None				
7.551	13	None	7.60	9.9		
4.253	19	None				
3.844	11	None				
3.797	6.8	None	3.80	5.0		
3.672	4.7	4.7				
3.466	2.7	None			3.47	3.6
3.336	41	None				
3.253	3.7	None				
3.029	100	None			[3.03	2.5]
					<2.957	3.2>

2.8148	24	None					2.821	24		
2.6813	4.0	None							2.6855	4.7
2.6021	7.0	None							2.5953	0.4*
" "	"								2.5905	0.4*
2.4903	15	None	2.495	16					[2.4915	0.8]
2.4528	7.7	None			2.4569	7.8			[2.4520	1.0]
2.2810	22	None	2.285	21	[2.2815	6.9]			[2.2906	0.1]
2.2348	2.7	None			2.2361	3.5				
2.2117	3.3	None							2.2189	2.0
2.1252	3.1	None			2.1277	5.2				
2.1195	3.2	None								
2.0909	18	None	2.095	21					[2.0836	2.3]
1.9911	9.8	None					1.994	13		
					<1.9799	3.5>				
1.9231	8.4	None	1.927	5.7						
1.9093	19	None	1.913	19						
1.8726	21	None	1.875	19						
1.8152	15	None			1.8180	11			[1.8113	1.6]
1.7771	2.4	None							1.7764	1.3
1.7320	2.4	None								
					<1.6717	3.5>				
1.6640	2.9	None							1.6621	1.0
1.6568	5.0	None			1.6592	1.7			1.6522	0.1*
" "	"									
1.6251	7.1	None	1.626	4.6			[1.628	3.6]	[1.6230	1.1]
1.6027	10	None	1.604	9.1					[1.5996	0.1]
1.5832	2.7	None	1.587	2.3					[1.5872	0.1]
1.5390	6.9	None			1.5415	7.8				
1.5340	4.7	4.4							1.5322	0.3*
1.5244	6.9	None	1.525	5.7					[1.5229	0.1]
1.5185	5.6	None	1.518	4.6					" "	"
" "	"								[1.5194	0.1]
1.5078	4.3	None	1.510	3.4					[1.5109	0.3]
1.4721	3.3	None	1.473	2.3						
1.4389	6.7	None	1.440	5.7					[1.4394	0.4]
1.4197	4.0	None	1.422	3.4	[1.4184	0.9]			[1.4203	0.1]
1.4091	2.9	None					1.410	1.4		
					<1.3821	5.2>				
1.3737	15	9			1.3750	6.1				
1.3702	8.3	None			1.3719	4.3				

* = Obscured   <..> = Missing   [..] = Previously Removed

Summary Report (Part 2 of 2):

	Full	Resid	26-1286:	10%	19-0696:	4%
d	I	I	d	I	d	I
7.858	3.5	3.5				
7.642	12	None				
7.551	13	None	7.60	9.9		
4.253	19	None				
3.844	11	None				
3.797	6.8	None	3.80	5.0		
3.672	4.7	4.7				
3.466	2.7	None			3.47	3.6
3.336	41	None				
3.253	3.7	None				
3.029	100	None			[3.03	2.5]
					<2.957	3.2>

2.8148	24	None			[2.815	1.4]
2.6813	4.0	None				
2.6021	7.0	None	2.60	5.0		
" "	"					
2.4903	15	None				
2.4528	7.7	None				
			<2.301	4.0>	<2.317	2.9>
2.2810	22	None				
2.2348	2.7	None				
2.2117	3.3	None				
2.1252	3.1	None				
2.1195	3.2	None			2.116	2.2
2.0909	18	None				
1.9911	9.8	None				
			<1.947	4.0>		
1.9231	8.4	None			[1.922	0.22]
1.9093	19	None	[1.903	0.99]		
1.8726	21	None				
1.8152	15	None				
1.7771	2.4	None	[1.783	0.50]		
1.7320	2.4	None	1.735	2.0	[1.737	1.8]
1.6640	2.9	None			[1.664	0.72]
1.6568	5.0	None			1.660	1.4
" "	"				1.652	1.1
1.6251	7.1	None			[1.620	0.22]
1.6027	10	None			[1.603	0.36]
1.5832	2.7	None				
1.5390	6.9	None	[1.541	3.0]	[1.543	0.36]
1.5340	4.7	4.4				
1.5244	6.9	None				
1.5185	5.6	None			[1.515	0.72]
" "	"					
1.5078	4.3	None	[1.510	3.0]		
1.4721	3.3	None				
1.4389	6.7	None			[1.436	0.22]
1.4197	4.0	None				
1.4091	2.9	None			[1.408	0.22]
1.3737	15	9				
1.3702	8.3	None			[1.368	0.22]

* = Obscured   <..> = Missing   [..] = Previously Removed

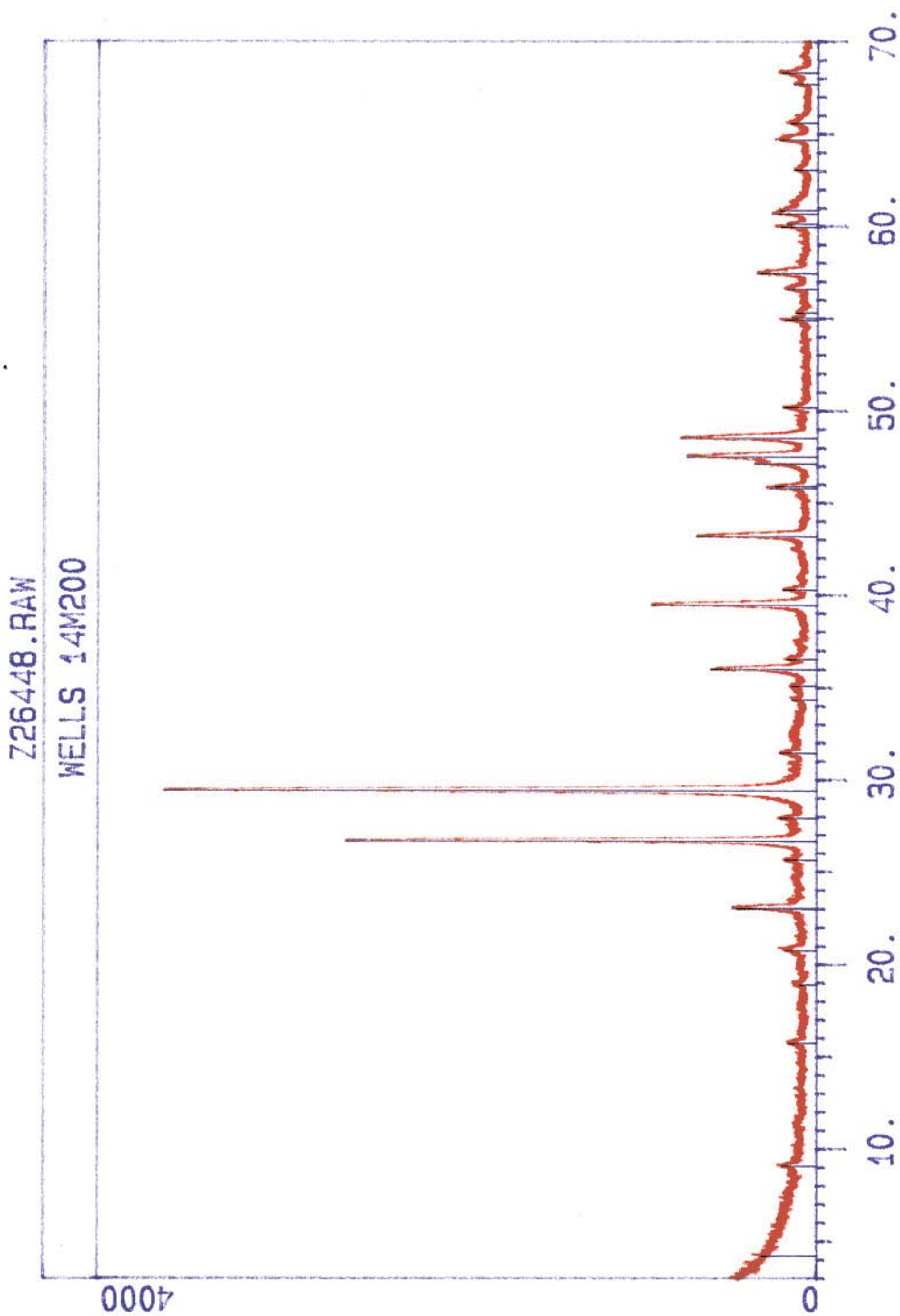
Z26448.RAW
WELLS 14M200
4000
0
10.
20.
30.
40.
50.
60.
70.

Input Pattern

WELLS 14M200

Peak search on 20-FEB-0410:45:32

d	I	d	I	d	I	d	I	d	I	d	I
20.80	8.5	3.469	4.9	2.4922	16	1.9272	9.6	1.6256	4.7	1.4404	6.0
9.697	5.4	3.339	72	2.4566	4.6	1.9126	20	1.6034	9.4	1.4224	4.2
5.609	4.4	3.191	5.7	2.2823	25	1.8748	21	1.5419	5.7	1.3837	3.8
4.686	2.6	3.033	100	2.2369	5.3	1.8167	5.4	1.5382	4.7	1.3726	5.6
4.271	4.9	2.8419	5.8	2.0931	19	1.6713	5.0	1.5253	7.1		
3.860	12	2.6086	3.9	1.9796	7.4	1.6679	3.9	1.5208	5.9		
3.852	13	2.5539	3.9	1.9755	6.6	1.6601	3.4	1.4734	3.7		

39 lines in pattern.

Identified Phases:

JCPDS#	SI	ML/X	At%	Identity . . .
5-0586*	281	16/1	118	*Calcium Carbonate / Calcite, syn = $CaCO_3$
	Ierr:50,150		derr:2.0	Bground:2.6 dmax/min:29.41/1.343
46-1045*	167	12/1	74	*Silicon Oxide / Quartz, syn = SiO_2
	Ierr:50,150		derr:2.0	Bground:2.6 dmax/min:29.41/1.343
41-1451*	71	7/3	14	*Calcium Aluminum Sulfate Hydroxide Hydrate / Ettringite, syn = $Ca_6Al_2(SO_4)_3(OH)_{12}.26H_2O$
	Ierr:50,150		derr:2.0	Bground:2.6 dmax/min:29.41/1.343
16-0895D	12	3/2	7.7	Iron Oxide = Fe_2O_3
	Ierr:50,150		derr:2.0	Bground:2.6 dmax/min:29.41/1.343
20-0452I	12	3/7	30	Calcium Aluminum Silicate Hydrate / Gismondine = $CaAl_2Si_2O_8.4H_2O$
	Ierr:50,150		derr:2.0	Bground:2.6 dmax/min:29.41/1.343
5-0017	20	2/0	22	Lead caproate = $C_{12}H_{22}O_4Pb$
	Ierr:50,150		derr:2.0	Bground:2.6 dmax/min:29.41/1.343

Summary Report (Part 1 of 2):

	Full	Resid	5-0586:118%		46-1045: 74%		41-1451: 14%		16-0895: 8%	
d	I	I	d	I	d	I	d	I	d	I
20.80	8.5	None								
9.697	5.4	None					9.72	14		
5.609	4.4	None					5.61	10		
4.686	2.6	None					4.689	2.3		
4.271	4.9	None			4.2550	12				
3.860	12	6					3.873	4.2		
3.852	13	None	3.86	14						
3.469	4.9	None					3.475	3.2		
3.339	72	None			3.3435	74				
							<3.240	2.9>		
3.191	5.7	None								
3.033	100	None	3.035	118						
									<2.98	4.6>
2.8419	5.8	None	2.845	3.5						

							<2.772	3.4>		
2.6086	3.9	None					2.614	2.2		
2.5539	3.9	None					2.560	4.0	[2.55	1.5]
2.4922	16	None	2.495	16			[2.485	0.3]		
2.4566	4.6	None			2.4569	6.7			[2.46	7.7]
2.2823	25	None	2.285	21	[2.2815	5.9]				
2.2369	5.3	None			2.2361	3.0	[2.230	1.1]	[2.24	4.6]
					<2.1277	4.5>	<2.206	3.0>		
2.0931	19	None	2.095	21						
1.9796	7.4	None			1.9799	3.0			1.98	2.3
1.9755	6.6	5.1					1.971	0.3*		
1.9272	9.6	None	1.927	5.9						
1.9126	20	None	1.913	20						
1.8748	21	None	1.875	20			[1.870	0.1]		
1.8167	5.4	None			1.8180	9.7				
									<1.74	4.6>
1.6713	5.0	None			1.6717	3.0				
1.6679	3.9	None							1.67	0.77
1.6601	3.4	None			1.6592	1.5	[1.662	0.7]		
1.6256	4.7	None	1.626	4.7						
1.6034	9.4	None	1.604	9.4	[1.6083	0.7]				
1.5419	5.7	None			1.5415	6.7				
1.5382	4.7	None							1.54	2.3
1.5253	7.1	None	1.525	5.9						
1.5208	5.9	None	1.518	4.7					[1.52	7.7]
			<1.510	3.5>						
1.4734	3.7	None	1.473	2.4					[1.47	7.7]
1.4404	6.0	None	1.440	5.9						
1.4224	4.2	None	1.422	3.5	[1.4184	0.7]				
1.3837	3.8	None			1.3821	4.5				
1.3726	5.6	None			1.3750	5.2				
" "	"				1.3719	3.7				

* = Obscured <..> = Missing [..] = Previously Removed

Summary Report (Part 2 of 2):

	Full	Resid	20-0452: 30%		5-0017: 22%	
d	I	I	d	I	d	I
20.80	8.5	None			20.70	22
9.697	5.4	None				
			<7.28	4.7>		
5.609	4.4	None				
			<4.91	4.7>		
4.686	2.6	None	[4.67	1.2]		
4.271	4.9	None	[4.27	10]	[4.26	0.2]
			<4.19	3.6>		
3.860	12	6			3.879	1.7
3.852	13	None				
3.469	4.9	None			[3.474	0.2]
3.339	72	None	[3.34	30]	[3.351	0.4]
3.191	5.7	None	3.19	5.3		
			<3.13	4.1>		
3.033	100	None			[3.046	0.2]
2.8419	5.8	None				
			<2.74	4.1>		
			<2.70	5.3>		

			<2.66	3.0>		
2.6086	3.9	None	[2.62	0.6]	[2.621	0.2]
2.5539	3.9	None	[2.56	0.6]	[2.546	0.2]
2.4922	16	None			[2.492	0.2]
2.4566	4.6	None	[2.46	2.4]	[2.452	0.2]
2.2823	25	None	[2.28	1.8]	[2.291	0.4]
2.2369	5.3	None	[2.24	1.2]		
2.0931	19	None			[2.100	0.6]
1.9796	7.4	None				
1.9755	6.6	5.1	1.981	1.2		
1.9272	9.6	None	[1.933	0.6]		
1.9126	20	None	[1.916	0.6]	[1.909	0.2]
1.8748	21	None				
1.8167	5.4	None	[1.819	4.7]		
1.6713	5.0	None				
1.6679	3.9	None	1.671	2.4		
1.6601	3.4	None				
1.6256	4.7	None				
1.6034	9.4	None	[1.608	0.6]	[1.608	0.2]
1.5419	5.7	None	[1.542	2.4]	[1.545	0.2]
1.5382	4.7	None	" "	"		
1.5253	7.1	None			[1.526	0.2]
1.5208	5.9	None				
1.4734	3.7	None				
1.4404	6.0	None	[1.438	0.6]	[1.439	0.2]
1.4224	4.2	None			[1.423	0.2]
1.3837	3.8	None	[1.384	1.2]	[1.387	0.2]
1.3726	5.6	None	[1.375	0.3]		
" "	"					

* = Obscured <..> = Missing [..] = Previously Removed

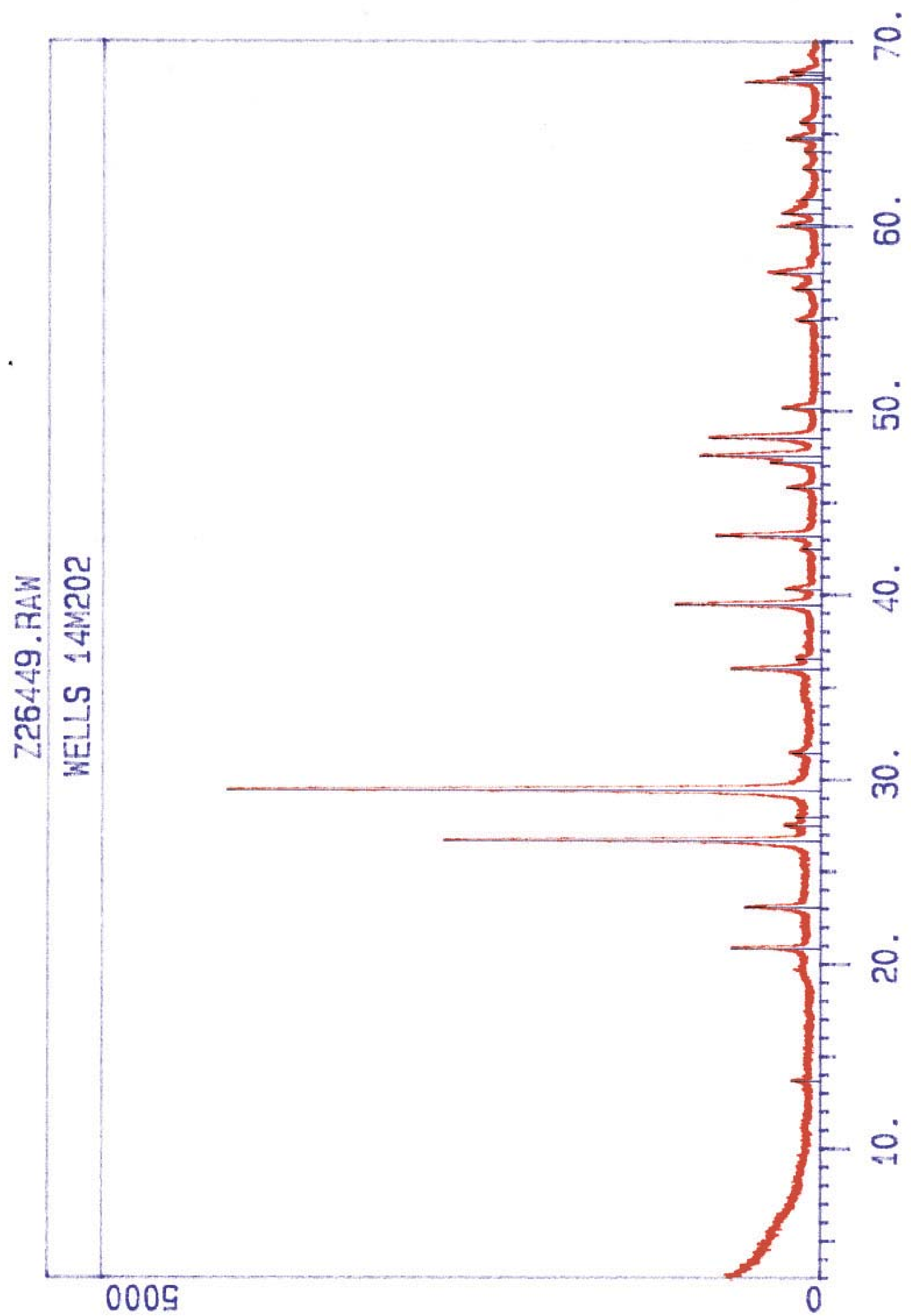
Z26449.RAW
WELLS 14M202
5000
0
10.
20.
30.
40.
50.
60.
70.

Input Pattern

WELLS 14M202

Peak search on 20-FEB-0411:20:04

d	I	d	I	d	I	d	I	d	I	d	I
6.464	5.0	3.034	100	2.1252	3.2	1.8187	6.8	1.5253	7.0	1.4224	4.0
4.252	15	2.8437	5.0	2.0931	18	1.6718	4.0	1.5083	3.6	1.3823	13
3.849	13	2.4927	15	1.9796	6.0	1.6256	4.7	1.4730	3.4	1.3790	7.8
3.340	64	2.4566	4.3	1.9241	8.8	1.6033	7.9	1.4532	3.2	1.3751	4.7
3.239	6.0	2.2828	25	1.9117	21	1.5423	7.3	1.4404	6.2	1.3719	5.7
3.187	4.2	2.2369	6.2	1.8749	19	1.5391	4.7	1.4380	5.0		

35 lines in pattern.

Identified Phases:

JCPDS#	SI	ML/X	At%	Identity . . .
5-0586*	283	16/1	114	*Calcium Carbonate / Calcite, syn = CaCO3
	Ierr:50,150			derr:2.0 Bground:3.2 dmax/min:29.41/1.343
46-1045*	216	13/0	88	*Silicon Oxide / Quartz, syn = SiO2
	Ierr:50,150			derr:2.0 Bground:3.2 dmax/min:29.41/1.343
46-1045*	23	2/0	46	*Silicon Oxide / Quartz, syn = SiO2
	Ierr:50,150			derr:2.0 Bground:3.2 dmax/min:29.41/1.343
2-0122D	13	2/3	4.6	Sodium Calcium Carbon Hydrate / Gaylussite = Na2Ca(CO3)2.5H2O
	Ierr:50,150			derr:2.0 Bground:3.2 dmax/min:29.41/1.343
2-0096D	12	2/3	4.7	Calcium Aluminum Silicate Hydrate / Gismondite = CaAl2Si2O8.4H2O
	Ierr:50,150			derr:2.0 Bground:3.2 dmax/min:29.41/1.343

Summary Report (Part 1 of 2):

	Full	Resid	5-0586:114%		46-1045: 88%		46-1045: 46%		2-0122: 5%	
d	I	I	d	I	d	I	d	I	d	I
6.464	5.0	None							6.41	4.6
									<4.45	3.2>
4.252	15	None			4.2550	14	[4.2550	7.3]		
3.849	13	None	3.86	14						
3.340	64	None			3.3435	88	[3.3435	46]		
3.239	6.0	None								
3.187	4.2	None							3.18	3.7
3.034	100	None	3.035	114					[3.02	1.8]
2.8437	5.0	None	2.845	3.4						
									<2.70	3.7>
									<2.61	3.7>
2.4927	15	None	2.495	16					[2.49	3.2]
2.4566	4.3	None			2.4569	7.9	[2.4569	4.1]		
2.2828	25	None	2.285	20	[2.2815	7.1]	[2.2815	3.7]		
2.2369	6.2	None			2.2361	3.5	[2.2361	1.8]		
2.1252	3.2	None			2.1277	5.3	[2.1277	2.8]	[2.12	1.8]
2.0931	18	None	2.095	20						
1.9796	6.0	None			1.9799	3.5	[1.9799	1.8]	[1.98	3.2]
1.9241	8.8	None	1.927	5.7						
1.9117	21	None	1.913	19					[1.91	3.7]

1.8749	19	None	1.875	19						
1.8187	6.8	None			1.8180	11	[1.8180	6.0]		
1.6718	4.0	None			1.6717	3.5	[1.6717	1.8]	[1.67	2.8]
1.6256	4.7	None	1.626	4.5						
1.6033	7.9	None	1.604	9.1	[1.6083	0.9]	[1.6083	0.5]	[1.60	1.8]
1.5423	7.3	None			1.5415	7.9				
1.5391	4.7	None					1.5415	4.1		
1.5253	7.0	None	1.525	5.7						
			<1.518	4.5>						
1.5083	3.6	None	1.510	3.4						
1.4730	3.4	None	1.473	2.3						
1.4532	3.2	None			1.4529	1.8	[1.4529	0.9]		
1.4404	6.2	None	1.440	5.7						
1.4380	5.0	5.0								
1.4224	4.0	None	1.422	3.4	[1.4184	0.9]	[1.4184	0.5]		
1.3823	13	None			1.3821	5.3	1.3821	2.8		
1.3790	7.8	7.8								
1.3751	4.7	None			1.3750	6.2	[1.3750	3.2]		
" "	"						[1.3719	2.3]		
1.3719	5.7	None			1.3719	4.4	[1.3750	3.2]		
" "	"						[1.3719	2.3]		

* = Obscured   <..> = Missing   [..] = Previously Removed

Summary Report (Part 2 of 2):

d	Full I	Resid I	2-0096: 5% d	I
			<7.30	4.7>
6.464	5.0	None		
4.252	15	None		
			<4.19	3.8>
3.849	13	None		
3.340	64	None		
3.239	6.0	None	3.24	4.7
3.187	4.2	None		
3.034	100	None		
2.8437	5.0	None		
			<2.73	4.7>
2.4927	15	None		
2.4566	4.3	None		
2.2828	25	None		
2.2369	6.2	None		
2.1252	3.2	None		
2.0931	18	None		
1.9796	6.0	None		
1.9241	8.8	None		
1.9117	21	None	[1.91	1.9]
1.8749	19	None	[1.88	1.9]
1.8187	6.8	None		
1.6718	4.0	None	[1.67	1.9]
1.6256	4.7	None		
1.6033	7.9	None		
1.5423	7.3	None		
1.5391	4.7	None		
1.5253	7.0	None		

1.5083	3.6	None		
1.4730	3.4	None		
1.4532	3.2	None		
1.4404	6.2	None		
1.4380	5.0	5.0		
1.4224	4.0	None	[1.42	2.4]
1.3823	13	None	1.38	2.4
1.3790	7.8	7.8		
1.3751	4.7	None		
" "	"			
1.3719	5.7	None		
" "	"			

* = Obscured <..> = Missing [..] = Previously Removed

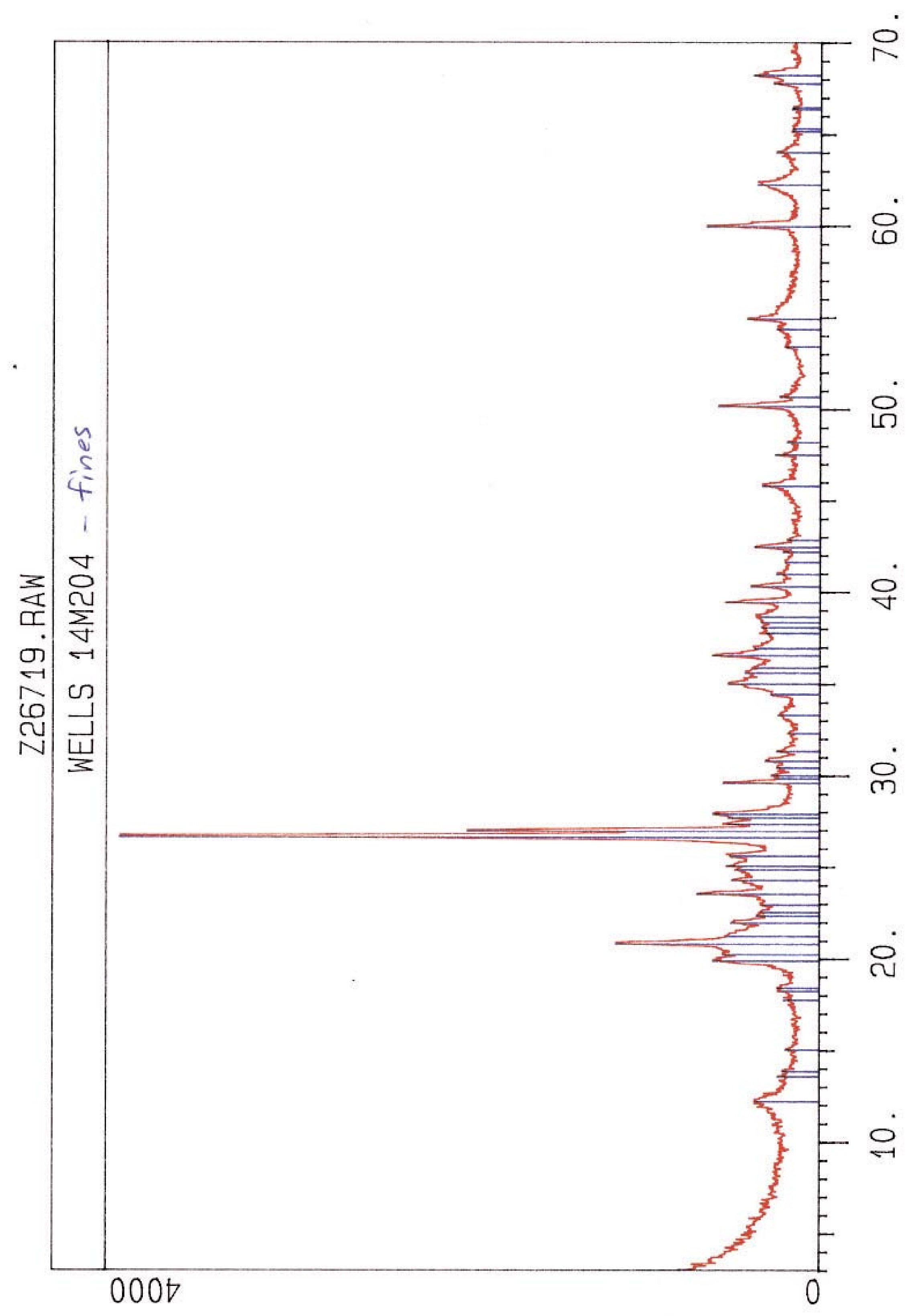

Z26719.RAW
WELLS 14M204 - fines
4000
0
10.
20.
30.
40.
50.
60.
70.

Input Pattern

WELLS 14M204 – fines
Peak search on 17-MAR-0417:58:40

d	I	d	I	d	I	d	I	d	I	d	I
7.215	9.3	3.969	9.0	3.192	15	2.4982	9.4	2.1271	9.4	1.4536	6.4
6.495	6.0	3.934	8.4	3.013	14	2.4550	15	2.1082	4.7	1.4309	4.1
6.371	5.3	3.867	8.2	2.9884	6.3	2.4296	9.3	1.9791	8.3	1.4280	4.0
5.867	4.9	3.772	18	2.9738	6.9	2.3800	7.7	1.9121	6.5	1.4079	4.2
4.978	5.1	3.659	13	2.9324	6.2	2.3609	8.4	1.8862	4.7	1.4061	4.1
4.848	5.7	3.576	12	2.8972	7.8	2.3442	8.4	1.8177	15	1.3822	6.8
4.807	6.1	3.547	13	2.8504	6.1	2.3267	8.6	1.8006	5.8	1.3741	9.6
4.452	15	3.473	13	2.7675	4.4	2.2822	14	1.7147	5.1		
4.375	14	3.343	100	2.6862	6.0	2.2353	9.9	1.6868	6.3		
4.255	29	3.302	50	2.5998	7.0	2.1996	6.3	1.6710	11		
4.172	13	3.255	13	2.5591	13	2.1660	5.0	1.5420	16		
4.035	13	3.215	13	2.5170	11	2.1391	5.3	1.4905	9.1		

67 lines in pattern.

Identified Phases:

JCPDS#	SI	ML/X	At%	Identity . . .
31-0966*	408*	39/3	56	*Potassium Aluminum Silicate / Orthoclase = KAlSi3O8
	Ierr:100,200	derr:2.5	Bground:4.0	dmax/min:29.41/1.343
46-1045*	180	11/0	131	*Silicon Oxide / Quartz, syn = SiO2
	Ierr:100,200	derr:2.5	Bground:4.0	dmax/min:29.41/1.343
1-0527D	78	7/1	18	Aluminum Silicate Hydrate / Kaolinite = Al2Si2O5(OH)4
	Ierr:100,200	derr:2.5	Bground:4.0	dmax/min:29.41/1.343
76-0823C	31*	9/2	24	Potassium Aluminum Silicate / Potassium-Feldspar P2B = KAlSi3O8
	Ierr:100,200	derr:2.5	Bground:4.0	dmax/min:29.41/1.343
31-0966*	5*	3/0	21	*Potassium Aluminum Silicate / Orthoclase = KAlSi3O8
	Ierr:100,200	derr:2.5	Bground:4.0	dmax/min:29.41/1.343
9-0466*	57*	7/0	29	Sodium Aluminum Silicate / Albite, ordered = NaAlSi3O8
	Ierr:100,200	derr:2.5	Bground:4.0	dmax/min:29.41/1.343

Summary Report (Part 1 of 2):

	Full	Resid	31-0966: 56%		46-1045:131%		1-0527: 18%		76-0823: 24%	
d	I	I	d	I	d	I	d	I	d	I
7.215	9.3	None					7.20	14		
6.495	6.0	None	6.48	6.7					[6.5065	2.6]
6.371	5.3	None								
5.867	4.9	None	5.86	6.7					[5.8700	2.9]

4.978	5.1	5.1								
4.848	5.7	5.7								
4.807	6.1	6.1								
4.452	15	None					4.45	14		
4.375	14	14								
4.255	29	None	4.22	39	[4.2550	21]	[4.30	11]	[4.2296	16]
4.172	13	None					4.20	8.5		
4.035	13	None					4.04	5.7		
3.969	9.0	None							3.9475	5.3
3.934	8.4	None	3.94	8.9						
3.867	8.2	None	3.85	3.3					[3.8592	1.2]
3.772	18	None	3.77	44					[3.7814	19]
3.659	13	None								
" "	"									
			<3.61	8.9>						
3.576	12	None					3.59	18	[3.5462	2.6]
3.547	13	None	3.54	6.7					" "	"
3.473	13	None	3.47	25					[3.4676	12]
3.343	100	None			3.3435	131			[3.3193	24]
3.302	50	None	3.31	56					" "	"
" "	"		3.29	33					[3.2886	14]
3.255	13	None	3.25	11					[3.2533	8.4]
" "	"								[3.2338	19]
3.215	13	None	3.24	36					" "	"
3.192	15	None								
3.013	14	None							2.9959	14
2.9884	6.3	None	2.992	28						
2.9738	6.9	None	" "	"						
2.9324	6.2	None	2.934	4.4					[2.9350	2.2]
2.8972	7.8	None	2.901	17					[2.9063	6.0]
" "	"								[2.8958	5.0]
2.8504	6.1	None								
" "	"									
2.7675	4.4	None	2.769	11					[2.7691	4.8]
2.6862	6.0	6.0								
2.5998	7.0	None	2.601	10					[2.6069	4.3]
									<2.5787	8.9>
2.5591	13	None	2.571	17			[2.56	8.5]	[2.5526	2.2]
" "	"		2.553	4.4						
2.5170	11	None	2.515	4.4					2.5240	2.2
2.4982	9.4	None					2.50	8.5	[2.4874	1.0]
" "	"									
2.4550	15	None			2.4569	12				
" "	"									
2.4296	9.3	None	2.415	5.6					[2.4200	1.9]
2.3800	7.7	None	2.380	5.6					[2.3877	2.6]
2.3609	8.4	8.4								
2.3442	8.4	None					2.34	14		
2.3267	8.6	None	2.328	3.3					2.3242	1.4
2.2822	14	None			2.2815	10				
2.2353	9.9	None			2.2361	5.2				
2.1996	6.3	None	2.200	2.2					2.2038	1.0
2.1660	5.0	None	2.163	14					[2.1688	5.8]
" "	"								[2.1619	3.4]
2.1391	5.3	None							2.1287	2.6
2.1271	9.4	None	2.124	4.4	[2.1277	7.9]			[2.1215	1.9]
" "	"									
2.1082	4.7	None	2.113	2.2					[2.1148	1.7]
" "	"		2.108	2.2						
			<2.005	6.7>			<1.99	5.7>		
1.9791	8.3	None	1.971	4.4	[1.9799	5.2]			[1.9737	2.6]
			<1.922	5.6>						

1.9121	6.5	None	1.911	3.3					[1.9145	1.4]
1.8862	4.7	None	1.884	2.2						
1.8177	15	None			1.8180	17			[1.8105	1.2]
1.8006	5.8	None	1.807	2.2	[1.8017	1.3]	[1.80	1.4]	[1.7988	6.7]
" "	"		1.801	8.9						
" "	"		1.798	4.4						
1.7147	5.1	5.1								
1.6868	6.3	6.3								

1.6710	11	None	1.675	2.2*	1.6717	5.2	[1.67	7.1]	[1.6767	1.2]
1.5420	16	None			1.5415	12	[1.54	2.8]		
									<1.4989	5.0>
1.4905	9.1	None	1.495	6.7			[1.49	9.9]		
1.4536	6.4	None	1.450	2.2	1.4529	2.6			[1.4543	1.2]
1.4309	4.1	None							1.4353	1.4
" "	"								1.4328	1.0
" "	"								1.4300	1.9
1.4280	4.0	None	1.424	2.2					[1.4271	1.0]
1.4079	4.2	3.4								
1.4061	4.1	None	1.405	2.2						
1.3822	6.8	None	1.384	2.2	1.3821	7.9				
1.3741	9.6	None			1.3750	9.2				
" "	"				1.3719	6.6				

* = Obscured   <..> = Missing   [..] = Previously Removed

Summary Report (Part 2 of 2):

	Full	Resid	31-0966: 21%		9-0466: 29%	
d	I	I	d	I	d	I
7.215	9.3	None				
6.495	6.0	None	[6.48	2.5]		
6.371	5.3	None			6.39	5.7
5.867	4.9	None	[5.86	2.5]	[5.94	0.6]
4.978	5.1	5.1				
4.848	5.7	5.7				
4.807	6.1	6.1				
4.452	15	None				
4.375	14	14				
4.255	29	None	[4.22	15]		
4.172	13	None				
4.035	13	None			4.03	4.6
3.969	9.0	None	[3.94	3.4]		
3.934	8.4	None	" "	"		
3.867	8.2	None	[3.85	1.3]	[3.857	2.3]
3.772	18	None	[3.77	17]	[3.780	7.2]
3.659	13	None			3.684	5.7
" "	"				3.663	4.6
3.576	12	None				
3.547	13	None	[3.54	2.5]		
3.473	13	None	[3.47	9.5]	[3.484	0.6]
3.343	100	None				
3.302	50	None	[3.31	21]		
" "	"		[3.29	13]		
3.255	13	None	[3.25	4.2]		
" "	"		[3.24	14]		
3.215	13	None	" "	"		
3.192	15	None			3.196	29
3.013	14	None	[2.992	11]		
2.9884	6.3	None	" "	"		
2.9738	6.9	None	" "	"	[2.964	2.9]
2.9324	6.2	None	[2.934	1.7]	[2.933	4.6]
2.8972	7.8	None	[2.901	6.3]		
" "	"					
2.8504	6.1	None			2.866	2.3
" "	"				2.843	0.6
2.7675	4.4	None	[2.769	4.2]		
2.6862	6.0	6.0				
2.5998	7.0	None	[2.601	3.8]		

2.5591	13	None	[2.571	6.3]	[2.563	2.3]
" "	"		[2.553	1.7]		
2.5170	11	None	[2.515	1.7]	[2.511	0.6]
2.4982	9.4	None			" "	"
" "	"				[2.496	1.7]
2.4550	15	None			[2.460	1.7]
" "	"				[2.443	1.1]
2.4296	9.3	None	[2.415	2.1]	" "	"
2.3800	7.7	None	[2.380	2.1]	[2.388	1.1]
2.3609	8.4	8.4				
2.3442	8.4	None				
2.3267	8.6	None	2.328	1.3	[2.320	1.1]
2.2822	14	None			[2.278	0.6]
2.2353	9.9	None				
2.1996	6.3	None	2.200	0.8	[2.189	1.1]
2.1660	5.0	None	[2.163	5.3]		
" "	"					
2.1391	5.3	None				
2.1271	9.4	None	[2.124	1.7]	[2.125	2.3]
" "	"				[2.119	1.7]
2.1082	4.7	None	[2.113	0.8]	" "	"
" "	"					
1.9791	8.3	None	[1.971	1.7]	[1.980	1.1]
1.9121	6.5	None	[1.911	1.3]		
1.8862	4.7	None	[1.884	0.8]	[1.889	2.3]
1.8177	15	None			[1.824	5.1]
1.8006	5.8	None	[1.807	0.8]	[1.804	1.7]
" "	"		[1.801	3.4]		
" "	"		[1.798	1.7]		
1.7147	5.1	5.1				
1.6868	6.3	6.3				
1.6710	11	None	[1.675	0.8]		
1.5420	16	None				
1.4905	9.1	None	[1.495	2.5]		
1.4536	6.4	None	[1.450	0.8]		
1.4309	4.1	None				
" "	"					
" "	"					
1.4280	4.0	None	[1.424	0.8]		
1.4079	4.2	3.4	1.405	0.8		
1.4061	4.1	None				
1.3822	6.8	None	[1.384	0.8]		
1.3741	9.6	None				
" "	"					

* = Obscured <..> = Missing [..] = Previously Removed

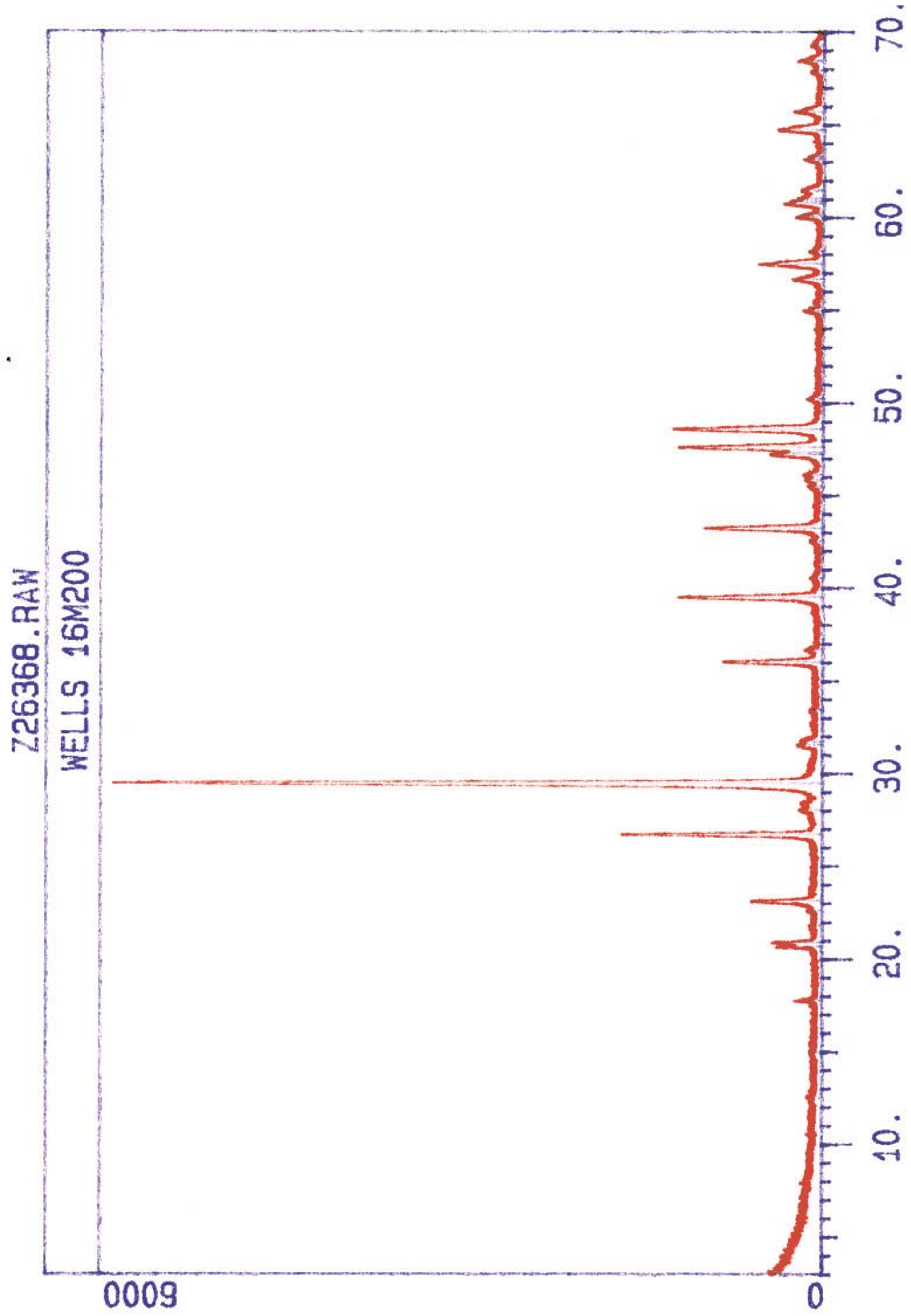
Z26368.RAW
WELLS 16M200
6000
0
10.
20.
30.
40.
50.
60.
70.

Input Pattern

WELLS 16M200
Peak search on 13-FEB-0411:33:58

d	I	d	I	d	I	d	I	d	I	d	I
7.081	2.2	3.338	28	2.2824	20	1.9211	6.2	1.5862	2.0	1.4700	2.2
5.930	1.5	3.184	3.3	2.2253	1.7	1.9104	20	1.5415	4.0	1.4403	6.5
4.994	3.9	3.031	100	2.1252	1.6	1.8739	21	1.5386	3.0	1.4213	4.2
4.299	6.4	2.8354	3.6	2.0925	17	1.8167	2.3	1.5249	5.6	1.3808	1.8
4.251	7.1	2.8210	2.5	1.9944	2.1	1.6713	2.8	1.5217	4.7	1.3712	3.8
4.077	1.7	2.6797	1.6	1.9796	2.5	1.6662	2.0	1.5185	3.5	1.3570	1.6
3.934	2.1	2.4922	14	1.9690	2.8	1.6252	4.4	1.5087	3.0		
3.848	10	2.4501	2.2	1.9254	7.5	1.6033	9.2	1.4725	2.8		

46 lines in pattern.

Identified Phases:

JCPDS#	SI	ML/X	At%	Identity . . .
5-0586*	339	19/0	108	*Calcium Carbonate / Calcite, syn = $CaCO_3$
	Ierr:50,150		derr:2.0	Bground:1.5 dmax/min:29.41/1.343
46-1045*	130	10/1	36	*Silicon Oxide / Quartz, syn = SiO_2
	Ierr:50,150		derr:2.0	Bground:1.5 dmax/min:29.41/1.343
71-0962C	55	6/0	7.2	Sodium Aluminum Silicate Hydrate = $Na_6Al_6Si_{10}O_{32}(H_2O)_{12}$
	Ierr:50,150		derr:2.0	Bground:1.5 dmax/min:29.41/1.343
5-0586*	26	3/0	44	*Calcium Carbonate / Calcite, syn = $CaCO_3$
	Ierr:50,150		derr:2.0	Bground:1.5 dmax/min:29.41/1.343
20-0452I	16	5/7	20	Calcium Aluminum Silicate Hydrate / Gismondine = $CaAl_2Si_2O_8.4H_2O$
	Ierr:50,150		derr:2.0	Bground:1.5 dmax/min:29.41/1.343

Summary Report (Part 1 of 2):

	Full	Resid	5-0586:108%		46-1045: 36%		71-0962: 7%		5-0586: 44%	
d	I	I	d	I	d	I	d	I	d	I
7.081	2.2	None					7.1015	7.2		
5.930	1.5	None								
4.994	3.9	None					5.0215	1.9		
4.299	6.4	None								
4.251	7.1	None			4.2550	5.7				
4.077	1.7	None					4.1000	4.4		
3.934	2.1	2.1								
3.848	10	None	3.86	13					[3.86	5.3]
3.338	28	None			3.3435	36				
3.184	3.3	None					3.1759	5.0		
3.031	100	None	3.035	108					[3.035	44]

2.8354	3.6	None	2.845	3.2					[2.845	1.3]
2.8210	2.5	2.1								
2.6797	1.6	None					2.6841	2.6		
2.4922	14	None	2.495	15					[2.495	6.1]
2.4501	2.2	None			2.4569	3.2				
2.2824	20	None	2.285	19	[2.2815	2.8]			[2.285	7.9]
2.2253	1.7	1.7								
2.1252	1.6	None			2.1277	2.1				
2.0925	17	None	2.095	19					[2.095	7.9]
1.9944	2.1	2.1								
1.9796	2.5	None			1.9799	1.4				
1.9690	2.8	1.9					1.9696	0.86		
1.9254	7.5	None	1.927	5.4						
1.9211	6.2	None							1.927	2.2
1.9104	20	None	1.913	18					[1.913	7.5]
1.8739	21	None	1.875	18					[1.875	7.5]
1.8167	2.3	None			1.8180	4.6				
1.6713	2.8	None			1.6717	1.4	[1.6738	0.58]		
1.6662	2.0	None								
1.6252	4.4	None	1.626	4.3			[1.6292	0.43]	[1.626	1.8]
1.6033	9.2	None	1.604	8.6	[1.6083	0.4]			[1.604	3.5]
1.5862	2.0	None	1.587	2.2			[1.5879	0.22]	[1.587	0.9]
1.5415	4.0	None			1.5415	3.2				
1.5386	3.0	None								
1.5249	5.6	None	1.525	5.4						
1.5217	4.7	None							1.525	2.2
1.5185	3.5	None	1.518	4.3			[1.5140	0.07]	[1.518	1.8]
1.5087	3.0	None	1.510	3.2					[1.510	1.3]
1.4725	2.8	None	1.473	2.2						
1.4700	2.2	None							1.473	0.9
1.4403	6.5	None	1.440	5.4					[1.440	2.2]
1.4213	4.2	None	1.422	3.2	[1.4184	0.4]	[1.4203	0.29]	[1.422	1.3]
1.3808	1.8	None			1.3821	2.1				
					<1.3750	2.5>				
1.3712	3.8	None			1.3719	1.8				
1.3570	1.6	None	1.356	1.1					[1.356	0.4]

* = Obscured   <..> = Missing   [..] = Previously Removed

Summary Report (Part 2 of 2):

d	Full I	Resid I	20-0452: 20% d	I
			<7.28	3.3>
7.081	2.2	None		
5.930	1.5	None	5.93	0.4
4.994	3.9	None	[5.01	0.8]
			<4.91	3.3>
4.299	6.4	None	4.27	7.1
4.251	7.1	None		
			<4.19	2.4>
4.077	1.7	None	[4.05	0.8]
3.934	2.1	2.1		
3.848	10	None		
3.338	28	None	[3.34	20]
3.184	3.3	None	[3.19	3.7]
			<3.13	2.9>
3.031	100	None		

2.8354	3.6	None		
2.8210	2.5	2.1	2.82	0.4
			<2.74	2.9>
			<2.70	3.7>
2.6797	1.6	None		
			<2.66	2.0>
2.4922	14	None		
2.4501	2.2	None	[2.46	1.6]
2.2824	20	None	[2.28	1.2]
2.2253	1.7	1.7		
2.1252	1.6	None	[2.13	1.2]
2.0925	17	None		
1.9944	2.1	2.1		
1.9796	2.5	None	[1.981	0.8]
1.9690	2.8	1.9		
1.9254	7.5	None		
1.9211	6.2	None	[1.916	0.4]
1.9104	20	None	" "	"
1.8739	21	None		
1.8167	2.3	None	[1.819	3.3]
1.6713	2.8	None		
1.6662	2.0	None	1.671	1.6
1.6252	4.4	None		
1.6033	9.2	None	[1.608	0.4]
1.5862	2.0	None		
1.5415	4.0	None		
1.5386	3.0	None	1.542	1.6
1.5249	5.6	None		
1.5217	4.7	None		
1.5185	3.5	None		
1.5087	3.0	None		
1.4725	2.8	None		
1.4700	2.2	None		
1.4403	6.5	None	[1.438	0.4]
1.4213	4.2	None		
1.3808	1.8	None	[1.384	0.8]
1.3712	3.8	None		
1.3570	1.6	None		

* = Obscured   <..> = Missing   [..] = Previously Removed

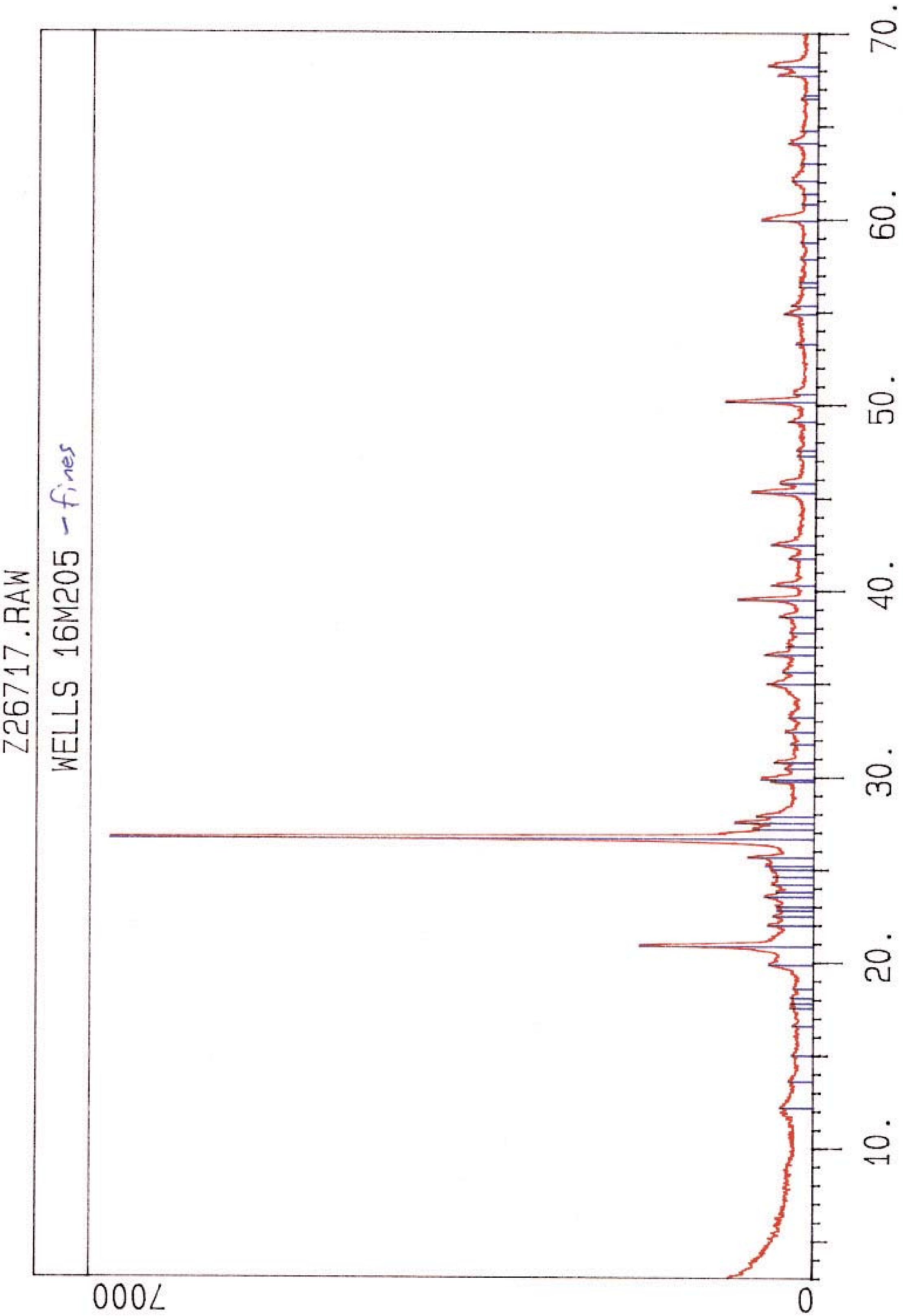
Z26717.RAW
WELLS 16M205 - fines
7000
0
10.
20.
30.
40.
50.
60.
70.

Input Pattern

WELLS 16M205

Peak search on 17-MAR-0417:09:14

d	I	d	I	d	I	d	I	d	I	d	I
7.239	4.7	3.892	5.2	3.198	8.2	2.4265	4.1	1.8177	13	1.4946	3.7
6.487	3.5	3.859	5.3	2.9982	6.3	2.3794	3.6	1.8031	3.3	1.4744	2.5
5.884	3.0	3.772	7.1	2.9881	7.6	2.3296	5.1	1.7182	3.0	1.4520	4.3
5.325	3.0	3.731	5.4	2.9310	4.3	2.2790	11	1.6714	4.8	1.4388	2.3
5.039	3.3	3.670	5.8	2.8991	4.4	2.2361	6.4	1.6586	3.7	1.4061	2.5
4.969	3.1	3.612	5.8	2.8989	5.8	2.1626	3.8	1.6314	2.6	1.4023	2.1
4.888	3.2	3.555	6.0	2.8130	3.4	2.1263	6.4	1.6248	2.6	1.3831	5.8
4.758	2.9	3.526	7.0	2.7594	4.2	2.0007	9.2	1.5927	2.4	1.3744	7.2
4.460	6.4	3.466	9.4	2.6951	3.7	1.9799	5.2	1.5704	2.4		
4.251	25	3.341	100	2.5630	6.9	1.9218	2.7	1.5430	8.0		
4.034	6.5	3.279	8.8	2.5177	4.6	1.9104	2.8	1.5224	2.3		
3.947	5.8	3.237	11	2.4559	7.3	1.8541	4.0	1.5100	2.2		

68 lines in pattern.

Identified Phases:

JCPDS#	SI	ML/X	At%	Identity . . .
76-0824C	421*	48/2	34	Potassium Aluminum Silicate / Potassium-Feldspar P2A = K.931Na0.055Ca.009Ba.005Al0.97Si3.03O8
	Ierr:100,200	derr:2.5	Bground:2.1	dmax/min:29.41/1.343
20-0452I	191	18/8	64	Calcium Aluminum Silicate Hydrate / Gismondine = CaAl2Si2O8.4H2O
	Ierr:100,200	derr:2.5	Bground:2.1	dmax/min:29.41/1.343
46-1045*	41	4/0	57	*Silicon Oxide / Quartz, syn = SiO2
	Ierr:100,200	derr:2.5	Bground:2.1	dmax/min:29.41/1.343
82-1572C	9*	4/1	19	Silicon Oxide = SiO2
	Ierr:100,200	derr:2.5	Bground:2.1	dmax/min:29.41/1.343

Triclinic

Summary Report:

	Full	Resid	76-0824: 34%		20-0452: 64%		46-1045: 57%		82-1572: 19%	
d	I	I	d	I	d	I	d	I	d	I
7.239	4.7	None			7.28	10				
6.487	3.5	None	6.4940	3.4						
5.884	3.0	None	5.8694	3.7	[5.93	1.3]				
					<5.76	2.5>			<5.6808	3.9>
5.325	3.0	None			5.28	1.3				
5.039	3.3	None			5.01	2.5				
4.969	3.1	3.1								
4.888	3.2	None			4.91	10				
4.758	2.9	2.9								
					<4.67	2.5>				
4.460	6.4	None			4.47	2.5			[4.4417	19]
4.251	25	None	4.2277	21	[4.27	22]	[4.2550	9.1]	[4.2809	3.2]
					<4.19	7.6>				
4.034	6.5	None			4.05	2.5			[4.0252	2.6]
3.947	5.8	None	3.9456	6.7						

3.892	5.2	5.2								
3.859	5.3	None	3.8555	2.0						
3.772	7.1	None	3.7750	26						
3.731	5.4	None							3.7185	4.3
3.670	5.8	5.8								
3.612	5.8	None	3.6166	5.4	[3.61	1.3]				
3.555	6.0	None	3.5430	4.0						
3.526	7.0	None							3.5302	5.4
3.466	9.4	None	3.4693	17					[3.4688	6.4]
3.341	100	None	3.3153	34	3.34	64	[3.3435	57]	[3.3140	1.5]
3.279	8.8	None	3.2898	20						
3.237	11	None	3.2470	12						
" "	"		3.2352	29						
3.198	8.2	None			3.19	11			[3.1816	12]
					<3.13	8.9>				
2.9982	6.3	None	2.9926	18	[2.99	1.3]				
2.9881	7.6	None	" "	"	" "	"				
2.9310	4.3	None	2.9347	2.7						
2.8991	4.4	None	2.8957	8.4						
2.8989	5.8	None	2.9021	8.7						
2.8130	3.4	None			2.82	1.3				
2.7594	4.2	None	2.7681	6.4						
					<2.74	8.9>				
2.6951	3.7	None			2.70	11			[2.6957	4.7]
			<2.6063	6.4>	<2.66	6.4>				
2.5630	6.9	None	2.5751	12	[2.56	1.3]			[2.5622	6.4]
" "	"		2.5524	3.4						
2.5177	4.6	None	2.5215	3.0	[2.51	1.3]				
2.4559	7.3	None			2.46	5.1	[2.4569	5.1]		
2.4265	4.1	None	2.4161	2.7					[2.4128	1.3]
2.3794	3.6	None	2.3851	3.4					[2.3736	1.7]
" "	"		2.3795	2.0						
2.3296	5.1	None	2.3255	1.7	2.34	1.3			[2.3360	3.6]
" "	"								[2.3294	3.0]
2.2790	11	None			2.28	3.8	2.2815	4.6		
2.2361	6.4	None			2.24	2.5	[2.2361	2.3]	[2.2435	2.1]
2.1626	3.8	None	2.1647	7.0						
" "	"		2.1568	4.0						
2.1263	6.4	None	2.1262	3.0	[2.13	3.8]	[2.1277	3.4]	[2.1186	2.6]
" "	"		2.1197	2.7						
2.0007	9.2	None	2.0100	4.0	[2.01	1.3]				
1.9799	5.2	None	1.9728	3.7	[1.981	2.5]	[1.9799	2.3]		
1.9218	2.7	None	1.9278	3.4	[1.916	1.3]				
" "	"		1.9222	2.7						
1.9104	2.8	None	1.9146	2.0	" "	"				
1.8541	4.0	None	1.8553	2.0	[1.850	1.3]				
1.8177	13	None			1.819	10	[1.8180	7.4]		
1.8031	3.3	None	1.8083	1.3			[1.8017	0.6]		
" "	"		1.8001	8.4						
" "	"		1.7966	6.4						
					<1.754	2.5>				
1.7182	3.0	3.0								
1.6714	4.8	None	1.6758	1.7	1.671	5.1	[1.6717	2.3]		
1.6586	3.7	None	1.6615	0.3*			1.6592	1.1	[1.6616	0.7]
" "	"		1.6576	0.3*						
					<1.641	2.5>				

1.6314	2.6	None	1.6303	2.0					[1.6370	0.7]
1.6248	2.6	1.9							1.6285	0.7
1.5927	2.4	None	1.5945	1.7					[1.5919	0.7]
1.5704	2.4	None	1.5696	1.7					[1.5735	0.2]
1.5430	8.0	None			1.542	5.1	[1.5415	5.1]	[1.5472	0.6]
1.5224	2.3	1.9							1.5173	0.4*
1.5100	2.2	None	1.5145	2.3						
" "	"		1.5109	1.3						
1.4946	3.7	None	1.4963	5.7	[1.499	1.3]			[1.4996	0.9]
1.4744	2.5	2.3							1.4704	0.2*
1.4520	4.3	None	1.4528	1.3	[1.454	1.3]	[1.4529	1.1]	[1.4540	0.2]
" "	"		1.4504	1.7						
1.4388	2.3	None	1.4393	2.7	[1.438	1.3]			[1.4430	0.6]
			<1.4290	2.3>						
1.4061	2.5	2.5								
1.4023	2.1	1.5							1.3978	0.6
1.3831	5.8	None			1.384	2.5	[1.3821	3.4]	[1.3845	0.2]
1.3744	7.2	None			1.375	0.6*	1.3750	4.0		
" "	"						1.3719	2.9		

* = Obscured   <..> = Missing   [..] = Previously Removed

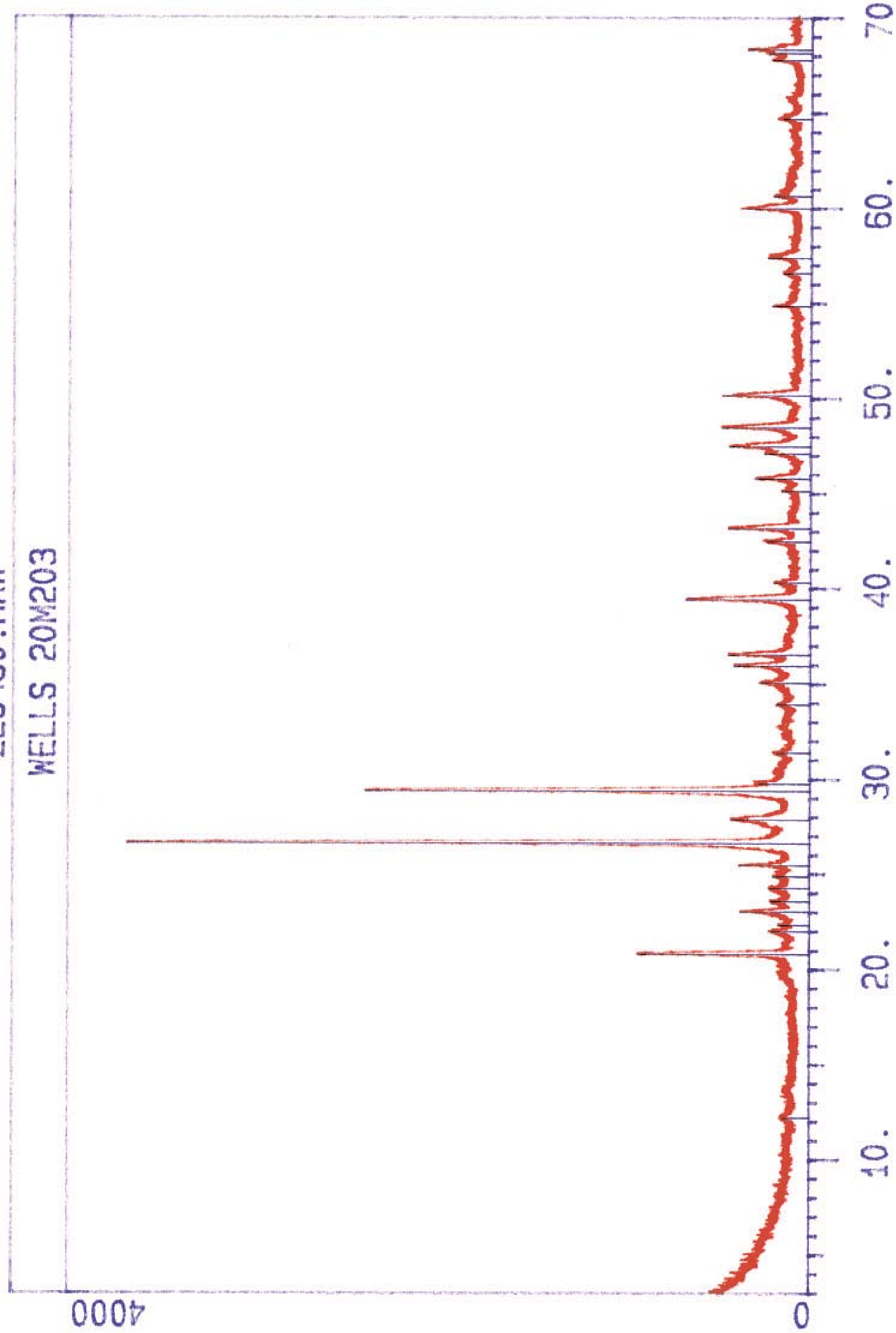
Z26450.RAW
WELLS 20M203
4000
0
10.
20.
30.
40.
50.
60.
70.

Input Pattern

WELLS 20M203

Peak search on 20-FEB-0411:57:12

d	I	d	I	d	I	d	I	d	I	d	I
7.231	4.0	3.573	5.5	2.6398	5.1	2.0943	12	1.6730	5.8	1.3762	6.5
4.258	25	3.493	10	2.5567	7.3	2.0078	4.3	1.6261	4.1	1.3726	9.5
4.029	5.6	3.344	100	2.4938	11	1.9804	8.2	1.6054	6.4		
3.969	4.7	3.197	12	2.4572	12	1.9280	6.8	1.5419	9.6		
3.854	10	3.036	65	2.2839	18	1.9141	12	1.5267	5.6		
3.767	5.8	2.9982	7.6	2.2358	5.4	1.8762	13	1.4408	4.3		
3.660	6.0	2.8472	4.9	2.1261	6.5	1.8180	13	1.3826	5.8		

37 lines in pattern.

Identified Phases:

JCPDS#	SI	ML/X	At%	Identity . . .
46-1045*	232	13/0	125	*Silicon Oxide / Quartz, syn = SiO2
	Ierr:50,150		derr:2.0	Bground:4.0 dmax/min:29.41/1.343
5-0586*	227	13/0	77	*Calcium Carbonate / Calcite, syn = CaCO3
	Ierr:50,150		derr:2.0	Bground:4.0 dmax/min:29.41/1.343
20-0452I	20	4/6	51	Calcium Aluminum Silicate Hydrate / Gismondine = CaAl2Si2O8.4H2O
	Ierr:50,150		derr:2.0	Bground:4.0 dmax/min:29.41/1.343
9-0457D	37	6/6	8.8	*Sodium Calcium Aluminum Silicate / Albite, calcian, ordered = (Na,Ca)(Si,Al)4O8
	Ierr:50,150		derr:2.0	Bground:4.0 dmax/min:29.41/1.343

Summary Report:

	Full	Resid	46-1045:125%		5-0586: 77%		20-0452: 51%		9-0457: 9%	
d	I	I	d	I	d	I	d	I	d	I
7.231	4.0	None					7.28	8.2		
							<4.91	8.2>	<6.38	5.3>
4.258	25	None	4.2550	20			[4.27	18]		
							<4.19	6.2>		
4.029	5.6	None					4.05	2.1	4.03	7.0
3.969	4.7	4.7								
3.854	10	None			3.86	9.2			[3.86	4.4]
3.767	5.8	None							3.76	6.2
									<3.69	5.3>
3.660	6.0	None							3.66	5.3
3.573	5.5	5.5								
3.493	10	6							3.49	4.4
3.344	100	None	3.3435	125			[3.34	51]	[3.36	4.4]
3.197	12	None					3.19	9.2	[3.20	7.0]
" "	"								[3.18	8.8]
							<3.13	7.2>	<3.15	4.4>
3.036	65	None			3.035	77				
2.9982	7.6	6.6					2.99	1.0*		
									<2.98	5.3>
									<2.93	6.2>
2.8472	4.9	None			2.845	2.3			[2.84	5.3]
							<2.74	7.2>		
							<2.70	9.2>		
							<2.66	5.1>		

2.6398	5.1	None							2.65	4.4
2.5567	7.3	None					2.56	1.0*	2.55	5.3
2.4938	11	None			2.495	11				
									<2.47	4.4>
2.4572	12	None	2.4569	11			[2.46	4.1]		
2.2839	18	None	2.2815	10	2.285	14	[2.28	3.1]		
2.2358	5.4	None	2.2361	5.0			[2.24	2.1]		
2.1261	6.5	None	2.1277	7.5			[2.13	3.1]		
2.0943	12	None			2.095	14				
2.0078	4.3	3.3					2.01	1.0		
1.9804	8.2	None	1.9799	5.0			[1.981	2.1]		
1.9280	6.8	None			1.927	3.8	[1.933	1.0]		
1.9141	12	None			1.913	13	[1.916	1.0]		
1.8762	13	None			1.875	13				
1.8180	13	None	1.8180	16			[1.819	8.2]		
1.6730	5.8	None	1.6717	5.0			[1.671	4.1]		
1.6261	4.1	None			1.626	3.1				
1.6054	6.4	None	1.6083	1.2*	1.604	6.1	[1.608	1.0]		
1.5419	9.6	None	1.5415	11			[1.542	4.1]		
1.5267	5.6	None			1.525	3.8				
1.4408	4.3	None			1.440	3.8	[1.438	1.0]		
1.3826	5.8	None	1.3821	7.5			[1.384	2.1]		
1.3762	6.5	None	1.3750	8.7			[1.375	0.5]		
1.3726	9.5	None	1.3719	6.2			" "	"		

* = Obscured <..> = Missing [..] = Previously Removed

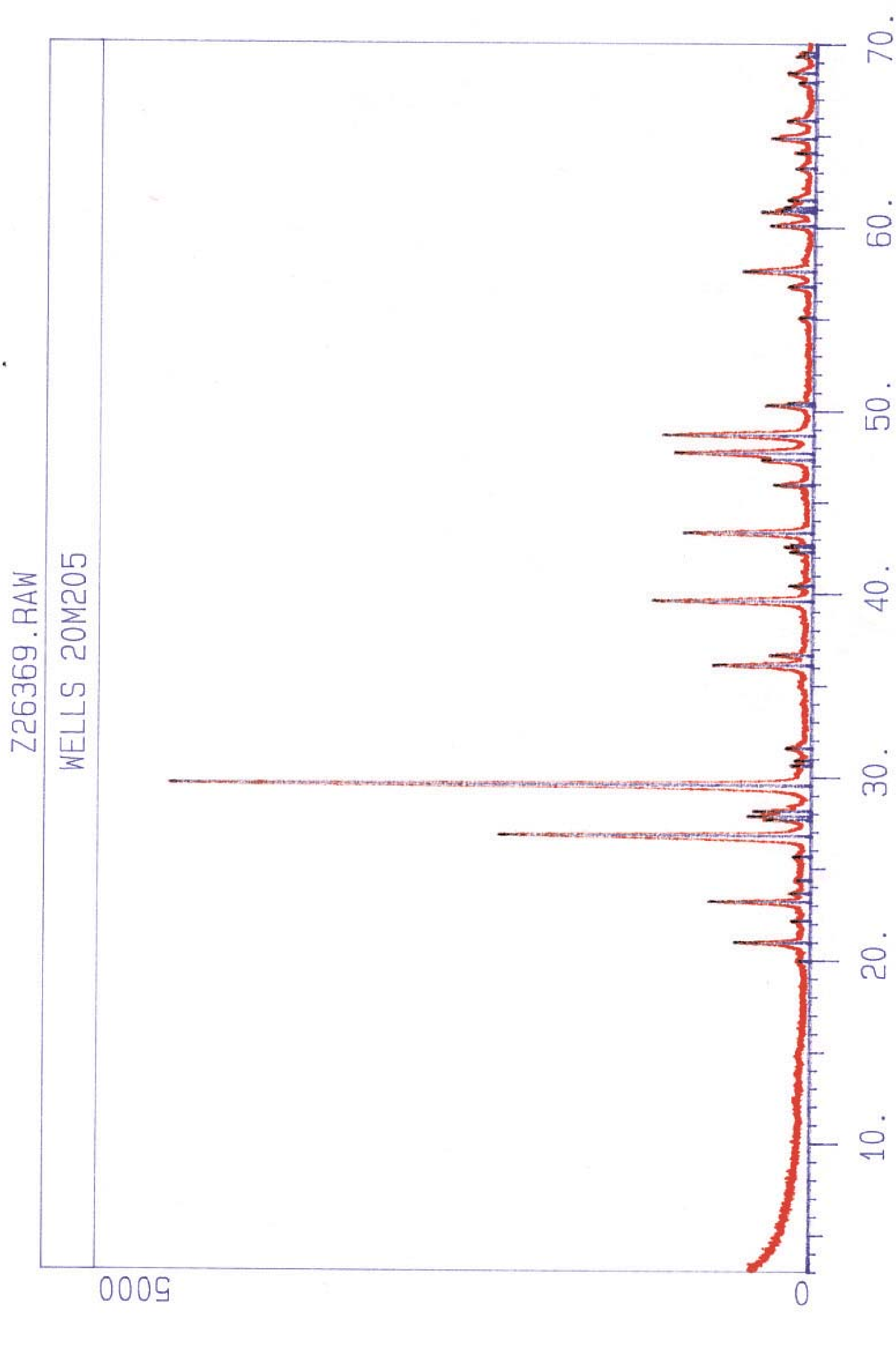
Z26369.RAW
WELLS 20M205
5000
0
10.
20.
30.
40.
50.
60.
70.

Input Pattern

WELLS 20M205
Peak search on 13-FEB-0412:11:14

d	I	d	I	d	I	d	I	d	I	d	I
4.453	1.8	3.227	7.0	2.4533	6.7	1.9766	6.2	1.6013	11	1.4386	6.9
4.241	12	3.205	10	2.2788	25	1.9220	8.1	1.5406	6.9	1.4194	4.6
4.015	2.9	3.175	9.0	2.2327	3.7	1.9084	22	1.5229	8.5	1.3812	2.7
3.840	16	3.025	100	2.2327	3.7	1.8719	24	1.5208	5.3	1.3719	4.5
3.764	3.1	2.9198	3.3	2.1386	3.6	1.8154	7.5	1.5172	4.8	1.3559	3.1
3.657	2.0	2.8958	2.6	2.1252	4.4	1.8106	4.0	1.5083	4.3	1.3525	2.0
3.477	2.7	2.8367	4.1	2.1204	3.3	1.6679	2.3	1.4713	3.0		
3.333	49	2.4886	16	2.0901	20	1.6225	4.0	1.4540	2.9		

46 lines in pattern.

Identified Phases:

JCPDS#	SI	ML/X	At%	Identity . . .
5-0586*	276	18/1	123	*Calcium Carbonate / Calcite, syn = CaCO3
	Ierr:50,150			derr:2.0 Bground:1.8 dmax/min:29.41/1.343
46-1045*	178	13/0	64	*Silicon Oxide / Quartz, syn = SiO2
	Ierr:50,150			derr:2.0 Bground:1.8 dmax/min:29.41/1.343
79-1149C	82	12/7	15	Sodium Calcium Aluminum Silicate / Andesine - from Hogarth Ranges, Australia = Na.499Ca.491(Al1.488Si2.506O8)
	Ierr:50,150			derr:2.0 Bground:1.8 dmax/min:29.41/1.343
71-0706C	29	5/1	6.8	Magnesium Iron Calcium Silicate / Pigeonite = (Mg.39Fe.52Ca.09)SiO3
	Ierr:50,150			derr:2.0 Bground:1.8 dmax/min:29.41/1.343

Summary Report:

	Full	Resid	5-0586:123%		46-1045: 64%		79-1149: 15%		71-0706: 7%	
d	I	I	d	I	d	I	d	I	d	I
4.453	1.8	None							4.4364	0.95
4.241	12	None			4.2550	10				
4.015	2.9	None					4.0450	9.7		
							<3.8958	2.2>		
3.840	16	None	3.86	15						
3.764	3.1	None					3.7547	7.1		
3.657	2.0	None					3.6449	4.0		
3.477	2.7	None					3.4755	1.5		
							<3.3696	2.8>		
3.333	49	None			3.3435	64			[3.3263	1.1]
3.227	7.0	None					3.2325	6.3	[3.2075	3.7]
3.205	10	None					3.2072	15	" "	"
3.175	9.0	None					3.1828	12		
							<3.1390	4.8>		
3.025	100	None	3.035	123			[3.0216	2.5]	[3.0183	6.8]
							<2.9507	2.8>		

2.9198	3.3	None					2.9335	2.2	[2.9178	2.9]
" "	"						2.9160	1.2		
2.8958	2.6	None							2.9010	3.6
2.8367	4.1	None	2.845	3.7			[2.8402	2.5]		
							<2.5232	3.9>	<2.5762	3.1>
							<2.5081	2.2>		
2.4886	16	None	2.495	17					[2.4861	3.4]
2.4533	6.7	None			2.4569	5.8			[2.4579	1.8]
2.2788	25	None	2.285	22	[2.2815	5.2]	[2.2876	0.8]		
2.2327	3.7	None			2.2361	2.6				
2.2327	3.7	None					2.2271	0.6	2.2300	1.0
2.1386	3.6	None					2.1416	1.1	2.1451	2.5
" "	"								2.1383	1.6
2.1252	4.4	None			2.1277	3.9	[2.1219	0.8]		
2.1204	3.3	None					2.1254	1.4	[2.1144	0.48]
2.0901	20	None	2.095	22						
1.9766	6.2	3.6			1.9799	2.6				
1.9220	8.1	None	1.927	6.1			[1.9258	1.1]		
1.9084	22	None	1.913	21						
1.8719	24	None	1.875	21			[1.8773	0.9]		
1.8154	7.5	None			1.8180	8.4				
1.8106	4.0	4.0								
							<1.7747	2.3>		
1.6679	2.3	None			1.6717	2.6			[1.6631	0.14]
1.6225	4.0	None	1.626	4.9			[1.6200	0.2]	[1.6254	1.9]
1.6013	11	None	1.604	9.8			[1.6062	0.3]	[1.6038	0.07]
			<1.587	2.5>						
1.5406	6.9	None			1.5415	5.8			[1.5432	0.54]
1.5229	8.5	None	1.525	6.1					[1.5247	0.07]
1.5208	5.3	5.2							1.5212	0.07*
1.5172	4.8	None	1.518	4.9					[1.5149	0.07]
1.5083	4.3	None	1.510	3.7					[1.5075	0.34]
1.4713	3.0	None	1.473	2.5			[1.4754	0.6]	[1.4707	0.34]
1.4540	2.9	None			1.4529	1.3	[1.4579	0.6]		
1.4386	6.9	None	1.440	6.1						
1.4194	4.6	None	1.422	3.7	[1.4184	0.6]			[1.4191	0.34]
1.3812	2.7	None			1.3821	3.9				
1.3719	4.5	None			1.3750	4.5			[1.3736	0.41]
" "	"				1.3719	3.2				
1.3559	3.1	None	1.356	1.2						
1.3525	2.0	2.0								

* = Obscured <..> = Missing [..] = Previously Removed

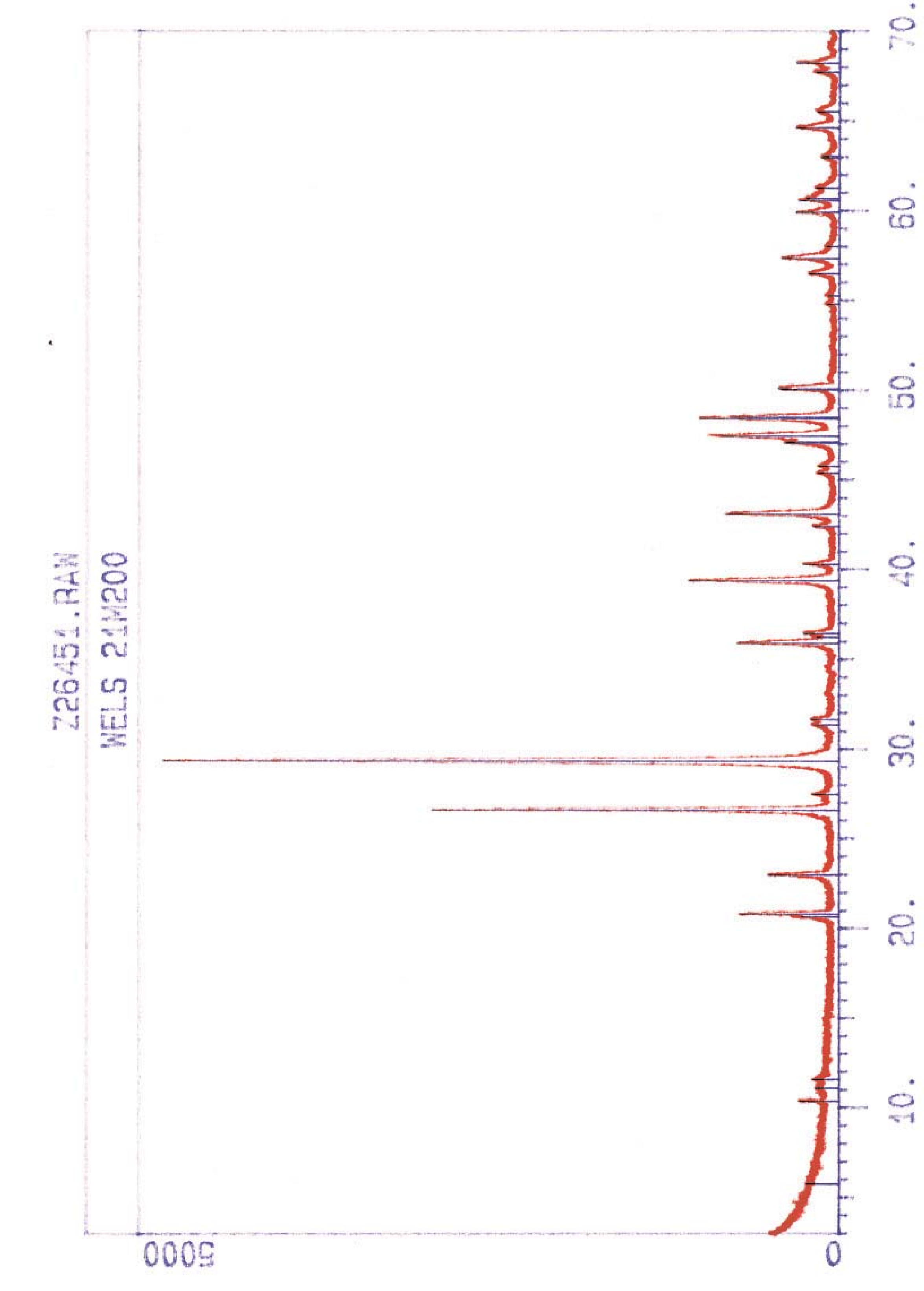
Z26451.RAW
WELS 21M200
5000
0
10.
20.
30.
40.
50.
60.
70.

Input Pattern

WELS 21M200
Peak search on 26-FEB-0410:46:44

d	I	d	I	d	I	d	I	d	I	d	I
15.17	4.9	3.241	4.0	2.2359	5.3	1.8774	21	1.5887	1.9	1.4235	3.3
8.495	5.9	3.040	100	2.1290	3.8	1.8741	16	1.5424	6.4	1.3826	3.5
7.943	3.5	2.8490	3.7	2.0964	17	1.8215	8.5	1.5271	6.0	1.3736	6.3
7.616	3.9	2.8227	4.1	1.9961	3.1	1.8197	9.0	1.5244	4.9		
4.291	5.5	2.4972	15	1.9804	3.0	1.6741	1.9	1.5114	3.4		
4.259	15	2.4749	3.3	1.9295	8.1	1.6607	1.7	1.4755	2.7		
3.861	10	2.4609	5.3	1.9272	7.8	1.6278	4.5	1.4734	2.4		
3.347	60	2.2865	22	1.9142	17	1.6057	8.5	1.4412	6.5		

43 lines in pattern.

Identified Phases:

JCPDS#	SI	ML/X	At%	Identity . . .
5-0586*	300	17/1	103	*Calcium Carbonate / Calcite, syn = CaCO3
	Ierr:50,150		derr:2.0	Bground:1.7 dmax/min:29.41/1.343
46-1045*	195	13/0	68	*Silicon Oxide / Quartz, syn = SiO2
	Ierr:50,150		derr:2.0	Bground:1.7 dmax/min:29.41/1.343
5-0586*	41	4/1	64	*Calcium Carbonate / Calcite, syn = CaCO3
	Ierr:50,150		derr:2.0	Bground:1.7 dmax/min:29.41/1.343
78-1252C	24	2/0	32	Silicon Oxide / Quartz alpha - synthetic = SiO2
	Ierr:50,150		derr:2.0	Bground:1.7 dmax/min:29.41/1.343
75-0306C	26	3/0	12	Sodium Chloride / Halite = NaCl
	Ierr:50,150		derr:2.0	Bground:1.7 dmax/min:29.41/1.343
46-1405*	21	3/4	21	Calcium Aluminum Silicate Hydrate / Cowlesite = CaAl2Si3O10.6H2O
	Ierr:50,150		derr:2.0	Bground:1.7 dmax/min:29.41/1.343

Summary Report (Part 1 of 2):

	Full	Resid	5-0586:103%		46-1045: 68%		5-0586: 64%		78-1252: 32%	
d	I	I	d	I	d	I	d	I	d	I
15.17	4.9	None								
8.495	5.9	4.5								
7.943	3.5	3.5								
7.616	3.9	None								
4.291	5.5	None							4.2602	5.8
4.259	15	None			4.2550	11				
3.861	10	None	3.86	12			[3.86	7.7]		
3.347	60	None			3.3435	68			[3.3458	32]
3.241	4.0	2.9								
3.040	100	None	3.035	103			[3.035	64]		

2.8490	3.7	None	2.845	3.1			[2.845	1.9]		
2.8227	4.1	None								
2.4972	15	None	2.495	14			[2.495	9.0]		
2.4749	3.3	3.3								
2.4609	5.3	None			2.4569	6.1			[2.4596	1.6]
2.2865	22	None	2.285	19	[2.2815	5.4]	[2.285	12]	[2.2821	1.6]
2.2359	5.3	None			2.2361	2.7			[2.2387	0.3]
2.1290	3.8	None			2.1277	4.1			[2.1301	1.3]
2.0964	17	None	2.095	19			[2.095	12]		
1.9961	3.1	None								
1.9804	3.0	None			1.9799	2.7			[1.9817	0.3]
1.9295	8.1	None					1.927	3.2		
1.9272	7.8	None	1.927	5.2						
1.9142	17	None	1.913	18			[1.913	11]		
1.8774	21	None					1.875	11		
1.8741	16	None	1.875	18						
1.8215	8.5	None							1.8190	4.2
1.8197	9.0	None			1.8180	8.8				
1.6741	1.9	None			1.6717	2.7			[1.6729	0.6]
1.6607	1.7	None			1.6592	1.4			[1.6594	0.3]
1.6278	4.5	None	1.626	4.1			[1.626	2.6]		
1.6057	8.5	None	1.604	8.3	[1.6083	0.7]	[1.604	5.2]	[1.6102	0.3]
1.5887	1.9	None	1.587	2.1			[1.587	1.3]		
1.5424	6.4	None			1.5415	6.1			[1.5432	1.6]
1.5271	6.0	None					1.525	3.2		
1.5244	4.9	None	1.525	5.2						
			<1.518	4.1>			<1.518	2.6>		
1.5114	3.4	None	1.510	3.1			[1.510	1.9]		
1.4755	2.7	None					1.473	1.3		
1.4734	2.4	None	1.473	2.1						
1.4412	6.5	None	1.440	5.2			[1.440	3.2]		
1.4235	3.3	None	1.422	3.1			[1.422	1.9]	[1.4201	0.3]
1.3826	3.5	None			1.3821	4.1			[1.3833	1.0]
1.3736	6.3	None			1.3750	4.7			[1.3756	1.6]
" "	"				1.3719	3.4				

* = Obscured   <..> = Missing   [..] = Previously Removed

Summary Report (Part 2 of 2):

d	Full I	Resid I	75-0306: 12% d	I	46-1405: 21% d	I
15.17	4.9	None			15.239	21
8.495	5.9	4.5			8.489	1.4
7.943	3.5	3.5				
7.616	3.9	None			7.637	3.1
4.291	5.5	None				
4.259	15	None				
3.861	10	None				
					<3.826	2.5>
3.347	60	None				
3.241	4.0	2.9	3.2563	1.1		
					<3.062	2.1>
3.040	100	None				
					<2.975	2.7>
					<2.938	2.9>
2.8490	3.7	None				
2.8227	4.1	None	2.8200	12	[2.831	1.0]
2.4972	15	None			[2.508	0.2]
2.4749	3.3	3.3				
2.4609	5.3	None				

2.2865	22	None		
2.2359	5.3	None		
2.1290	3.8	None		
2.0964	17	None		
1.9961	3.1	None	1.9940	7.0
1.9804	3.0	None		
1.9295	8.1	None		
1.9272	7.8	None		
1.9142	17	None		
1.8774	21	None		
1.8741	16	None		
1.8215	8.5	None		
1.8197	9.0	None		
1.6741	1.9	None		
1.6607	1.7	None		
1.6278	4.5	None	[1.6281	2.0]
1.6057 ·	8.5	None		
1.5887	1.9	None		
1.5424	6.4	None		
1.5271	6.0	None		
1.5244	4.9	None		
1.5114	3.4	None		
1.4755	2.7	None		
1.4734	2.4	None		
1.4412	6.5	None		
1.4235	3.3	None		
1.3826	3.5	None		
1.3736	6.3	None		
" "	"			

* = Obscured   <..> = Missing   [..] = Previously Removed

APPENDIX I: FTIR RESULTS

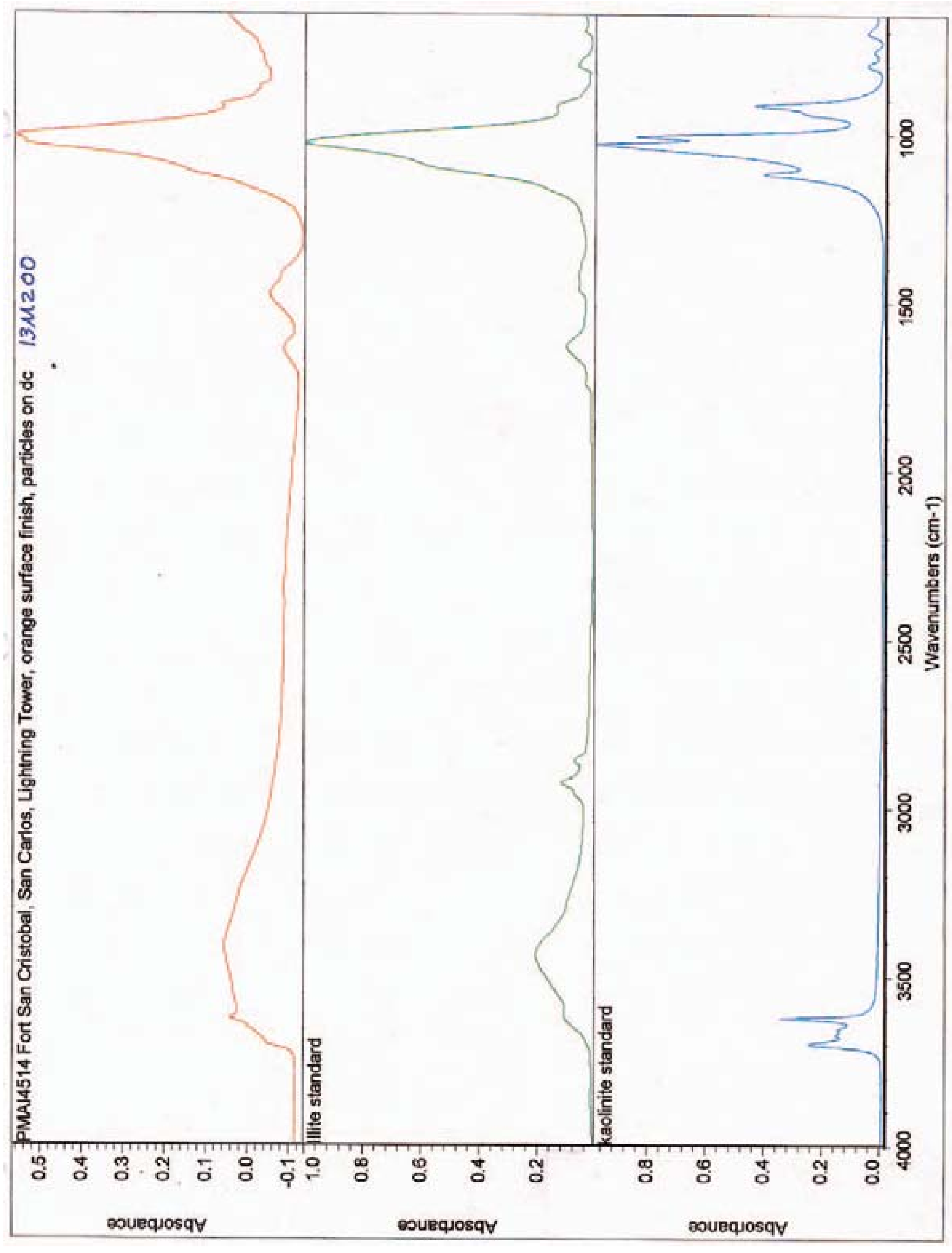
PMAI4514 Fort San Cristobal, San Carlos, Lightning Tower, orange surface finish, particles on dc
13M200
Illite standard
kaolinite standard
Absorbance
Absorbance
Absorbance
Wavenumbers (cm-1)

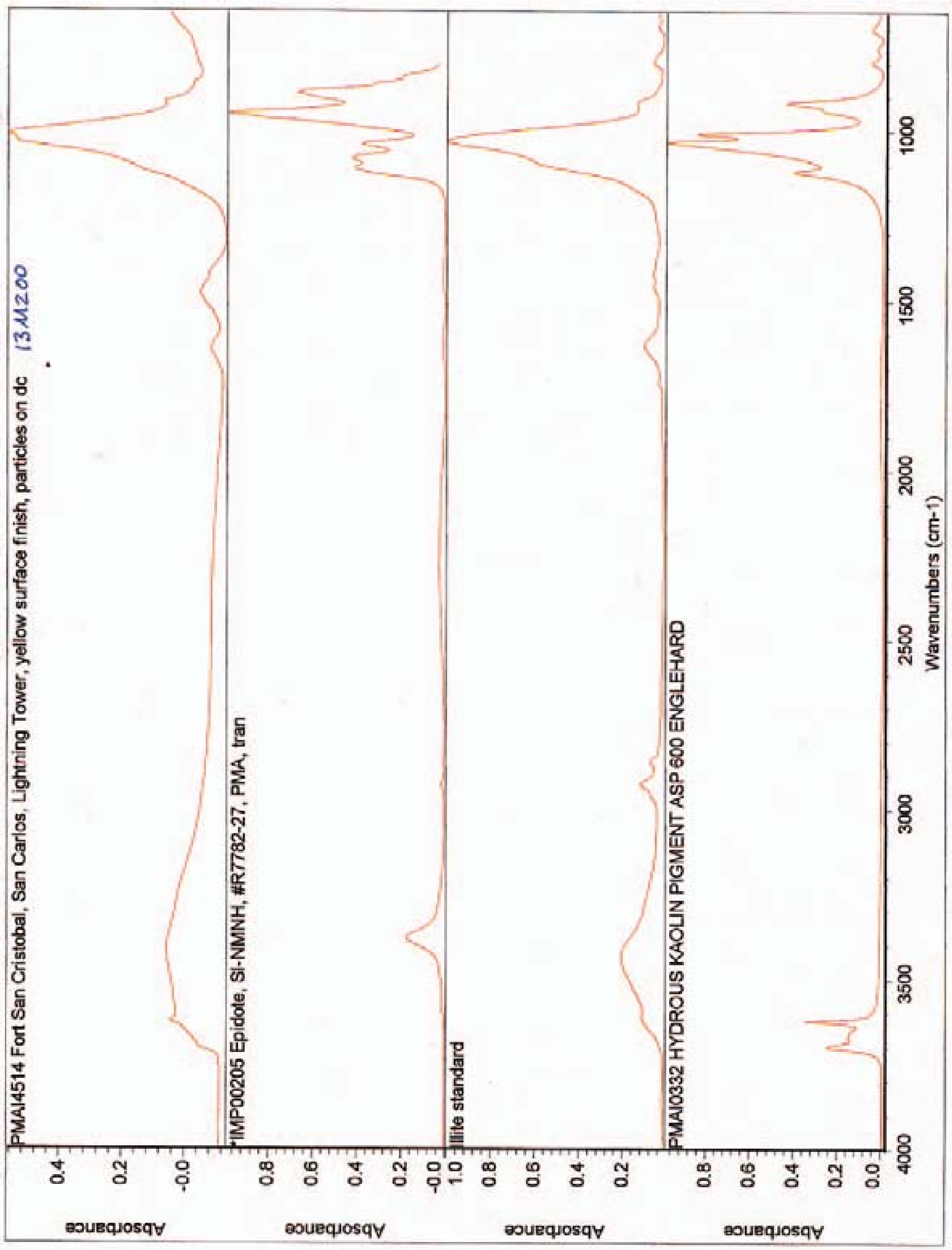
PMAI4514 Fort San Cristobal, San Carlos, Lightning Tower, yellow surface finish, particles on dc
*IMP00205 Epidote, SI-NMNH, #R7782-27, PMA, tran
Illite standard
PMAI0332 HYDROUS KAOLIN PIGMENT ASP 600 ENGLEHARD
Absorbance
Wavenumbers (cm-1)

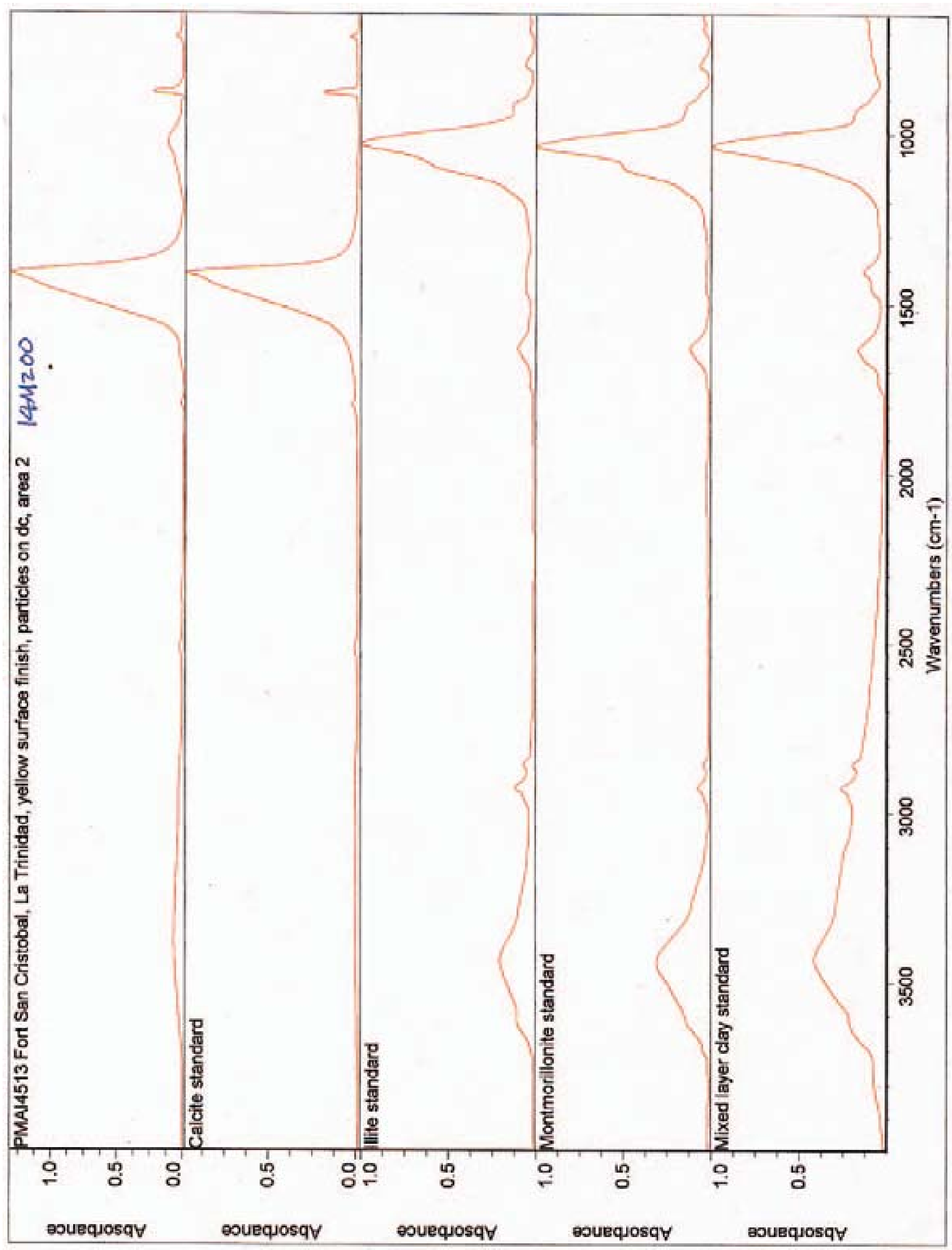
PMAI4513 Fort San Cristobal, La Trinidad, yellow surface finish, particles on dc, area 2
Calcite standard
Illite standard
Montmorillonite standard
Mixed layer clay standard
Absorbance
Absorbance
Absorbance
Absorbance
Absorbance
1.0
0.5
0.0
Wavenumbers (cm-1)
3500
3000
2500
2000
1500
1000

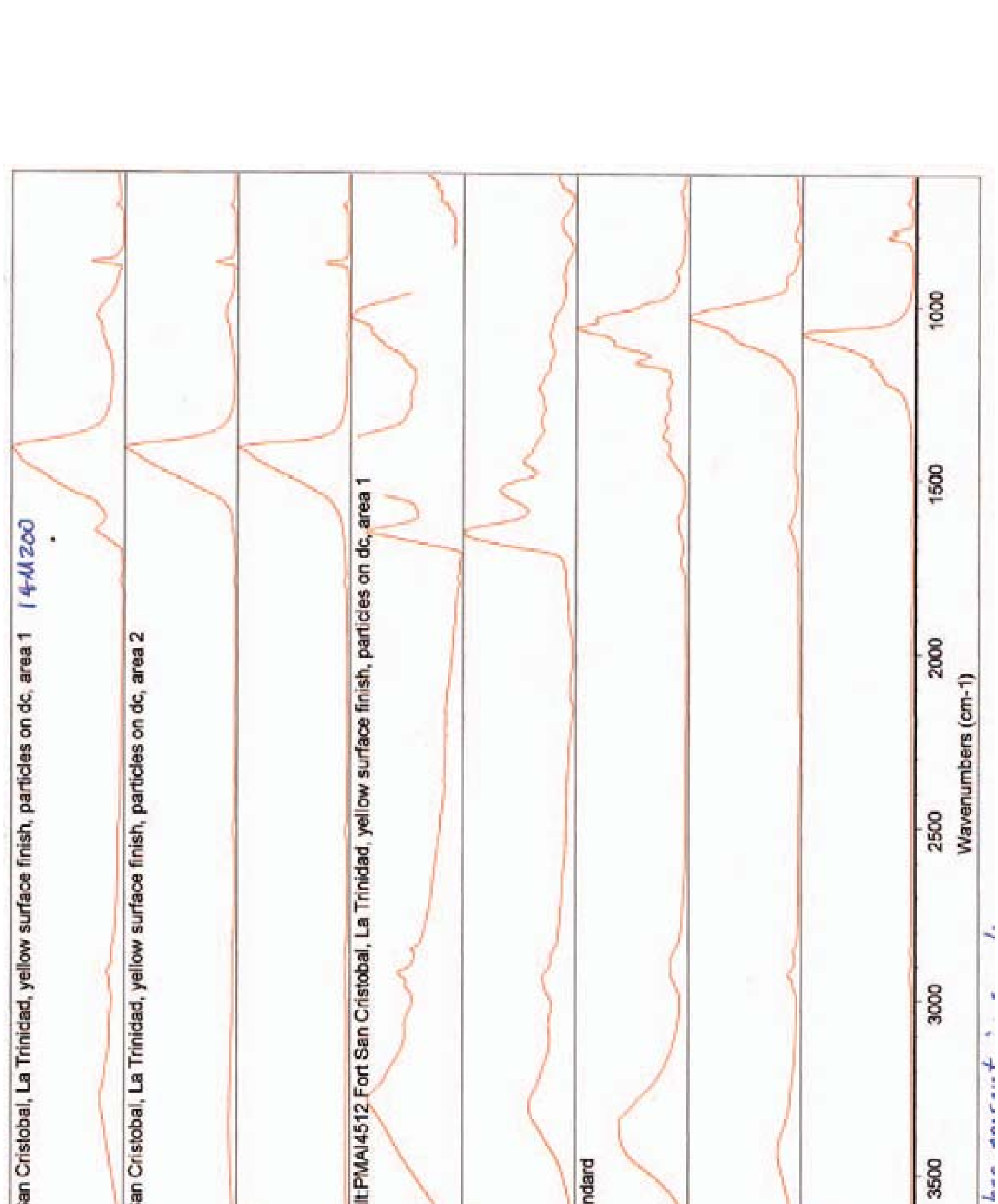
PMAI4512 Fort San Cristobal, La Trinidad, yellow surface finish, particles on dc, area 1
PMAI4513 Fort San Cristobal, La Trinidad, yellow surface finish, particles on dc, area 2
Calcite standard
Subtraction Result:PMAI4512 Fort San Cristobal, La Trinidad, yellow surface finish, particles on dc, area 1
Protein standard
Carbohydrate standard
Illite standard
quartz standard
Absorbance
Wavenumbers (cm-1)
4000
3500
3000
2500
2000
1500
1000

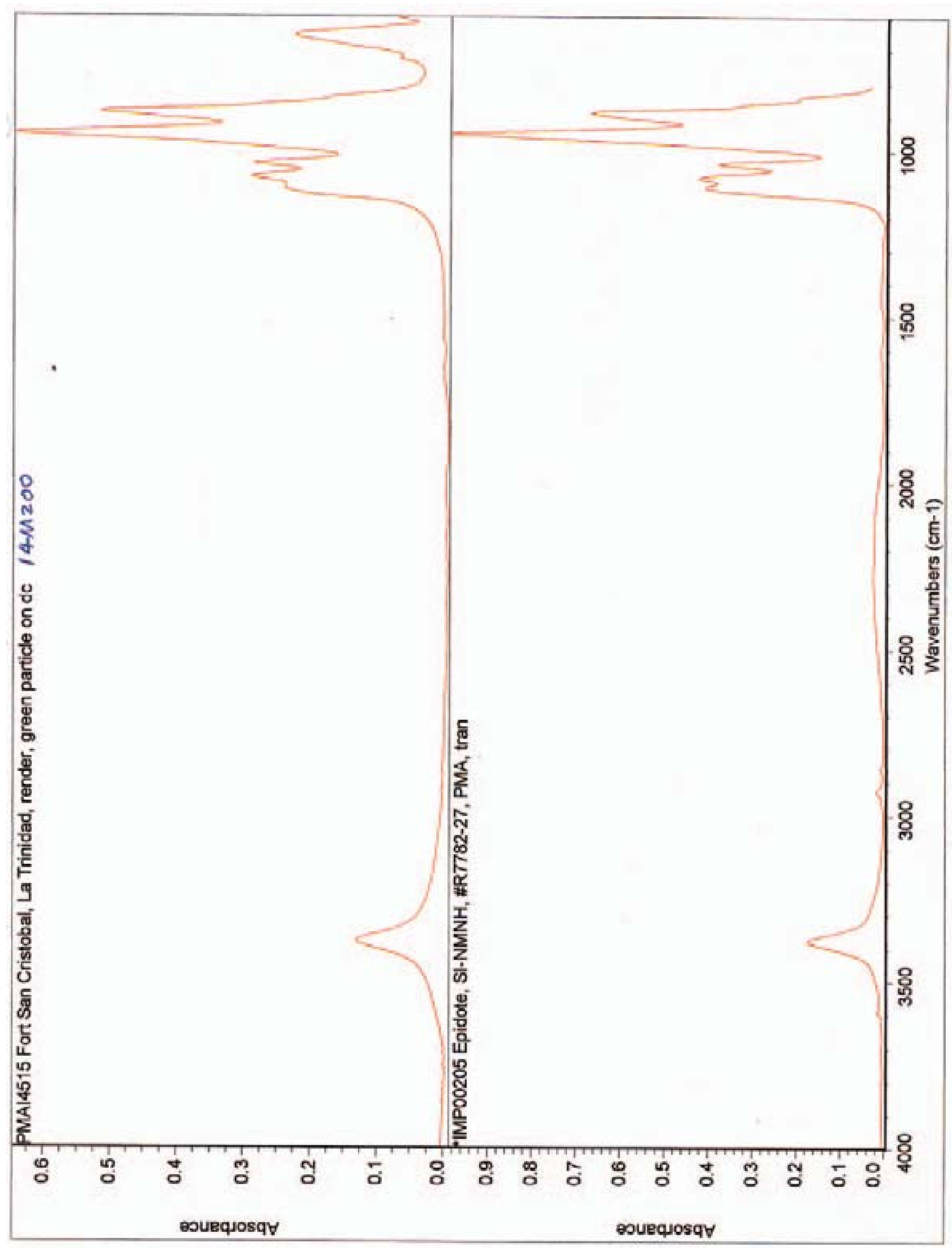
PMAI4515 Fort San Cristobal, La Trinidad, render, green particle on dc
*IMP00205 Epidote, SI-NMNH, #R7782-27, PMA, tran
Absorbance
Absorbance
Wavenumbers (cm-1)
4000
3500
3000
2500
2000
1500
1000
0.0
0.1
0.2
0.3
0.4
0.5
0.6
0.7
0.8
0.9

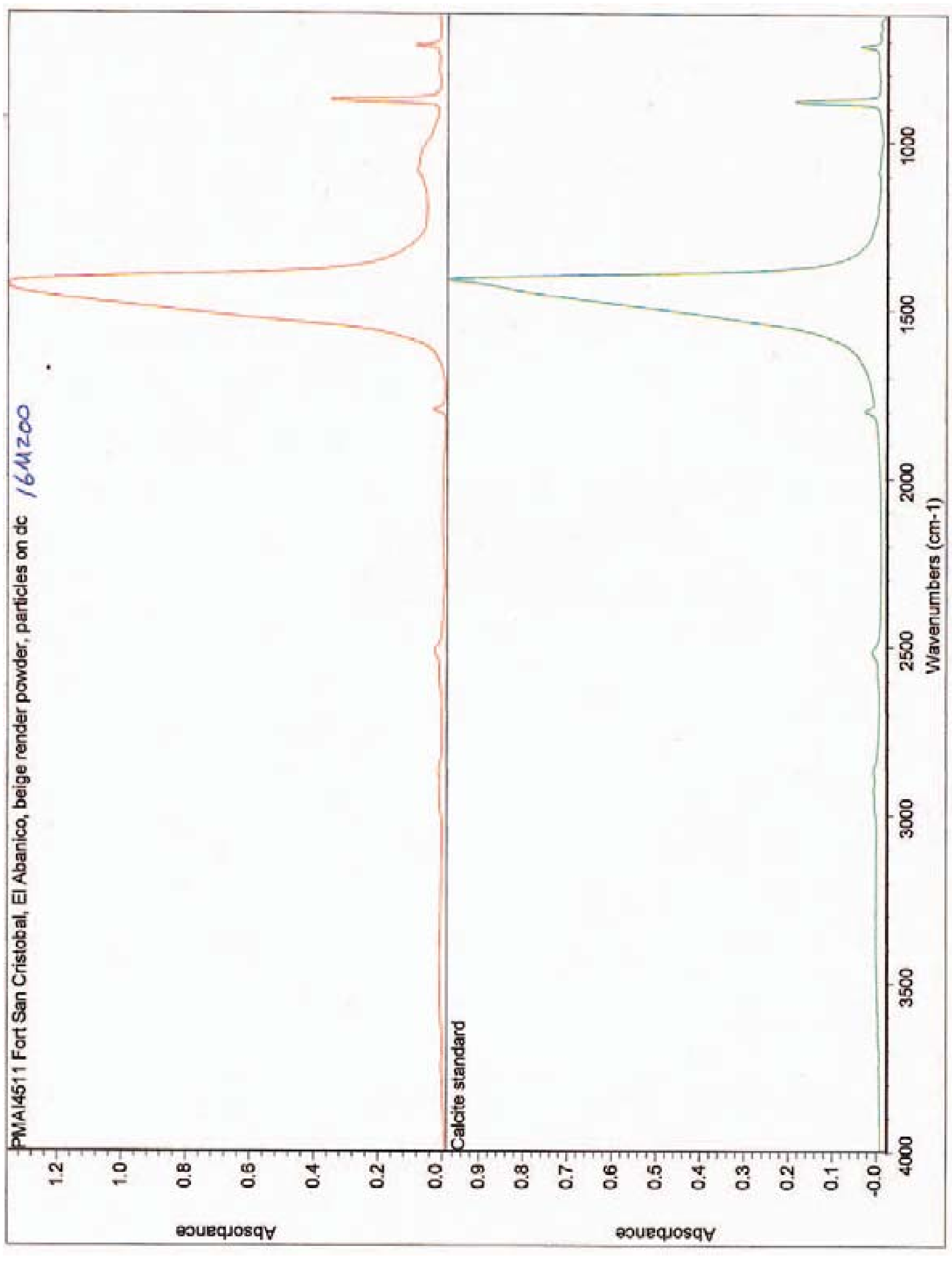
PMAI4511 Fort San Cristobal, El Abanico, beige render powder, particles on dc
16M200
Calcite standard
Absorbance
Absorbance
Wavenumbers (cm-1)

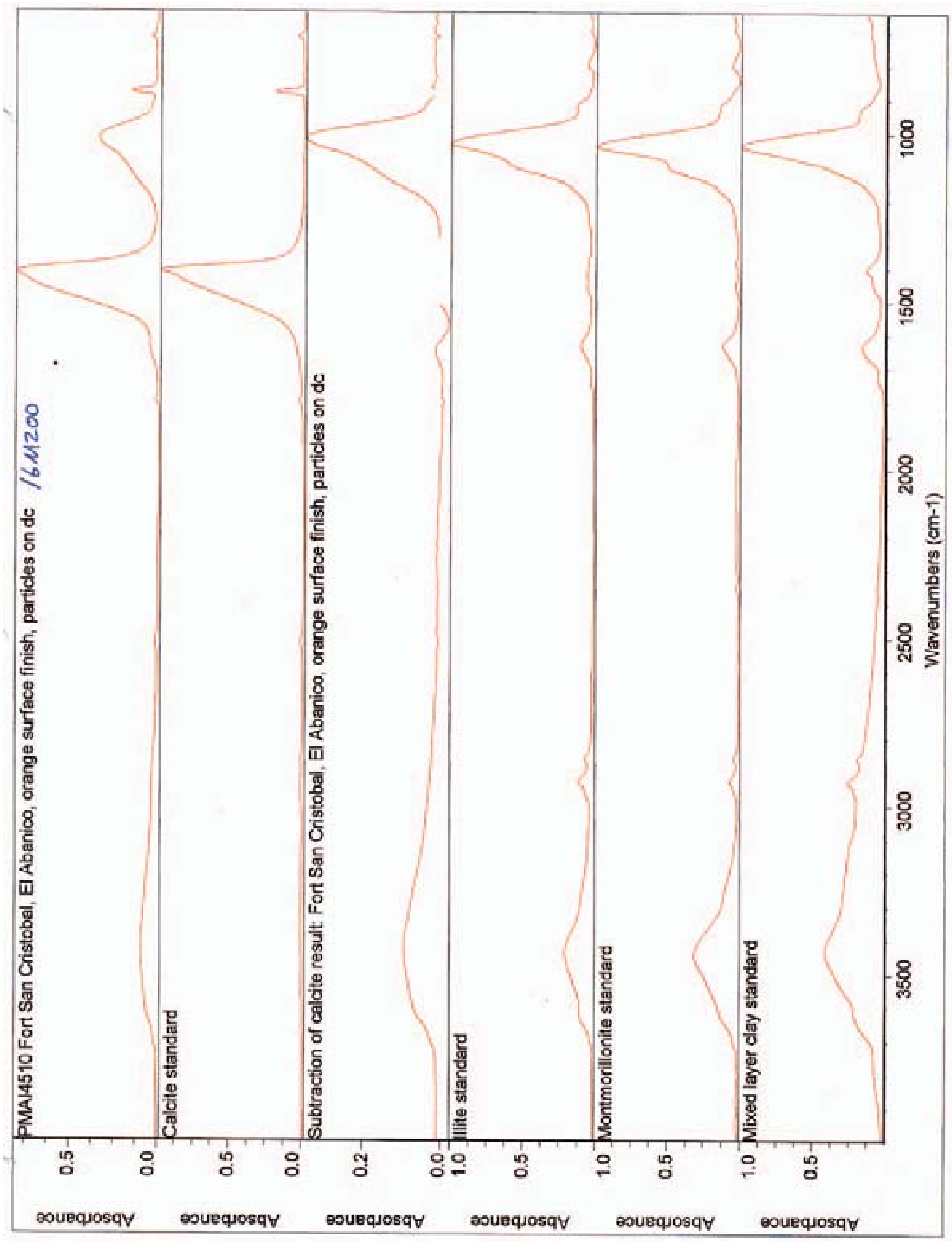
PMAI4510 Fort San Cristobal, El Abanico, orange surface finish, particles on dc
/611200
Calcite standard
Subtraction of calcite result: Fort San Cristobal, El Abanico, orange surface finish, particles on dc
Illite standard
Montmorillonite standard
Mixed layer clay standard
Absorbance
Wavenumbers (cm-1)
1000
1500
2000
2500
3000
3500
0.5
0.0
0.2
1.0

APPENDIX J: SEM/EDS RESULTS

Fort San Cristobal

16/03/2004 17.56:04

Project: Fort San Cristobal
Owner: PMA
Site: upper layer

Sample: orange surface finish
Type: Particles
ID: 13M200

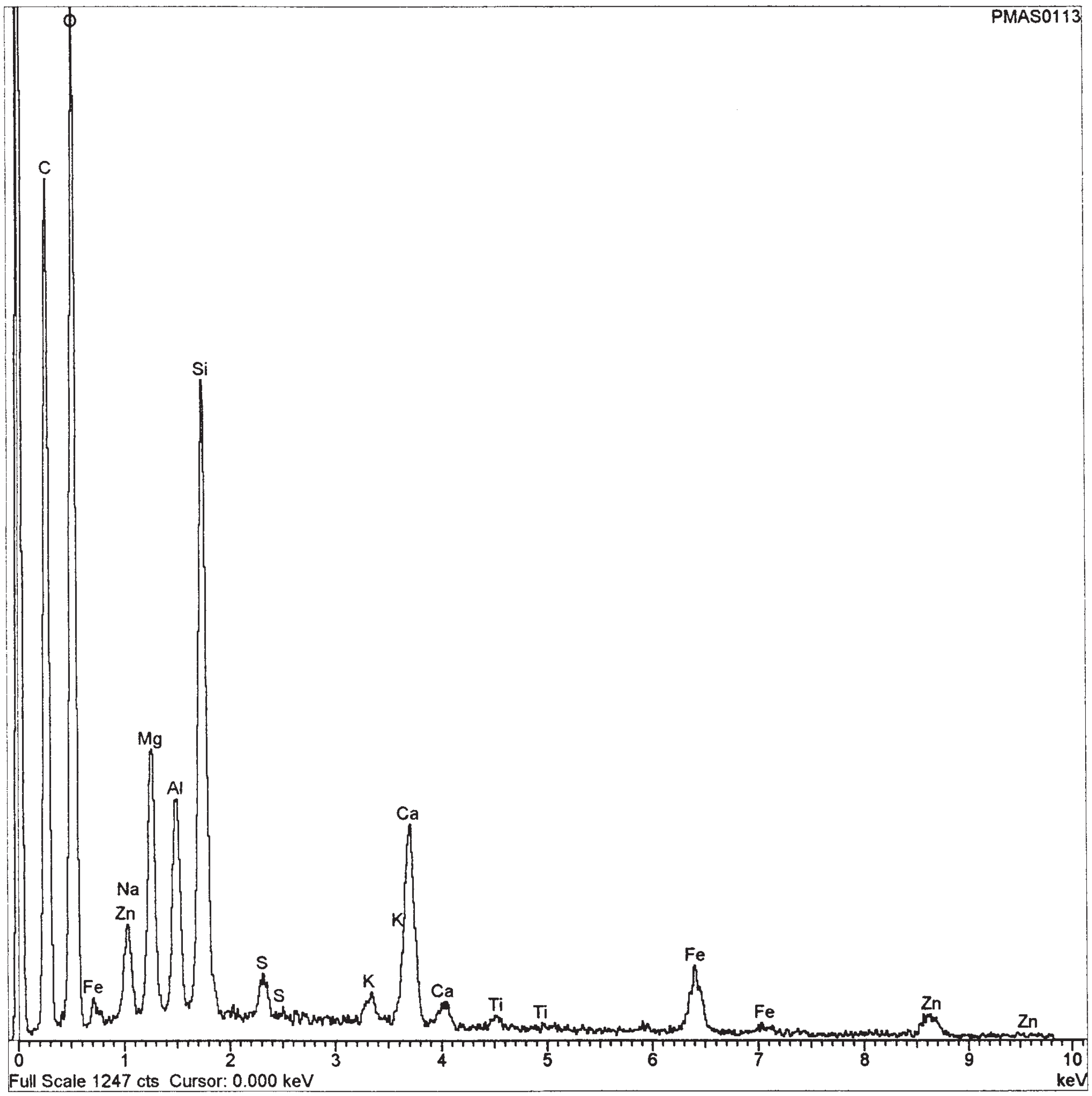

Comment: San Carlos Lightning Tower Orange Particles 13M200

Fort San Cristobal

16/03/2004 17:46:08

Project: Fort San Cristobal
Owner: PMA
Site: render

Sample: red particle in render
Type: Particles
ID: 14M200

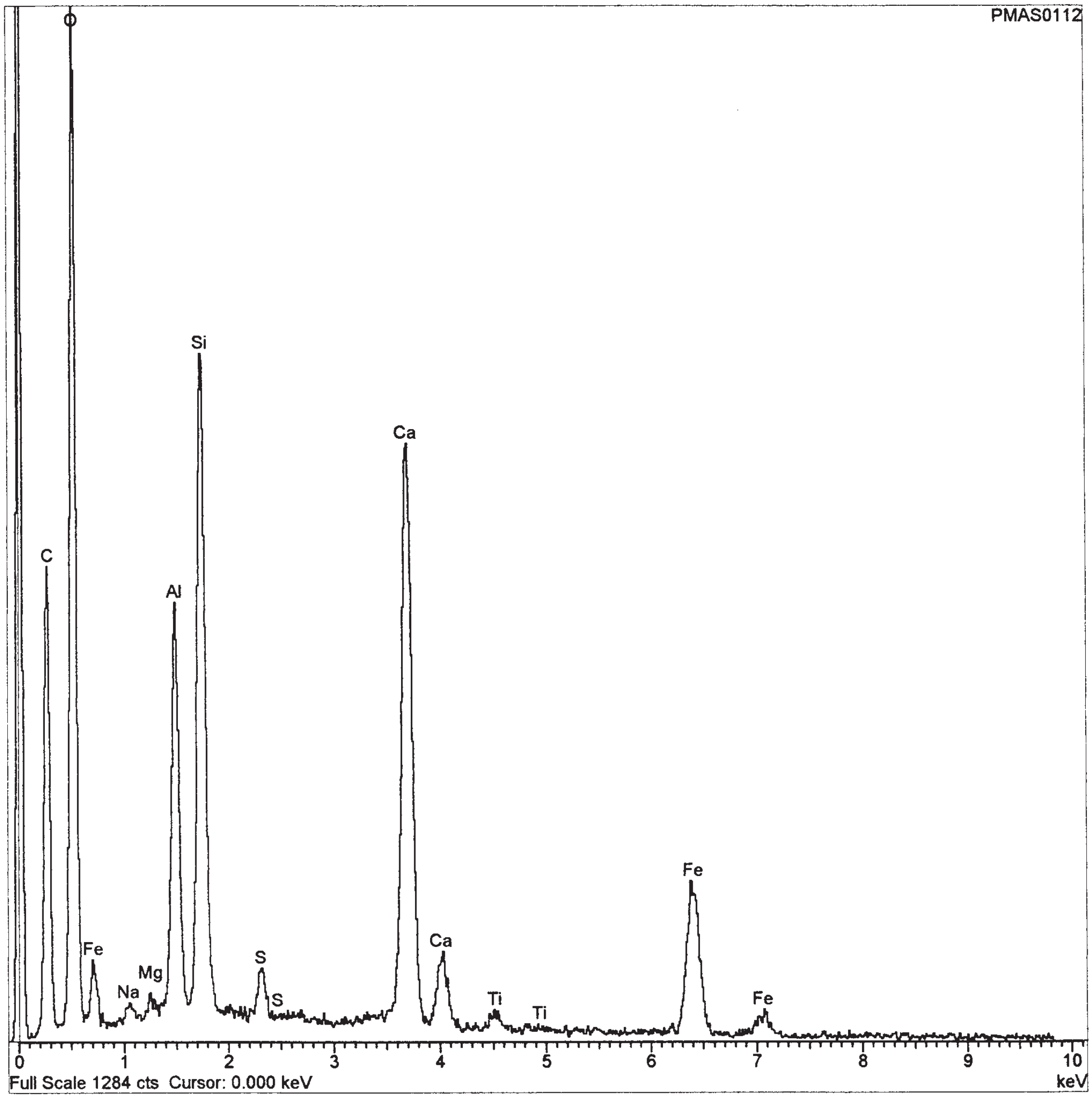

Comment: La Trinidad red particle in render 14 M200

Fort San Cristobal

16/03/2004 18 07:05

Project: Fort San Cristobal
Owner: PMA
Site: lower layer

Sample: [redacted] render body
Type: Particles
ID: 14M200

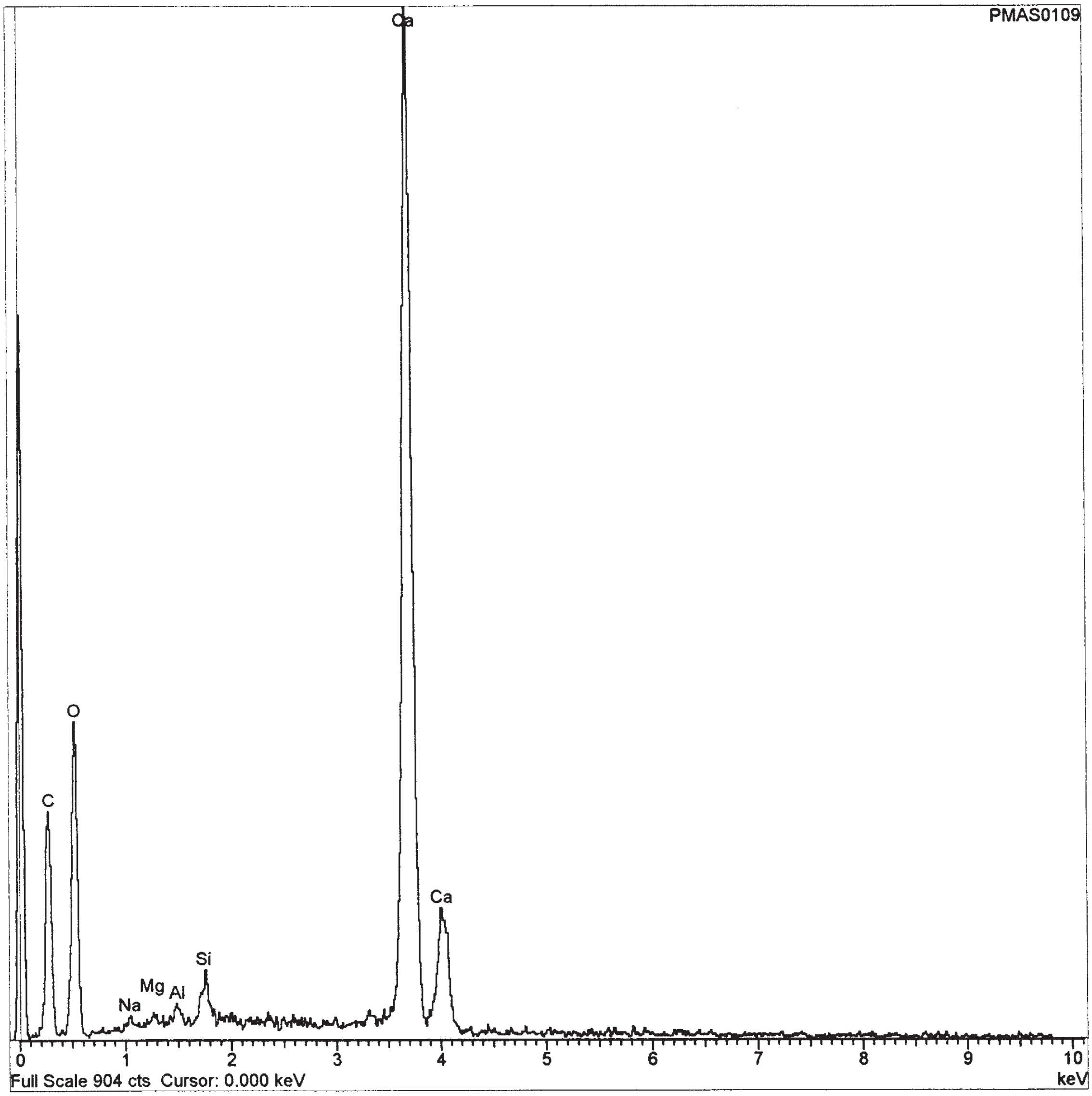

Comment: El Abanico Render 14M200

Fort San Cristobal

16/03/2004 17:36:24

Project: Fort San Cristobal
Owner: PMA
Site: surface finish

Sample: yellow surface finish
Type: Particles
ID: 14M200

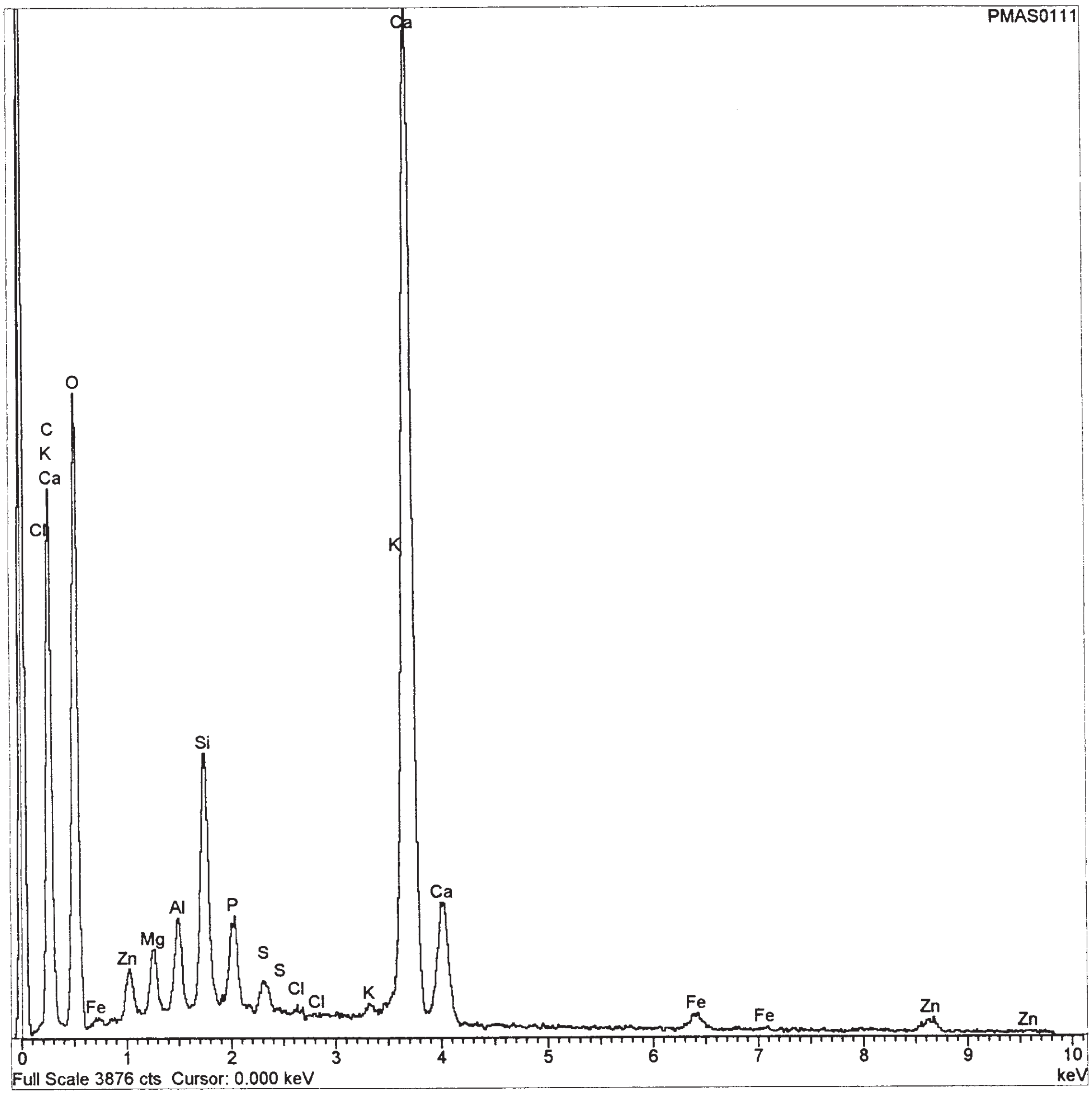

Comment: La Trinidad yellow surface finish 14M200

Fort San Cristobal

16/03/2004 18:00:11

Project: Fort San Cristobal
Owner: PMA
Site: upper layer

Sample: Orange surface finish
Type: Particles
ID: 16M200

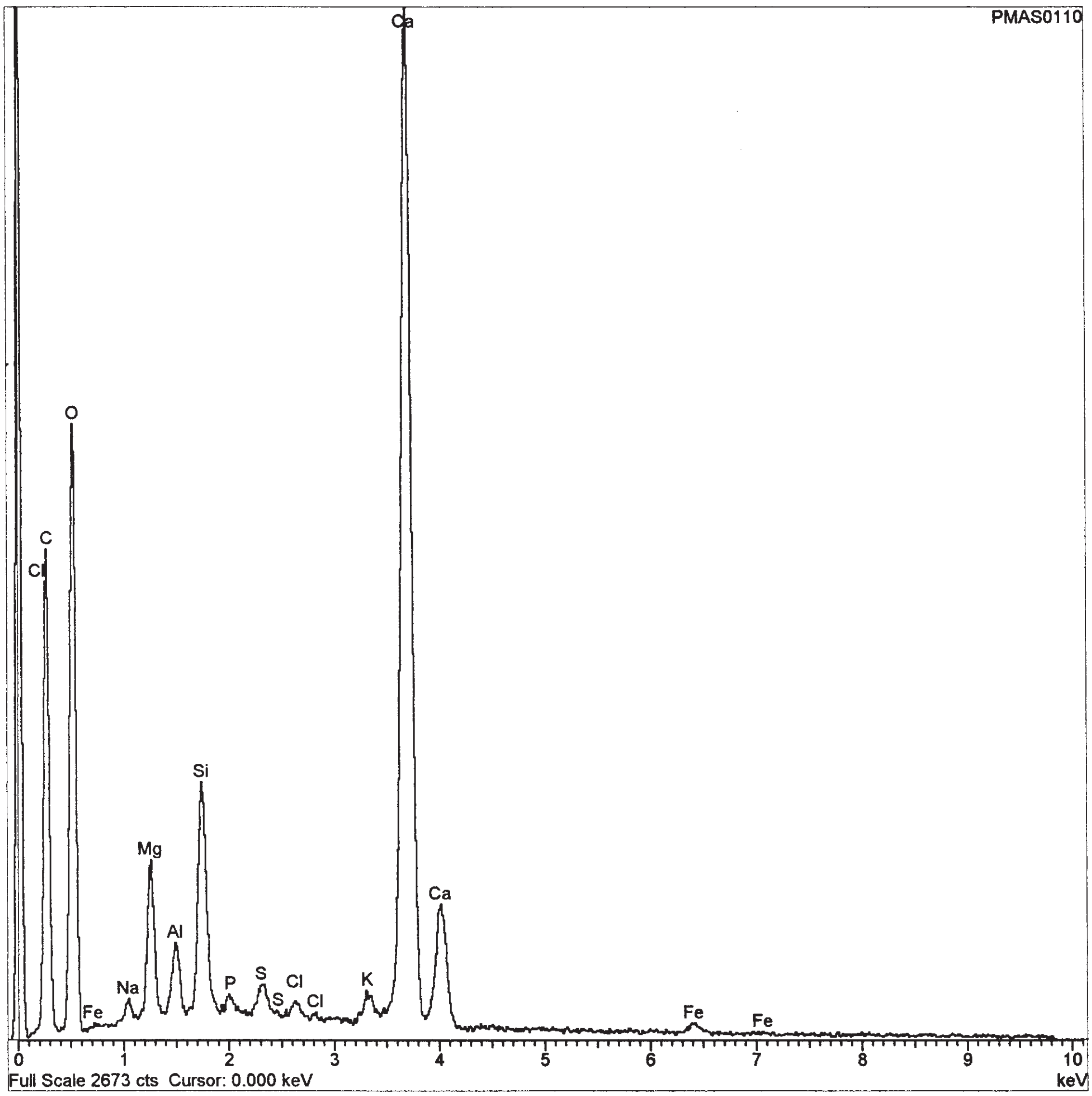

Comment: El Abanico Orange surface finish 16M200

BIBLIOGRAPHY

Adams, James E., and William A. Kneller. 1988. Thermal analysis (TA) of medieval mortars from Gothic cathedrals of France. In *Engineering geology of ancient works, monuments and historical sites: Preservation and protection, proceedings of an international symposium organized by the Greek national group of IAEG, Athens 1988*, edited by P. G. Marinos and G. C. Koukis. Rotterdam: Balkema.

Alba, Almyr M. 1995. Architectural exterior finishes in the Spanish Caribbean. Case studies: San Geronimo and Santa Elena powder magazines, Graduate Program in Historic Preservation, University of Pennsylvania, Philadelphia.

Alberti, Leon Battista. 1986. *The ten books of architecture*. Translated by Giacomo Leoni 1755 ed. New York: Dover Publications.

Anderson, Helle Dam, Hans Dieter Zimmerman, Henrik Friis, and Ulrich Schnell. 2000. Examination of hydraulic lime mortars of medieval churches in Denmark. In *International RILEM workshop on historic mortars: Characteristics and Tests; Paisley, Scotland, 12th - 14th May 1999*, edited by P. Barton, C. Groot and J. J. Hughes. Cachan, France: RILEM Publications.

Arana, Luis R. 1988. Construction at Castillo de San Marcos 1784-1821. *Escribano* 25:135-145.

Architectural practice in Mexico City. 1987. Translated by M. K. Schuetz. Tucson, AZ: The University of Arizona Press.

ASTM. 1999. *ASTM C144-99: Standard specification for aggregate for masonry mortar*. West Conshohocken, PA: ASTM.

Barnett, William K. 1991. Optical petrography as a tool for examining gypsum and lime plaster pyrotechnology. *Journal of Field Archeology* 18:253-256.

Berkowitz, Joan, E. Blaine Cliver, Judy Jacob, Frank Matero, and Barbara Yocum. 1991. *The fortifications of San Juan National Historic Site; Historic structure report, volume II: El Fuerte de San Cristóbal*. Atlanta, GA: Southeast Regional Office, National Park Service.

Berlucchi, N., and Ginanni R. Corradini. 1995. Experimentation of a chemical-physical methodology for the reconstruction of historic mortars. In *Methods of evaluating products for the conservation of porous building materials in monuments, international colloquium, Rome, 19-21 June 1995, preprints*. Rome: ICCROM.

Bläuer Böhm, Christine. 1996. Assessment of quantitative salt analysis by the water extraction method on lime mortars. In *Proceedings of the 8th international congress on deterioration and conservation of stone, Berlin, 30 Sept. - 4 Oct. 1996*, edited by J. Riederer. Berlin: Moller Druck & Verlag.

Bläuer Böhm, Christine. 2000. Analysis of mortars containing pozzolanas. In *International RILEM workshop on historic mortars: Characteristics and Tests; Paisley, Scotland, 12th - 14th May 1999*, edited by P. Barton, C. Groot and J. J. Hughes. Cachan, France: RILEM Publications.

Briggs, R. P., and P. A. Gelabert. 1962. Preliminary report of the geology of the Barranquitas Triangle, Puerto Rico; Map I-336. Washington, DC: U.S. Geological Survey.

Calderón Quijano, José Antonio. 1996. *Las fortificaciones Españolas en América y Filipinas*. Madrid: Mapfre.

Callebaut, K., J. Elsen, K. Van Balen, and W. Viaene. 2000. Historical and scientific study of hydraulic mortars from the 19th century. In *International RILEM workshop on historic mortars: Characteristics and Tests; Paisley, Scotland, 12th - 14th May 1999*, edited by P. Barton, C. Groot and J. J. Hughes. Cachan, France: RILEM Publications.

Callebaut, K., W. Viaene, K. Van Balen, and Ottenburgs R. 2000. Petrographical, mineralogical and chemical characterisation of lime mortars in the Saint Michael's Church (Leuven, Belgium). In *International RILEM workshop on historic mortars: Characteristics and Tests; Paisley, Scotland, 12th - 14th May 1999*, edited by P. Barton, C. Groot and J. J. Hughes. Cachan, France: RILEM Publications.

Casal, Francisco. 1990. Insolita tradicion de tapial en Cuba. In *ADOBE 90, 6th international conference on the conservation of earthen architecture*. Los Angeles: The Getty Conservation Institute.

Charola, A. E. 2001. Mortar analysis: A comparison of European procedures. *US/ICOMOS Scientific Journal: Historic Mortars & Acidic Deposition on Stone* 3 (1):2-5.

Charola, A. E., Michel Dupas, Richard P. Sheryll, and Gregory G. Freund. 1986. Characterization of ancient mortars: Chemical and instrumental methods. In *Scientific methodologies applied to works of art: proceedings of the symposium, Florence, Italy 2-5 May 1984*, edited by P. Parrini. Milan: Montedison Progretto Cultura.

Charola, A. Elena. 2000. Salts in the deterioration of porous materials: an overview. *Journal of the American Institute for Conservation* 39:327-343.

Charola, A. Elena, and Silvia A. Centeno. 2002. Analysis of gypsum-containing lime mortars: Possible errors due to the use of different drying conditions. *Journal of the American Institute for Conservation* 41:269-278.

Crisson, Richard C. 1996. San Juan historic structure report stucco project. In *Third international symposium of historic preservation on Puerto Rico and the Caribbean*, edited by M. F. Román. Puerto Rico: National Park Service.

Doebley, Carl E., and Donald S. Spitzer. 1996. Guidelines and standards for testing historic mortars. In *Standards for preservation and rehabilitation (STP 1258)*, edited by S. J. Kelley. West Conshohocken, PA: ASTM.

Draffin, Jasper O. 1976. A brief history of lime, cement, concrete, and reinforced concrete. In *A selection of historic American papers on concrete, 1876-1926*, edited by H. Newlon, Jr. Detroit: American Concrete Institute.

Duffy, Christopher. 1985. *The fortress in the age of Vauban and Frederick the Great 1660-1789*. London: Routledge & Kegan Paul.

Ellis, P. R. 2000. Analysis of mortars (to include historic mortars) by differential thermal analysis. In *International RILEM workshop on historic mortars: Characteristics and Tests; Paisley, Scotland, 12th - 14th May 1999*, edited by P. Barton, C. Groot and J. J. Hughes. Cachan, France: RILEM Publications.

English Heritage. 2000. *The English Heritage directory of building sands and aggregates*. Edited by S. Chapman and J. Fidler. Dorset: Donhead.

Erhardt, David, Walter Hopwood, Mary Baker, and David von Endt. 1988. A systematic approach to the instrumental analysis of natural finishes and binding media. In *The American Institute for Conservation of Historic and Artistic Works preprints of papers presented at the sixteenth annual meeting, New Orleans, LA.* Washington, D.C.: American Institute for Conservation of Historic and Artistic Works.

Erlin, Bernard, and William G. Hime. 1985. Methods for analyzing mortar. In *Proceedings of the third North American masonry conference*, edited by J. H. Matthys and J. G. Borchelt. Arlington, TX: The University of Texas at Arlington.

FitzPatrick, Ewart Adsil. 1984. *Micromorphology of soils*. London; New York: Chapman and Hall.

Goins, Elizabeth. 2001. A standard method for the characterization of historic cementitious materials. *US/ICOMOS Scientific Journal: Historic Mortars & Acidic Deposition on Stone* 3 (1):6-7.

Goren, Yuval, and Paul Goldberg. 1991. Petrographic thin sections and the development of neolithic plaster production in northern Israel. *Journal of Field Archeology* 18:131-138.

Guillou, Robert B., and Jewell J. Glass. 1957. *A reconnaissance study of the beach sands of Puerto Rico; Geological survey bulletin 1042-I*. Washington, DC: United States Government Printing Office.

Gurcke, Karl. 1987. *Bricks and brickmaking*. Moscow, ID: The University of Idaho Press.

Hansen, Eric. 2001. Some factors to be considered in the analysis of high lime mortars of archaeological provenance. *US/ICOMOS Scientific Journal: Historic Mortars & Acidic Deposition on Stone* 3 (1):9, 10.

Haynes, R. 1984. *Optical microscopy of materials*. Glasgow, Scotland: International Textbook Company.

Hostos, Adolfo De. 1948. *Cuidad murada; Ensayo acerca del proceso de la civilización en la cuidad española de San Juan Bautista de Puerto Rico*. Havana, Cuba: Editorial Lex.

Hughes, Quentin. 1991. *Military Architecture*. Hants, U.K.: Beafort Publishing.

Iñiguez, Diego Angulo. 1942. *Bautista Antonelli; Las fortificaciones Americanas del siglo XVI*. Madrid: Hauser and Menet.

Jacob, Judy, and Gregory J. Cavallo. 1992. Masonry mortars in the Castillo de San Felipe del Morro, San Juan, Puerto Rico: A method for categorization. In *Conservation of the Iberian and Latin American cultural heritage: Preprints of the contributions to the Madrid Congress, 9-12 September 1992*, edited by H. W. M. Hodges, J. S. Mills and P. Smith. London: The International Institute for Conservation of Historic and Artistic Works.

Jedrzejewska, Hanna. 1960. Old mortars in Poland: A new method of investigation. *Studies in Conservation* 5 (4):132-138.

———. 1982. Ancient mortars as criterion in analyses of old architecture. In *Mortars, cements and grouts used in the conservation of historic buildings, symposium 3-6.11.1981*. Rome: ICCROM.

Johnston, Sean. 1991. *Fourier transform infrared*. New York: Ellis Horwood.

Jonsson, Marita, and E. Blaine Cliver. 2003. Coloring historic stucco: The revival of a past technique in San Juan, Puerto Rico. *APT Bulletin* 33 (4):31-36.

Kaye, Clifford A. 1959. *Geology of the San Juan metropolitan area, Puerto Rico; Geological survey professional paper 317-A*. Washington, DC: U.S. Government Printing Office.

Klemm, Dietrich D., and R. Klemm. 1990. Mortar evolution in the old kingdom of Egypt. In *Archaeometry '90*, edited by E. Pernicka and G. A. Wagner. Basel: Birkhäuser Verlag.

Lawes, Grahame. 1987. *Scanning electron microscopy and X-ray microanalysis*. Chichester, UK: John Wiley & Sons.

Lewin, Seymor Z. 1982. X-Ray diffraction and scanning electron microscope analysis of conventional mortars. In *Mortars, cements and grouts used in the conservation of historic buildings, symposium 3-6.11.1981*. Rome: ICCROM.

Manuncy, Albert C. 1952. Tapia or tabby. *Journal of the Society of Architectural Historians* 11 (4):32-33.

———. 1983. Building materials in colonial San Augustin. *El Escribano* 20:60.

Manuncy, Albert, and Ricardo Torres-Reyes. 1973. *Puerto Rico and the forts of Old San Juan*. Riverside, CT: The Chatham Press, Inc.

Martinet, Gilles, and Bernard Quenee. 2000. Proposal for a useful methodology for the study of ancient mortars. In *International RILEM workshop on historic mortars: Characteristics and Tests; Paisley, Scotland, 12th - 14th May 1999*, edited by P. Barton, C. Groot and J. J. Hughes. Cachan, France: RILEM Publications.

Meeks, Carroll L. V. 1949. Books and buildings, 1449-1949. One hundred great architectural books most influential in shaping the architecture of the Western World. *Journal of the Society of Architectural Historians* 8 (1/2):55-67.

Middendorf, B., G. Baronio, K. Callebaut, and J. Hughes. 2000. Chemical-mineralogical and physical-mechanical investigations of old mortars. In *International RILEM workshop on historic mortars: Characteristics and Tests; Paisley, Scotland, 12th - 14th May 1999*, edited by P. Barton, C. Groot and J. J. Hughes. Cachan, France: RILEM Publications.

Mitchell, Herbert. 1994. An unrecorded issue of Philibert Delorme's Le premier tome de l'architecture, annotated by Sir Henry Wotton. *Journal of the Society of Architectural Historians* 53:20-29.

Moore, J., and J. Stewart. 1982. Chemical techniques of historic mortars analysis. In *Mortars, cements and grouts used in the conservation of historic buildings, symposium 3-6.11.1981*. Rome: ICCROM.

National Park Service. 1996. *The Forts of Old San Juan*. Washington, D.C.: U.S. Department of the Interior.

Palladio, Andrea. 1965. *The four books of architecture*. Translated by Isaac Ware 1738 ed. New York: Dover Publications.

Phillips, Morgan. 1994. An actual mortar analysis. *APT Bulletin* 25 (3-4):54, 55.

Price, Beth A., Janice H. Carlson, Richard Newman, Kate Duffy, and Kendra E. Roth. 1996. Application of FTIR microspectroscopy to the identification of naturally occurring minerals in works of art. In *5th international conference on non-destructive testing microanalytical methods and environmental evaluation for the study and conservation of works of art, Budapest*. Roma: Instituto Centrale per il Restauro and Associazione Italiana Prove non Distruttive.

Reedy, Chandra L. 1994. Thin-section petrography in studies of cultural materials. *Journal of the American Institute for Conservation* 33 (2):115-129.

Reynolds, R. J., and K. Aldous. 1970. *Atomic absorption spectroscopy*. London: Charles Griffin & Company Ltd.

Rothrock, George A. 1966. Positional warfare: A reappraisal. *Military Review* 46 (4):77-88.

Russell, J. D. 1981. Infrared methods. In *A handbook of determinative methods in clay mineralogy*, edited by M. J. Wilson. New York: Chapman and Hall.

Sagredo, Diego de. 1986. *Medidas del romano*. Madrid: Instituto de Conservacion y Restauracion de Bienes Culturales.

Serlio, Sebastiano. 1996. *Sebastiano Serlio on architecture: Books I-V of tutte l'opere d'architettura et prospetiva*. New Haven, CT: Yale University Press.

Smykatz-Kloss, Werner. 1974. *Differential thermal analysis*. Berlin: Springer-Verlag.

Steed, John, Captain. 1688. *Fortification and military discipline*. London: Robert Morden.

Tellez, German. 1997. Caribbean fortification design and technology, comments. In *Fortificaciones del Caribe; Memorias de la reunion de expertos, 31 de Julio, 1 y 2 de Agosto de 1992, Cartagena de Indias, Columbia*. Columbia: Colcultura.

Teutonico, Jeanne Marie, Iain McCaig, Colin Burns, and John Ashurst. 1994. The Smeaton Project: Factors affecting the properties of lime-based mortars. *APT Bulletin* 25 (3-4).

Torres-Reyes, Ricardo. 1965. *Construction history of San Cristobal*. Puerto Rico: National Park Service.

Van Balen, K., E.-E. Toumbakari, M.-T. Blanco, J. Aguilera, F. Puertas, C. Sabbioni, G. Zappia, C. Riontino, and G. Gobbi. 2000. Procedure for mortar type identification: A proposal. In *International RILEM workshop on historic mortars: Characteristics and Tests; Paisley, Scotland, 12th - 14th May 1999*, edited by P. Barton, C. Groot and J. J. Hughes. Cachan, France: RILEM Publications.

Van Middeldyk, R. A. 1903. *The history of Puerto Rico*. New York: D. Appleton and Company.

Vauban, Sébastien LePrestre de. 1968. *A manual of siegecraft and fortification*. Translated by G. A. Rothrock. Ann Arbor: The University of Michigan Press.

Vitruvius, Marcus. 1960. *The ten books on architecture*. Translated by M. H. Morgan. New York: Dover.

Warren, B. E. 1969. *X-ray diffraction*. Reading, MA: Addison-Wesley Publishing Company.

Weaver, Martin, and Frank Matero. 1997. *Conserving buildings: Guide to techniques and materials*. New York: John Wiley and Sons.

INDEX